Uniwersytet Medyczny w Białymstoku

DZIEDZINA: nauki medyczne i nauki o zdrowiu

DYSCYPLINA: nauki medyczne

ROZPRAWA DOKTORSKA

Wpływ kształtu i rozmiaru nanocząstek złota na efekt przeciwbakteryjny i przeciwgrzybiczy ceragenin związanych z ich powierzchnią – badania *in vitro*

Karol Skłodowski

Promotor: Prof. dr hab. Robert Bucki
Promotor pomocniczy: Dr n. med. Sylwia Joanna Chmielewska-Deptuła

Zakład Mikrobiologii Lekarskiej i Inżynierii Nanobiomedycznej
Kierownik jednostki: Prof. dr hab. Robert Bucki
Rozprawa doktorska została zrealizowana w ramach kształcenia w Szkole Doktorskiej UMB

Białystok, 2024

Medical University of Bialystok

Field of Medical and Health Sciences

Scientific discipline: Medical Sciences

Doctoral Thesis

Impact of the shape and size of ceragenin-coated gold nanoparticles on the antimicrobial and antifungal effects - *in vitro* studies

Karol Skłodowski

Supervisor: Prof. Robert Bucki, M.D., PhD
Assisting supervisor: Sylwia Joanna Chmielewska-Deptuła, M.Sc., PhD

Department of Medical Microbiology and Nanobiomedical Engineering
Head of Department: Prof. Robert Bucki, M.D., PhD
The doctoral thesis was carried out as a part of education at the Doctoral School of UMB

Bialystok, 2024

Spis treści

1. Wykaz publikacji włączonych do rozprawy doktorskiej

Praca przeglądowa (publikacja nr 1, P.1):

Karol Skłodowski, Sylwia Joanna Chmielewska-Deptuła, Ewelina Piktel, Przemysław Wolak, Tomasz Wollny, Robert Bucki. *Metallic Nanosystems in the Development of Antimicrobial Strategies with High Antimicrobial Activity and High Biocompatibility*. International Journal of Molecular Sciences, 2023, 24(3), 2104. DOI: 10.3390/ijms24032104. Data publikacji: 20.01.2023 r.

IF: 5,6; MEiN: 140.

Praca oryginalna (publikacja nr 2, P.2):

Karol Skłodowski, Sylwia Joanna Chmielewska, Joanna Depciuch, Piotr Deptuła, Ewelina Piktel, Tamara Daniluk, Magdalena Zakrzewska, Michał Czarnowski, Mateusz Cieśluk, Bonita Durnaś, Magdalena Parlińska-Wojtan, Paul B. Savage, Robert Bucki. *Ceragenin-Coated Non-Spherical Gold Nanoparticles as Novel Candidacidal Agents*. Pharmaceutics, 2021, 13, 1940. DOI: 10.3390/pharmaceutics13111940. Data publikacji: 16.11.2021 r.

IF: 6,525; MEiN: 100.

2. Zestawienie publikacji

Rodzaj publikacji	Liczba	Impact Factor	Punktacja MEiN
Prace włączone do rozprawy doktorskiej	2	12,125	240
Prace, które nie zostały włączone do rozprawy doktorskiej	13	67,202	1600
Streszczenia zjazdowe	5	-	-
Razem	20	79,327	1840

3. Spis skrótów

A549 – ludzkie komórki gruczolakoraka płuc

ABC – ang. *ATP-binding cassette*; kaseta wiążąca ATP

AmpC – ang. *βeta-lactamase class C according to Ambler*; βeta-laktamaza klasy C wg Amblera

ATCC – ang. *American Type Culture Collection*

ATP – ang. *adenosine triphosphate*; adenozynotrifosforan

Au NPs – ang. *gold nanoparticles*; nanocząstki złota

Au NPs@CSAs – nanocząstki złota, których powierzchnia została sfunkcjonalizowana cerageninami

AuR/AuP/AuS NPs@CSA – nanocząstki złota w kształcie patyczków (AuR)/fistaszków (AuP)/gwiazdek (AuS) sfunkcjonalizowane cerageninami

BSA – ang. *bovine serum albumin*; surowicza albumina bydlęca

CAUTI – ang. *catheter-associated urinary tract infections*; odcewnikowe zakażenia dróg moczowych

CDC – ang. *Centers for Disease Control and Prevention*; Centra Kontroli i Zapobiegania Chorobom

CFU- ang. *colony-forming unit*; jednostka tworząca kolonię

CSAs – ang. *cationic steroid antimicrobials*; kationowe steroidowe środki przeciwdrobnoustrojowe, cerageniny

DAPI – ang. *4',6-diamidino-2-phenylindole*; 4',6-diamidino-2-fenyloindol

DFCH-DA – ang. *2',7'-Dichlorofluorescein diacetate*; dioctan 2',7'-dichlorofluoresceiny

Disc(3) – ang. *3,3'-Dipropylthiadicarbocyanine iodide*; jodek 3,3'-dipropylotiadikarbocyjaniny

DMEM – ang. *Dulbecco's modified Eagle's medium*

DNA – ang. *deoxyribonucleic acid*; kwas deoksyrybonukleinowy

EPS – ang. *extracellular polymeric substances*; zewnątrzkomórkowe substancje polimerowe

ERG11 – gen kodujący 14α-demetylazę lanosterolu

ESBL – ang. *extended-spectrum βeta-lactamases*; β-laktamazy o rozszerzonym spektrum działania

ESKAPE – akronim obejmujący nazwy sześciu wysoce zjadliwych i opornych na antybiotyki patogenów bakteryjnych: *Enterococcus faecium*, *Staphylococcus aureus*, *Klebsiella pneumoniae*, *Acinetobacter baumannii*, *Pseudomonas aeruginosa* i *Enterobacter* spp.

EUCAST – ang. *European Committee on Antimicrobial Susceptibility Testing*; Europejski Komitet ds. Oznaczania Lekowrażliwości

FBS – ang. *fetal bovine serum*; płodowa surowica bydlęca

FITC – ang. *fluorescein isothiocyanate*; izotiocyjanian fluoresceiny

IMP – ang. *imipenemase*; imipenemaza

LB – ang. *Luria-Bertani*; pożywka Lurii-Bertaniego

LPS – ang. *lipopolysaccharides*; lipopolisacharyd

MATE – ang. *multidrug and toxin extrusion*; białka ekstruzji wielolekowej i toksyn

MBC – ang. *minimum bactericidal concentration*; minimalne stężenie bakteriobójcze

MDR – ang. *multidrug-resistant bacteria*; bakterie wielolekooporne

MFC – ang. *minimum fungicidal concentration*; minimalne stężenie grzybobójcze

MFS – ang. *major facilitator superfamily*; nadrodzina białek transportu błonowego

MHDA – ang. *16-mercaptohexadecanoic acid*; kwas 16-merkaptoheksadekanowy

MIC – ang. *minimum inhibitory concentration*; minimalne stężenie hamujące

MOPS – ang. *3-(N-Morpholino)propanesulfonic acid*; kwas 3-(N-morfolino) propanosulfonowy

MRSA – ang. *methicyllin-resistant Staphylococcus aureus*; gronkowiec złocisty oporny na metycylinę

MTT – ang. *3- (4,5-Dimethylthiazol-2-Yl) -2,5-Diphenyltetrazolium Bromide*; bromek 3-[4,5-dimetylotiazol-2-ylo]-2,5-difenylotetrazoliowy

NDM-1 – ang. *New Delhi metallo-β-lactamase*; metalo-β-laktamaza

NPN – ang. *N-Phenyl-1-naphthylamine*; N-fenylo-1-naftyloamina

NPs – ang. *nanoparticles*; nanocząstki

OD – ang. *optical density*; gęstość optyczna

OMP – ang. *outer membrane proteins*; białka błony zewnętrznej

OprD – ang. *outer membrane protein D*; białko D błony zewnętrznej

PACE – ang. *proteobacterial antimicrobial compound efflux*; rodzina białek transportowych u proteobakterii

PBS – ang. *phosphate buffered saline*; sól fizjologiczna buforowana fosforanami

PFA – ang. *paraformaldehyde*; paraformaldehyd

RBC – ang. *red blood cell*; krwinka czerwona

RND – ang. *resistance-nodulation-division*; transportery z rodziny RND

ROS – ang. *reactive oxygen species*; reaktywne formy tlenu

RPMI – ang. *Roswell Park Memorial Institute*

rRNA – ang. *ribosomal ribonucleic acid*; rybosomalny kwas rybonukleinowy

SMR – ang. *small multidrug resistance*; rodzina SMR integralnych białek błonowych

STEM – ang. *scanning transmission electron microscopy*; skaningowy transmisyjny mikroskop elektronowy

TEM – ang. *transmission electron microscopy*; transmisyjny mikroskop elektronowy

TSST-1 – ang. *toxic shock syndrome toxin-1*; toksyna-1 zespołu wstrząsu toksycznego

VRE – ang. *vancomycin-resistant Enterococcus*; enterokoki oporne na wankomycynę

VREF – ang. *vancomycin-resistant Enterococcus faecium*; oporny na wankomycynę *Enterococcus faecium*

WHO – ang. *World Health Organization*; Światowa Organizacja Zdrowia

XDR – ang. *extensively drug-resistant*; bakterie oporne na szeroką gamę leków

ZUM – zakażenie układu moczowego

4. Wstęp

Zakażenia wywoływane przez drobnoustroje lekooporne, stanowią istotny problem zdrowotny, epidemiologiczny oraz ekonomiczny (1). Szacuje się, iż w 2019 roku zakażenia bakteryjne były przyczyną śmierci około 7,7 miliona osób (z czego 4,95 miliona zgonów było spowodowane przez drobnoustroje lekooporne). Równocześnie, szacuje się, iż zakażenia grzybicze każdego roku są przyczyną śmierci 1,7 miliona osób (2-4). Najnowsze prognozy wskazują, iż do 2050 roku zakażenia wywołane przez drobnoustroje lekooporne będą powodować 10 milionów zgonów rocznie, a liczba zgonów z powodu zakażeń bakteryjnych będzie główną przyczyną śmierci ludności, przewyższając umieralność wywołaną przez choroby nowotworowe (5, 6).

Jedną z głównych przyczyn niepowodzenia antybiotykoterapii jest narastająca lekooporność mikroorganizmów spowodowana (i) nadmiernym stosowaniem antybiotyków, zwłaszcza w rolnictwie oraz (ii) ich niewłaściwym stosowaniem w medycynie, wynikającym z braku znajomości zasad racjonalnej antybiotykoterapii, a także (iii) formowaniem biofilmu przez mikroorganizmy patogenne (7-9). W kontekście hodowli zwierząt, rutynowo stosuje się antybiotyki zarówno celem profilaktyki chorób, jak i zwiększenia przyrostu masy ciała (10). W przypadku leczenia ludzi, nieprawidłowe stosowanie antybiotyków obejmuje między innymi stosowanie środków przeciwbakteryjnych w zakażeniach górnych dróg oddechowych o etiologii wirusowej, samodzielne stosowanie antybiotyków bez konsultacji z lekarzem, nieprzestrzeganie zaleceń dotyczących dawkowania, bądź przedwczesne przerwanie kuracji, co sprzyja generowaniu i selekcji opornych szczepów bakterii (11). Ponadto, zdolność mikroorganizmów do tworzenia wielokomórkowych struktur biofilmu jest istotnym czynnikiem wpływającym na niepowodzenie stosowanej terapii, gdyż komórki bakterii oraz grzybów chronione w macierzy biofilmu są nawet 1000-krotnie bardziej oporne na środki dezynfekcyjne oraz stosowane leczenie w porównaniu do planktonicznej formy wzrostu (12). Niepokojący jest fakt, iż większość obecnie stosowanych antybiotyków jedynie zmniejsza liczbę komórek bakteryjnych lub grzybiczych znajdujących się w strukturze biofilmu, nie prowadząc do ich całkowitej eradykacji, czego konsekwencją jest rozwój przewlekłych i/lub nawracających zakażeń (13). Z tego też względu, konieczne jest poszukiwanie nowych środków przeciwdrobnoustrojowych, skutecznych w stosunku do patogenów tworzących biofilm.

5.1 Zakażenia bakteryjne wywoływane przeze patogeny z grupy ESKAPE

Akronimem ESKAPE, zdefiniowanym po raz pierwszy w roku 2008, określa się grupę lekoopornych bakterii, które ze względu na swoją niewrażliwość na powszechnie stosowane antybiotyki, wynikającą z obecności różnych mechanizmów oporności, stały się istotnym problemem epidemiologicznym o charakterze globalnym (14). Do grupy tej zalicza się: *Enterococcus faecium*, *Staphylococcus aureus*, *Klebsiella pneumoniae*, *Acinetobacter baumannii*, *Pseudomonas aeruginosa* oraz *Enterobacter* spp. (15). Wagę problemu podkreśla umieszczenie patogenów z grupy ESKAPE na priorytetowej liście Światowej Organizacji Zdrowia (WHO), uwzgledniającej mikroorganizmy w stosunku do których występuje pilna potrzeba opracowania nowych środków przeciwdrobnoustrojowych. W szczególności, oporne na karbapenemy *A. baumannii* i *P. aeruginosa* zostały wymienione w priorytecie krytycznym, a oporne na wankomycynę *E. faecium* (VREF) oraz oporne na metycylinę/wankomycynę *S. aureus* (MRSA/VRSA) zostały sklasyfikowane w grupach o wysokim priorytecie (16).

E. faecium jest fakultatywnie beztlenowym, Gram-dodatnim ziarenkowcem, który jako komensal powszechnie wywołuje zakażenia szpitalne u pacjentów z obniżoną odpornością. Infekcje związane z *E. faecium* obejmują odcewnikowe zakażenia dróg moczowych (CAUTI), bakteriemię, infekcje w obrębie jamy brzusznej czy zapalenie wsierdzia. Enterokoki oporne na wankomycynę (VRE) zostały po raz pierwszy wyizolowane w latach osiemdziesiątych XX wieku i w dalszym ciągu stanowią istotny czynnik etiologiczny zakażeń (17).

S. aureus to Gram-dodatni ziarenkowiec obecny w mikrobiomie skóry. Gronkowiec złocisty może powodować wiele infekcji, począwszy od infekcji ran i tkanek miękkich, przez zapalenie wsierdzia, sepsę, aż po zapalenie płuc. *S. aureus* jest zdolny do tworzenia biofilmu na implantach medycznych (18). Dodatkowo, około 20% naturalnych izolatów gronkowca złocistego wytwarza egzotoksynę TSST-1 (toksyna-1 zespołu wstrząsu toksycznego), która jest odpowiedzialna za wywoływanie zespołu wstrząsu toksycznego (19). Szczep MRSA został wyizolowany po raz pierwszy w 1961 roku, po zaledwie 2 latach od wprowadzenia antybiotyków β-laktamowych i w dalszym ciągu pozostaje istotnym problemem zdrowotnym na całym świecie (18).

K. pneumoniae jest Gram-ujemną pałeczką klasyfikowaną do rzędu Enterobacterales. Szacuje się, iż bakteria ta odpowiedzialna jest za około 30% wszystkich infekcji wywoływanych przez bakterie Gram-ujemne, stanowiąc częsty czynnik etiologiczny zapalenia płuc, zakażeń układu moczowego, posocznicy, zakażeń ran chirurgicznych oraz wsierdzia. Ze względu na produkcję β-laktamazy o rozszerzonym spektrum działania (ESBL), występowanie

wielolekoopornych (MDR) i skrajnie lekoopornych (XDR) fenotypów, bakteria ta stanowi poważne wyzwanie w zwalczaniu zakażeń (20, 21).

A. baumannii oporny na karbapenemy jest jednym z patogenów, który wymaga podjęcia natychmiastowych działań celem wdrożenia nowych terapii przeciwdrobnoustrojowych. A. baumannii jest oportunistyczną, Gram-ujemną pałeczką, która potrafi przystosować się do niekorzystnych warunków środowiska. Najczęstszymi postaciami klinicznymi zakażeń wywoływanych przez tę bakterię są zakażenia krwi związane z zastosowaniem centralnej linii naczyniowej oraz zapalenia płuc związane z wentylacją mechaniczną. Bakterie te cechują się zdolnością do długookresowego przetrwania w suchym środowisku, co możliwe jest ze względu na obecność polisacharydów otoczkowych, zbudowanych z powtarzających się jednostek węglowodanowych, działających jako tarcza glikanowa chroniąca przed szkodliwymi czynnikami zewnętrznymi oraz utratą wody (22). Aby zapobiec uszkodzeniom DNA w wyniku alkilacji, utleniania, delecji zasad czy pękania nici, które mogą wystąpić w wyniku odwodnienia, A. baumannii wykorzystuje białko RecA28, które pełni funkcję enzymu niezbędnego do homologicznej rekombinacji i naprawy DNA (23, 24). Dodatkowo, ze względu na nasilony stres oksydacyjny podczas wysuszania, A. baumannii istotnie zwiększa ekspresję katalazy, co jest skutkiem obecności w genomie sekwencji insercyjnej ISAba1. Dzięki temu mechanizmowi możliwa jest skuteczna neutralizacja reaktywnych form tlenu (ROS) (25). W ostatnim czasie odnotowano pojawienie się szczepów A. baumannii wytwarzających karbapenemazy: MBL typu IMP, kodowaną przez bla_{IMP} oraz oksacylinazy - β-laktamazy serynowej klasy D, kodowanej przez bla_{OXA}. Szczepy wielolekooporne A. baumannii charakteryzują się produkcją: (i) β-laktamaz (AmpC, karbapenemazy Oxa-23 czy MBL typu IMP), (ii) białek błony zewnętrznej (OmpA, CarO, OmpW, NlpE), (iii) enzymów modyfikujących leki (tj. acetylotransferazy aminoglikozydowe, transferazy adenylowe, fosfotransferazy), (iv) transporterów leków (białko HlyD; pompy efflux AcrB-AdelJK) oraz (v) poryny DcaP pełniącej istotną rolę podczas tworzenia biofilmu (26-28).

P. aeruginosa to Gram-ujemna pałeczka tlenowa, która jest częstym czynnikiem etiologicznym zapalenia płuc u pacjentów z mukowiscydozą i zakażeń ran oparzeniowych. Posiada słabo przepuszczalną błonę zewnętrzną dla wielu klas związków, gdzie współczynnik przepuszczalności jest od 10 do 500 razy niższy niż w przypadku Escherichia coli, wykazuje zdolność produkcji cefalosporynaz, a także posiada liczne systemy transportu, które zapewniają wrodzoną oporność na wiele antybiotyków (29, 30). Ponadto, modyfikacje i zmniejszona ekspresja białek porynowych OprD przyczyniają się do zmniejszonego wychwytu leku, co

skutkuje opornością na imipenem (31). Bakteria ta posiada również geny kodujące β-laktamazy typu AmpC, nadające oporność na leki β-laktamowe, takie jak cefuroksym i ceftriakson (32). Niski poziom produkcji AmpC nie skutkuje wysokim poziomem oporności na karbapenemy ze względu na ich niski potencjał hydrolizy karbapenemów, ale ich nadprodukcja wraz ze zmniejszoną przepuszczalnością poryn przez błonę zewnętrzną i/lub nadekspresją pompy wypływowej przyczyniają się do wysokiego poziomu oporności na karbapenemy (33, 34). *P. aeruginosa* posiada pompy efflux z rodziny RND, które aktywnie wydalają toksyczne związki z przestrzeni peryplazmatycznej i cytoplazmy, zwłaszcza pompy wypływowe MexAB-OprM i MexXY-OprM. Nadekspresja MexXY-OprM jest związana z opornością *P. aeruginosa* na aminoglikozydy, fluorochinolony i cefalosporyny. Co więcej, wiele klinicznych izolatów *P. aeruginosa* wykazuje ekspresję systemów wypływu MexCD-OprJ i MexEF-OprN (15). *P. aeruginosa* może również nabywać oporność poprzez mutacje punktowe w istniejących wcześniej genach (mutacje punktowe gyrazy DNA/topoizomerazy IV warunkujące oporność na fluorochinolony) lub horyzontalny transfer determinantów oporności (35).

Enterobacter spp. to grupa Gram-ujemnych pałeczek fakultatywnie beztlenowych, wywołujących sepsę, infekcje dróg moczowych, zakażenia miejsca operowanego czy infekcje dróg oddechowych. *E. cloacae*, *E. aerogenes* (obecnie *Klebsiella aerogenes*) i *E. hormaechei* są to gatunki najczęściej izolowane w zakażeniach klinicznych, szczególnie u pacjentów z obniżoną odpornością oraz pacjentów hospitalizowanych na oddziałach intensywnej terapii (36). Szczepy *Enterobacter* są naturalnie oporne na penicyliny oraz cefalosporyny pierwszej i drugiej generacji ze względu na niski poziom ekspresji chromosomalnych genów *ampC* kodujących indukcyjną cefalosporynazę typu AmpC (37). W przypadku długotrwałej ekspozycji na działanie leków β-laktamowych może dojść do powstania indukcyjnych fenotypów cefalosporynazy AmpC, warunkujących oporność na cefalosporyny trzeciej generacji (38). Możliwość nabycia plazmidów, w których pośredniczą geny kodujące ESBL, nadaje *Enterobacter* oporność na większość antybiotyków β-laktamowych. Dodatkowo, bakterie mogą nabywać oporność na kolistynę, poprzez plazmidowy gen *mcr*, gen *ecr* lub dwuskładnikowe systemy phoPQ, pmrAB, które prowadzą do modyfikacji lipidu A (39, 40).

W związku z powyższymi rozważaniami, istotne staje się opracowanie nowych strategii terapeutycznych przeciwko omawianym patogenom. Bakterie z grupy ESKAPE, wykazujące oporność na wiele antybiotyków, są czynnikami etiologicznymi infekcji mogących skutkować śmiercią, przede wszystkim wśród pacjentów o obniżonej odporności.

5.2 Zakażenia grzybicze o etiologii *Candida*

W ostatnich latach zaobserwowano istotny wzrost częstości występowania infekcji grzybiczych wywołanych przez grzyby z rodzaju *Candida* (41). Szacuje się, że śmiertelność związana z kandydemią wynosi od 10% do 47%, przy czym ryzyko zgonu jest ściśle powiązane z wiekiem pacjenta, gatunkiem *Candida* odpowiedzialnym za zakażenie, stosowaniem leków immunosupresyjnych, obecnością cewnika naczyniowego, a także istniejącą wcześniej dysfunkcją nerek i innymi chorobami współistniejącymi (42-46).

Głównym czynnikiem etiologicznym ogólnoustrojowych zakażeń grzybiczych, potencjalnie zagrażającym życiu są grzyby zaliczane do *Candida* spp. (47). Chociaż *Candida albicans* jest najczęstszym gatunkiem izolowanym od pacjentów z kandydozą, w ostatnim czasie wzrosła rola innych gatunków, takich jak *C. glabrata* (obecnie *Nakaseomyces glabrata*), *C. tropicalis*, *C. parapsilosis* i *C. krusei* (obecnie *Pichia kudriavzeveii*) (48-51). Wszystkie pięć gatunków *Candida* izoluje się w ponad 90% inwazyjnych zakażeń grzybiczych (52, 53). Warto podkreślić, że na całym świecie odnotowuje się prawie 10 milionów przypadków kandydozy błon śluzowych, a ponad 150 milionów ludzi jest dotkniętych poważnymi chorobami grzybiczymi (54).

Mimo utrzymującego się istotnego zagrożenia związanego z kandydozą, dostępność skutecznych leków przeciwgrzybiczych w terapii pozostaje nadal ograniczona (55, 56). Ponadto, rosnąca oporność grzybów na dostępne leki przeciwgrzybicze stanowi poważne wyzwanie dla sektora opieki zdrowotnej (54). Z wielkim niepokojem obserwuje się systematyczny wzrost liczby grzybów lekoopornych, w tym szczepów MDR (57, 58). Powagę problemu podkreśla raport opublikowany przez Centrum Kontroli i Prewencji Chorób (CDC), który ostrzega przed lekoopornymi szczepami *Candida*, określając je jako poważne zagrożenie, wymagające natychmiastowego opracowania nowych metod leczenia (59).

Lekooporność grzybów negatywnie wpływa na wyniki leczenia pacjentów z inwazyjną kandydozą. Najistotniejsze mechanizmy oporności na leki przeciwgrzybicze obejmują (i) zmniejszenie wewnątrzkomórkowej akumulacji leku poprzez aktywację związanych z błoną pomp wypływowych, (ii) zmniejszenie powinowactwa leków do docelowego miejsca działania, a także (iii) zmiany w strukturze i składzie błony komórkowej, które mogą wpływać na przepuszczalność dla leków (60-63).

Chociaż nastąpił postęp w profilaktyce, diagnostyce i terapii, inwazyjne zakażenia *Candida* wywołane przez oporne szczepy w dalszym ciągu przyczyniają się do znacznej

śmiertelności, szczególnie u pacjentów z obniżoną odpornością, co podkreśla pilną potrzebę opracowania nowych leków przeciwgrzybiczych (54, 64).

5.3 Mechanizmy oporności drobnoustrojów

Wiek dwudziesty to „złota era" rozwoju antybiotyków. Odkryto wówczas wiele nowych środków przeciwdrobnoustrojowych i wprowadzono je do medycyny praktycznej. Jednak rozwój leków przeciwbakteryjnych i przeciwgrzybiczych uległ znacznej stagnacji. Najnowszą klasę antybiotyków, jaką są lipopeptydy, opisano w latach osiemdziesiątych XX wieku, natomiast echinokandyny stanowią najmłodsza grupę środków przeciwgrzybiczych, wprowadzono do praktyki lekarskiej na początku obecnego stulecia (65, 66).

Chemiczna modyfikacja i rozkład leku stanowią jedną z wielu strategii, które mogą być wykorzystywane przez mikroorganizmy w celu rozwoju oporności. Mechanizmy te pozwalają drobnoustrojom unikać lub zneutralizować działanie leku, co prowadzi do utraty jego skuteczności. Mikroorganizmy, a zwłaszcza bakterie mogą wytwarzać enzymy zdolne do bezpośredniego rozkładu lub modyfikacji struktury chemicznej leku. Bakteryjne β-laktamazy są jednymi z szeroko badanych enzymów pod kątem oporności na antybiotyki i charakteryzują się zdolnością do rozszczepiania wiązania amidowego pierścienia β-laktamowego obecnego w penicylinach, cefalosporynach, monobaktamach i karbapenemach (67). Penicylinazy, cefalosporynazy, ESBL, metalo-β-laktamazy czy karbapenemazy to główne typy laktamaz odpowiedzialnych za degradację leku (68). Również niektóre enzymy bakteryjne mają zdolność chemicznej modyfikacji antybiotyków poprzez acetylację, fosforylację czy adenylację, zapobiegając wiązaniu się antybiotyku z miejscem docelowym w komórce bakteryjnej. Modyfikacje te obejmują acetylację zależną od acetylo-CoA, a także dwa odrębne procesy zależne od ATP: fosforylację i adenylację. Geny kodujące różne izoformy enzymów odpowiedzialnych za powyższe modyfikacje są obecne na mobilnych elementach genetycznych, co sprawia, że istnieje różnorodność w regiospecyficzności chemicznych modyfikacji antybiotyków (69). Acetylacja jest najczęściej stosowanym mechanizmem modyfikacji przez bakterie takich antybiotyków jak aminoglikozydy, chloramfenikole, streptograminy czy fluorochinolony. Enzymy modyfikujące aminoglikozydy uczestniczą w kowalencyjnej zmianie grup hydroksylowych, bądź aminowych cząsteczki aminoglikozydu, prowadząc do utraty aktywności antybiotyku (70, 71). Główne kategorie enzymów modyfikujących antybiotyki obejmują enzymy modyfikujące aminoglikozydy, fosfomycyny czy rifamycyny, acetylotransferazy chloramfenikolu, fosfotransferazy makrolidowe oraz

monooksygenazy zależne od flawiny (69). Możliwe, że mechanizm rozkładu leku przez enzymy komórkowe występuje również u grzybów. Ostatnie badania dowiodły, iż indukowany układ enzymatyczny dermatofitów doprowadził do degradacji leku do mało aktywnych lub nieaktywnych pochodnych (72).

Pompy wypływowe odpowiadają za usuwanie antybiotyków z komórki drobnoustroju, a u szczepów MDR obserwuje się nadekspresję różnego rodzaju tych białek (73). Geny kodujące pompy wypływowe mogą być obecne albo w genomie bakterii, albo w mobilnych elementach genetycznych, takich jak plazmidy. Do tej pory opisano sześć rodzin bakteryjnych pomp wypływowych, a mianowicie: nadrodzinę ABC (ATP-binding cassette), rodzinę MATE (multidrug and toxin extrusion), nadrodzinę MFS (major facilitator superfamily), nadrodzinę RND (resistance-nodulation-cell division), rodzinę SMR (small multidrug resistance) oraz rodzinę PACE (proteobacterial antimicrobial compound efflux) (74). Natomiast ostatnie badania wskazują, że grzyby posiadają co najmniej dwa systemy usuwania leku za pomocą pompy wypływowej. Należą do niej białka nadrodziny MFS i ABC (75).

Drobnoustroje chronią się przed działaniem antybiotyków poprzez modyfikację miejsca docelowego działania leku. Te modyfikacje obejmują mutacje w genie kodującym białko docelowe, chemiczną zmianę miejsca interakcji bądź zastąpienie/ominięcie docelowego miejsca działania (71). Wiele antybiotyków wywiera swoje działanie przeciwbakteryjne po połączeniu z podjednostkami rybosomów (50S i 30S). Antybiotyki aminoglikozydowe oddziałują z 16S rRNA podjednostki 30S i utrudniają interakcję aminoacylo-tRNA z antykodonem, co ostatecznie prowadzi do zahamowania translacji. Jednak w wyniku metylacji N7 guaniny (1405) lub N1 adeniny (1408) 16S rRNA przez metylotransferazy, dochodzi do uzyskania oporności na większość aminoglikozydów (76). W przypadku makrolidów, linkozamidów czy streptogramin ich celem działania są białka rybosomalne podjednostki 50S oraz niektóre rRNA (5S i 23S rRNA) (77). Podobnie, bakteryjne cele antybiotyków są modyfikowane przez transferazy fosfoetanoloaminy i enzymy modyfikujące peptydoglikan. Przykładem modyfikacji docelowego miejsca działania u grzybów są mutacje punktowe w genie *ERG11*, który koduje enzym 14α-demetylazę lanosterolu. Mutacje w *ERG11* powodują zmiany w strukturze przestrzennej kodowanego białka i zmniejszają powinowactwo pomiędzy białkiem i azolem (78).

Zapobieganie napływowi antybiotyków jest wynikiem tworzenia barier lub modyfikacji struktur powierzchownych komórek mikroorganizmów, które uniemożliwiają antybiotykom penetrację do ich wnętrza. Zewnętrzna błona bakterii Gram-ujemnych zawiera białka zwane

porynami, które biorą udział w tworzeniu kanałów umożliwiających przemieszczanie się antybiotyków do wnętrza komórki. *A. baumannii*, który wykazywał wyraźną utratę białka błony zewnętrznej (OMP) był niewrażliwy na działanie imipenemu (79). Z kolei białko OprD jest obecne w błonie zewnętrznej *P. aeruginosa*, natomiast obniżenie poziomu OprD umożliwiło bakteriom nabycie oporności na imipenem (33). W przypadku grzybów zmiany w składzie steroli i/lub fosfolipidów błony komórkowej grzybów mogą wpływać na penetrację leku przeciwgrzybiczego do wnętrza komórki. Ostatnie badania dowiodły, iż zmienione profile fosfolipidów i kwasów tłuszczowych wpływają na przepuszczalność komórek *C. albicans* czyniąc je bardziej opornymi na mikonazol (80). W innym badaniu wykazano, że mutant *C. albicans* oporny na azole i polieny miał większą zawartość lipidów i niższy stosunek lipidów polarnych do lipidów obojętnych niż szczepy wrażliwe na azole (81).

Zdolność tworzenia biofilmu jest jednym z kluczowych mechanizmów, które mikroorganizmy wykorzystują w celu rozwijania oporności na antybiotyki, co stanowi poważne wyzwanie dla skutecznej terapii antybiotykowej. Biofilm to zorganizowana, złożona i wielokomórkowa struktura, w skład której wchodzą polisacharydy, kwasy nukleinowe, białka i lipidy (82). Macierz biofilmu stanowi fizyczną barierę, która nie tylko zabezpiecza przed mechanicznym usunięciem, ale także działaniem środków przeciwdrobnoustrojowych oraz umożliwia unikanie odpowiedzi immunologicznej gospodarza. Bakterie w formie biofilmu wykorzystują szereg strategii, aby uniknąć wykrycia przez układ odpornościowy gospodarza. Obniżają one swoją aktywność metaboliczną, dzięki czemu są mniej podatne na działanie komórek odpornościowych, których celem są aktywnie rosnące mikroorganizmy (83). Ponadto, aby uniknąć wykrycia przez układ odpornościowy gospodarza, biofilm może podlegać zmianom antygenowym i uwalniać substancje chemiczne, które tłumią sygnalizację i aktywność immunologiczną (84).

Polimerowe składniki macierzy zewnątrzkomórkowej (EPS) jako bariera ograniczająca dyfuzję substancji przeciwdrobnoustrojowych, uniemożliwia ich penetrację do głębszych warstw biofilmu (85). Ograniczone przenikanie antybiotyków przez matrycę biofilmu wynika między innymi z reakcji środków przeciwdrobnoustrojowych z EPS (86), umożliwiając inaktywację lub degradację tych środków przez enzymy obecne w matrycy biofilmu (87). Ograniczona penetracja antybiotyków przez biofilm prowadzi do konieczności stosowania wysokich dawek leków lub wydłużenia antybiotykoterapii, co z kolei zwiększa ryzyko toksyczności w stosunku do komórek gospodarza oraz rozwój oporności na antybiotyki. Dodatkowo, biofilm może stanowić źródło wtórnych infekcji, gdyż nawet po zakończeniu

antybiotykoterapii, bakterie wewnątrz struktury biofilmu mogą przetrwać, pozostając potencjalnym źródłem ponownej infekcji (88). Podsumowanie mechanizmów oporności drobnoustrojów przedstawiono na **Rycinie 1**.
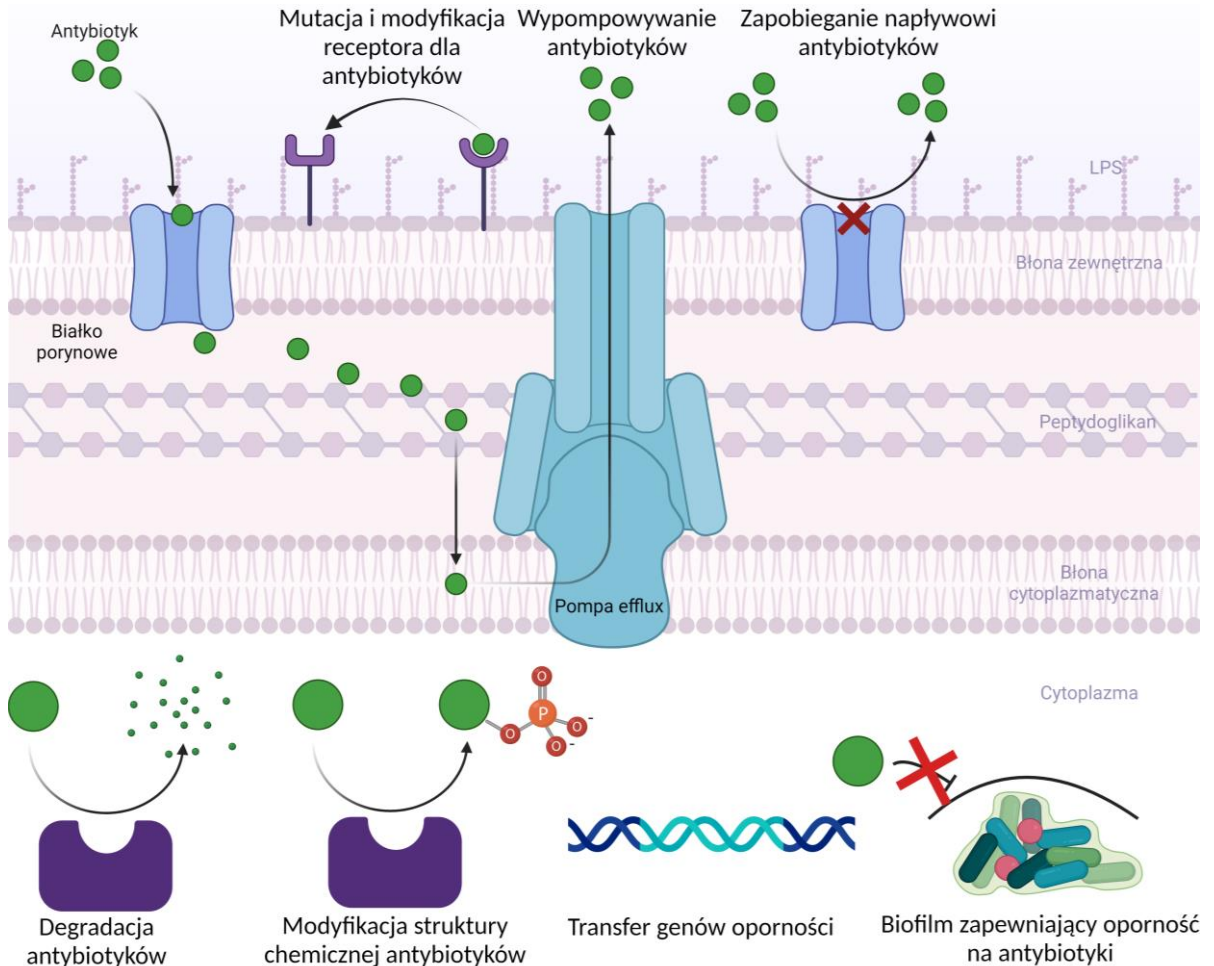
Rycina 1. Zasadnicze mechanizmy oporności drobnoustrojów na antybiotyki.

5.4 Serageniny - kationowe lipidy przeciwdrobnoustrojowe

Alternatywą dla współcześnie stosowanych antybiotyków mogą być serageniny (CSAs), będące lipidowymi analogami naturalnych peptydów przeciwdrobnoustrojowych (89). Struktura seragenin opiera się na kwasie cholowym, będącym naturalnym steroidowym związkiem chemicznym, który nadaje serageninom charakterystyczne właściwości. CSAs wykazują ampifatyczny charakter – zawierają zarówno regiony hydrofilowe umożliwiające interakcje z wodą oraz innymi substancjami polarnymi, podczas gdy regiony hydrofobowe zapewniają interakcje z hydrofobowymi elementami błon lipidowych, dzięki temu serageniny mogą łatwo wbudowywać się w błonę lipidową. Serageniny, w przeciwieństwie do kwasu cholowego, posiadają grupy funkcyjne z dodatnim ładunkiem. Kationowy charakter CSAs

19

umożliwia ich oddziaływanie z ujemnie naładowanymi cząsteczkami na powierzchni komórek mikroorganizmów (90, 91).

Główny mechanizm działania przeciwdrobnoustrojowego CSAs obejmuje bezpośrednią interakcję elektrostatyczną z ujemnie naładowanymi błonami komórkowymi drobnoustroju, co po wbudowaniu CSAs w strukturę błony prowadzi do zmian w organizacji fosfolipidów błony oraz jej depolaryzacji. Mechanizm działania ceragenin obejmuje również stymulację wytwarzania wolnych rodników co prowadzi do stresu oksydacyjnego. Tym samym, skutkiem oddziaływania ceragenin z komórkami bakterii jest (i) utrata integralności błony komórkowej, zwiększenie jej przepuszczalności i utrata składników wewnątrzkomórkowych, a także (ii) uszkodzenie materiału genetycznego komórki oraz zaburzenia w procesie replikacji i naprawy DNA.

Uważa się, że CSAs stanowią alternatywę dla antybiotyków ze względu na szerokie spektrum działania obejmujące bakterie Gram-dodatnie i Gram-ujemne, grzyby, a także szczepy wielolekooporne (89, 90, 92). Ceragateniny wykazują także działanie przeciwbiofilmowe, sporobójcze, przeciwwirusowe, przeciwpasożytnicze i przeciwnowotworowe (93-98). Co więcej, ceragateniny, w porównaniu z klasycznymi antybiotykami, charakteryzują się mniejszą tendencją do indukcji lekooporności (90). Do chwili obecnej, nie opisano szczepów bakteryjnych lub grzybiczych wykazujących oporność na ceragateniny (99, 100). Potencjał terapeutyczny CSAs podkreśla także ich niska toksyczność, stabilność w warunkach fizjologicznych i niskie koszty produkcji (99). Dodatkowo, ceragateniny posiadają szereg korzystnych cech farmakokinetycznych i farmakodynamicznych, takich jak (i) amfipatyczny charakter chemiczny, (ii) niespecyficzny, błonowy mechanizm działania, (iii) niewrażliwość na proteazy, a także (iv) wysoką aktywność przeciwdrobnoustrojową w płynach ustrojowych (101-104).

5.5 Nanocząstki złota sfunkcjonalizowane ceragateninami

W obliczu ciągłego wzrostu oporności na antybiotyki wśród drobnoustrojów, zastosowanie nanocząstek (NPs) metali stanowi innowacyjne podejście w rozwoju nowych metod terapii zakażeń (105). Nanocząstki metaliczne, w tym złota (Au NPs), zyskują coraz większe zainteresowanie ze względu na unikalne właściwości fizykochemiczne, takie jak (i) korzystny stosunek powierzchni do objętości, (ii) możliwość funkcjonalizacji czynnikami diagnostyczno-terapeutycznymi, (iii) łatwość modyfikacji sposobu syntezy oraz

(iv) właściwości przeciwbakteryjne i immunomodulujące (106-108). Rodzaje nanocząstek przedstawiono na **Rycinie 2**.
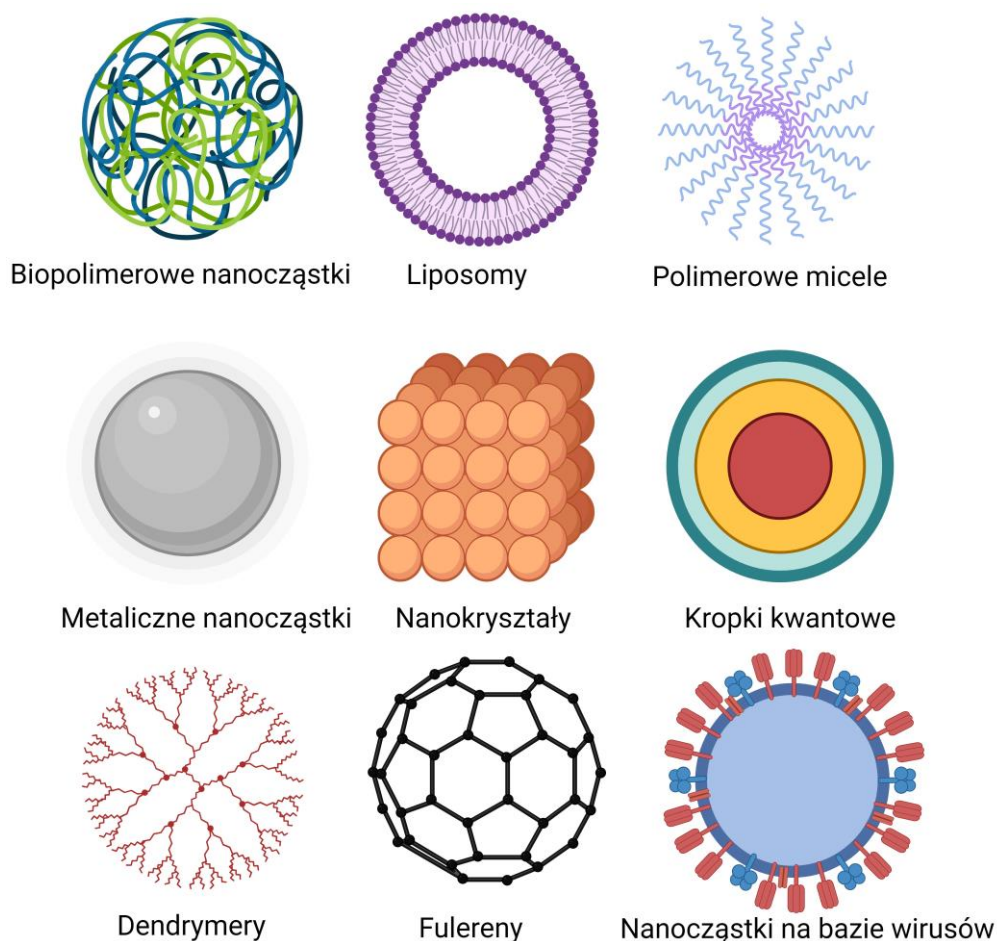
Rycina 2. Główne rodzaje nanocząstek będących przedmiotem badań w nanomedycynie.

Funkcjonalizacja nanocząstek substancjami przeciwdrobnoustrojowymi jest jedną ze strategii stosowanych w celu zwiększenia skuteczności leków przeciwko patogenom (109). W wyniku zwiększonej penetracji przez błony biologiczne, która jest ograniczona przez wysoce polarne środowisko błon drobnoustrojów, ich aktywność jest zachowana (110). Nanocząstki metali oddziałują z błoną komórkową bakterii poprzez oddziaływania elektrostatyczne, hydrofobowe, receptor-ligand lub siły van Der Waalsa, prowadząc do zmiany potencjału błony komórkowej i integralności komórek drobnoustrojów (111, 112). Ze względu na możliwość przyłączenia do powierzchni nanocząstek środka przeciwdrobnoustrojowego w wysokim stężeniu, zwiększoną penetrację przez błonę biologiczną oraz większe wchłanianie przez komórkę bakteryjną, efektywne dostarczane stężenie środka przeciwdrobnoustrojowego jest zwiększone (113, 114). Ważnym aspektem dostarczania leków przeciwdrobnoustrojowych w oparciu o NPs jest poprawa stabilności antybiotyków. Nanocząstki metali jako nośniki mogą

chronić leki przed degradacją i podtrzymywać uwalnianie leku, co skutkuje zwiększoną biodostępnością (115). W niektórych przypadkach funkcjonalizacja powierzchni metalicznych nanocząstek antybiotykami, na które pierwotnie drobnoustroje są oporne, sprawia, że stają się one podatne na działanie tych antybiotyków. Oporny na karbapenemy *A. baumannii* jest wrażliwy na sfunkcjonalizowane imipenemem nanocząstki srebra (116), natomiast szczep *C. albicans* oporny na flukonazol jest wrażliwy na nanocząstki złota sfunkcjonalizowane tym lekiem (117). Potencjał terapeutyczny nanocząsteczek podkreśla także fakt, iż leki zimmobilizowane na powierzchni nanocząstek metalicznych często charakteryzują się lepszymi parametrami farmakokinetycznymi w stosunku do natywnych wolnych antybiotyków, głównie w zakresie rozpuszczalności, wydłużenia okresu półtrwania, bądź przedłużenia czasu, w którym lek obecny jest w płynach ustrojowych (107).

W porównaniu z innymi nanocząstkami, nanocząstki metali szlachetnych takich jak miedź, platyna, srebro czy złoto, coraz częściej przyciągają uwagę badaczy (118). Spośród nich, nanocząstki złota są najbardziej stabilne i wykazują silne właściwości przeciwdrobnoustrojowe (119-121). W szczególności Au NPs mają szanse na szerokie zastosowane w medycynie ze względu na ich zadowalającą biokompatybilność, która wynika z wysokiej stabilności chemicznej i fizycznej, odporności na utlenianie, unikalne właściwości optyczne oraz łatwość przyłączania cząsteczek białek do powierzchni (122, 123). Au NPs mogą bezpośrednio oddziaływać z przeciwciałami, enzymami, kwasami nukleinowymi czy barwnikami fluorescencyjnymi (124). Nanocząstki złota wykazują odmienne właściwości w porównaniu do złota w skali makro i w zależności od metody syntezy można nadawać im różny kształt (125).

Ponieważ aktywność biologiczna nanocząstek złota zależy od właściwości fizykochemicznych, takich jak ich wielkości, kształtu i ładunku powierzchniowego (126, 127), zasadnym wydaje się stwierdzenie, iż cechy te będą bezpośrednio wpływać na ich efektywność jako nośniki leków. Jak wykazano na przykładzie nanocząstek tlenku cynku, zmniejszenie rozmiaru istotnie nasila aktywność przeciwdrobnoustrojową, co uwarunkowane jest korzystniejszym stosunkiem powierzchni do objętości, co umożliwia większą internalizację do wnętrza komórki drobnoustroju, co z kolei pozwala na zwiększenie efektów wewnątrzkomórkowych NPs (128). W aspekcie funkcjonalizacji powierzchni nanocząstek czynnikami o aktywności przeciwdrobnoustrojowej, stosunek powierzchni do objętości decyduje również o liczbie cząsteczek, które mogą być związane na ich powierzchni i tym samym, ich zdolności do interakcji z błoną komórkową drobnoustrojów czy macierzą biofilmu (129). Warto jednak podkreślić, iż nanocząstki metaliczne o mniejszym rozmiarze mogą

wykazywać silniejszy efekt toksyczny w stosunku do komórek gospodarza (130). Tym samym, celem zaprojektowania nośnika leku o odpowiednim stosunku efektywności do bezpieczeństwa wymaga kompleksowej analizy.

Mechanizm działania nanocząstek na bazie metali obejmuje między innymi zaburzenie struktury błony komórkowej, prowadzące do zwiększenia przepuszczalności w wyniku oddziaływania elektrostatycznego między ujemnie naładowanymi elementami błony komórkowej mikroorganizmu a dodatnio naładowanymi nanocząstkami (131, 132), co prowadzi do zaburzeń potencjału błonowego i zwiększonego wytwarzania ROS (133). Stres oksydacyjny prowadzi do utleniania glutationu, zaburzając antyoksydacyjne mechanizmy obronne komórek drobnoustrojów. W wyniku tych zaburzeń dochodzi do nadmiernej produkcji ROS, które oddziałują z lipidami błonowymi i powodują uszkodzenie DNA, białek i hamowanie aktywności enzymatycznej (131, 134-138). W wyniku addytywnego działania powyższych czynników ostatecznie dochodzi do apoptozy komórki drobnoustroju (139). Mechanizm działania Au NPs prowadzący do śmierci komórki bakteryjnej schematycznie przedstawiony jest na **Rycinie 3**.
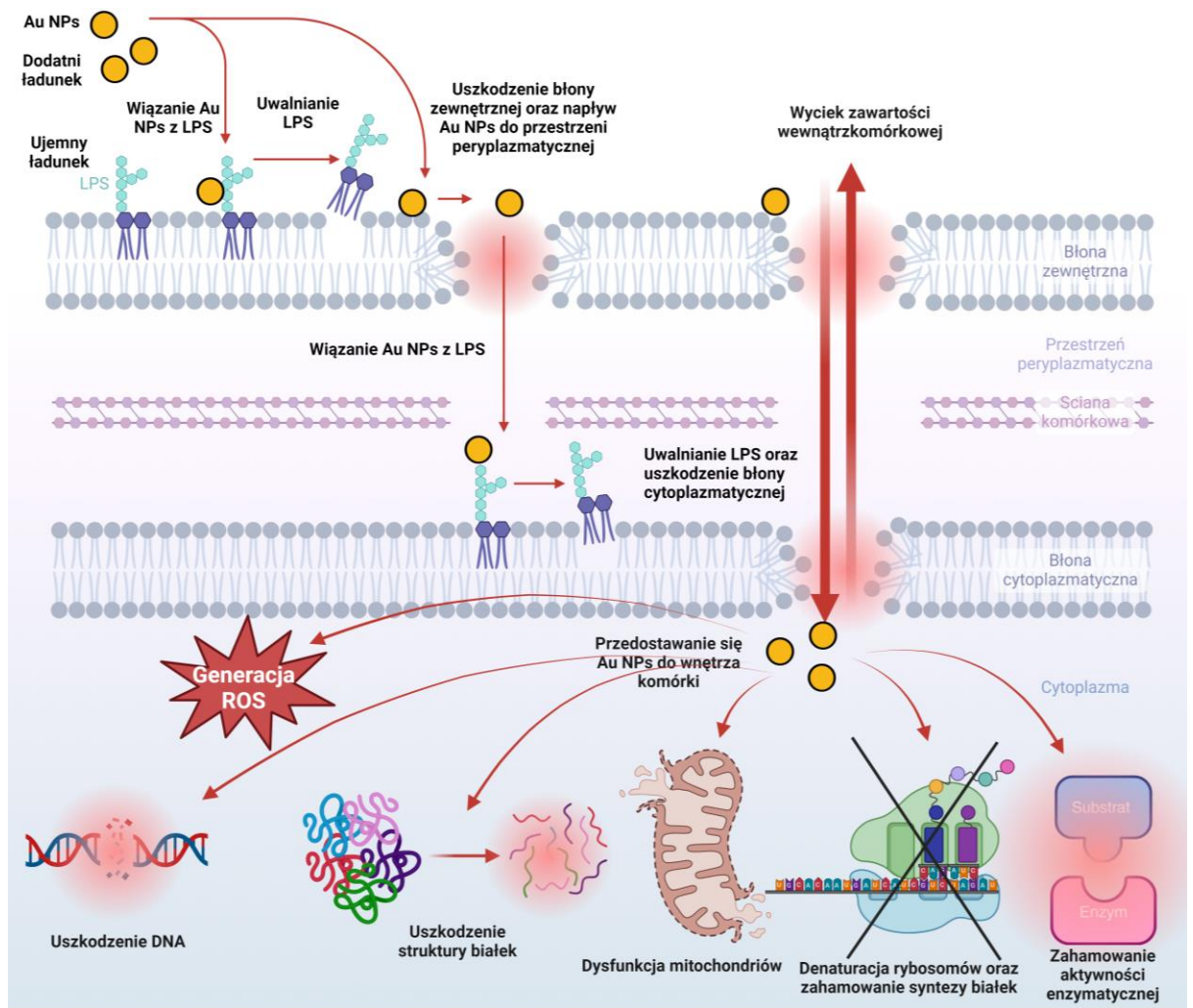
Rycina 3. Mechanizm działania nanocząstek złota.

5. Cel pracy

Narastająca oporność bakterii i grzybów na antybiotyki stanowi globalne wyzwanie współczesnej medycyny. Nanotechnologia jest postrzegana jako obiecujące narzędzie w walce z narastającą opornością obserwowaną wśród drobnoustrojów identyfikowanych jako czynniki etiologiczne zakażeń. W związku z tym, celem tej pracy było:

1. Określenie aktywności przeciwbakteryjnej i przeciwgrzybiczej nanocząstek złota sfunkcjonalizowanych cerageninami wobec bakterii z grupy ESKAPE oraz grzybów drożdżopodobnych.

2. Ocena wpływu kształtu oraz wielkości nanocząstek złota sfunkcjonalizowanych ceragoninami na aktywność przeciwbakteryjną oraz przeciwgrzybiczą.

3. Określenie przeciwgrzybiczego mechanizmu działania badanych nanosystemów.

4. Ocena indukcji oporności na nanocząstki złota sfunkcjonalizowane ceragoninami u wybranych szczepów *Candida*.

5. Określenie aktywności badanych nanosystemów w stosunku do zewnątrzkomórkowych oraz wewnątrzkomórkowych patogenów z grupy ESKAPE.

6. Ocena toksyczności badanych nanocząstek złota sfunkcjonalizowanych ceragoninami w stosunku do komórek gospodarza.

6. Materiały i metody

Szczegółowe informacje dotyczące materiałów i metod zostały zaprezentowane w pracy oryginalnej wchodzącej w skład rozprawy doktorskiej (publikacja nr 2):

Karol Skłodowski, Sylwia Joanna Chmielewska, Joanna Depciuch, Piotr Deptuła, Ewelina Piktel, Tamara Daniluk, Magdalena Zakrzewska, Michał Czarnowski, Mateusz Cieśluk, Bonita Durnaś, Magdalena Parlińska-Wojtan, Paul B. Savage, Robert Bucki.

Ceragenin-Coated Non-Spherical Gold Nanoparticles as Novel Candidacidal Agents. Pharmaceutics, 2021, 13, 1940.

Materiały, metody oraz wyniki dotyczące aktywności badanych ceragenin i nanosystemów wobec bakterii z grupy ESKAPE zostały opisane w rozdziale 6 i 7.

6.1 Szczepy bakteryjne, grzyby, podłoża hodowlane oraz warunki wzrostu

Szczep wzorcowy *E. faecium* ATCC 700221 (VRE) zakupiono z American Type Culture Collection (ATCC, VA, USA), natomiast pozostałe szczepy kliniczne bakterii z grupy ESKAPE uzyskano z kolekcji izolatów klinicznych Zakładu Mikrobiologii Lekarskiej i Inżynierii Nanobiomedycznej, Uniwersytetu Medycznego w Białymstoku. Szczep kliniczny *A. baumannii* wykazywał oporność na karbapenemy, aminoglikozydy i fluorochinolony, natomiast szczep kliniczny *K. pneumoniae* był oporny na antybiotyki β-laktamowe (produkcja NDM-1 oraz ESBL), aminoglikozydy i fluorochinolony. Szczepy bakteryjne przechowywano w temperaturze -80°C, a następnie hodowano w przypadku *K. pneumoniae* oraz *A. baumannii* na podłożu MacConkeya (Biomaxima, Lublin, Polska), a *E. faecium* na Columbia agar z 5% krwią baranią (Biomaxima) w temperaturze 37°C.

Dodatkowo, wykorzystano dwa szczepy referencyjne grzybów: *C. albicans* ATCC 26790 i *C. albicans* 1408 oraz 19 klinicznych izolatów grzybów pobranych od pacjentów hematoonkologicznych Świętokrzyskiego Centrum Onkologii w Kielcach. Identyfikacja i wrażliwość przeciwgrzybicza szczepów *Candida* została określona przy użyciu systemu VITEK® 2 (bioMérieux, Marcy-l'Etoile, Francja). Zamrożone szczepy przechowywano w temperaturze -80°C, a następnie hodowano na agarze Sabouraud z dodatkiem dekstrozy i chloramfenikolu (Biomaxima) w temperaturze 37°C.

6.2 Hodowla komórkowa

Ludzkie komórki gruczolakoraka płuc A549 (#CCL-185, ATCC), hodowano w temperaturze 37°C w obecności 5% CO_2 w medium wzrostowym Dulbecco's Modified Eagle's Medium (DMEM, ATCC) z dodatkiem 10% płodowej surowicy bydlęcej (FBS, PAN Biotech, Aidenbach, Niemcy) oraz 1% roztworem antybiotyków zawierającym penicylinę, streptomycynę i amfoterycynę B (Sigma-Aldrich, MO, USA). Wszystkie eksperymenty oparte na hodowli komórkowej, z wyjątkiem testów MTT, przeprowadzono w medium wolnym od FBS.

6.3 Związki przeciwdrobnoustrojowe

6.3.1 Cerageniny oraz antybiotyki

Cerageniny: CSA-13, CSA-44 i CSA-131 w ramach współpracy naukowej zostały udostępnione przez Pana Profesora Paula B. Savage'a z Wydziału Chemii i Biochemii Uniwersytetu Brighama Younga (Provo, Utah, USA). CSAs rozpuszczano w soli fizjologicznej buforowanej fosforanami (PBS) i przechowywano w temperaturze 4°C. Imipenem zakupiono z Sigma-Aldrich, natomiast wankomycynę z Pol-Aura (Morąg, Polska).

6.3.2 Nanocząstki złota sfunkcjonalizowane CSA-13, CSA-44 oraz CSA-131

Nanocząstki złota w kształcie patyczków (AuR NPs), fistaszków (AuP NPs) i gwiazdek (AuS NPs) zsyntezowane metodą „seed-mediated" zostały udostępnione w ramach współpracy naukowej przez Panią Profesor dr hab. inż. Magdalenę Parlińską-Wojtan oraz dr hab. Joannę Depciuch z Zakładu Nanomateriałów Funkcjonalnych Instytutu Fizyki Jądrowej im. Henryka Niewodniczańskiego Polskiej Akademii Nauk w Krakowie. Podczas przygotowywania nanosystemów użyto MHDA w nadmiarze, aby mieć pewność, iż wszystkie cząsteczki ceragenin sfunkcjonalizują powierzchnię Au NPs.

6.4 Metody

6.4.1 Określenie właściwości fizykochemicznych badanych nanocząstek złota

Za pomocą skaningowej transmisyjnej mikroskopii elektronowej (STEM, FEI, OR, USA) określono morfologię i rozmiar otrzymanych nanocząstek złota. Rozkład wielkości cząstek uzyskano na podstawie obrazów STEM, zliczając średnią wielkość ze 100 nanocząstek

umieszczonych w różnych obszarach siatek TEM. Rozkład potencjału zeta określono za pomocą metody mikroelektroforetycznej. Każdą wartość obliczono jako średnia z trzech odrębnych serii zawierającą co najmniej 20 pomiarów. Do określenia efektywności funkcjonalizacji nanocząstek i immobilizacji ceragenin wykorzystano spektroskopię Ramana z transformacją Fouriera (FT-Raman, Thermo Fisher Scientific, MA, USA). W celu uzyskania informacji o potencjale zeta otrzymanych nanocząstek wykorzystano Zetasizer Nano Series (Worcestershire, UK).

6.4.2 Określenie wartości MIC/MBC/MFC

Do określenia wartości minimalnego stężenia hamującego (MIC) badanych środków przeciwdrobnoustrojowych wykorzystano inokulum bakterii lub grzybów o zawartości komórek około $2{\times}10^5$ CFU (jednostek tworzących kolonie/mL). Wykorzystano metodę mikrorozcieńczeń opisaną w wytycznych Europejskiego Komitetu ds. Oznaczania Lekowrażliwości (EUCAST). Końcowe stężenia badanych związków wahały się od 0,1 do 51,2 μg/mL. Wartości MIC zostały określone wizualnie i potwierdzone spektrofotometrycznie w pożywce Muellera-Hintona dla bakterii (Sigma-Aldrich) oraz w RPMI (Sigma-Aldrich) uzupełnionej MOPS (Sigma-Aldrich) i D-(+)-glukozą (Sigma-Aldrich) wobec grzybów, przy najniższym stężeniu badanych związków, gdzie nie zaobserwowano widocznego wzrostu drobnoustrojów po 24 godzinach inkubacji w temperaturze 37°C. Minimalne stężenie bakteriobójcze (MBC) określono poprzez posiew każdej próbki (10 μL) na Columbia agar z 5% krwią baranią (dla *E. faecium*) oraz na MacConkey agar (dla *K. pneumoniae* oraz *A. baumannii*), z kolei minimalne stężenie grzybobójcze (MFC) poprzez posiew na agarze Sabouraud z dekstrozą i chloramfenikolem. Następnie płytki agarowe hodowano od 24 do 48 godzin w temperaturze 37°C, a wzrost drobnoustrojów określono wizualnie.

6.4.3 Test zliczania kolonii (killing assay)

W celu określenia aktywności bakteriobójczej antybiotyków (wankomycyny oraz imipenemu) oraz nanosystemów złota zawierających cerageniny: AuR NPs@CSA-13, AuP NPs@CSA-13 oraz AuS NPs@CSA-13 wobec bakterii z grupy ESKAPE przeprowadzono test zaliczania kolonii. Poszczególne hodowle zawieszano w ilości około 10^8 CFU/mL i seryjnie rozcieńczono do 10^5 CFU/mL w sterylnym PBS. Do badań wykorzystano antybiotyki oraz nanosystemy w zakresie stężeń 1–100 μg/mL. Po 60 minutach inkubacji z wytrząsaniem w temperaturze 37°C płytki zawierające zawiesinę badanych drobnoustrojów przeniesiono na

podkłady chłodzące, a następnie próbki rozcieńczono seryjnie od 10 do 1000-krotnie. Następnie 10 µL próbki każdego rozcieńczenia wysiewano na agar MacConkeya (dla *K. pneumoniae* oraz *A. baumannii*), bądź Columbia agar wzbogaconego 5% krwią baranią (dla *E. faecium*) oraz inkubowano przez 24 godziny w temperaturze 37°C w celu ustalenia liczby kolonii. Jednostki tworzące kolonie poszczególnych próbek określono na podstawie współczynnika rozcieńczenia.

6.4.4 Ocena kinetyki wzrostu bakterii z użyciem resazuryny

W celu zbadania kinetyki zabijania komórek *E. faecium* ATCC 700221, *K. pneumoniae* oraz *A. baumannii* indukowanego przez wankomycynę, imipenem, AuR NPs@CSA-13, AuP NPs@CSA-13 oraz AuS NPs@CSA-13, bakterie zawieszone w bulionie Luria-Bertani (LB, Sigma-Aldrich), przenoszono do 96-dołkowych czarnych płytek (Sigma-Aldrich), a następnie poddawano działaniu testowanych związków w zakresie stężeń 1-10 µg/mL. Sól sodową resazuryny (Sigma-Aldrich) o końcowym stężeniu 200 µg/mL dodano do mieszaniny bakterii, a obserwowane zmiany w emisji światła fluorescencyjnego (wskazujące pośrednio na żywotność i zdolność do proliferacji traktowanych komórek drobnoustrojów) rejestrowano przez 60 minut przy użyciu czytnika mikropłytek Varioskan Lux (Thermo Fisher Scientific) przy długości fali wzbudzenia/emisji wynoszącej odpowiednio 520/590 nm.

6.4.5 Indukcja oporności *C. albicans* ATCC 26790 oraz *C. krusei* na NPs sfunkcjonalizowane cerageninami

Wartości MIC dla AuR NPs@CSA-13, AuR NPs@CSA-44 i AuR NPs@CSA-131 w stosunku do *C. albicans* ATCC 26790 oraz *C. krusei* określono wizualnie i potwierdzono spektrofotometrycznie. Po 24 godzinach inkubacji rozpoczęto pasażowanie, wykorzystując komórki grzybów rosnące w stężeniu sub-MIC (stężenie poniżej wartości MIC, które nie jest grzybobójcze dla komórek) i zaszczepiając je w świeżym podłożu RPMI. Po 18-24-godzinnym okresie inkubacji, komórki rosnące w najwyższym stężeniu środka przeciwdrobnoustrojowego z poprzedniego pasażu były ponownie pobierane i oznaczano wartość MIC. Proces ten powtarzano przez 25 pasaży.

6.4.6 Test adhezji i internalizacji

W celu oceny aktywności badanych związków w stosunku do patogenów zewnątrzkomórkowych, komórki A549 wysiewano w ilości 4×10^4 komórek/szkiełko,

a następnie hodowano w temperaturze 37°C z dodatkiem 5% CO_2 do utworzenia monowarstwy. Przed nałożeniem komórek szkiełka były oczyszczane i sterylizowane. Następnie medium usunięto, a szkiełka przepłukano trzykrotnie PBS. W następnym etapie na poszczególne szkiełka dodano imipenem lub AuP NPs@CSA-13 w medium komórkowym, w stężeniach 2 μg/mL oraz 5 μg/mL na 1 godzinę w temperaturze 37°C. Po trzykrotnym przepłukaniu PBS, na każde szkiełko (poza kontrolą negatywną) dodano kliniczny szczep *K. pneumoniae* w fazie logarytmicznego wzrostu, aby stosunek liczby bakterii do komórek wynosił w przybliżeniu 100:1 (4×10^6 komórek bakteryjnych) i inkubowano przez 2 godziny w temperaturze 37°C. Komórki przepłukano trzykrotnie PBS w celu eliminacji komórek, które nie uległy adhezji do komórek A549. Następnie preparaty utrwalono w 3,7% roztworze paraformaldehydu (PFA, Sigma-Aldrich) w PBS przez 15 minut w temperaturze pokojowej. Po permeabilizacji (0,1% Triton X-100, Sigma-Aldrich; 10 min; temperatura pokojowa) i blokowaniu niespecyficznych wiązań (0,1% surowicza albumina bydlęca (BSA; Sigma-Aldrich) w PBS; 30 min; temperatura pokojowa) komórki przemyto i wybarwiono falloidyną znakowaną czerwienią teksańską (Thermo Fisher Scientific) w celu uwidocznienia aktyny w rozcieńczeniu 1:40 przez 1 godzinę, w temperaturze pokojowej, chroniąc przed dostępem do światła. Po przepłukaniu PBS, za pomocą DAPI (4′,6-diamidino-2-fenyloindol) o stężeniu 1 μg/mL inkubując przez 20 minut w temperaturze pokojowej w ciemności, wybarwiano jądra komórkowe. Bezpośrednio przed dodaniem na szkiełka, komórki bakteryjne zostały wybarwione za pomocą izotiocyjanianu fluoresceiny (FITC, Sigma-Aldrich). W tym celu przygotowano roztwór FITC w dimetylosulfotlenku (DMSO, Sigma-Aldrich) o stężeniu 10 mg/mL, który zastosowano w rozcieńczeniu 1:100 i przeprowadzono inkubację w ciemności w temperaturze pokojowej z wytrząsaniem. Następnie bakterie przemyto trzykrotnie za pomocą 0,1 M buforu wodorowęglanu sodu (Chempur, Piekary Śląskie, Polska) poprzez ultrawirowanie (10 000 x g; 4°C; 5 min) w celu usunięcia niezwiązanego FITC. W celu utrwalenia i zabezpieczenia wybarwionych preparatów przed utratą intensywności fluorescencji zastosowano Anti-Fade Fluorescence Mounting Medium (Abcam, Cambridge, Wielka Brytania). Zdjęcia fluorescencyjne wykonano za pomocą mikroskopu konfokalnego Olympus FV1200 (Olympus, Tokio, Japonia).

W celu oceny aktywności badanych związków w stosunku do patogenów wewnątrzkomórkowych, komórki A549 wysiewano w ilości $2,5 \times 10^4$ komórek/dołek w 24-dołkowych płytkach przeznaczonych do hodowli komórkowej (Sarstedt, NC, USA) i hodowano w temperaturze 37°C z dodatkiem 5% CO_2 do utworzenia monowarstwy. Następnie medium

usuwano, a dołki przepłukiwano trzykrotnie PBS. W następnym etapie do dołków dodawano imipenem i AuP NPs@CSA-13 w zakresie stężeń 1-20 μg/mL na 1 godzinę w temperaturze 37°C. Po trzykrotnym przepłukaniu PBS, do każdej studzienki (poza kontrolą negatywną) dodawano kliniczny szczep *A. baumannii* w fazie logarytmicznego wzrostu, aby stosunek liczby bakterii do komórek wynosił w przybliżeniu 100:1 ($2,5 \times 10^6$ komórek bakteryjnych) i inkubowano przez 2 godziny w temperaturze 37°C. Komórki przepłukiwano trzykrotnie PBS, natomiast do każdego dołka dodawano 5 μg/mL gentamycyny (Sigma-Aldrich, antybiotyk niepenetrujący błony komórek A549) w celu wyeliminowania bakterii, które nie uległy internalizacji, a płytki pozostawiono na 2-godzinną inkubację. Po zakończonej inkubacji, komórki przemywano trzykrotnie PBS i poddawano lizie za pomocą 0,1% roztworu Tritonu X- 100 w PBS przez 10 minut w temperaturze 37°C. W celu określenia żywotności bakterii, które uległy internalizacji po traktowaniu badanymi związkami, uzyskane próbki rozcieńczano 10- do 1000-krotnie, a 10 μL próbki przenoszono na płytki MacConkeya i hodowano przez 24 godziny w temperaturze 37°C. CFU poszczególnych próbek określono na podstawie współczynnika rozcieńczenia.

6.4.7 Analiza odpowiedzi izolatów grzybów na nanosystemy złota w kształcie patyczków, fistaszków i gwiazdek sfunkcjonalizowanych cerageninami oraz ceragenin w postaci wolnej

Eksperymenty przedstawione w **Tabeli 1** przeprowadzono w zakresie stężeń badanych związków wynoszących 1-10 μg/mL, natomiast końcowe inokulum w PBS odpowiadało OD600 ~ 0,5. Pomiary intensywności fluorescencji przeprowadzono z użyciem 96-dołkowych czarnych płytek.

Tabela 1. Testy zastosowane do analizy odpowiedzi komórek *Candida* na badane związki.

Test	Wskaźnik reakcji	Warunki inkubacji	Odczyt wyników
Wytwarzanie ROS	dioctan 2′,7′-dichlorofluoresceiny (DFCH-DA)	Inkubacja 60 minut w temperaturze 37°C z 20 μM DCFH-DA w PBS	emisja fluorescencji przy długości fali 488/535 nm, mikroskopia fluorescencyjna

Permeabilizacja błony zewnętrznej	N-fenylo-1-naftyloamina (NPN)	Inkubacja 5 minut w temperaturze 37°C z 0,5 mM NPN	intensywność fluorescencji λex = 348 nm/λem = 408 nm
Depolaryzacja błony komórkowej	Jodek 3,3′-dipropylotiadikarbocyjaniny (diSC$_{(3)}$)	Inkubacja 60 minut w temperaturze pokojowej z 0,4 µM diSC$_{(3)}$, następnie inkubacja przez 5 minut z 100 mM KCl	emisja fluorescencji przy długości fali 622/670 nm
Wyciek białka z komórki	Coomassie Brilliant Blue G-250 (odczynnik Bradforda)	Inkubacja 60 minut w temperaturze 37°C, następnie 10 minut wirowania (5000 obr/min) i inkubacja supernatantu z odczynnikiem Bradforda (stosunek 1:1) przez 10 minut w ciemności	poziom absorbancji przy długości fali 595 nm

6.4.8 Ocena aktywności hemolitycznej oraz cytotoksyczności badanych związków

Test hemolizy wykonano na 5% ludzkich krwinkach czerwonych (RBC) zawieszonych w PBS w obecności wolnych CSA-13, CSA-44 i CSA-131, jak i nanocząstek złota w kształcie patyczków, fistaszków i gwiazdek sfunkcjonalizowanych CSA-13, CSA-44 i CSA-131. Krew pobrano od zdrowych ochotników. Związki w zakresie stężeń 1-50 µg/mL inkubowano z RBC przez 1, 6 i 12 godzin w temperaturze 37°C. Po inkubacji, płytki odwirowywano (2500 obr./min, 10 min), a następnie absorbancję nadsączu mierzono przy długości fali wynoszącej 595 nm za pomocą czytnika płytek Varioskan Lux. Supernatant z próbek poddanych działaniu 1% Tritonu X-100 wykorzystano jako kontrolę pozytywną (100% hemolizy), natomiast jako kontrolę negatywną - supernatant z zawiesiny RBC w PBS (0% hemolizy). Względna absorbancja w porównaniu do absorbancji poddanej działaniu 1% Tritonu X-100 została zdefiniowana jako procent hemolizy.

Za pomocą testu MTT z użyciem bromku 3-[4,5-dimetylotiazol-2-ylo]-2,5-difenylotetrazoliowym (Sigma-Aldrich) oceniono aktywność cytotoksyczną wankomycyny,

imipenemu oraz nanosystemów złota wobec ludzkich komórek gruczolakoraka płuc A549. 1×10^4 komórek A549/dołek inkubowano przez 1, 6 oraz 24 godziny w 96-dołkowej płytce. Następnie komórki przepłukano PBS i dodano badane związki w stężeniach 1, 2, 5, 10, 25 oraz 50 µg/mL. Po zakończonej inkubacji supernatant usuwano, płytki płukano trzykrotnie PBS, a do dołków dodano MTT (końcowe stężenie 0,5 mg/mL) i inkubowano przez kolejne 4 godziny. Wytrącony formazan rozpuszczono w DMSO i odczytano absorbancję przy długości fali wynoszącej 540 nm za pomocą Varioskan Lux. Żywotność komórek A549 obliczono w procentach w porównaniu do kontroli, którą były nietraktowane związkami komórki.

6.4.9 Analiza statystyczna

Wszystkie analizy statystyczne przeprowadzono przy użyciu programu Graph Pad Prism, wersja 8 (San Diego, CA, USA). Wyniki zostały przedstawione jako średnia ± odchylenie standardowe (SD) składające się z trzech niezależnych eksperymentów. Do określenia istotności statystycznej różnic zastosowano dwustronny test-t Studenta. Wartość $p \leq 0,05$ uznano za istotną statystycznie.

7. Wyniki

Szczegółowy opis uzyskanych wyników dotyczący aktywności badanych ceragenin i nanosystemów wobec *Candida* spp. znajduje się w niżej wymienionej pracy oryginalnej włączonej do rozprawy (publikacja nr 2):

Karol Skłodowski, Sylwia Joanna Chmielewska, Joanna Depciuch, Piotr Deptuła, Ewelina Piktel, Tamara Daniluk, Magdalena Zakrzewska, Michał Czarnowski, Mateusz Cieśluk, Bonita Durnaś, Magdalena Parlińska-Wojtan, Paul B. Savage, Robert Bucki.

Ceragenin-Coated Non-Spherical Gold Nanoparticles as Novel Candidacidal Agents. Pharmaceutics, 2021, 13, 1940.

7.1 Właściwości fizykochemiczne nanocząstek złota w kształcie patyczków, fistaszków i gwiazdek sfunkcjonalizowanych cerageninami

Przeprowadzona synteza nanocząstek złota pozwoliła na uzyskanie Au NPs w kształcie patyczków (AuR) **(Fig.1 A1 i A2, P.2)**, fistaszków (AuP) **(Fig. 1 B1 i B2, P.2)** i gwiazdek (AuS) **(Fig. 1 C1 i C2, P.2)**. Rozmiary mierzone w osi podłużnej i poprzecznej AuP NPs i AuR NPs, wykorzystano do porównania badanych NPs. W przypadku AuR NPs rozmiary osi wynosiły odpowiednio 37-53 nm i 7-13 nm, podczas gdy w przypadku AuP NPs rozmiary wynosiły odpowiednio 55-65 nm i 24-34 nm. Rozmiar AuS NPs wynosił 243 nm. Badania potencjału zeta AuR NPs, AuP NPs i AuS NPs wykazały, że wszystkie nanocząstki złota były naładowane dodatnio w całym zakresie pH **(Fig. 1 D, P.2)**.

Skuteczną funkcjonalizację i immobilizację ceragenin na powierzchni nanocząstek zweryfikowano za pomocą spektroskopii Ramana. W reprezentatywnych widmach ramanowskich zaobserwowano pasma w zakresie drgań rozciągających wiązania pomiędzy atomami złota, a atomami siarki przy 278 cm^{-1} (Au-S) **(Fig. 1 E, P.2)**. Dodatkowo, immobilizacja ceragenin na powierzchni AuR NPs, AuP NPs i AuS NPs została potwierdzona przez obecność pasm przy 1680 cm^{-1}, odpowiadających drganiom N-H (azot-wodór) utworzonym między grupami -COOH (grupa karboksylowa) z MHDA i grupami -NH$_2$ (grupa aminowa) z CSA-13, CSA-44 i CSA-131 **(Fig. 1 E, P.2)**.

7.2 Wrażliwość badanych szczepów z grupy ESKAPE oraz *Candida* na antybiotyki, cerageniny w postaci wolnej oraz nanosystemy złota

Wartości MIC, MBC i MFC są wykorzystywane do określenia potencjału terapeutycznego środków przeciwdrobnoustrojowych. W przeprowadzonym badaniu, wykorzystano szczepy *Candida* oporne na flukonazol, średnio wrażliwe na kaspofunginę oraz worykonazol. Aktywność ceragenin zimobilizowanych na powierzchni nanocząstek złota była wyższa (wartości MIC w zakresie od 0,4 do 3,2 µg/mL) w porównaniu do samych ceragenin: CSA-13, CSA-44 i CSA-131 (MIC w zakresie od 0,8 do 6,4 µg/ml). Co więcej, nanocząstki złota sfunkcjonalizowane CSA-13 i CSA-131 wykazywały wyższą aktywność w porównaniu do nanocząstek sfunkcjonalizowanych CSA-44 (**Fig. 2 A-C, P.2**).

W przypadku bakterii z grupy ESKAPE wartości MIC/MBC dla badanych związków przedstawiono w **Tabeli 2**.

Tabela 2. Wartości MIC i MBC imipenemu, wankomycyny, AuR NP@CSA-13, AuP NPs@CSA-13 oraz AuS NP@CSA-13 w stosunku do badanych szczepów bakterii. „-" – nie określono.

Związek	MIC/MBC [µg/mL]		
	E. faecium ATCC 700721	*A. baumannii*	*K. pneumoniae*
Imipenem	–	64/64	32/32
Wankomycyna	>256/>256	–	–
AuR NPs@CSA-13	0,8/1,6	3,2/3,2	3,2/3,2
AuP NPs@CSA-13	0,8/1,6	3,2/3,2	3,2/3,2
AuS NPs@CSA-13	0,8/1,6	3,2/3,2	3,2/3,2

7.3 AuR NPs@CSA-13, AuP NPs@CSA-13 oraz AuS NPs@CSA-13 wykazały silną aktywność przeciwbakteryjną w teście zliczania kolonii

AuR NPs@CSA-13, AuP NPs@CSA-13 i AuS NPs@CSA-13 wykazały silne działanie przeciwbakteryjne wobec bakterii z grupy ESKAPE. Użyte w tym eksperymencie nanosystemy w stężeniu 10 µg/mL spowodowały całkowite zahamowanie wzrostu *E. faecium* ATCC 700721 oraz dwóch szczepów klinicznych *A. baumannii* i *K. pneumoniae*. Dla porównania wankomycyna oraz imipenem, nie zahamowały wzrostu drobnoustrojów przy stężeniu 100 µg/mL (**Rycina 4, A-C**).
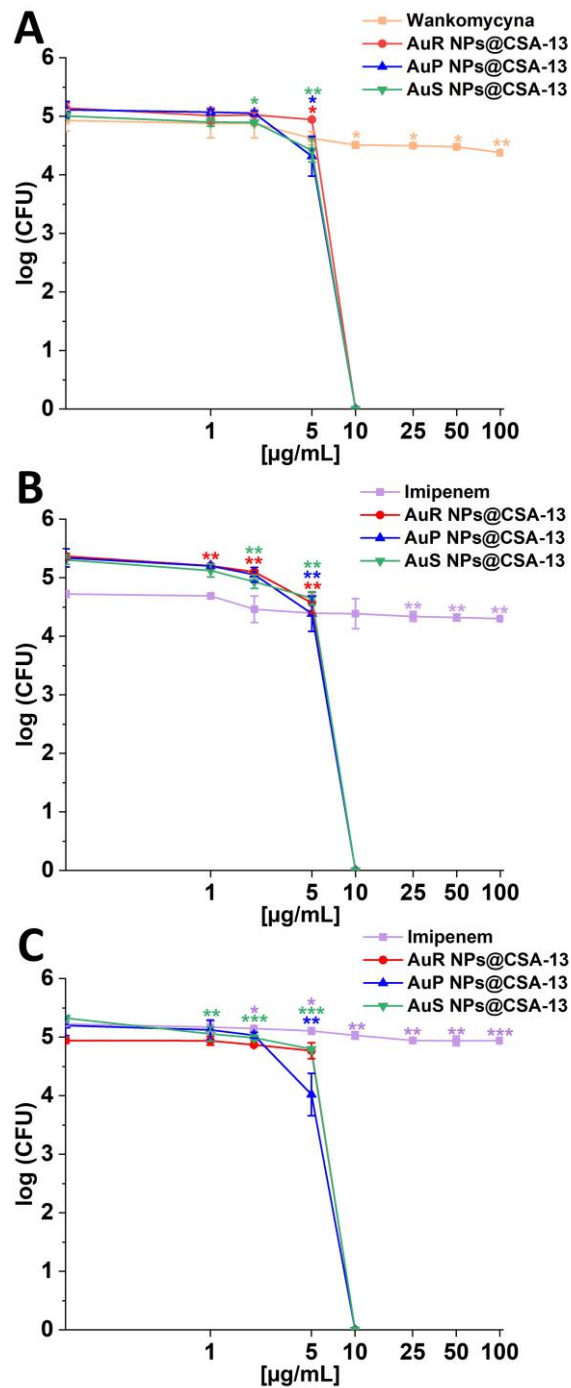
Rycina 4. Działanie bakteriobójcze wankomycyny, imipenemu, AuR NP@CSA-13, AuP NP@CSA-13 oraz AuS NP@CSA-13, w stosunku do *E. faecium* ATCC 700221 (panel A), *A. baumannii* (panel B) oraz *K. pneumoniae* (panel C). Aktywność bakteriobójczą badanych związków w stężeniach 1–100 µg/mL określono z wykorzystaniem testu zliczania kolonii. Wyniki stanowią średnią ± SD z trzech pomiarów. * oznacza istotność statystyczną przy ≤0,05, ** <0,01 i *** <0,001.

7.4 AuR-, AuP- oraz AuS-NPs@CSA-13 ograniczają tempo wzrostu bakterii z grupy ESKAPE

Zależne od dawki zahamowanie wzrostu bakterii odnotowano dla wszystkich badanych nanosystemów. Analiza krzywych uzyskanych dla kontroli oraz próbek traktowanych badanymi związkami wykazała, iż najwyższy stopień zahamowania wzrostu (zarówno w dawce 5 µg/mL i 10 µg/mL) zaobserwowano dla nanocząstek złota w kształcie fistaszków (**Rycina 5, B, C, E, F, H, I**). Warto podkreślić, iż aktywność przeciwbakteryjna zastosowanych antybiotyków – wankomycyny i imipenemu była porównywalna do wzrostu nietraktowanych związkami bakterii (**Rycina 5, A-I**).
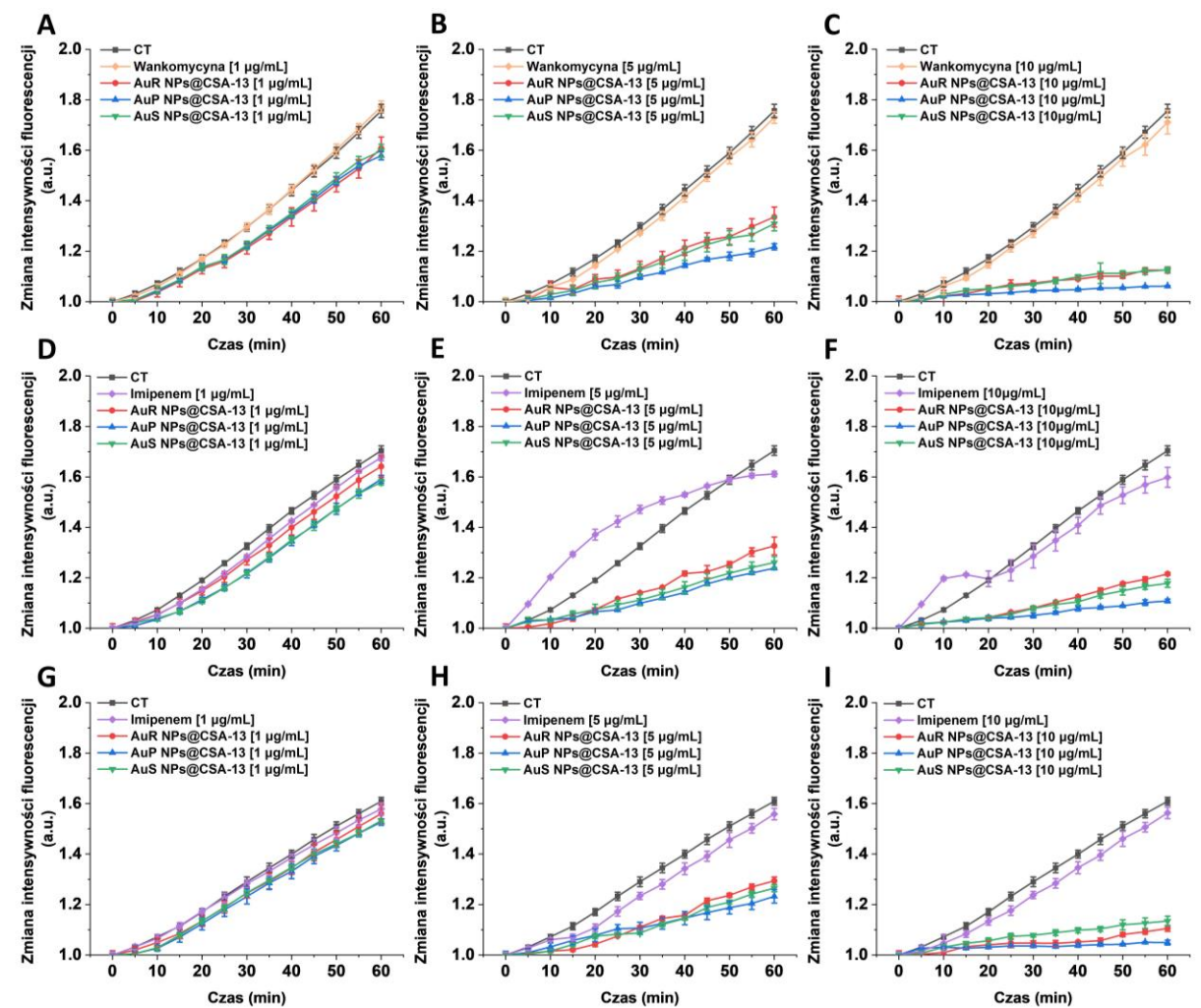
Rycina 5. Wpływ antybiotyków (imipenemu i wankomycyny) oraz nanocząstek złota sfunkcjonalizowanych cerageninami (AuR NPs@CSA-13, AuP NPs@CSA-13 i AuS NPs@CSA-13) na wzrostu bakterii z grupy ESKAPE, tj. *E. faecium* ATCC 700221 (panele A-C), *A. baumannii* (panel D-F) oraz *K. pneumoniae* (panel G-I) został określony w zakresie stężeń 1 µg/mL (panele A, D, G), 5 µg/mL (panele B, E, H) i 10 µg/mL (panele C, F, I) przy użyciu resazuryny.

7.5 AuR NPs@CSA-13, AuR NPs@CSA-44 i AuR NPs@CSA-131 nie indukowały oporności u szczepów *Candida*

Początkowe wartości MIC dla AuR NPs@CSA-13, AuR NPs@CSA-44 i AuR NPs@CSA-131 dla *C. albicans* ATCC 26790 wynosiły odpowiednio 1,6 µg/mL, 3,2 µg/mL i 1,6 µg/mL, natomiast po przeprowadzeniu 25 pasaży wartości MIC wzrosły jedynie do wartości odpowiednio 6,4 µg/mL (dla AuR NPs@CSA-13 i AuR NPs@CSA-44) oraz 3,2 µg/mL (dla AuR NPs@CSA-131) **(Fig. 3 A, C, E, P.2)**. W przypadku szczepu klinicznego *C. krusei*, początkowe wartości MIC dla AuR NPs@CSA-13, AuR NPs@CSA-44 i AuR NPs@CSA-131 wynosiły odpowiednio 0,8 µg/mL, 1,6 µg/mL i 0,8 µg/mL. Po przeprowadzeniu indukcji oporności, ich końcowe wartości MIC wynosiły odpowiednio 0,8 µg/mL, 3,2 µg/mL i 1,6 µg/mL **(Fig. 3 B, D, F, P.2)**.

7.6 Wysoka aktywność przeciwbakteryjna nanocząstek złota sfunkcjonalizowanych cerageninami w stosunku do patogenów zewnątrz- i wewnątrzkomórkowych

Zaobserwowano, że nanocząstki złota sfunkcjonalizowane CSA-13 w kształcie fistaszków skutecznie uniemożliwiają adhezję komórek *A. baumannii* do ludzkich komórek gruczolakoraka płuc, a tym samym zmniejszają ich zdolność do wywołania zakażenia. Dawka 2 i 5 µg/mL AuP NPs@CSA-13 w znaczny sposób zmniejszyła ilość bakterii przylegających do komórek A549 w porównaniu do 2 i 5 µg/mL imipenemu. Dodatkowo, zdolność imipenemu do hamowania adhezji, zarówno w dawce 2 µg/mL, jak i 5 µg/mL, nie wykazywała istotnych różnic w porównaniu do nietraktowanej związkami kontroli **(Rycina 6, A-F)**.

Internalizacja bakterii do komórek gospodarza jest istotnym zjawiskiem w przebiegu wielu infekcji. AuP NPs@CSA-13 skutecznie zahamowały wzrost *K. pneumoniae* wewnątrz komórek A549 już w dawce 5 µg/mL, podczas gdy imipenem w dawce 20 µg/mL spowodował nieznaczny spadek ilości bakterii w stosunku do nietraktowanej antybiotykiem kontroli **(Rycina 6, G)**.
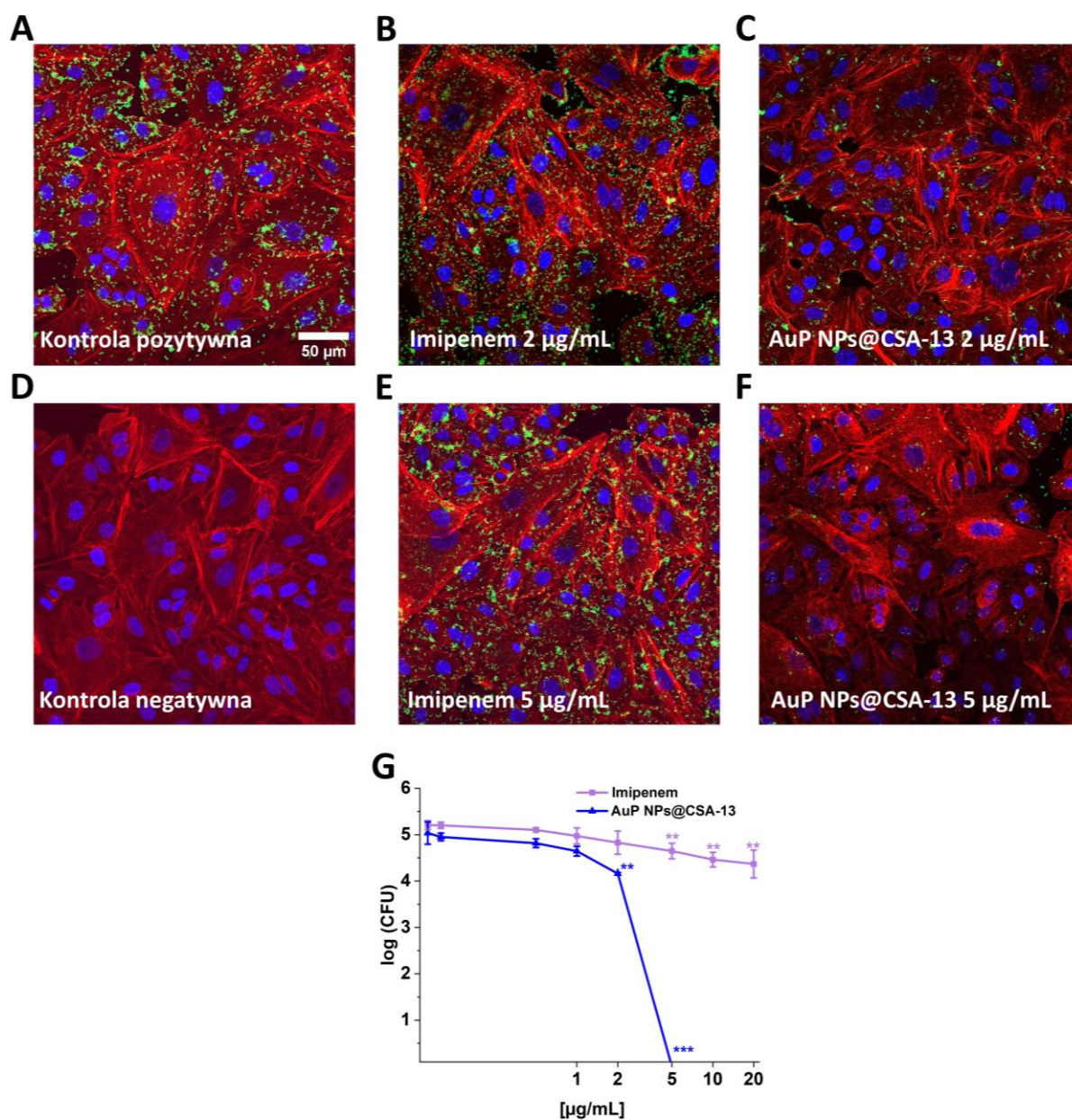
Rycina 6. Ocena aktywności imipenemu oraz AuP NPs@CSA-13 w stosunku do *K. pneumoniae* oraz *A. baumannii*. W teście adhezji (panele A-F) imipenem oraz AuP NPs@CSA-13 użyto w stężeniu 2 µg/mL i 5 µg/mL, na kolor czerwony wybarwiono aktynę komórek A549, na kolor niebieski jądra komórkowe, a na kolor zielony – bakterie (*K. pneumoniae*). Aktywność bakteriobójczą badanych związków w teście internalizacji w stosunku do *A. baumannii* (panel G) przeprowadzono w zakresie stężeń 1–20 µg/mL Wyniki pokazują średnią ± SD z trzech pomiarów. ** oznacza istotność statystyczną przy <0,01 i *** <0,001.

7.7 Mechanizm aktywności przeciwgrzybiczej nanosystemów obejmuje wytwarzanie reaktywnych form tlenu, depolaryzację oraz uszkodzenie błony komórkowej

Reaktywne formy tlenu (ROS) są syntetyzowane w różnych szlakach metabolicznych podczas redukcji i utleniania. Zastosowanie nanocząstek złota sfunkcjonalizowanych cerageninami w stężeniu 10 μg/mL spowodowało maksymalnie ponad dwukrotny wzrost wytwarzania ROS w porównaniu z 5 mM nadtlenkiem wodoru. Co istotne, efekt ten zaobserwowano dla wszystkich opracowanych nanosystemów. Z drugiej strony wolne cerageniny, tj. CSA-13, CSA-44 i CSA-131, zwiększały wytwarzanie ROS w przedziale 1,22 do 1,7-raza w stosunku do 5 mM nadtlenku wodoru (**Fig. 4 A-C, P.2**). Podczas inkubacji *C. albicans* 1408 bez stosowania badanych związków, nie odnotowano obecności jakiegokolwiek sygnału fluorescencyjnego. W przeciwieństwie do tego, zaobserwowano intensywny sygnał z sondy fluorescencyjnej DFCH-DA po dodaniu nanosystemów do zawiesiny komórek *C. albicans* 1408 (**Fig. 5, P.2**).

Zdolność ceragenin oraz nanocząstek złota sfunkcjonalizowanych cerageninami do indukcji depolaryzacji błony cytoplazmatycznej została określona przy użyciu barwnika diSC$_{(3)}$. Największy wzrost sygnałów fluorescencyjnych zaobserwowano dla nanocząstek złota w kształcie fistaszków sfunkcjonalizowanych CSA-13 oraz CSA-131 (AuP NPs@CSA-13 i AuP NPs@CSA-131). Należy podkreślić, że zastosowanie nanosystemów w stężeniu 10 μg/mL skutkowało około 1,27 do 2,30-krotnym wzrostem sygnału fluorescencji w porównaniu do 1 μg/mL amfoterycyny B. W przeciwieństwie do tego, ta sama dawka CSA-13, CSA-44 i CSA-131 spowodowała jedynie o 1,22 do 1,41-krotny wzrost sygnału fluorescencji w porównaniu do 1 μg/mL amfoterycyny B (**Fig. 6 A-C, P.2**).

Zdolność nanosystemów zawierających cerageniny oraz samych ceragenin do zaburzenia integralności błony powierzchniowej *C. albicans* 1408 została określona za pomocą testu wychwytu NPN. Najwyższy poziom permeabilizacji błony obserwowano dla nanocząstek złota w kształcie patyczków. Aktywność przeciwgrzybicza nanosystemów była wyższa aniżeli ta obserwowana dla CSA-13, CSA-44 i CSA-131 w formie wolnej (**Fig. 7 A-C, P.2**).

Aby zweryfikować, czy traktowanie cerageninami i nanocząstkami złota sfunkcjonalizowanych cerageninami komórek *C. albicans* 1408 prowadzi do uwolnienia zawartości cytoplazmy, przeprowadzono test wycieku białka. Uzyskane wyniki wskazują na znaczne uwolnienie białek cytoplazmatycznych w wyniku uszkodzenia błony powierzchniowej komórek grzybów. Efekt ten zaobserwowano dla wszystkich zsyntetyzowanych nanosystemów w sposób zależny od dawki. Warto zauważyć, że w przypadku AuP NPs@CSA-131 wykryto

największy wypływ białek wewnątrzkomórkowych z 2,51-krotnym wzrostem w porównaniu do 1 μg/mL amfoterycyny B. W przypadku ceragenin zaobserwowano znacznie niższe wartości absorbancji w porównaniu do wartości absorbancji określonej dla nanosystemów (**Fig. 8 A-C, P.2**).

7.8 Biokompatybilność nanosystemów zawierających ceragenin w dawkach wykazujących działanie bakteriobójcze oraz grzybobójcze

Aby ocenić potencjalną toksyczność badanych nanosystemów, przeprowadzono test hemolizy w stężeniach odpowiadających zakresowi ich aktywności kandydobójczej. Badane związki nie indukowały znaczącej hemolizy w dawkach od 1 do 10 μg/mL, nawet po 12 godzinach inkubacji. Po 1 h inkubacji w stężeniach od 1 do 10 μg/mL hemoliza nie przekraczała 3,5%, po 6 godzinach – 9,60%, natomiast po 12 godzinach – 9,78% (**Fig. 9 A-I, P.2**).

Ocenę cytotoksyczności antybiotyków oraz AuR, AuP, AuS NPs@CSA-13 przeprowadzono na ludzkich komórkach gruczolakoraka płuc A549. W dawkach bakteriobójczych, żywotność komórek nie spadła poniżej 90% po godzinie inkubacji oraz poniżej 80% po 6 godzinach inkubacji. Po 24 godzinach inkubacji żywotność komórek A549 traktowanych nanosystemami w stężeniu 5 μg/mL wynosiła powyżej 76%. W przypadku wankomycyny i imipenemu żywotność komórek nie spadła poniżej 90% po 1, 6 i 24 godzinach (**Rycina 7, A-C**).
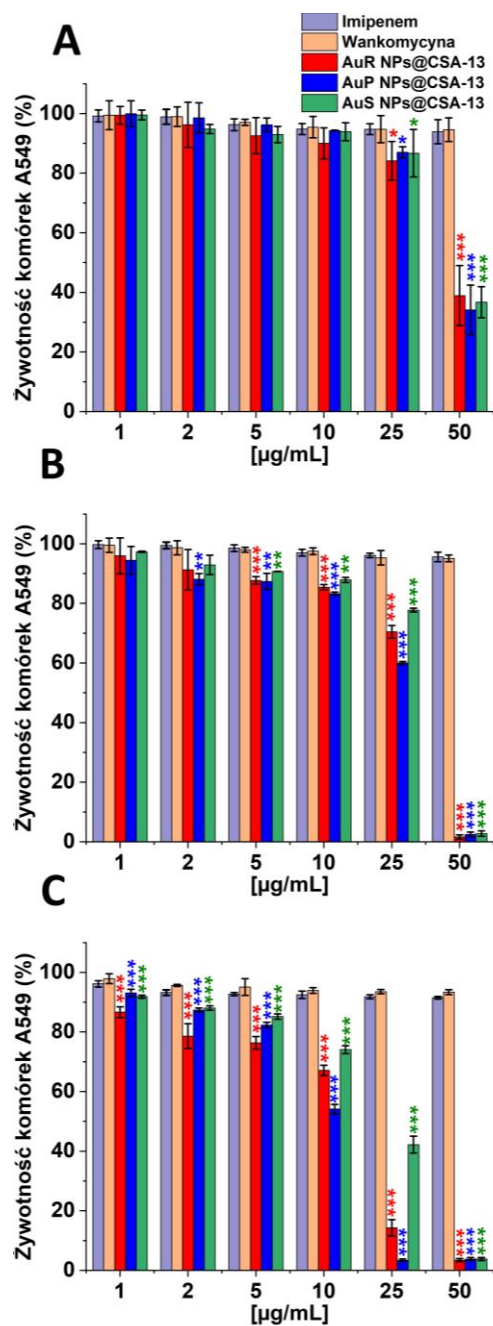
Rycina 7. Cytotoksyczność imipenemu, wankomycyny, AuR NPs@CSA-13, AuP NPs@CSA-13 oraz AuS NPs@CSA-13 w stosunku do komórek A549 w dawkach od 1 do 50 µg/mL po 1, 6 oraz 24 h inkubacji (odpowiednio panel A, B i C). Wyniki pokazują średnią ± SD z trzech pomiarów. * oznacza istotność statystyczną przy ≤0,05, ** <0,01 i *** <0,001.

8. Wnioski

1. Nanocząstki złota sfunkcjonalizowane cerageninami wykazują wysoką aktywność bakteriobójczą i grzybobójczą.

2. Mechanizm aktywności przeciwdrobnoustrojowej nanosystemów obejmuje wytwarzanie reaktywnych form tlenu, depolaryzację oraz uszkodzenie błony komórkowej.

3. Nanocząstki złota sfunkcjonalizowane cerageninami nie indukowały oporności zarówno u szczepu wzorcowego *C. albicans*, jak i szczepu klinicznego *C. krusei*.

4. Badane nanosystemy charakteryzuje wysoka aktywność przeciwbakteryjna zarówno w stosunku do bakterii zewnątrz- jak i wewnątrzkomórkowych.

5. Niska aktywność hemolityczna badanych nanosystemów w dawkach bakteriobójczych oraz grzybobójczych wskazuje na ich duży potencjał w opracowywaniu nowych metod zwalczania infekcji wywoływanych przez bakterie z grupy ESKAPE oraz grzyby z rodzaju *Candida*.

6. Nanocząstki złota w kształcie fistaszków sfunkcjonalizowane cerageninami wykazują większą aktywność przeciwbakteryjną i przeciwgrzybiczą w porównaniu do patyczków i gwiazdek.

9. Publikacja nr 1 (P.1)

Review

Metallic Nanosystems in the Development of Antimicrobial Strategies with High Antimicrobial Activity and High Biocompatibility

Karol Skłodowski [1], Sylwia Joanna Chmielewska-Deptuła [1], Ewelina Piktel [2], Przemysław Wolak [3] [ID], Tomasz Wollny [4] and Robert Bucki [1,3,* [ID]

[1] Department of Medical Microbiology and Nanobiomedical Engineering, Medical University of Bialystok, 15-222 Bialystok, Poland
[2] Independent Laboratory of Nanomedicine, Medical University of Bialystok, 15-222 Bialystok, Poland
[3] Institute of Medical Science, Collegium Medicum, Jan Kochanowski University of Kielce, IX Wieków Kielce 19A, 25-317 Kielce, Poland
[4] Holy Cross Oncology Center of Kielce, Artwińskiego 3, 25-734 Kielce, Poland
* Correspondence: buckirobert@gmail.com; Tel.: +48-85-748-5493; Fax: +48-85-748-5416

Abstract: Antimicrobial resistance is a major and growing global problem and new approaches to combat infections caused by antibiotic resistant bacterial strains are needed. In recent years, increasing attention has been paid to nanomedicine, which has great potential in the development of controlled systems for delivering drugs to specific sites and targeting specific cells, such as pathogenic microbes. There is continued interest in metallic nanoparticles and nanosystems based on metallic nanoparticles containing antimicrobial agents attached to their surface (core shell nanosystems), which offer unique properties, such as the ability to overcome microbial resistance, enhancing antimicrobial activity against both planktonic and biofilm embedded microorganisms, reducing cell toxicity and the possibility of reducing the dosage of antimicrobials. The current review presents the synergistic interactions within metallic nanoparticles by functionalizing their surface with appropriate agents, defining the core structure of metallic nanoparticles and their use in combination therapy to fight infections. Various approaches to modulate the biocompatibility of metallic nanoparticles to control their toxicity in future medical applications are also discussed, as well as their ability to induce resistance and their effects on the host microbiome.

Keywords: antibiotic resistance; metallic nanoparticles; synergy; biocompatibility; modulation of antimicrobial activity

1. Introduction

Antimicrobial resistance (AMR) is a natural phenomenon that occurs when microorganisms are exposed to antimicrobial agents [1]. The speed of this natural process has been drastically affected by the use of antibiotics not only in medicine, but also in other sectors. The list of causes of increasing antibiotic resistance includes: (i) excessive use of antimicrobials in veterinary medicine/agriculture, where the addition of antibiotics to feed for farm animals not only ensures the prevention of intestinal infections but also results in improved absorption of nutrients and, thus, faster weight gain while causing the selection and development of bacterial strains with mechanisms of resistance and further release of these strains into the environment [2], (ii) over-use of antimicrobials due to the over-prescription of antibiotics (approximately 90% of all antibiotic prescriptions are issued by general practitioners and respiratory infections are the main reason for prescribing them, however, they are mainly caused by viruses) [3], (iii) improper selection of doses, which prevents the complete elimination of pathogens, which then favors changes in gene expression, increased mutagenesis or horizontal gene transfer and, thus, increasing

44

resistance to antibiotics and the spread of these strains, especially in the hospital environment [4,5], (iv) the duration of antibiotic therapy, with a longer duration of therapy being associated with an increased risk of antimicrobial resistance [6]. Due to the overuse of antimicrobials in veterinary medicine [7], inappropriate use of antibiotics resulting from a lack of knowledge on the principles of rational antibiotic therapy [3], biofilm formation by pathogenic microorganisms [8], an increasing number of infections with multidrug-resistant strains (MDR) has been observed [9], making antimicrobial resistance one of the biggest public health challenges of our time [10,11]. A report published by the Centers for Disease Control (CDC) indicates the highest number of infections in United States caused by drug-resistant *Streptococcus pneumoniae* with 900,000 cases, followed by 550,000 infections caused by drug-resistant *Neisseria gonorrhoeae*, and in third place were 448,400 infections caused by drug-resistant *Campylobacter* [12]. Importantly, it is estimated by World Health Organization (WHO) that the drug resistance of microorganisms is already responsible for at least 700,000 deaths each year, including 230,000 people dying from multidrug-resistant tuberculosis [13]. The seriousness of the problem in the treatment of infectious diseases is evidenced by analyses conducted by scientists, who predict that by the end of 2050, untreatable infections will be the most common cause of death, causing more than 10 million deaths per year, overtaking cancer and cardiovascular diseases [14].

The problem of increasing resistance is a growing concern as the number of new antibiotics approved since the late 1970s has declined [15]. Evidently, the propensity of microbes to develop resistance occurs much faster than the ability of humans to develop new agents; therefore, new antimicrobial compounds are being sought and nanomaterials appear to be a promising alternative to conventional antimicrobials due to their unique physical and chemical properties [16,17].

Nanotechnology is the science of materials/devices defined by size (the nanoscale range is 1–100 nm in one dimension). The term nanotechnology was introduced by American physicist and Nobel Prize winner Richard Feynman in 1959 during a lecture entitled "There's Plenty of Room at the Bottom". Dr. Richard Feynman considered some of the consequences of the possibility of manipulating matter on the atomic scale and mentioned the ability to create nanoscale machines [18]. Fifteen years later, the term "nanotechnology" was defined by Professor Norio Taniguchi from Tokyo Science University in the 1974 paper: 'Nano-technology' mainly consists of the processing of, separation, consolidation, and deformation of materials by one atom or by one molecule" [19].

A steadily increasing number of reports indicate that nanomaterials may be also developed as alternative to currently used antibiotics and antifungal drugs [20]. Nanomaterials, among which four categories can be distinguished, depend on their material type. (i) The first group includes carbon-based nanomaterials such as fullerenes, carbon nanotubes, graphene and its derivatives, graphene oxide, nanodiamonds, or carbon-based quantum dots [21]. In their pure state, most carbon-based nanomaterials have limited antimicrobial capacity and show low selective toxicity against bacteria over mammalian cells. By modifying their physicochemical properties, their antimicrobial activity and targeting efficiency can be modulated [22] through surface functionalization to modulate physicochemical parameters or modification of their synthesis methods [23] (using covalent and non-covalent modification, among others [24]). In addition, to improve the water solubility and dispersion of carbon-based nanomaterials, surfactants and polymer are used to increase both the probability of contact and the strength of interaction with bacteria [25]. In order to enhance antibacterial efficacy, carbon-based nanomaterials are functionalized with functional groups and bioactive molecules [26]. The second group represents (ii) inorganic-based nanomaterials consisting of metal (e.g., Au, Ag, Pt) [27], metal oxide NPs (nanoparticles) (e.g., TiO_2, MnO, ZnO) and semiconductors such as silicon and ceramics [28]. Inorganic-based nanomaterials are of great interest due to a number of features such as optical properties including surface plasmon resonance (SPR) with the ability to control optical field, the possibility to modify the surface of nanoparticles to control solubility, stability and interaction with the environment (it is possible, among

other things, to increase the circulation time of NPs by reducing non-specific uptake by the mononuclear phagocyte system), mechanisms of action quite different from those described for traditional antibiotics, irrespective of the pathogen resistance mechanism, synthetic versatility, which allows the control of their size, shape and surface properties, surface functionalization of NPs with an appropriate functional groups for the labelling, targeting and conjugation of pharmacological molecules, synthesis by simple, cost-effective, and easy methods [29–34]. Another negative trait of inorganic-based nanomaterials is their toxicity, which can be modulated by changing the shape and size of the particles and modifying their surface, leading to nanoparticles with desired properties but without toxic effects [35,36]. The third group represents (iii) organic-based nanomaterials which include molecules made of organic material as cationic polymers NPs, solid lipid NPs, lipid NPs, biomimetic NPs, dendrimer nanoparticles or protein-based NPs [37]. A key advantage of organic-based nanomaterials NPs is the tunability of the lipid layer, which can be further functionalized to produce nanomaterials with the desired properties. In addition, they have advantageous characteristics such as chemical diversity, high loading capacity and intrinsic biodegradability [38] and biocompatibility [39,40]. However, compared to inorganic materials, they are less stable by nature, especially at higher temperatures [41], and the presence of potential problems related to immunogenicity and challenges in loading of a wide variety of drugs [42] or poor mechanical and processing properties or insolubility in common organic solvents [43]. The last group represents (iv) composite-based nanomaterials that are comprised of two or more components at the nanoscale where mutual contact interfaces occur between the individual components. Composites can be any combination of metal, carbon, or organic based-NMs (nanomaterials) with any form of metal or polymer materials [44]. The advantages of composite-based nanomaterials include the film uniformity, biocompatibility, available hydroxyl and carboxyl groups or amines, improve physical properties of ions and their releasing, possibility of functionalizing the surface, environmental stability, simple doping process or tunable conductivity [45,46]. The disadvantages of these nanomaterials include uncertain cytotoxicity, component stability, long-term stability, structural integrity, mechanical and corrosion properties or the tendency of nanomaterials to agglomerate [47,48]. From among the above-mentioned categories, the most promising are metallic nanoparticles, which show strong antimicrobial activity both against planktonic bacteria and in biofilm form in a large number of studies, which is why this review focuses on metallic NPs.

Due to their unique physicochemical properties such as (i) a large surface to the volume ratio, (ii) the ability to functionalize with diagnostic and therapeutic factors, (iii) ease of modification of the method of synthesis, (iv) antibacterial and immunomodulatory properties [49–55], nanoparticles are of growing interest in medicine. It is noteworthy that due to the nanometer scale size and appropriate surface charge, a strong interaction of nanoparticles with the biological membranes of the pathogen is possible [56,57]. Moreover, in respect of their relatively low potential to induce drug resistance [58,59], metal nanoparticles are proposed as an alternative to antimicrobial agents. They are also receiving increasing recognition as highly effective drug carriers [60].

The mechanism of action of metallic nanoparticles includes, among others: (i) disruption of the cell walls, thus, increasing their permeability as a result of electrostatic interaction between negatively charged molecules of the cell wall of the microorganism and positively charged nanoparticles resulting in a leakage of cytoplasmic contents [61,62] and causing membrane potential disorder [63]; (ii) another mechanism comprises of the generation of toxic Reactive Oxygen Species (ROS). Oxidative stress leads to oxidation of glutathione, disrupting the antioxidant defense mechanisms of bacteria against ROS. The excessive production of ROS causes disturbances in redox homeostasis, which results in oxidative stress, thus, affecting the membrane lipids and modifies DNA as well as the protein structure [61,64]; (iii) a further mechanism involves the binding to intracellular components among other things, causing damaged DNA, proteins and inhibition of the enzymatic activity [65]. The interaction of metallic nanoparticles with DNA can denature

or shear the DNA and disrupt cell division [66,67]. In addition, metallic NPs can inhibit protein synthesis by denaturing ribosomes [68]. As a result of the additive effect of the above factors, (iv) apoptotic cell death eventually occurs [69]. A schematic representation of the different mechanisms of nanoparticles action is illustrated in Figure 1.
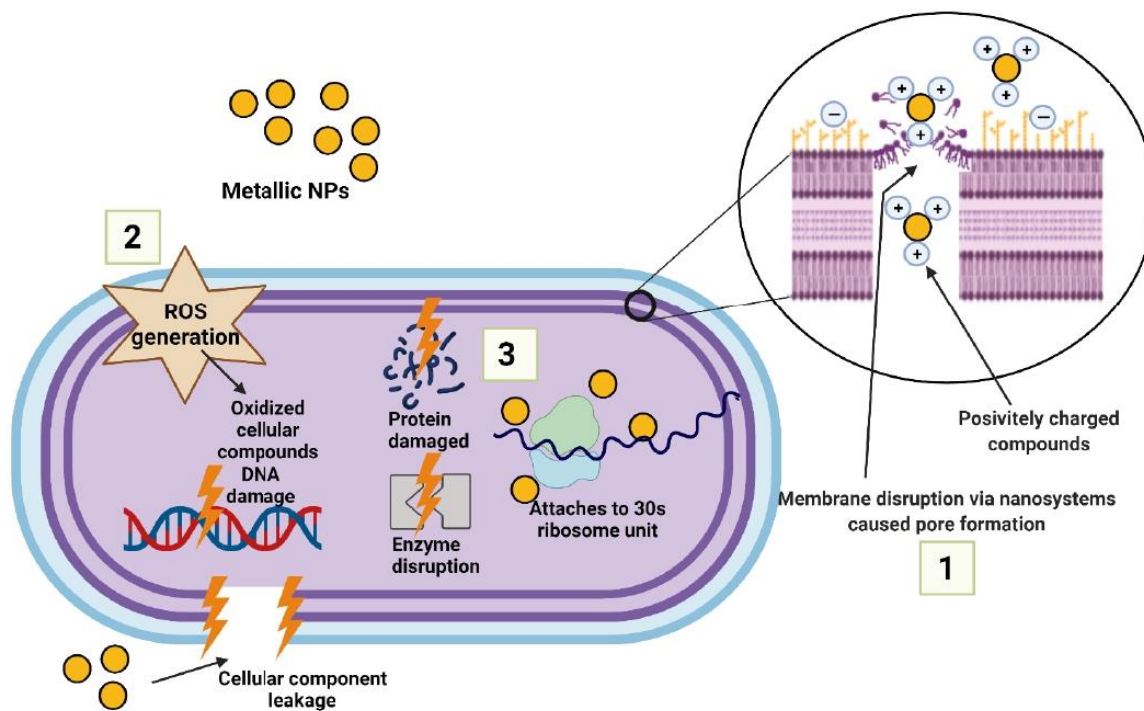

Figure 1. The main mechanisms of antimicrobial activity of metal nanoparticles include: (1) disruption of the pathogen cell wall resulting in increased permeability, (2) generation of ROS disrupting redox homeostasis and damaging cellular structures, (3) binding to intracellular structures causing their dysfunction.

Here, we provide a throughfall characterization and discussion of the latest achievements in synthesis and design of metallic nanoparticles and metallic nanoparticle-based nanosystems as potent antimicrobials with the potential to be used for the treatment of drug-resistant bacterial and fungal infections.

2. Synergistic Effects of Metallic Nanoparticles

Over the past few decades, antibiotic-resistant bacteria have become increasingly prevalent; the number of infections caused by multidrug-resistant (MDR) bacteria is increasing and the risk of untreatable infections is rising [70].

Among metallic nanoparticles, silver (Ag), gold (Au), copper oxide (CuO), iron oxide (Fe_3O_4) titanium oxide (TiO_2) or zinc oxide (ZnO) are commonly used as antimicrobial agents after their strong antimicrobial activity is well known [16,71]. There are many studies showing that various metal and metal oxide nanoparticles exhibit biocidal activity against gram-positive and gram-negative bacteria, fungi or viruses [72]. A key influence on the antimicrobial properties of metallic NPs is their high specific surface area high surface-to-volume ratio and nanoscale size, which allows strong interaction with the membranes of micro-organisms causing its disruption, penetration into cells followed by damage to internal cellular structures ultimately leading to the cell death [52]. The mechanisms associated with metallic nanoparticles ability to overcome antibiotic resistance

involved their unique physicochemical properties enabling the exploitation of multiple novel bactericidal pathways to achieve antimicrobial activity [73]. Due to the binding between metal ions and microbials' biomolecules, which is generally non-specific, metallic nanoparticles exhibit a broad spectrum of activity [74]. Specific metal ions such as iron, zinc or copper are essential for the biochemistry of life in all organisms, and their deficiency can cause damage to the structure of cell membranes and DNA or disrupt enzymatic functions [75]. However, an excess of these ions or the presence of other, less essential ions such as gold or silver can be lethal to pathogens' cells. Released from the extracellular space, metal ions are able to enter the cell and disrupt biological processes where, inside the cell, they can induce the production of ROS and affect cellular structures by disrupting cellular functions as a result of forming strong coordination bonds with nitrogen, oxygen and sulfur atoms, which are abundant in organic compounds and biomolecules [61].

Due to the increasing prevalence of microbial resistance, combinations of nanoparticles and antimicrobials have been shown to possess superior efficacy compared to antimicrobials alone [76–78]. Such combinations can reduce the development of antimicrobial resistance as well as shorten the duration and dose requirements of antimicrobial treatment [79,80]. The use of combination therapy is common in clinical practice for many reasons, including: (i) the prevention of antimicrobial resistance [81], (ii) antimicrobials can mutually enhance antimicrobial activity [77], (iii) when a critically ill patient is admitted with suspected sepsis of unknown etiology, several antimicrobials are used to broaden the spectrum against unknown pathogenic species [82,83], (iv) killing bacteria in a dormant state [84].

Based on the type of components that comprise the combination of metallic nanoparticles, they can be divided into several categories: (i) monometallic nanoparticles, (ii) metallic nanoparticles in combination with conventional antibiotics/fungicides or compounds other than antimicrobial agents, (iii) multimetallic nanoparticles alone and (iv) in combination with antibiotics/fungicides, (v) metallic nanoparticles, whose surface has been further functionalized with antibiotics/fungicides or compounds other than antimicrobial agents. The functionalization of metallic NPs surfaces with the desired compound utilizes various types of covalent and non-covalent bonds—these include electrostatic forces, hydrogen bonds and van der Waals interactions, resulting in the integration of a variety of organic and inorganic molecules at the nanoscale [85]. In order to form covalent and non-covalent bonds between ligands and NPs surfaces, a number of linker molecules are used, such as organic materials, within which various polymers (polyethylene glycol (PEG), polyvinyl alcohol (PVA), chitosan, dextran, alginate, polyacrylic acid, citrates, phosphates, amines [86]) or inorganic substances (metals and metal oxides, silicas [87–89]) are used. The non-covalent functionalization approach is based on a large number of weak interactions such as ionic interactions, van der Walls, hydrophobic interactions, electrostatic interactions, hydrogen bonds that are applied to metallic and silica nanoparticles [90–92]. The advantages of using non-covalent modifications include the simplicity and lack of influence on the structures of the particles used and their interaction with docked biological substances, while the disadvantage is that non-covalent interactions are easily influenced by factors such as pH or ionic strength [93]. The surface modification of NPs using covalent bonds can be achieved using a number of alternative approaches, depending on the composition of the NPs [94–96] by means of modifications at several levels using sequential functionalization, so that structures with multiple functions can be obtained [97,98].

2.1. Monometallic Nanoparticles

Monometallic NPs consist of a single metal species, which, depending on the atomic type and properties, may exist in various forms such as metallic, magnetic, transition metal and oxide. Monometallic NPs are the most popular inorganic nanoparticles, which represent a promising solution in the fight against resistance to traditional antibiotics, not only because of their completely different mechanisms of action from commonly used antibiotics, showing activity against bacteria that have developed resistance, but

also because they target many biomolecules that impede the development of resistant strains [99].

Among monometallic NPs, silver and gold nanoparticles are leading the way. Silver NPs are of great interest as antimicrobial agents due to their exceptional antimicrobial activity against a broad spectrum of pathogenic microorganisms [100,101]. Within the antimicrobial action of silver nanoparticles, three main mechanisms of action can be distinguished: firstly, the interaction and penetration of nanoparticles into the membrane of microorganisms [102], which results in protein inactivation and membrane lipid peroxidation, leading to structural modification of membrane integrity, transport protein dysfunction and leakage of cellular contents [103,104]. Secondly, there is damage to intrinsic structures, which triggers ROS generation, leading to the disruption of redox hemostasis, affecting the Na^+/K^+ ATPase pump and signal transduction pathways [105]. As a result of the interaction of ions and nanoparticles with DNA, protein inactivation occurs, ultimately leading to cell death [106]. Thirdly, there is the release of Ag^+ ions (whose rate of release depends largely on the size, shape, concentration, capping agent or colloidal state of NPs [107,108]), which occurs in parallel with the other two, which, due to their size and charge, can interact with cell components to alter metabolic pathways and even genetic material [109,110]. It is also important to keep in mind the type of bacterial species that respond differently to the activity of Ag NPs, which is caused by the different composition and thickness of the cell wall [111].

Gold nanoparticles (AuNPs) are one of the most important nanoparticles due to their simple and controlled synthesis, inertness, biocompatibility and low toxicity compared with other nanomaterials. Gold nanoparticles, such as silver nanoparticles, disrupt the integrity and structure of the cell membrane, causing leakage of intracellular components [112–114]. It can be compared to apoptosis-like cell death, where gold nanoparticles cause depolarization of the bacterial cell membrane and a continuous increase in the concentration of calcium ions in the cytoplasm, induction of DNA fragmentation, resulting in apoptosis-like death (overexpression of caspase-subunit proteins was observed as well) [115]. Additionally, membrane potential is altered and ATP synthase activity is reduced, resulting in metabolic dysfunction [116]. On the other hand, our studies with gold nanoparticles coated with ceragenin CSA-131 confirmed that cell membrane depolarization and cytoplasmic protein leakage occur when ESCAPE strains are targeted [117] (Figure 2 adopted from [117]).

The interaction of Au NPs with intracellular biomolecules results in translation inhibition [118]. The antimicrobial mechanism of Au NPs also involves an increase in intracellular ROS levels [119]. Additionally, our previous results show that gold nanoparticles display antibiofilm activity against *Candida* by reducing pathogen cell adhesion, resulting in the inhibition of biofilm growth. Interestingly, peanut shaped gold nanoparticles were found to reduce the viscosity of the biofilm formed by *Pseudomonas*, which may be important in the case of cystic fibrosis where thick mucus are formed, making it difficult for antimicrobial agents to penetrate and subsequently eradicate the pathogens causing infection. (Figures 3 and 4 from [120,121] respectively).
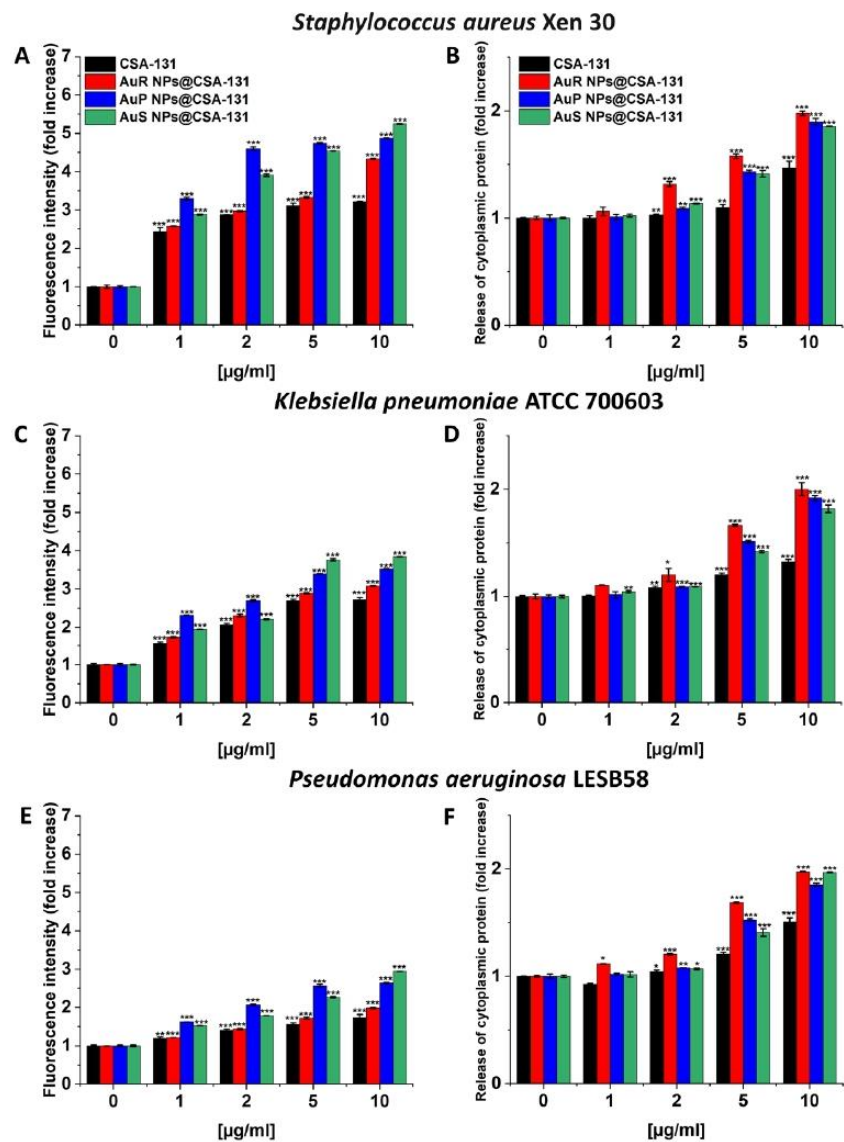
Figure 2. Bacterial membrane depolarization of multidrug-resistant strains: *Staphylococcus aureus* Xen 30 (**A**), *Klebsiella pneumoniae* ATCC 700603 (**C**), *Pseudomonas aeruginosa* LESB58 (**E**), was assessed using the 3,3′-dipropylthiadicarbocyanine iodide (diSC$_{(3)}$) assay, where bacterial cells were treated with gold nanosystems functionalized with ceragenin CSA-131 with rod-shaped (AuR NP@CSA-131), peanut-shaped (AuP NP@CSA-131), and star-shaped (AuS NP@CSA-131) metal cores and free ceragenin CSA-131. The release of cytoplasmic proteins from the bacteria *Staphylococcus aureus* Xen 30 (**B**), *Klebsiella pneumoniae* ATCC 700603 (**D**), *Pseudomonas aeruginosa* LESB58 (**F**), treated with AuR NP@CSA-131, AuP NP@CSA-131, AuS NP@CSA-131 and CSA-131 was assessed using the Bradford protein assay. Concentrations of the tested compounds ranged from 1–10 μg/mL. Results show the mean ± SD, n = 3; * indicates statistical significance at p ≤ 0.05, ** ≤0.01, and *** ≤0.001. Adapted from Pharmaceutics [117].

Figure 3. Height and adhesion images of *Candida albicans* strain 1408 using atomic force microscopy (**A**). Figures (**B**,**C**) show the adhesion distribution of *Candida albicans* strain treated with rod-shaped gold nanoparticles at doses of 0.125 ng/mL and 1 ng/mL compared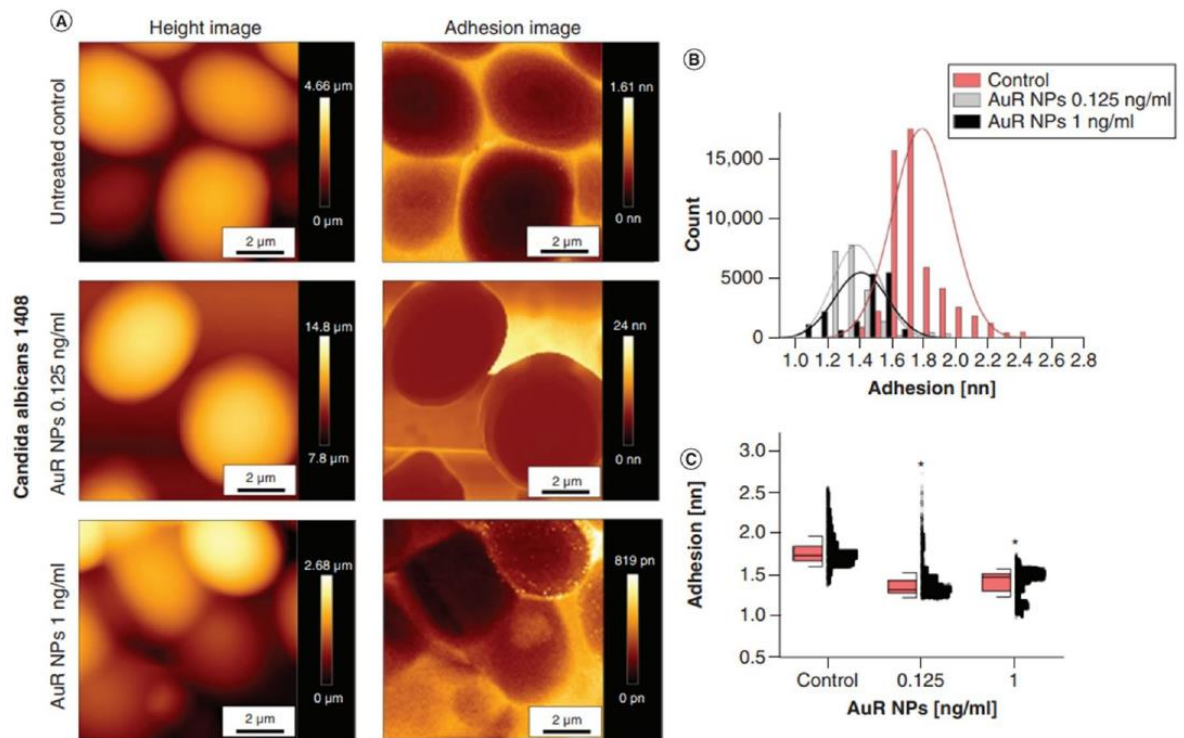 to control cells. * indicates statistical significance ($p < 0.05$) compared to untreated control. Reprinted with permission from [120]. 2022, Medical University of Bialystok.

Among other factors, antimicrobial activity is strongly influenced by the shape [107] and size [122] of nanoparticles, even for nanoparticles with the same surface-to-volume ratio. Typically, nanoparticles of smaller size have higher antimicrobial activity [123,124], but there are reports that larger nanoparticles are more effective, which may suggest that size alone is not the most important factor in their activity and toxicity [125] and, thus, it can be hypothesized that with certain metallic NP systems, antimicrobial activity may be largely controlled by the extent of electrostatic interactions with the microbial cell wall. In order to verify this hypothesis indicating shape influence on the activity of metallic nanoparticles, metallic NPs in different shapes were synthesized, then their antimicrobial activity was evaluated. Cheon et al. [126] synthesized Ag NPs with spherical, triangular plate and disk shapes in aqueous solution. Based on the zone of bacterial growth inhibition, the highest antibacterial activity was recorded for spherical Ag NPs, followed by disc shaped Ag NPs, while the lowest activity was recorded for triangular plate Ag NPs. The difference in antimicrobial activity of these Ag NPs was explained by the release rate of Ag ions from the surface. In another study by El-Zahry et al. [127] spherical, triangular and hexagonal Ag NPs of the same size were synthetized by chemical reduction. The results of this work show that hexagonal Ag NPs exhibit the highest antimicrobial activity compared to spherical and triangular NPs, which is associated with a larger surface area, allowing a stronger antimicrobial effect. In our research with metallic nanoparticles, we also observed shape-dependent activity of Au NPs. For ceragenin-containing gold nanoparticles in the shape of rods (AuR NPs@CSA-131), peanuts (AuP NPs@CSA-131) and

stars (AuS NPs@CSA-131), the antimicrobial activity of peanut-shaped gold nanoparticles was lower compared to those in rod and star shapes [117]. Another important factor governing the antimicrobial activity of NPs is their charge. Positively charged metallic nanoparticles are able to alter the function of the electron transport chain in bacteria, leading to the neutralization of the surface electrical charge of the bacterial membrane and altering its permeability, ultimately causing bacterial death [128]. However, there are some discrepancies regarding the activity of metallic nanoparticles against gram-positive and gram-negative bacteria. Some researchers reported that gram-positive bacteria are more sensitive to nanoparticles, due to the fact that the cell wall structure of gram-negative bacteria is more complex [129]. On the opposite side, researchers believe that gram-negative bacteria are more susceptible to antibacterial Ag nanoparticles due to the easier passage of Ag ions through the thinner cell walls [130].

The activity of metallic nanoparticles can be modulated by doping with suitable compounds, such as transition metals. Singh et al. evaluated how the antimicrobial activity of ZnO NPs doped with Fe, and CdS doped with Fe and Co would change. The results showed that Fe-doped ZnO nanoparticles exhibited decreased antibacterial activity against gram-negative bacteria, which could be due to the decrease in the positive surface charge carried by the nanoparticles, and also the change in the surface morphology of ZnO nanoparticles as a result of Fe doping, while Fe atom-doped CdS NPs increased the antibacterial activity of the nanoparticles with no change in the activity of cobalt-doped CdS NPs [131]. As a result of the doping of metallic nanoparticles with transition metals, changes in the NPs' charge and size were observed, which is a key factor in their antimicrobial activity. An increase in the antimicrobial activity of copper ferrite NPs doped with nickel [132] or Mg-doped ZnO nanoparticles [133] was also observed. In one of our studies, magnetic nanoparticles functionalized with gold displayed strong bacteriostatic activity against *Pseudomonas aeruginosa*. We assumed that the gold present on the surface of magnetic nanoparticles interacts with bacterial proteins through disulfide bonds, which can have a significant impact on the microbial cells metabolism and redox system of [134].

The antimicrobial properties of metallic nanoparticles can be improved by increasing the solubility of nanoparticles in aqueous media. By synthesizing silver nanoparticles using an aqueous solution of an extract from the plant *Pulicaria glutinosa*, it was determined how the solubility of Ag NPs affects their activity. The results indicate that with the increase in the solubility of silver nanoparticles obtained by increasing the concentration of the plant extract used for the synthesis (from 4% to 21%), a decrease in the values of the half maximal inhibitory concentration were observed against *Escherichia coli*, *Pseudomonas aeruginosa*, *Staphylococcus aureus* and *Micrococcus luteus* strains [135]. Although metallic nanoparticles exhibit high antimicrobial activity to effectively combat pathogens, their inherent characteristic of low solubility causes a significant loss of antimicrobial capacity and leads to increased toxicity [136], where solubility determines many important properties of nanoparticles, including their surface area, which makes it possible to control the interaction between nanoparticles and microorganisms [136].
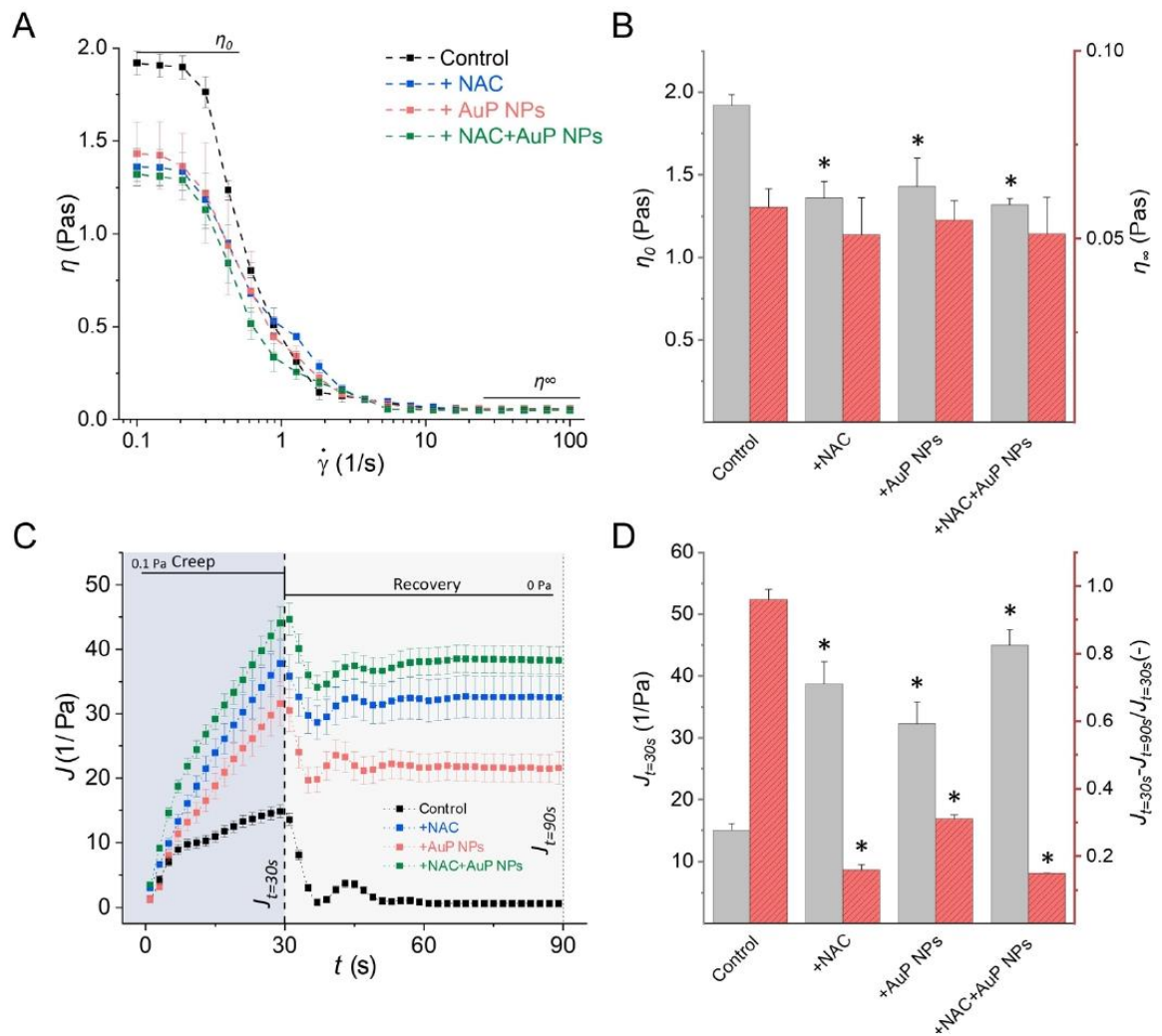
Figure 4. Rheological properties of *Pseudomonas aeruginosa* biofilm under the influence of N-acetyl-cysteine (NAC) and peanut-shaped gold nanoparticles (AuP NPs): (**A**) dynamic viscosity as a function of shear rate for control samples, and samples treated with tested compounds; (**B**) zero-shear viscosity $\eta 0$ and infinity-shear viscosity $\eta\infty$ determined from the viscosity curves; (**C**) compliance as a function of time in creep-recovery tests; (**D**) mean maximal creep compliance values (at 30 s Jt = 30 s) and the ratio of difference between Jt = 30 s and unrecovered creep compliance (at 90 s Jt = 90 s) to maximal creep compliance calculated from creep-recovery curves. * indicates statistical significance ($p < 0.05$) compared to untreated control. Infection and Drug Resistance 2022:15 851-871. Originally published by and used with permission from Dove Medical Press Ltd. [121].

The activity of metallic nanoparticles can also be governed by modulating their surface to improve their functionality as antimicrobial compounds. By functionalizing the surface of iron oxide nanoparticles with L-tyrosine, a significant difference in antimicrobial activity was observed between nanoparticles whose surface was modified, compared with non-functionalized iron oxide nanoparticles [137]. For the non-functionalized iron oxide nanoparticles, no antimicrobial activity was observed against *Staphylococcus aureus*

and *Salmonella typhimurium*, whereas the functionalized iron oxide nanoparticles showed antimicrobial activity against these strains, as a result of the formation by L-tyrosine functionalization of more stable NPs with different functional groups on the surface, providing a better binding interaction with microorganisms [138]. Nijonshuti et al. [139] compared the activity of Ag NPs and Ag NPs whose surface was functionalized with polydopamine (PDA). The results indicated that the PDA coating acted in synergy with Ag NPs, significantly increasing the potency of Ag NPs against bacteria, and suggest that higher valence/oxidation state increases the antimicrobial potency of Ag [140] and coordination between Ag and PDA mainly through the catechol group, which may play an important role in regulating the antimicrobial activity of PDA-Ag NPs [141]. In our study, as a result of the functionalization of the surface of gold nanoparticles with a cationic steroid antimicrobial (CSA), we obtained enhanced antimicrobial activity against gram-positive bacteria, gram-negative bacteria, and fungi, regardless of the resistance mechanism, as well as against microorganisms both in planktonic form and growing in biofilm as a result of the permeabilization of the cell membrane and release of protein content and generation of ROS [117,119,142]. Similarly, in the case of magnetic nanoparticles that were functionalized with compounds such as PBP10 peptide, 1,4-dihydropyridine, ceragenin, LL-37, chlorhexidine, increased antimicrobial activity of the functionalized nanoparticles was obtained compared with nanoparticles alone and compounds in the free form [143–147].

The antimicrobial activity of metallic nanoparticles is influenced by their method of synthesis. In a study by Garibo et al., silver nanoparticles synthesized by green synthesis using an extract from *Lysiloma acapulcensis* possessed higher antimicrobial potency than chemically produced Ag NPs. Antimicrobial activity was determined using the disk diffusion method and minimal inhibitory concentrations (MICs) and minimal bactericidal concentrations (MBCs) against four clinical strains: *Escherichia coli*, *Pseudomonas aeruginosa*, *Staphylococcus aureus* and *Candida albicans*. Both a larger zone of inhibition and lower MICs and MBCs of biogenic Ag NPs were observed in comparison with Ag NPs synthesized by the chemical method [148]. In the case of the study provided by Ghetas et al. the antimicrobial activity of biologically synthesized Ag NPs using an extract from *Origanum vulgare* and Ag NPs synthesized chemically was assessed. Using the disk-diffusion method, their activity against *Streptococcus agalactiae*, *Aeromonas hydrophila*, *Vibrio alginolyticus*, *Aspergillus flavus*, *Fusarium moniliforme*, *Candida albicans* was determined. Against both bacteria and fungi, the zone of growth inhibition and, thus, the antimicrobial activity was higher for biologically synthesized Ag NPs than for chemically synthesized Ag NPs [149]. Mohammad Musawi-Khattat et al. observed that besides higher antimicrobial activity of Ag NPs synthesized by green synthesis method compared to chemically synthesized Ag NPs, they also exhibited more desirable characteristics and biological activities such as narrow size range, spherical shape, high antioxidant and DNA cleavage activity [150]. Also in the case of gold nanoparticles, the green synthesis method results in higher antifungal activity and smaller size of the resulting nanoparticles compared to the chemical synthesis method [151]. Similarly, biosynthesized titanium and iron oxide nanoparticles were observed to have higher antimicrobial activity compared to chemically synthesized nanoparticles [152,153]. On the other hand, zinc nanoparticles synthesized by the chemical method had high thermal stability compared to ZnO NPs synthesized by the green synthesis method, while the antimicrobial activity was insignificantly higher for ZnO NPs prepared by the chemical method over by the green synthesis at 50 and 100 ppm, but no difference at 150 ppm against *Pseudomonas aeruginosa* and *Bacillus subtilis* with comparable activity against *Staphylococcus aureus* [154]. Recent studies on the antimicrobial activity of monometallic NPs are summarized in Table 1.

54

Table 1. Antimicrobial activity of monometallic NPs. Abbreviations: Au, gold; Ag, silver; Fe$_3$O$_4$, iron (II, III) oxide; Pd, palladium; TiO$_2$, titanium dioxide; ZnO, zinc oxide; Se, selenium.

NPs	Size (nm)	Synthesis	Pathogens	Mechanism of Action	Reference
Au	~37–53 (AuR), ~55–65 (AuP), ~243 (AuR)	Chemical reduction	Staphylococcus aureus, Staphylococcus epidermidis, Klebsiella pneumoniae, Klebsiella oxytoca, Pseudomonas aeruginosa	Induction of oxidative stress, increase of cellular membranes permeability, cell membrane depolarization, protein leakage from the bacteria, destruction of pathogen's membranes	[117]
Au	~37–53	Chemical reduction	Candida glabrata, Candida krusei, Candida albicans, Aspergillus fumigatus, Aspergillus flavus, Cladosporium herbarum, Fusarium oxysporum	disrupt the outer fungal membrane and increased permeability of Candida cells, the release of proteins from damaged Candida cells, ROS generation	[120]
Ag	~11–18	Green sythesis (plant)	Staphylococcus aureus	Disruption of membrane integrity and permeability, membrane depolarization, decline in efflux pump activity	[155]
Ag	~15–37	Green sythesis (plant)	Ralstonia solanacearum, Xanthomonas axonopodis pv. punicae	Generation of ROS, disruption of replication and DNA damage	[156]
Fe$_3$O$_4$	~9	Co-precipitate methods	Escherichia coli, Pseudomonas aeruginosa, Staphylococcus aureus, Candida albicans	Nonspecific interaction with membrane compounds, disorganization of lipid packing in the membrane of the microorganism, disruption of transport across the membrane, disruption of cell division	[157]
Pd	13–18	Biosynthesis (plant)	Staphylococcus auerus, Streptococcus pyogenes, Bacillus subtilis, Enterobacter aerogenes, Klebsiella pneumoniae, Proteus vulgaris	The cell membrane destruction and cell apoptosis	[158]
TiO$_2$	2–23	Laser ablation in liquid	Escherichia coli, Pseudomonas aeruginosa, Proteus vulgaris, Staphylococcus aureus	The interaction between NPs and the cell wall of the microorganism, leading to the microorganism oxidation and finally death	[159]

Table 1. *Cont.*

NPs	Size (nm)	Synthesis	Pathogens	Mechanism of Action	Reference
ZnO	15–30	Biosynthesis (plant)	*Staphylococcus aureus, Pseudomonas aeruginosa, Escherichia coli, Aspergillus niger, Aspergillus flavus, Aspergillus fumigates*	The production of ROS leading to DNA damaging, denaturation of proteins, rupture of enzymes, and depletion in antioxidant glutathione level causing the cell death	[160]
Se	~110	Biosynthesis (cow urine)	*Staphylococcus aureus, Escherichia coli, Klebsiella pneumoniae; Pseudomonas spp., Serratia marcescens, Proteus mirabilis*	The generation of ROS and proteins denaturation	[161]
Se	~55	Biosynthesis (plant)	*Bacillus subtilis, Escherichia coli*	The cell wall destruction, inhibiting cell wall synthesis or inactivating other cellular processes	[162]

2.2. Metallic Nanoparticles in Combination with Antibiotics

Due to the antimicrobial activity possessed by metallic nanoparticles, they can overcome resistance mechanisms such as: (i) reduced permeability of bacterial cells, (ii) enzymatic modifications of antimicrobial substance, (iii) modification within target sites/enzymes, (iv) active removal of antimicrobials by overexpression of scavenger pumps to escape the antimicrobial effect of antimicrobials, or (v) overexpression of an enzyme inactivated by an antimicrobial [163–165]. Additionally, the coupling of metallic nanoparticles with antibiotics shows synergistic effects against bacteria in planktonic, as well as biofilm forms or also against multidrug resistant strains [166,167]. When combined with optimally selected antibiotics, nanoparticles exhibit synergy and in the future may contribute to the reduction of the global crisis of emerging microbial resistance [168]. The benefit of this combination is an increase in antibiotic or fungicidal activity due to a synergistic effect, resulting in a faster antimicrobial action and, thus, reducing the possibility of the emergence of resistant microorganisms, as well as an antimicrobial action against biofilm-forming pathogens and an increase in the penetration of antimicrobial agents into cells and tissues [169]. It is also worth pointing out that metallic nanoparticles do not have much potential for the induction of microorganisms resistance [58,142] and that antibiotic resistance is of little relevance to nanoparticles, because the action of nanoparticles takes place through direct contact with the cell walls of pathogens without the need to penetrate microbial cells, or use of the specific pathogen's targets that might be modified by microbes in response to presence of nanoparticles [170].

Although broad-spectrum antibiotics and antifungal agents play a very important role in the control of bacterial and fungal infections, they also have a disadvantageous side to their use, namely, the selection and spread of resistance among many bacterial and fungal species and the deleterious effect they can have on the host microbiome [1,171–173]. Problems related to conventional antimicrobial therapy also include, but are not limited to, a narrow spectrum of antimicrobial activity, where the agent used is directed at a well-defined target of infection, or problems related to the safety and tolerability of the antimicrobial agent, which can cause harmful side effects such as toxicity or allergic reactions [174,175]. One of the major limitations of conventional antimicrobial therapy is also the inefficient delivery of drugs, where they may be non-specifically distributed in the body causing systemic side effects. In addition, there may be problems related to drug absorption and metabolism [176]. By increasing the potency of antibiotics by combining them with nanoparticles, it is possible to shorten the duration of treatment, reducing the concentration of administered drug to the patient, resulting in, among other things, in decreased systemic toxicity [177].

Colistin is considered as an antibiotic of last line of defense for the control of infections of some pathogens such as *Pseudomonas aeruginosa* resistant to all commonly used antimicrobial drugs. However, due to the dose-dependent side effects of colistin, the possibility of bacteria treating using colistin and seeking same therapeutic effect, but at a lower dose, is being sought. To achieve these goals, silver nanoparticles have been used in combination with colistin by Khaled et al. [178]. Additionally, the synergism of imipenem with Ag NPs was investigated. The synergistic effect of antibiotics with silver nanoparticles was determined against pandrug-resistant *Acinetobacter baumannii*. The results obtained indicate a synergistic effect leading to a reduction in the MIC values of colistin, imipenem and silver nanoparticles where a more than fourfold reduction was observed. Due to the synergistic effect of metallic nanoparticles with an antimicrobial agent, it is possible to target not only planktonic cells, but also cells growing within biofilm structure. Our research also confirms the synergism between metallic nanoparticles and antibiotics. As a result of the combination of the classical antibiotics such as vancomycin and colistin, synthetic ceragenins CSA-13 and CSA-131 and the human antimicrobial peptide cathelicidin LL-37 with core-shell magnetic nanoparticles against methicillin-resistant *Staphylococcus aureus* and *Pseudomonas aeruginosa*, an additive or synergistic effect was observed, as well as a strong suppression of biofilm

formation. The interaction of magnetic nanoparticles with bacterial cell wall compounds results in increased insertion and/or uptake of membrane-active agents such as colistin or vancomycin, destruction of the membrane and leakage of intracellular contents, as well as induction of oxidative stress by the magnetic nanoparticles, causing damage to bacteria cell' organelles [179]. Also, in the case of the combination of gold nanoparticles with tobramycin against tobramycin-resistant strains of *Pseudomonas aeruginosa*, a strong combinatorial effect of nanoparticles with an antibiotic was achieved, enabling the reduction of biofilm formation and, thus, increasing the effectiveness of antimicrobial therapies [121].

As a result of the combination of silver nanoparticles with amphotericin B and fluconazole, Ag NPs showed a synergistic effect with amphotericin B and fluconazole against biofilms formed by *Candida albicans*. As a consequence penetration of silver nanoparticles through the cell membrane due to their small size, the integrity of the membrane is disrupted, resulting in easy passage of drugs through the cell membrane leading to their action at the target site [180]. The metallic nanoparticles also showed high activity against fungal spores. Silver nanoparticles were synthesized by green synthesis using agro-waste material, strawberry leaf as reducing agents and completely large germination inhibition of *Botrytis cinerea* spores at 100 ppm as a result of the increased density of the solution, causing cohesion/sticking of the fungal hyphae [181]. In addition to the search for synergistic interactions between metallic nanoparticles and antimicrobial or fungicidal agents, other potential compounds are being explored to enhance the antimicrobial activity of the metallic nanoparticle-factor A complex. An example of this is the study by Al-Tawarah et al. of a synergistic interaction between silver nanoparticles and the essential oil of *Varthemia iphionoides*. The results showed a significant increase in antimicrobial activity of Ag NPs complex with essential oil against multi-drug resistant strains of *Enterobacter aerogenes*, *Pseudomonas aeruginosa*, *Staphylococcus epidermidis* and *Staphylococcus aureus*. The Ag NPs resulted in an increase in surface area, leading to greater surface contact with the bacteria and, thus, improved bactericidal activity, perforation and lysis of the bacterial cell wall, followed by generation of free radicals and DNA breakdown [182]. On the other hand, Abdelsattar et al. [183] evaluated the synergistic effect of silver nanoparticles with ZCSE2 phage against *Salmonella enteritidis*. Synergistically treating bacteria with a sublethal dose of Ag NPs enabled them to be readily lysed by phages even at low concentrations. As a result of the combination of Ag NPs and phages, a new prospect of nanoparticles with greatly improved antibacterial properties and therapeutic efficacy appeared.

Recent work on the synergistic effect of metallic nanoparticles in combination with antibiotics/fungicides and compounds other than antimicrobial agents is shown in Table 2.

Table 2. Antimicrobial activity of metallic NPs in combination with conventional antibiotics/fungicides or compounds other than antimicrobial agents. Abbreviations: Ni, nickel; Cu, Copper; Zn, zinc; AZI, azithromycin; GEN, gentamycin; OXA, oxacillin; CEFO, cefotaxime; NEO, neomycin; AMP, ampicillin; SUL, sulbactam; CEFU, cefuroxime; FOS, fosfomycin; CHL, chloramphenicol; OXY, oxytetracycline; ERY, erythromycin; CEP, cephacothin; CLI, clindamycin; TET, tetracycline; AMO, amoxycillin; CIP, ciprofloxacin; CEFP, cefpodoxime; CEFI, cefixime; KET, ketoconazole; STR, streptomycin; AMB, amphotericin B; FLU, fluconazole; PVA, polyvinyl alcohol; PAH, polyallylamine hydrochloride; H₂O₂, hydrogen peroxide; NAC, N-acetyl-cysteine; TOB, tobramycin.

NPs	Size (nm)	Synthesis	Pathogens	Mechanism of Action	Reference
Ag NPs, ZnO NPs in combination with: AZI, GEN, OXA, CEFO, NEO, AMP/SUL, CEFU, FOS, CHL, OXY	15–16 (Ag NPs), 187–188 (ZnO NPs)	biosynthesis (plant)	*Staphylococcus aureus, Salmonella enterica* subsp. *Bukuru, Escherichia coli, Candida albicans*	The electrostatic interaction between positively charged nanoparticles and negatively charged bacterial cell, release of ions, disruption the cellular respiratory chain, inhibition of unwinding of DNA, the ROS generation	[77]
Ag NPs in combination with: ERY, AMP, CHL, CEP, CLI, TET, GEN, AMO, CIP, CEFP, CEFU	~26	chemical reduction	*Staphylococcus aureus, Streptococcus mutans, Streptococcus oralis, Streptococcus gordonii, Enterococcus faecalis, Escherichia coli, Aggregatibacter actinomycetemcomitans, Pseudomonas aeruginosa*	The attachment to the bacterial cell membrane and pore formation, interacting with intracellular biomolecules such as DNA, cause inhibition of DNA replication leading to the cell death, disruption the respiratory chain, transport of hydrophilic antibiotics to the cell surface	[166]
Ag NPs, Ni NPs, Cu NPs, Zn NPs in combination with: CEFI	~17–41	chemical reduction, biosynthesis (plants)	*Salmonella typhi*	Change in the membrane permeability, ROS generation, ATP depletion, DNA damage and disruption, interaction with sulfur and phosphorus-containing molecules	[184]
Ag NPs in combination with: KET	11–19	chemical reduction	*Malassezia furfur*	The attachment and anchoring to the surface of the fungus, ROS generation, leading to structural changes and damage, such as permeability and the membrane potential, forming pores causing leakage of various substances, disrupting the activity of respiratory chain enzymes	[185]

Table 2. Cont.

NPs	Size (nm)	Synthesis	Pathogens	Mechanism of Action	Reference
Ag NPs in combination with: STR, AMB, FLU	11–15	biogenic synthesis	*Pseudomonas aeruginosa, Escherichia coli, Klebsiella pneumoniae, Bacillus cereus, Candida albicans, Candida glabrata*	The interaction with the bacterial cell wall, membrane damage, destruction the proton pump, blocking the metabolism and respiration, pores that disrupt the membrane electrical potential, ROS generation, DNA damage, depletion of glutathione, lipid peroxidation, release of Ag^+ ions, translation inhibition	[186]
Au NPs in combination with: colicin	35–70	green method	*Klebsiella pneumoniae*	No data	[187]
PVA@Ag NPs and PAH@Ag NPs in combination with: H_2O_2	11–15 (PAH@Ag NPs) 17–26 (PVA@Ag NPs)	chemical reduction	*Escherichia coli, Staphylococcus aureus*	The electrostatic interaction with the bacterial cell wall, ROS generation, disruption of bacterial cell membrane	[188]
Ag NPs in combination with: ebselen	2–24	biosynthesis (microbes and plant)	*Escherichia coli, Staphylococcus aureus*	The ROS generation, interruption of bacterial antioxidant system	[189]
ZnO NPs in combination with guava leaf extract	15–30	chemical reduction	*Escherichia coli*	No data	[190]
Au NPs in combination with: NAC, TOB	~44 (spherical NPs), ~60 (rod-shaped NPs), ~144 (star-shaped NPs)	chemical reduction	*Pseudomonas aeruginosa*	Induction of oxidative stress leading to subsequent permeabilization of microbial membranes and leakage of intracellular contents	[121]

2.3. Multimetallic Nanoparticles

Multimetallic NPs are nanoparticles composed of at least two different metals that form alloy or core-shells nanostructures. Multimetallic nanoparticles are of growing interest due to an increased spectrum of properties compared to monometallic NPs [191]. The bactericidal mechanism of action of multimetallic nanoparticles is usually related to the release of metal ions and the induction of oxidative stress, while non-oxidative mechanisms may also take place [191]. The joined action of various metals and metallic oxides in chemical transformation results in enhanced catalytic performance of multimetallic nanoparticles [192]. With regard to the synergistic effects between various metals, multimetallic NPs with bimetallic, ternary and quaternary combinations exhibit special features with improved chemical, optical and catalytic performance compared to mono- and bimetallic NPs [193].

By using a combination of metal compounds, it is possible to obtain synergistic antimicrobial properties of the newly synthesized compound compared to the properties of the individual components used alone. The antimicrobial activity of silver nanoparticles involves the anchoring and penetration of NPs in the bacterial cell wall while once inside the cell, they contribute to the formation of free radicals, generating intracellular oxidative stress and ultimately leading to cell death [194]. On the other hand, iron can interact with amino acids present in bacterial cell wall proteins, including the -SH groups of cysteine. The thiol side chain of cysteine has been shown to be the most susceptible to electron capture from oxidative species [195]. By synthesizing bimetallic silver and iron nanoparticles, Padilla-Cruz et al. [196] suggest that the mechanism of synergistic action of the two metals involved oxidation of the thiol side chains in cysteine leads to changes in protein structure, resulting in an increase in bacterial cell wall permeability and ultimately cell death (iron was responsible for this effect). As a result of the increased permeability of the cell wall, there is an increased influx of bimetallic nanoparticles into the cell. Eventually, with the release of silver ions into the cytoplasm, oxidative stress is induced, causing DNA changes and disruption of membrane morphology. In this way, synergistically acting silver and iron contribute to the destruction of cell structures, disruption of intracellular biological functions leading to cell death. In another study, Zhao et al. [197] noted that monometallic gold (Au), rhodium (Rh) and ruthenium (Ru) NPs did not cause disruption of bacteria cell structures of *Escherichia coli*, bacterial membranes treated with monometallic NPs had no visible damage. In contrast, the application of bimetallic gold- rhodium (Au-Rh) NPs and gold- ruthenium (Au-Ru) NPs caused significant changes in the cell membrane structure-cell membrane was dramatically ruffled and severely damaged, thus, can induce bacterial cell lysis, leading to leakage of cell substrates and bacterial death. The mechanism of action of the bimetallic nanoparticles also included a decrease in bacterial membrane potential and an increase in ATP and ROS levels. The above results suggest that monometallic nanoparticles (Au, Rh and Ru NPs) exhibit lower antimicrobial activity under the given experimental conditions (they do not cause noticeable changes in the cell membrane), compared to bi-metallic nanoparticles (Au-Rh and Au-Ru NPs), significant changes in the bacterial cell membrane were observed as a result of synergistic action of their constituent metals. Moreover, the application of bimetallic silver-platinum (Ag-Pt) NPs [198] not only killed the bacteria, but also limited their growth by reducing the density of bacteria, which shows that they are bacteriostatic agents; stopping bacteria from reproducing. The activity of multi-metallic nanoparticles covers a broad spectrum, not only against Gram-positive and Gram-negative bacteria, but also against multidrug resistant fungi such as *Candida auris*. Exposure of fungal cells to trimetallic silver-copper-cobalt (Ag-Cu-Co) NPs [199] influenced the level of apoptosis markers, manifested by phosphatidylserine translocation and collapse of mitochondrial membrane potential. The nanoparticles resulted in a direct inhibition of the cell cycle, arresting cells in the G2/M phase.

Some bacterial species have a remarkable ability to adapt to the administration of antibiotics by developing resistance mechanisms such as *Mycobacterium tuberculosis*, which is made possible by the rapid export of drugs from the cytosol. One of the targets of the silver and zinc oxide nanoparticles is to weaken the stability of the membrane, resulting in an increase in its permeability to antibiotics [200,201]. The use by Ellis et al. [202] of bimetallic nanoparticles in pulmonary delivery of antitubercular drugs to the endosomal system of *Mycobacterium tuberculosis*-infected macrophages in combination with rifampicin resulted in an increase in the potency of the antibiotic by as much as 76%, causing a decrease in the integrity of the *Mycobacterium tuberculosis* cell envelope due to the interaction of bimetallic nanoparticles with the mycobacterial envelope, which is reflected in an increase in its permeability. Due to this interaction, an increased penetration of rifampicin into the cytosol of the bacteria is possible, which results in an enhanced potency of the drug. The use of multi-metallic nanoparticles proved to be an effective drug delivery vehicle that can be used to transport TB drugs, among others, while increasing the potency of the drug [202].

Most bacterial infections are associated with biofilm formation, where the microbial cells that make up the biofilm structure have been shown to be 10–1000 times more resistant to antibiotics than planktonic cells [203]. As a result, it is necessary to develop new bactericides that can effectively combat biofilm-associated infections. One example of such agents represents the silver-platinum nanohybrids synthesized by Ranpariya et al. [204], which significantly inhibited bacterial biofilm formation and exhibited strong antimicrobial synergy when combined with antibiotics such as streptomycin, rifampicin, chloramphenicol, novobiocin, and ampicillin against strains of *Escherichia coli*, *Pseudomonas aeruginosa*, and *Staphylococcus aureus*. For example, they found that rifampicin activity in the presence of Ag-ZnO NPs increased as much as 15-fold against *Staphylococcus aureus*, while Ag-ZnO NPs inhibited biofilm against *Escherichia coli* and *Pseudomonas aeruginosa* by about 76%. Bimetallic nanoparticles Ag-Au NPs synthesized by the core-shell method [205] showed synergistic antimicrobial activity of bimetallic nanoparticles conjugated with doxycycline against *Pseudomonas aeruginosa* and *Escherichia coli*, where the combinatorial effect led to higher drug binding affinity and enhanced antimicrobial efficacy. Synergy of antibiotic with bimetallic nanoparticles may be the current approach with the most promise for the significant improvement of patients treatment with complicated skin infections.

Recent studies on the antimicrobial activity of multi-metallic NPs are summarized in Table 3. Quadrometallic nanoparticles, such as silver-copper-platinum-palladium (Ag-Cu-Pt-Pd) [206] or silver-platinum-gold-palladium (Ag-Pt-Au-Pd) [207], are also being synthesized, but so far no studies have been conducted on the antimicrobial properties of quadrometallic nanoparticles.

As a result of the generation of reactive oxygen species, the antioxidant defense system is disrupted, which leads to mechanical damage to the cell membrane. A large number of studies on multimetallic nanoparticles describe their mechanism of action as the adhesion of multimetallic NPs to microbial cells and destruction of the cell wall by interaction between the positively charged surface of multimetallic NPs and the negatively charged surfaces of pathogen cells, leading to the generation of ROS, the penetration of multimetallic NPs into the cell, causing damage to proteins and DNA, as well as oxidative stress [191]. Considering the wide spectrum of action of multimetallic nanoparticles, and the diversity of their mechanisms of action against pathogens, including multidrug-resistant strains, they may prove to be an effective tool to combat infections.

Table 3. Antimicrobial activity of multimetallic NPs. Abbreviations: Pt, platinum; CdO, cadmium (II) oxide; NiO, nickel(II) oxide; Fe_2O_3, iron(III) oxide; CuO, copper(II) oxide.

NPs	Size (nm)	Synthesis	Pathogens	Mechanism of Action	Reference
Au-Pt	1–3	chemical reduction (Turkevich method)	Candida albicans; Pseudomonas aeruginosa; Staphylococcus aureus	ROS generation	[208]
Ag-Au	3–40	chemical reduction	Xanthomonas oryzae; Magnaporthe grisea	The damage the bacterial cell wall and release of metal ions	[209]
Ag-Cu and Cu-Zn	80 (Ag-Cu), 100 (Cu-Zn)	biosynthesis (plant)	Alcaligenes faecalis, Staphylococcus aureus, Citrobacter freundii, Klebsiella pneumoniae, Clostridium perfringens	ROS generation	[210]
Au-Pt-Ag	35–40	biosynthesis (plant)	Staphylococcus aureus, Enterococcus faecalis, Escherichia coli, Candida albicans	Interaction with cell membranes (membrane disruption, changes in its permeability); ROS generation, inactivation of some enzymes; destruction of microbial DNA/RNA; lysis of microbial cells	[211]
CdO-NiO-Fe$_2$O$_3$	~7–28	self-combustion method	Escherichia coli, Pseudomonas aeruginosa, Moraxella catarrhalis, Staphylococcus aureus	The ROS generation, release of heavy-metal ions, interaction of nanoparticles with the cell wall of bacteria	[212]
CuO-NiO-ZnO	5–9	co-precipitation method	Escherichia coli, Staphylococcus aureus	The interaction between nanoparticles and bacterial cell wall. The bacterial cells are ruptured and cracked with the release of intracellular components	[213]
Ag-ZnO-TiO	80–140	sol-gel method	Escherichia coli	The inhibition the enzymes for ATP hydrolysis and expression of ribosomal proteins by hindering DNA replication of bacteria and ROS generation	[214]

63

2.4. Metallic Nanoparticles as Carriers for Molecules with Antimicrobial Activity

Metallic nanoparticles have great potential in medicine as carriers of small molecules such as drugs, genes, proteins, and enzymes [215–217]. The efficacy of some antibiotics can be enhanced by increasing the cell permeability or weakening the cell envelope, therefore, when metal nanoparticles are combined with antibiotics, they can show better efficacy in certain therapies by reducing the side effects associated with individual drug [218]. Functionalization of antimicrobial agents with nanoparticles is one of the strategies used to enhance the efficacy of drugs against pathogens.

Functionalization of metallic nanoparticles with antimicrobial agents enables strong antimicrobial activity as a result of enhanced ability to penetrate biological membranes. Penetration of hydrophobic antimicrobials is limited by the highly polar environment within bacterial membranes, which impairs their activity [73]. Metallic nanoparticles interact with the bacterial cell membrane through electrostatic, hydrophobic, receptor-ligand interactions or van Der Waals forces, leading to a change in the cell membrane potential and bacterial integrity [219,220]. Due to the high surface-to-volume ratio and the possibility of loading the metallic NPs onto the surface with a high concentration of antimicrobial agent, increased permeability towards the biological membrane or higher uptake by the bacterial cell, the effective delivered concentration of antimicrobial agent is increased [221,222]. As a result of the increased porosity of the pathogen's structure, antibiotic molecules conjugated with metallic NPs gained easy access to the bacterial cell. The hypothesis proposed by Shaikh et al. is that conjugation on the surface of nanoparticles can result in increased concentrations of the administered antibiotic, which is able to saturate antibiotic-degrading enzymes and inhibit the growth of resistant bacterial strains containing degrading enzymes [222]. On the other hand, Sreedharan et al. proposed a hypothesis regarding the increased permeation of ciprofloxacin (AuF NPs@ciprofloxacin) bound on the surface of gold nanorods by: (i) the binding of AuF NPs@ciprofloxacin to the cell wall or membrane of the microorganism resulting in the release of carried drug within the cell wall or membrane or (ii) the nanoparticle-antibiotic complex binds to the bacterial cell wall that may serve as a reserve for the continuous release of the antibiotic, which could then penetrate into the microorganisms [223]. In addition, efflux pumps, whose activity is increased in antibiotic-resistant bacterial cells, play an important role in multidrug resistance, whereby antimicrobials are actively transported outside the bacterial cells [224]. As a result of the functionalization of metallic nanoparticles with agents with antimicrobial activity, it is possible to block the efflux pump, increasing the accumulation of antibiotics inside bacterial cells [225]. Brown et al. showed that gold nanoparticles functionalized with ampicillin were observed to block the efflux pump and the multivalent presentation of ampicillin were the reason for the more effective action of the functionalized gold nanoparticles versus the antibiotic compared with the antibiotic alone [226].

Another advantage of the functionalization of metallic nanoparticles is the improved stability of the metallic NPs-antimicrobial agent. Higher stability and antimicrobial activity under conditions such as room temperature, UV exposure or heat stress (increasing temperature up to 90 °C) was reported for the conjugate of Au NPs with ampicillin, streptomycin and kanamycin compared to the free forms of the antibiotics (except for Au NPs@ampicillin, where at room temperature the conjugated ampicillin was precipitated out of solution) [227]. Metallic nanoparticles are also a good carrier, providing high antimicrobial peptide (AMP) activity in the presence of proteases and enzymes [228]. The stability of metallic nanoparticles in different buffer solutions and biological fluids such as water, Dulbecco phosphate buffered saline (DPBS, in different pH range) in various concentrations of NaCl and in the presence of fetal bovine serum confirms that they are a promising approach in drug delivery [229].

An important aspect of antimicrobial drug delivery based on metallic nanoparticles is the improvement in the pharmacokinetic properties of the drug in the form of increased solubility of poorly soluble drugs, prolonged drug half-life and systemic circulation time, as well as prolonged and stimulus-controlled drug release, resulting in lower dosage and drug frequency, reducing the toxic effect of the drug [163]. By functionalizing the surface of metallic nanoparticles with antimicrobial agents, it is possible to overcome their poor solubility and aggregation in solution, thereby achieving an increase in antimicrobial efficacy and a decrease in cytotoxicity [230,231]. Metallic nanoparticles as carriers for antimicrobial agents can protect drugs from premature degradation and sustain drug release in order to result in prolonged half-life and bioavailability [232]. The conjugation of gentamicin with gold nanoparticles confirms that metallic nanoparticles are a very good carrier for continuous release of the antibiotic over a few days, making it possible to reduce the number of administrations [233]. By coupling antimicrobial agents to metallic nanoparticles, it is also possible to improve antimicrobial properties and overcome resistance mechanisms among microorganisms. Our research confirms that metallic nanoparticles are an effective carrier for antimicrobial agents. When conjugated to gold nanoparticles with ceragenins, they show higher antimicrobial activity against both multidrug-resistant strains regardless of resistance mechanism [117], strains causing otitis media [119] and fungal strains [142]. In addition, the magnetic nanoparticles prove to be a very good carrier for the PBP10 peptide, which shows good antimicrobial activity against both planktonic and biofilm forming of bacteria and fungi [143]. Also, the conjugation of 1,4-dihydropyridine on the surface of magnetic nanoparticles significantly increases antimicrobial activity compared to nanoparticles alone which is due, among other things, to the high affinity of the nanosystems for microbial cell wall components, while antimicrobial activity is still high in the presence of human body fluids such as serum, saliva, cerebrospinal fluid or abdominal fluid [144]. A microorganism that is originally resistant to a given antimicrobial agent becomes susceptible to the nanosystems conjugated with metallic nanoparticles. Carbapenem-resistant *Acinetobacter baumannii* was found to be sensitive to conjugated Ag NPs with imipenem [234], where were observed (i) reversal of drug resistance by protecting the β-ring of carbapenem from hydrolysis by metallo-β-lactamases (MBLs) through zinc ion chelation of MBLs, resulting in the deactivation of MBLs, and (ii) enhanced antibacterial efficacy with increased production of reactive oxygen species and membrane damage, (iii) effects on cell wall formation and metabolic pathways, as well as the downregulation of ompA gene expression, which can mediate fibronectin-mediated attachment to host cells and induce the biofilm formation. Despite the presence of beta-lactamase and carbapenemase resistance genes in *Acinetobacter baumannii*, the combination of AgNPs with imipenem is effective antimicrobial agent against carbapenem-resistant strains, showing potent antimicrobial activity [235]. Ampicillin-resistant *Escherichia coli* also proved to be sensitive after exposure to ampicillin-conjugated gold nanoparticles, where an accumulation of Au NPs@ampicillin on the bacterial cell surface was observed, resulting in the formation of pores in the bacterial membrane, allowing the nanoparticles to penetrate the interior of pathogen cells [236]. The results obtained by Memarian et al. confirm that the fluconazole-resistant strain became sensitive to Au NPs@fluconazole. The MIC value for fluconazole alone was 64 μg/mL, while that for the tested nanosystem was 2 μg/mL [237].

Another advantage of functionalizing metallic nanoparticles with antimicrobial agents is the reduction of toxic effects where using nanoparticles as carriers for drug delivery not only improves efficacy, but it also enables a reduction in adverse effects compared to conventional therapy. Functionalization of gold nanoparticles with ciprofloxacin resulted in lower hemolytic activity of Au NPs@ciprofloxacin than the antibiotic in free form thereby reducing the toxicity of the antibiotic [238]. Similarly, conjugation of amphotericin B (AMB), which exhibits nephrotoxicity due to its poor water solubility and aggregation on the surface of gold nanoparticles allowed the negative effects to be reduced, resulting in a water-soluble covalent gold nanoparticle conjugate with AmB with increased antimicrobial efficacy and reduced cytotoxicity [230]. Our studies also confirmed that conjugated ceragenins, peptide LL-37 chlorhexidine and polyene antibiotics (amphotericin B and nystatin) on the surface of magnetic nanoparticles showed not only lower toxicity, but also increased antimicrobial activity compared with antimicrobial agents in a free form, which is a very promising approach to reduce the side effects of conventional therapies and increase the success of therapies [145–147,239].

By functionalizing metallic nanoparticles with specific antibodies, it is possible to obtain a system that might serve for rapid identification of the pathogens and target treatment to combat infection. Gold and silver nanoparticles conjugated with antibodies specific for *Staphylococcus aureus* peptidoglycan are proving to be a promising treatment method, which can be used alone or in addition to existing conventional antibiotic therapy to achieve complete eradication of the pathogen by means of which extended and selective bacterial death can be achieved [240–242]. Also, the conjugation of antibodies to protein A on the surface of gold nanoparticles both in vitro and in vivo in a mouse model resulted in a significant reduction in the viability of methicillin-resistant *Staphylococcus aureus* (MRSA) cells and the ability of the antibody-nanoparticle conjugate to selectively kill pathogens in an animal model [243]. Goat anti-*Escherichia coli* O157:H7 antibodies were also successfully conjugated on the surface of silver nanoparticles, which effectively bind to the target pathogen [244]. An important aspect of the successful treatment of infections is the correct identification of the pathogen. Hashemi et al. confirmed that with rabbit antibodies to *Candida* and *Gardnerella* species, it is possible to correctly identify vaginal infections with very high sensitivity and specificity [245].

Recent studies on the antimicrobial activity of metallic NPs functionalized with antibiotics/fungicides or compounds other than antimicrobial agents are summarized in Table 4.

Table 4. Antimicrobial activity of metallic nanoparticles functionalized with antibiotics/fungicides or compounds other than antimicrobial agents. Abbreviations: STR, streptomycin; AMP, ampicillin; Au NFs, gold nanoflowers; CIP, ciprofloxacin; IMI, imipenem; GNRs, gold nanorods; FLU, fluconazole; CAS, caspofungin; Fe_2O_3, iron(III) oxide; AMB, amphotericin B; NYS, nystatin; ZrO_2, zirconium dioxide; GA, glutamic acid; CuO, copper(II) oxide; GLYMO, (3-glycidyloxypropyl)trimethoxysilane; 4-HPBA, 4-hydroxyphenylboronic acid; CH, chitosan; PVP, polyvinylpyrrolidone; MPA, 2-mercaptopropanoic acid; CHX, chlorhexidine; Fe_3O_4 NPs@NH_2, aminosilane-functionalized iron(II,III) oxide nanoparticles.

NPs	Size (nm)	Synthesis	Pathogens	Mechanism of Action	Reference
Ag NPs@STR	~31–119	green synthesis	*Escherichia coli, Staphylococcus aureus*	The interaction between NPs and microorganism's cell wall	[218]
Au NPs@AMP	25–50	chemical reduction	*Escherichia coli, Bacillus subtilis, Staphylococcus aureus, Flavobacterium devorans*	The interaction between positively charged nanoparticles and negatively charged bacterial cell, disruption of bacterial membrane integrity, enhanced entry of antibiotic, inhibition of the bacterial proliferation	[236]
Au NFs@ CIP	No data	adsorption method	*Bacillus subtilis, Staphylococcus aureus, Escherichia coli, Pseudomonas aeruginosa*	The interaction between nanoparticles and bacterial cell wall, release of the carried drugs	[223]
Ag NPs@IMI	~63–65	co-reduction method	*Pseudomonas* spp.	The assembly on the bacterial surface, reduction of the expression of Verona imipenemase (VIM) and Imipenemase (IMP) genes involved in resistance, changes in morphology: chromatin condensation and fragmented nuclei	[246]

Table 4. *Cont.*

NPs	Size (nm)	Synthesis	Pathogens	Mechanism of Action	Reference
GNRs @FLU	72–75	chemical reduction	*Candida albicans*	Conjugating fluconazole with AuR NPs enhanced the delivery efficiency of fluconazole to the cell wall of the fungal cells and accelerated their cellular uptake	[247]
Au NPs@CAS	30–50	chemical reduction	*Candida* spp.	The membrane damage as well as cell wall and cell death	[248]
Fe_2O_3 NPs@AMB, Fe_2O_3 NPs@NYS	12–16 nm (Fe_2O_3 NPs@amphotericin B), 13–17 nm (Fe_2O_3 NPs@nystatin)	co-precipitation (Massart method)	*Candida* spp.	Membrane disruption, induction of oxidative stress	[239]
ZrO_2 NPs@GA	~2.5	solvothermal method	*Rhodotorula mucilaginosa, Rothia dentocariosa, Streptococcus mitis,* and *Streptococcus mutans*	The interaction between nanoparticles and pathogen cell wall or cellular constituents	[249]
CuO NPs@ GLYMO/4-HPBA	117–125	precipitation method	*Escherichia coli, Rhodococcus rhodochrous*	The ROS generation, leading to peroxidation of lipids from the bacterial cell membrane, interaction ROS with the cell organelles, electrostatic interaction between nanoparticles and bacterial cell wall, release of free Cu^{2+} ions	[250]
Ag NPs@CH	13–42	green synthesis	*Staphylococcus aureus, Pseudomonas aeruginosa, Candida albicans*	The electrostatic interaction between nanoparticles and bacterial cell wall leading to the leakage of the intracellular components, penetration the cell wall of the fungus and interaction with sulfur-containing membrane proteins and phosphorus-containing DNA nitrogenous bases	[251]

Table 4. Cont.

NPs	Size (nm)	Synthesis	Pathogens	Mechanism of Action	Reference
AgNPs@PVP	6–10	chemical reduction	*Acinetobacter baumannii*	The ROS generation, changing the expression level of proteins	[252]
Au NPs@ MPA-cationic dipeptide	10–14	chemical reduction (Turkevich method)	*Escherichia coli, Staphylococcus aureus, Candida albicans, Candida glabrata*	The disruption of the cell wall	[253]
Fe_2O_3 NPs@CHX	10–14	co-precipitation (Massart method)	*Staphylococcus aureus, Enterococcus faecalis, Escherichia coli, Pseudomonas aeruginosa, Candida spp.*	Depolarization of mitochondria, induction of oxidative stress and oxidation of pathogen structures	[147]
Fe_3O_4 NPs @Au, Fe_3O_4 NPs @NH_2	10 (Fe_3O_4 @Au), 13 (Fe_3O_4 @NH_2)	co-precipitation (Massart method)	*Pseudomonas aeruginosa*	Attach to the bacterial membrane and loss of its integrity, electrostatic interactions with the bacterial cell wall resulting in damage to the cell wall, increased membrane permeability, perforation of the plasma membrane, disruption of cell metabolism	[134]

3. Biocompatibility of Metallic Nanoparticles

An important aspect of the biomedical application of various types of nanoparticles is biocompatibility, i.e., the property of a substance determining its correct functioning in a living organism, which should show a lack of toxicity, not affect the body's immune system and do not induce hemolysis. In order to ensure the effective and safe use of nanomaterials, the interactions between the nanoparticle and the cells of the host must be considered, with particular attention being paid to the environment in which the test compounds act. A great number of information/trends regarding the toxicity of nanoparticles are obtained in cancer research and in studies that are not focused on antimicrobial activity. On the basis of such studies, certain effects can be expected, even their possible therapeutic potential [254,255]. The toxicity of nanoparticles is highly affected by their physical and chemical properties, such as shape, size, surface area and charge or catalytic activity [256].

Therefore, different methods are used to assess the biocompatibility of nanoparticles, ranging from quantitative assays using conversion of compounds such as 3-(4, 5-dimethylthiazol-2-yl)-2, 5-diphenyltetrazolium bromide (MTT) [257], 2, 3-bis-(2-methoxy-4-nitro-5-sulfophenyl)-2H-tetrazolium-5-carboxanilide (XTT) [258] or lactate dehydrogenase (LDH) [257], through qualitative studies (live and/or dead cell staining assays using dyes such as calcein-AM with propidium iodide [259] and dual acridine orange/ethidium bromide staining [260]) and finally blood hemolysis assays [261] and animal model [262] to assess biocompatibility.

A very important factor associated with the toxic properties of metallic nanoparticles is their size. Due to their small size, NPs have a much larger surface area per unit mass compared to their bulk counterparts, which translates into higher reactivity, which is associated with a higher risk of cytotoxic effects. As their size decreases, the number of metal atoms per surface area increases exponentially, resulting in higher reactivity of nanoparticles in biological systems [263]. Due to their small size, many nanoparticles are able to bypass or cross the blood-brain barrier where they can reach and accumulate in the brain parenchyma, including the striatum and hippocampus [264]. Depending on the size of the nanoparticles, a differentiated subcellular distribution is observed in the accumulated organs. In a study provided by Lopez-Chaves et al. gold nanoparticles with three sizes of 10 nm, 30 nm, 60 nm were observed to accumulate. Au NPs of 10 nm in size gathered within the cell nucleus, while particles larger than 10 nm in the cytoplasm [265]. Xia et al. determined the effect of cytotoxicity of gold nanoparticles depending on their size (5, 20 and 50 nm) against HepG2 cancer cells and healthy L02 cells, where Au NPs of 5 nm size showed higher cytotoxicity than those of 20 and 50 nm size. In contrast, in mouse in vivo studies, 50 nm Au NPs showed the longest circulation in the blood and the highest distribution in the liver and spleen, while 5 nm Au NPs caused an increase in neutrophil counts and little hepatotoxicity in a mice [266]. In addition, the size of metallic NPs may determine the aggregation process. Results presented by Wozniak et al. showed that 4–28 nm Au nanospheres aggregate at high concentrations and long incubation times increasing cytotoxicity in contrast to larger 130 nm star-shaped Au nanoparticles, which are rather monodisperse and non-toxic [267].

With the help of changing the shape of nanoparticles, it is possible to modulate their cytotoxicity. Nanoparticles can have different shapes and geometries including spheres, ellipsoids, cylinders, stars, octahedral sheets, cubes, spikes, rods, triangles, prisms, which significantly affects their toxicity. The star-shaped AuNPs had the highest anticancer potential but also exhibited the highest cytotoxicity, while the spheres of AuNPs, which were the least cytotoxic, showed weak anticancer activity [268]. Lee et al. synthesized chitosan-coated gold nanoparticles in the shape of nanospheres, nanostars and nanowires and determined the effect of their shape on cytotoxicity against human hepatocyte cancer cells (HepG2). Cytotoxicity was highest for Au NPs in the shape of nanorods, followed by nanostars and lowest for nanospheres [269]. Whereas Wozniak et al. performed the synthesis of Au NPs with different shapes: spherical (~10 nm), nanorods (~41 nm), nanoprisms

(~160 nm), nanostars (~240 nm) and nanoflowers (~370 nm) against cancer cells—HeLa and normal cells—HEK293T. The obtained results indicated that spherical and rod-shaped Au NPs were found to be more toxic than star-, flower- and prism-shaped Au NPs, which the authors suggest may be due to the aggregation process and their small size. The above results indicate that the selection of the appropriate shape for the synthesis of metallic nanoparticles affects their cytotoxic activity [267]. Our results provided information that ceragenin-functionalized gold nanoparticles (CSA-13, CSA-44 and CSA-131) with the peanut-shape induce the greatest hemolysis compared with rod- and star- shaped [117,142], while non-functionalized gold nanoparticles in rod-shaped induced slightly greater hemolysis compared to peanut-shaped Au NPs.

The toxicity of nanoparticles may also depend on their chemical composition. The degradation of nanoparticles that can occur depends on environmental conditions, such as a change in pH, ionic strength, or ionic valence, resulting in the leakage of metal ions from the core of metallic nanoparticles [270]. The resultant release of metal ions, such as silver, cobalt, chromium, or nickel, is toxic to cells and causes cell damage, whereas the release of metal ions from the nanoparticles alters the bioactivity and thus the toxic effect of the nanoparticle-metal ion complex [271]. Free ions can cause, among other things, oxidative stress with the release of cytokines [272]. In turn, other metal ions such as iron or zinc, which are the main micronutrients necessary for the proper functioning of the body, however, as a result of exceeding a certain concentration can adversely affect the functioning of cells by negatively affecting cellular pathways and thus cause high toxicity. The toxic effect of released metal ions can be reduced by using, among other things, appropriate surface modifications, thanks to which their properties can be improved and such system can be stabilized by preventing the release of ions from the interior, preventing oxidation of nanoparticle surface and inhibiting aggregation and subsequent agglomeration of nanoparticles [273]. Results obtained by Soenen et al. indicated that coating silver nanoparticles with a thin layer of SiO_2 minimized their toxicity as a result of blocking ion release and bacterial and/or cell contact. In addition, the composition of the core can be changed by the addition of other metals, thereby achieving increased chemical stability against degradation of the metallic nanoparticles and consequently against unwanted leakage of metal ions into the body [274].

The surface charge of nanoparticles plays an important role in their toxicity, as it determines to a large extent the interaction of nanoparticles with biological systems [275]. The relationship between high toxicity and positive charge on the surface of NPs is explained by their ability to penetrate into cells resulting from electrostatic interactions between negatively charged cell membrane glycoproteins and positively charged NPs, where in the case of neutrally or negatively charged NPs such interactions are not observed [256]. The surface charge of metallic nanoparticles can be modified by non-covalent modification of the nanoparticle surface by coating or wrapping with biological molecules to make more biocompatible NPs using polymers, peptides, proteins, or surfactants. The second way to modify the surface charge are covalent modifications involving the formation of chemical bonds between functional groups present on the nanoparticle surface and other biological molecules attached to that surface such as polyethylene glycol, peptides, or carbohydrates [276]. Chen et al. performed the synthesis of copper oxide nanoparticles modified with the polymers polyethylene glycol (PEG), polyvinylpyrrolidone (PVP), polydopamine (PDA) and polyvinyl alcohol (PVA) to determine the effect of surface modification of nanoparticles on their antimicrobial activity against *Escherichia coli*. The positive surface charge of CuO-PVP NPs enhanced antibacterial activity through electrostatic interactions with negatively charged surfaces of *Escherichia coli*. The authors concluded that the positive surface charge of CuO-PVP NPs resulted in enhanced antibacterial activity through electrostatic interactions with negatively charged *Escherichia coli* surfaces. It was also observed that the weakly negatively charged CuO-PDA NPs achieved better antibacterial activity, which the authors explain by the presence of lipophilic catecholamine structures on the nanoparticle surfaces, which enabled interaction with the lipid bilayer in the outer membrane of *Escherichia coli* [277]. In addition, Abbasadegan et al. synthesized silver

71

nanoparticles, obtaining three different electrical surface charges: positive, neutral and negative and determined the antibacterial activity of the nanoparticles. The authors concluded that the surface charge of Ag NPs was a significant factor affecting the bactericidal activity, where positively charged nanoparticles showed the highest bactericidal activity against both Gram-positive and Gram-negative bacteria, negatively charged nanoparticles showed the least antibacterial activity and neutral nanoparticles had intermediate activity [56].

The biocompatibility of metallic nanoparticles is also influenced by the method of synthesis and its conditions. Using the MTT assay, Amooaghaie et al. determined the toxicity of silver nanoparticles synthesized by two methods: green synthesis using *Nigella sativa* extract and chemical synthesis against bone-building stem cells of mice. The toxicity of the green synthesized Ag NPs was significantly lower than that of the chemical synthesized Ag NPs after 24, 48 and 72 h. After 72 h exposure of cells to the test compounds at a concentration of 0.2 mg/L, more than an 11-fold decrease in the number of viable cells was observed for chemically synthesized Ag NPs compared to Ag NPs synthesized by the green synthesis method [278]. Ghetas et al. determined the toxicity of chemically and biologically synthesized silver nanoparticles by means of a hemolysis assay using on chicken and goat red blood cells. The results indicate that chemically synthesized Ag NPs are in most cases more hemolytic than biologically synthesized Ag NPs [149]. Similarly, in the case of FeO NPs, the nanoparticles obtained by green synthesis are more biocompatible than the counterpart synthesized by the chemical method [279]. Slightly different results were obtained by Kummara et al. where, following exposure of non-small cell lung cancer cells (NCI-H460) and normal human skin fibroblast cells (HDFa) to silver nanoparticles by green synthesis and chemical methods, these biosynthesized Ag NPs were found to be more toxic than chemically synthesized Ag NPs. Both lower cell viability and greater inhibition of the cell proliferation were observed when exposed to green synthesized Ag NPs [280].

4. Metallic Nanoparticles—Development of Microbial Resistance and Their Impact on the Host Microbiome

Due to the rapid spread of resistance among microorganisms [281], a very important aspect of the potential use of metallic nanoparticles is whether pathogens can become resistant to them, and how quickly. Due to the different mechanisms of action of nanoparticles, pathogens do not easily acquire resistance with regard to the need to develop multiple mutations [52,99]. There are reports that metallic nanoparticles do not induce the development of resistance. Xie et al. synthesized quaternary gold nanoclusters coated with quaternary ammonium and did not observe an increase in the MIC for *Staphylococcus aureus* after 30 days of exposure [58]. Zheng et al. also observed no change in MIC values after 30 days of passaging *Staphylococcus aureus* with cercaptopyrimidine-conjugated gold nanoclusters. The results of our induction of resistance in *Candida* strains exposed to ceragenin-functionalized gold nanoparticles over 25 passages also confirmed the low potential for resistance development among fungi [142]. On the other hand, another published study investigated whether microorganisms may develop defense strategies to cope with the antimicrobial effects of metallic nanoparticles. Adaptive defense mechanisms include reduced uptake/adsorption of metallic NPs, where an important role is played by porins involved in the transport of ions through outer membranes to the periplasmic space, from which they undergo specific transport across the cytoplasmic membrane to the cell interior. As a result of the down-regulation of porins, it is possible to reduce the destructive effect of metal ions and, thus, pathogens become less susceptible to metallic nanoparticles [282,283]. Another defense mechanism is the increased pumping of metal ions to the interior of the cell. Thus, the exposure of pathogens to metallic nanoparticles might results in the upregulation of genes encoding efflux pumps [282,284]. It should be noted that due to the upregulation of genes encoding a wide variety of efflux systems, it is also possible to remove antibiotics from inside of the cell as well, and therefore develop resistance not only to metallic nanoparticles but also to other antimicrobial agents. The enhanced detoxification

of reactive oxygen species is also one mechanism. As a consequence of the exposure of pathogens to metallic nanoparticles, an increase in the expression of genes encoding ROS scavenging systems has been noted [285,286]. Furthermore, as a result of biofilm formation, a physical barrier is formed which impedes the penetration of metallic nanoparticles so that pathogen cells are exposed to lower doses of nanoparticles and are able to become resistant to the acting agent [287]. In respect of the influence of sublethal doses on the bacterial biofilm, Ouyang et al. [288] and Yang et al. [289] concluded not only the induction of quorum sensing gene expression and LPS (lipopolysaccharide) biosynthesis, but also the release of signaling molecules by *Pseudomonas putida* and *Pseudomonas aeruginosa* PAO1, respectively.

Another important aspect of metallic nanoparticles including, Ag NPs, TiO$_2$ NPs and ZnO NPs, is that they potentially interfere with the intestinal microbiome that can compromise the host health [290,291]. At the beginning, it should be mentioned that NPs may affect a complex of gastrointestinal (GI) environment. The non-absorbed fractions of NPs accumulate in the intestine and can indirectly affect the intestinal microbiota occurring within the gut lumen, as well as the mucus layer lining the epithelial surface. Subsequently, a portion of the NPs may translocate via the epithelial barrier and can be potentially captured by the intestinal immune cells (e.g., macrophages and dendritic cells) until reaching systemic circulation [290]. It should be explicitly underlined that intestinal microbiota plays a crucial role in numerous physiological functions as an indispensable element for host health. Apart from their contribution in the digestion of dietary fiber or the production of essential metabolites for the host, gut microbiota also participates in the maintenance of structural integrity of the mucosal barrier, the control of the immune response, and the protection against pathogens [290,292]. The intestinal microbiota consist of trillions of microorganisms comprising bacteria, viruses, fungi, archaea and protozoa [290,291,293]. It is estimated that in adults, the gastrointestinal tract (GIT) tract harbors 100 trillion bacteria, involving a minimum of several hundred species and more than 7000 strains [290]. Notably, 80% of fecal microbiota in a healthy adult representing the three dominant phyla i.e., Bacteroidetes, Firmicutes, and Actinobacteria [290,291]. Whereas other species are classified to the phyla Proteobacteria, Verrucomicrobia, Fusobacteria and Cyanobacteria [290]. A summary of the findings of research evaluating the impact of NPs on the intestinal flora is presented in Table 5.

Table 5. The influence of NPs such as Ag, TiO$_2$ and ZnO on the intestinal microbiota. Abbreviations: Ag, silver; TiO$_2$, titanium dioxide; ZnO, zinc oxide; F/B, Firmicutes/Bacteroidetes: ↑, increased bacteria; ↓ decreased bacteria.

NPs	Effect	Reference
Ag	↓ Firmicutes ↑ Bacteroidetes ↓ *Lactobacillus* ↑ *Bifidobacterium*	[291,294]
	↑ F/B ratio with dose ↑ *Coprococcus* ↑ *Lactobacillus* ↑ *Blautia* ↓ *Bacteroides* ↓ *Mucispirillum*	[291,295]
	↓ F/B ratio ↑ *Alistipes* ↑ *Bacteroides* ↑ *Prevotella* ↓ *Lactobacillus*	[291,296]

73

Table 5. *Cont.*

NPs	Effect		Reference
TiO$_2$	↓ Bacteroidetes i.e., *Bacteroides ovatus* ↓ *Eubacterium rectale* ↓ *Faecalibacterium prausnitzii* ↓ *Roseburia faecalis* and *Roseburia intestinalis* ↓ *Ruminococcus torques* ↑ *Escherichia col* i↑ *Raoultella* (sp.)		[290,297]
	↓ *Bacteroides ovatus* ↑ *Clostridium cocleatum*		[291,298]
	No considerable effect on gut microbiota. Microbial composition and GIT histology remained unchanged.		[291,296]
	↑ *Lactobacillus reuteri* ↓ *Romboutsia*		[291,299]
	↓ *Bacteroides ovatus* ↑ *Acidaminococcus intestini* ↑ *Clostridium cocleatum* ↑ *Eubacterium rectale* and *Eubacterium ventriosum*		[290,298]
ZnO	↑ Streptococcus ↓ *Lactobacillus*	Ileum	[290,291,300]
	↑ *Lactobacillus* ↓ *Oscillospira* ↓ *Prevotella*	Colon	
	↓ Firmicutes ↓ *Lactobacillus* ↑ Bacteroidetes ↑ *Fusobacteria* ↑ Bacilli		[291,301]

Considering all data, it should be highlighted that Ag NPs, TiO$_2$ NPs and ZnO NPs may affect the intestinal microbiota including the alteration of the F/B ratio (for example, an enhanced F/B ratio is related with obesity), a depletion of *Lactobacillus* strains and an elevated in the abundance of Proteobacteria. The above consequences can lead to obesity or even CRC (colorectal cancer) where gut dysbiosis play a significant role [290]. What is more, dysbiosis as a result of the action of the mentioned NPS may be associated with the development of inflammatory bowel disease (IBD), irritable bowel syndrome (IBS), and metabolic syndrome [290–292]. With regard to the above insights, additional investigations are needed for a better understanding of the changes among intestinal microbiota in the presence of Ag NPs, TiO$_2$ NPs and ZnO NPs.

5. Conclusions and Future Perspectives

In an era of increasing antimicrobial resistance, metallic nanoparticles appear to hold promise to improve current therapies and to develop new therapeutic agents of nanoscale nature. A possible way to increase the antimicrobial activity of conventional antibiotics is to use them in combination with metallic nanoparticles. This can be done either by synthesizing metallic nanoparticles with a modified surface, functionalization with suitable antimicrobial agents, or by designing a core of synergistically acting metals. It is also possible to select antimicrobial agents and use them in combination therapy (metallic nanoparticles + antimicrobial agents). The use of synergism in the nanotechnology context seems to be a very promising approach in the fight against various infections, whether of bacterial or fungal etiology, and against planktonic and biofilm-forming bacteria. Thus, the synergistic combination of metallic NPs with suitable compounds may be a potential

74

source of alternative antimicrobial agents and may play a significant role in the near future. Combining metallic nanoparticles with an antimicrobial agent not only demonstrated synergistic effects, but also improved drug delivery and increased antimicrobial agent efficacy, while reducing the side effects associated with the broad use of these agents. In addition, the synergistic action of metallic nanoparticles with an antimicrobial agent enabled resistance mechanisms to conventional antibiotics/fungicides, thereby providing a more effective use of antibiotics/fungicides available in the clinical practice.

In addition, the activity as well as the toxicity of metallic nanoparticles is influenced by their physical and chemical properties, where the size of nanoparticles has been found to have a significant effect due to the increase in specific surface area at nanoscale sizes, resulting in a higher number of cellular interactions and, consequently, toxicity. Other key factors influencing nanoparticle cytotoxicity include shape, surface charge, method of synthesis, nanoparticle surface modification and metal ion release. Therefore, the control of the physicochemical properties of NPs is crucial in order to obtain safer and more stable NPs. An important aspect of the use of nanotechnologies is the biocompatibility of the design materials. Although metallic nanoparticles in combination with antimicrobial agents have many advantages, they can also have adverse effects, as they have the potential to cross the natural barriers of living cells and tissues, causing toxic and inflammatory responses. The biocompatibility of metallic nanoparticles can be modulated by changing the size of the nanoparticles. It has been found that due to their small size, NPs have a much larger surface area per unit mass compared to their bulk counterparts, resulting in a greater reactivity with a greater risk of cytotoxic effects. By changing factors such as shape, chemical composition, surface charge, and method of synthesis, the biocompatibility of metallic NPs can be influenced. Therefore, it is believed that by controlling the physicochemical properties of nanoparticles, safer and more reliable nanoparticles with high antimicrobial activity can be obtained. Further research is still required to determine how nanoparticles affect the complex human body. In order to reduce the toxic effects of metallic nanoparticles, as well as in combination with other compounds, new methods are needed to reduce the negative effects of NPs while maintaining their activity. Much of the work to date confirms the low potential of metallic nanoparticles due to their divergent mechanisms of action against pathogens. However, there are also reports of the possibility of the development of resistance mechanisms as a result of exposure to nanoparticles, so a highly effective antimicrobial agent such as metallic NPs should be handled rationally to remain effective against various types of infections. Currently, the impact of NPs on intestinal microbiota has caught the increasing attention of researchers. It should be emphasized that there is a compelling amount of evidence indicating the correlation of Ag NPs, TiO_2 NPs and ZnO NPs in the development of obesity, IBD, IBS metabolic syndrome or even CRC. Nevertheless, the above mentioned findings raise the need for extended investigation in order to fully explain them, especially in humans.

For the safe use of metallic nanoparticles there is a need for future research, which should include the mechanisms of NPs' translocation, accumulation, long-term and long-lasting effects on the body, their interaction with cells, signaling pathways and receptors, and effects on fundamental processes such as phagocytosis. Understanding the relationship of potentially new nanotechnology-based antimicrobials to biological systems is a key to overcoming the limitations and toxicity barriers of metallic nanoparticles and to their future use in the treatment of bacterial or fungal infections. Although the results presented in this review are promising in the context of fighting infections by combining metallic nanoparticles with antimicrobial agents, at present, no existing product has been approved by the Food and Drug Administration (FDA) for clinical use. Therefore, future research should focus on the elucidation of the interaction of nanotechnology-based antimicrobials with cells, tissues or organs, their metabolism and accumulation in the body, and their effect on the natural flora in order to produce safe and effective means of combating microbial resistance in the next generation of drugs.

References

1. Aslam, B.; Wang, W.; Arshad, M.I.; Khurshid, M.; Muzammil, S.; Rasool, M.H.; Nisar, M.A.; Alvi, R.F.; Aslam, M.A.; Qamar, M.U.; et al. Antibiotic resistance: A rundown of a global crisis. *Infect. Drug Resist.* **2018**, *11*, 1645–1658. [CrossRef] [PubMed]
2. Peng, M.; Salaheen, S.; Biswas, D. Animal health: Global antibiotic issues. *Encycl. Agric. Food Syst.* **2014**, *346*, 346–357.
3. Llor, C.; Bjerrum, L. Antimicrobial resistance: Risk associated with antibiotic overuse and initiatives to reduce the problem. *Ther. Adv. Drug Saf.* **2014**, *5*, 229–241. [CrossRef] [PubMed]
4. Tariq, R.A.; Vashisht, R.; Sinha, A.; Scherbak, Y. *Medication Dispensing Errors and Prevention*; StatPearls Publishing: Tampa, FL, USA, 2018.
5. Ventola, C.L. The antibiotic resistance crisis: Part 1: Causes and threats. *Pharm. Ther.* **2015**, *40*, 277.
6. Cižman, M.; Srovin, T.P. Antibiotic consumption and resistance of gram-negative pathogens (collateral damage). *GMS Infect. Dis.* **2018**, *6*, Doc05. [CrossRef]
7. Palma, E.; Tilocca, B.; Roncada, P. Antimicrobial Resistance in Veterinary Medicine: An Overview. *Int. J. Mol. Sci.* **2020**, *21*, 1914. [CrossRef]
8. Abebe, G.M. The Role of Bacterial Biofilm in Antibiotic Resistance and Food Contamination. *Int. J. Microbiol.* **2020**, *2020*, 1705814. [CrossRef]
9. Van Duin, D.; Paterson, D.L. Multidrug-Resistant Bacteria in the Community: Trends and Lessons Learned. *Infect. Dis. Clin. North Am.* **2016**, *30*, 377–390. [CrossRef]
10. Jindal, A.K.; Pandya, K.; Khan, I.D. Antimicrobial resistance: A public health challenge. *Med. J. Armed Forces India* **2015**, *71*, 178–181. [CrossRef]
11. Tacconelli, E.; Pezzani, M.D. Public health burden of antimicrobial resistance in Europe. *Lancet Infect. Dis.* **2019**, *19*, 4–6. [CrossRef]
12. Centers for Disease Control and Prevention (CDC). Antibiotic Resistance Threats in the United States. 2019. Available online: https://www.cdc.gov/drugresistance/biggest-threats.html (accessed on 19 December 2022).
13. Available online: https://www.who.int/news/item/29-04-2019-new-report-calls-for-urgent-action-to-avert-antimicrobial-resistance-crisis (accessed on 19 December 2022).
14. O'Neill, J. Antimicrobial Resistance: Tackling a Crisis for the Health and Wealth of Nations. 2014. Available online: https://amr-review.org/sites/default/files/AMR%20Review%20Paper%20-%20Tackling%20a%20crisis%20for%20the%20health%20and%20wealth%20of%20nations_1.pdf (accessed on 6 June 2016).
15. Spellberg, B.; Blaser, M.; Guidos, R.J.; Boucher, H.W.; Bradley, J.S.; Eisenstein, B.I.; Gerding, D.; Lynfield, R.; Reller, L.B.; Rex, J.; et al. Combating antimicrobial resistance: Policy recommendations to save lives. *Clin. Infect. Dis.* **2011**, *52* (Suppl. 5), S397–S428. [CrossRef]
16. Beyth, N.; Houri-Haddad, Y.; Domb, A.; Khan, W.; Hazan, R. Alternative antimicrobial approach: Nano-antimicrobial materials. *Evid.-Based Complement. Altern. Med.* **2015**, *2015*, 246012. [CrossRef]
17. Gupta, A.; Landis, R.F.; Rotello, V.M. Nanoparticle-Based Antimicrobials: Surface Functionality is Critical. *F1000Research* **2016**, *5*, 364. [CrossRef]
18. Feynman, R. There's plenty of room at the bottom. In *Feynman and Computation*; CRC Press: Boca Raton, FL, USA, 2018; pp. 63–76.
19. Taniguchi, N. On the basic concept of nanotechnology. In Proceedings of the International Conference on Production Engineering (ICPE), Tokyo, Japan, 26–29 August 1974.
20. Mostafavi, E.; Soltantabar, P.; Webster, T.J. Nanotechnology and picotechnology: A new arena for translational medicine. In *Biomaterials in Translational Medicine*; Elsevier: Amsterdam, The Netherlands, 2019; pp. 191–212.

21. Patel, K.D.; Singh, R.K.; Kim, H.-W. Carbon-based nanomaterials as an emerging platform for theranostics. *Mater. Horiz.* **2019**, *6*, 434–469. [CrossRef]
22. Kang, S.; Mauter, M.S.; Elimelech, M. Physicochemical determinants of multiwalled carbon nanotube bacterial cytotoxicity. *Environ. Sci. Technol.* **2008**, *42*, 7528–7534. [CrossRef]
23. Hui, L.; Huang, J.; Chen, G.; Zhu, Y.; Yang, L. Antibacterial property of graphene quantum dots (both source material and bacterial shape matter). *ACS Appl. Mater. Interfaces* **2016**, *8*, 20–25. [CrossRef]
24. Georgakilas, V.; Otyepka, M.; Bourlinos, A.B.; Chandra, V.; Kim, N.; Kemp, K.C.; Hobza, P.; Zboril, R.; Kim, K.S. Functionalization of graphene: Covalent and non-covalent approaches, derivatives and applications. *Chem. Rev.* **2012**, *112*, 6156–6214. [CrossRef]
25. Bottini, M.; Rosato, N.; Bottini, N. PEG-modified carbon nanotubes in biomedicine: Current status and challenges ahead. *Biomacromolecules* **2011**, *12*, 3381–3393. [CrossRef]
26. Mocan, L.; Ilie, I.; Tabaran, F.A.; Iancu, C.; Mosteanu, O.; Pop, T.; Zdrehus, C.; Bartos, D.; Mocan, T.; Matea, C. Selective laser ablation of methicillin-resistant staphylococcus aureus with IgG functionalized multi-walled carbon nanotubes. *J. Biomed. Nanotechnol.* **2016**, *12*, 781–788. [CrossRef]
27. Yaqoob, A.A.; Ahmad, H.; Parveen, T.; Ahmad, A.; Oves, M.; Ismail, I.M.I.; Qari, H.A.; Umar, K.; Mohamad Ibrahim, M.N. Recent Advances in Metal Decorated Nanomaterials and Their Various Biological Applications: A Review. *Front. Chem.* **2020**, *8*, 341. [CrossRef] [PubMed]
28. Naseem, T.; Durrani, T. The role of some important metal oxide nanoparticles for wastewater and antibacterial applications: A review. *Environ. Chem. Ecotoxicol.* **2021**, *3*, 59–75. [CrossRef]
29. Klębowski, B.; Depciuch, J.; Parlińska-Wojtan, M.; Baran, J. Applications of noble metal-based nanoparticles in medicine. *Int. J. Mol. Sci.* **2018**, *19*, 4031. [CrossRef] [PubMed]
30. Sánchez-López, E.; Gomes, D.; Esteruelas, G.; Bonilla, L.; Lopez-Machado, A.L.; Galindo, R.; Cano, A.; Espina, M.; Ettcheto, M.; Camins, A. Metal-based nanoparticles as antimicrobial agents: An overview. *Nanomaterials* **2020**, *10*, 292. [CrossRef] [PubMed]
31. Liao, S.; Zhang, Y.; Pan, X.; Zhu, F.; Jiang, C.; Liu, Q.; Cheng, Z.; Dai, G.; Wu, G.; Wang, L. Antibacterial activity and mechanism of silver nanoparticles against multidrug-resistant Pseudomonas aeruginosa. *Int. J. Nanomed.* **2019**, *14*, 1469. [CrossRef]
32. Mba, I.E.; Nweze, E.I. The use of nanoparticles as alternative therapeutic agents against Candida infections: An up-to-date overview and future perspectives. *World J. Microbiol. Biotechnol.* **2020**, *36*, 163. [CrossRef]
33. Her, S.; Jaffray, D.A.; Allen, C. Gold nanoparticles for applications in cancer radiotherapy: Mechanisms and recent advancements. *Adv. Drug Deliv. Rev.* **2017**, *109*, 84–101. [CrossRef]
34. Li, J.; Li, Y.; Wu, H.; Naraginti, S.; Wu, Y. Facile synthesis of ZnO nanoparticles by Actinidia deliciosa fruit peel extract: Bactericidal, anticancer and detoxification properties. *Environ. Res.* **2021**, *200*, 111433. [CrossRef]
35. Buchman, J.T.; Hudson-Smith, N.V.; Landy, K.M.; Haynes, C.L. Understanding nanoparticle toxicity mechanisms to inform redesign strategies to reduce environmental impact. *Acc. Chem. Res.* **2019**, *52*, 1632–1642. [CrossRef]
36. Długosz, O.; Szostak, K.; Staroń, A.; Pulit-Prociak, J.; Banach, M. Methods for reducing the toxicity of metal and metal oxide NPs as biomedicine. *Materials* **2020**, *13*, 279. [CrossRef]
37. Khalid, K.; Tan, X.; Mohd Zaid, H.F.; Tao, Y.; Lye Chew, C.; Chu, D.T.; Lam, M.K.; Ho, Y.C.; Lim, J.W.; Chin Wei, L. Advanced in developmental organic and inorganic nanomaterial: A review. *Bioengineered* **2020**, *11*, 328–355. [CrossRef]
38. Sercombe, L.; Veerati, T.; Moheimani, F.; Wu, S.Y.; Sood, A.K.; Hua, S. Advances and challenges of liposome assisted drug delivery. *Front. Pharmacol.* **2015**, *6*, 286. [CrossRef]
39. De Barros, D.P.; Reed, P.; Alves, M.; Santos, R.; Oliva, A. Biocompatibility and Antimicrobial Activity of Nanostructured Lipid Carriers for Topical Applications Are Affected by Type of Oils Used in Their Composition. *Pharmaceutics* **2021**, *13*, 1950. [CrossRef]
40. Hou, Z.; Shankar, Y.V.; Liu, Y.; Ding, F.; Subramanion, J.L.; Ravikumar, V.; Zamudio-Vázquez, R.; Keogh, D.; Lim, H.; Tay, M.Y.F. Nanoparticles of short cationic peptidopolysaccharide self-assembled by hydrogen bonding with antibacterial effect against multidrug-resistant bacteria. *ACS Appl. Mater. Interfaces* **2017**, *9*, 38288–38303. [CrossRef]
41. Mubeen, B.; Ansar, A.N.; Rasool, R.; Ullah, I.; Imam, S.S.; Alshehri, S.; Ghoneim, M.M.; Alzarea, S.I.; Nadeem, M.S.; Kazmi, I. Nanotechnology as a Novel Approach in Combating Microbes Providing an Alternative to Antibiotics. *Antibiotics* **2021**, *10*, 1473. [CrossRef]
42. Mitragotri, S.; Stayton, P. Organic nanoparticles for drug delivery and imaging. *MRS Bull.* **2014**, *39*, 219–223. [CrossRef]
43. Jeevitha, D.; Amarnath, K. Chitosan/PLA nanoparticles as a novel carrier for the delivery of anthraquinone: Synthesis, characterization and in vitro cytotoxicity evaluation. *Colloids Surf. B Biointerfaces* **2013**, *101*, 126–134. [CrossRef]
44. Calandra, P.; La Parola, V.; Turco Liveri, V.; Lidorikis, E.; Finocchi, F. Composite nanoparticles. *J. Chem.* **2013**, *2013*, 536341. [CrossRef]
45. Maruthapandi, M.; Saravanan, A.; Gupta, A.; Luong, J.H.; Gedanken, A. Antimicrobial Activities of Conducting Polymers and Their Composites. *Macromol* **2022**, *2*, 78–99. [CrossRef]
46. Malhotra, B.D.; Ali, M.; Malhotra, B.; Ali, M. Chapter 5– Nanocomposite Materials: Biomolecular Devices. *Nanomater. Biosens.* **2018**, 145–159. [CrossRef]
47. Hanemann, T.; Szabó, D.V. Polymer-nanoparticle composites: From synthesis to modern applications. *Materials* **2010**, *3*, 3468–3517. [CrossRef]
48. Sahoo, N.G.; Pan, Y.Z.; Li, L.; He, C.B. Nanocomposites for bone tissue regeneration. *Nanomedicine* **2013**, *8*, 639–653. [CrossRef] [PubMed]

49. Sanità, G.; Carrese, B.; Lamberti, A. Nanoparticle Surface Functionalization: How to Improve Biocompatibility and Cellular Internalization. *Front. Mol. Biosci.* **2020**, 7, 587012. [CrossRef] [PubMed]

50. Siafaka, P.I.; Okur, N.; Karantas, I.D.; Okur, M.E.; Gündoğdu, E.A. Current update on nanoplatforms as therapeutic and diagnostic tools: A review for the materials used as nanotheranostics and imaging modalities. *Asian J. Pharm. Sci.* **2021**, 16, 24–46. [CrossRef] [PubMed]

51. Marinescu, L.; Ficai, D.; Oprea, O.; Marin, A.; Ficai, A.; Andronescu, E.; Holban, A.-M. Optimized Synthesis Approaches of Metal Nanoparticles with Antimicrobial Applications. *J. Nanomater.* **2020**, 2020, 6651207. [CrossRef]

52. Wang, L.; Hu, C.; Shao, L. The antimicrobial activity of nanoparticles: Present situation and prospects for the future. *Int. J. Nanomed.* **2017**, 12, 1227–1249. [CrossRef]

53. Khezerlou, A.; Alizadeh-Sani, M.; Azizi-Lalabadi, M.; Ehsani, A. Nanoparticles and their antimicrobial properties against pathogens including bacteria, fungi, parasites and viruses. *Microb. Pathog.* **2018**, 123, 505–526. [CrossRef]

54. Jiao, Q.; Li, L.; Mu, Q.; Zhang, Q. Immunomodulation of nanoparticles in nanomedicine applications. *Biomed. Res. Int.* **2014**, 2014, 426028. [CrossRef]

55. Feng, X.; Xu, W.; Li, Z.; Song, W.; Ding, J.; Chen, X. Immunomodulatory Nanosystems. *Adv. Sci.* **2019**, 6, 1900101. [CrossRef]

56. Abbaszadegan, A.; Ghahramani, Y.; Gholami, A.; Hemmateenejad, B.; Dorostkar, S.; Nabavizadeh, M.; Sharghi, H. The effect of charge at the surface of silver nanoparticles on antimicrobial activity against gram-positive and gram-negative bacteria: A preliminary study. *J. Nanomater.* **2015**, 2015, 53. [CrossRef]

57. Singh, J.; Vishwakarma, K.; Ramawat, N.; Rai, P.; Singh, V.K.; Mishra, R.K.; Kumar, V.; Tripathi, D.K.; Sharma, S. Nanomaterials and microbes' interactions: A contemporary overview. *3 Biotech* **2019**, 9, 68. [CrossRef]

58. Xie, Y.; Liu, Y.; Yang, J.; Liu, Y.; Hu, F.; Zhu, K.; Jiang, X. Gold Nanoclusters for Targeting Methicillin-Resistant Staphylococcus aureus In Vivo. *Angew. Chem. Int. Ed. Engl.* **2018**, 57, 3958–3962. [CrossRef]

59. Zheng, Y.K.; Liu, W.W.; Qin, Z.J.; Chen, Y.; Jiang, H.; Wang, X.M. Mercaptopyrimidine-Conjugated Gold Nanoclusters as Nanoantibiotics for Combating Multidrug-Resistant Superbugs. *Bioconjugate Chem.* **2018**, 29, 3094–3103. [CrossRef]

60. Patra, J.K.; Das, G.; Fraceto, L.F.; Campos, E.V.R.; Rodriguez-Torres, M.D.P.; Acosta-Torres, L.S.; Diaz-Torres, L.A.; Grillo, R.; Swamy, M.K.; Sharma, S.; et al. Nano based drug delivery systems: Recent developments and future prospects. *J. Nanobiotechnol.* **2018**, 16, 71. [CrossRef]

61. Stensberg, M.C.; Wei, Q.; McLamore, E.S.; Porterfield, D.M.; Wei, A.; Sepúlveda, M.S. Toxicological studies on silver nanoparticles: Challenges and opportunities in assessment, monitoring and imaging. *Nanomedicine* **2011**, 6, 879–898. [CrossRef]

62. Joshi, A.S.; Singh, P.; Mijakovic, I. Interactions of gold and silver nanoparticles with bacterial biofilms: Molecular interactions behind inhibition and resistance. *Int. J. Mol. Sci.* **2020**, 21, 7658. [CrossRef]

63. Warren, E.A.; Payne, C.K. Cellular binding of nanoparticles disrupts the membrane potential. *RSC Adv.* **2015**, 5, 13660–13666. [CrossRef]

64. Dwivedi, S.; Wahab, R.; Khan, F.; Mishra, Y.K.; Musarrat, J.; Al-Khedhairy, A.A. Reactive oxygen species mediated bacterial biofilm inhibition via zinc oxide nanoparticles and their statistical determination. *PLoS ONE* **2014**, 9, e111289. [CrossRef]

65. Makabenta, J.M.V.; Nabawy, A.; Li, C.-H.; Schmidt-Malan, S.; Patel, R.; Rotello, V.M. Nanomaterial-based therapeutics for antibiotic-resistant bacterial infections. *Nat. Rev. Microbiol.* **2021**, 19, 23–36. [CrossRef]

66. Hsueh, Y.-H.; Lin, K.-S.; Ke, W.-J.; Hsieh, C.-T.; Chiang, C.-L.; Tzou, D.-Y.; Liu, S.-T. The antimicrobial properties of silver nanoparticles in Bacillus subtilis are mediated by released Ag+ ions. *PLoS ONE* **2015**, 10, e0144306. [CrossRef]

67. Kumar, N.; Das, S.; Jyoti, A.; Kaushik, S. Synergistic effect of silver nanoparticles with doxycycline against Klebsiella pneumoniae. *Int. J. Pharm. Pharm. Sci.* **2016**, 8, 183–186.

68. Durán, N.; Nakazato, G.; Seabra, A.B. Antimicrobial activity of biogenic silver nanoparticles, and silver chloride nanoparticles: An overview and comments. *Appl. Microbiol. Biotechnol.* **2016**, 100, 6555–6570. [CrossRef] [PubMed]

69. Dakal, T.C.; Kumar, A.; Majumdar, R.S.; Yadav, V. Mechanistic basis of antimicrobial actions of silver nanoparticles. *Front. Microbiol.* **2016**, 7, 1831. [CrossRef] [PubMed]

70. Gajdács, M.; Albericio, F. Antibiotic resistance: From the bench to patients. *Antibiotics* **2019**, 8, 129. [CrossRef] [PubMed]

71. Zhang, X. Gold nanoparticles: Recent advances in the biomedical applications. *Cell Biochem. Biophys.* **2015**, 72, 771–775. [CrossRef]

72. Sharmin, S.; Rahaman, M.M.; Sarkar, C.; Atolani, O.; Islam, M.T.; Adeyemi, O.S. Nanoparticles as antimicrobial and antiviral agents: A literature-based perspective study. *Heliyon* **2021**, 7, e06456. [CrossRef]

73. Gupta, A.; Mumtaz, S.; Li, C.-H.; Hussain, I.; Rotello, V.M. Combatting antibiotic-resistant bacteria using nanomaterials. *Chem. Soc. Rev.* **2019**, 48, 415–427. [CrossRef]

74. Yuan, P.; Ding, X.; Yang, Y.Y.; Xu, Q.H. Metal nanoparticles for diagnosis and therapy of bacterial infection. *Adv. Healthc. Mater.* **2018**, 7, 1701392. [CrossRef]

75. Chandrangsu, P.; Rensing, C.; Helmann, J.D. Metal homeostasis and resistance in bacteria. *Nat. Rev. Microbiol.* **2017**, 15, 338–350. [CrossRef]

76. Khalil, M.; El Maghraby, G.; Allam, N.; Ateya, P. Enhanced efficacy of some antibiotics in presence of silver nanoparticles against multidrug resistant Pseudomonas aeruginosa recovered from burn wound infections. *Front. Microbiol.* **2021**, 12, 648560. [CrossRef]

77. Abo-Shama, U.H.; El-Gendy, H.; Mousa, W.S.; Hamouda, R.A.; Yousuf, W.E.; Hetta, H.F.; Abdeen, E.E. Synergistic and Antagonistic Effects of Metal Nanoparticles in Combination with Antibiotics Against Some Reference Strains of Pathogenic Microorganisms. *Infect. Drug Resist.* **2020**, *13*, 351–362. [CrossRef]

78. Hussain, M.A.; Ahmed, D.; Anwar, A.; Perveen, S.; Ahmed, S.; Anis, I.; Shah, M.R.; Khan, N.A. Combination Therapy of Clinically Approved Antifungal Drugs Is Enhanced by Conjugation with Silver Nanoparticles. *Int. Microbiol.* **2019**, *22*, 239–246. [CrossRef]

79. Fischbach, M.A. Combination therapies for combating antimicrobial resistance. *Curr. Opin. Microbiol.* **2011**, *14*, 519–523. [CrossRef]

80. Hwang, I.-S.; Hwang, J.H.; Choi, H.; Kim, K.-J.; Lee, D.G. Synergistic effects between silver nanoparticles and antibiotics and the mechanisms involved. *J. Med. Microbiol.* **2012**, *61*, 1719–1726. [CrossRef]

81. Gao, W.; Zhang, L. Nanomaterials arising amid antibiotic resistance. *Nat. Rev. Microbiol.* **2021**, *19*, 5–6. [CrossRef]

82. Soh, M.; Kang, D.W.; Jeong, H.G.; Kim, D.; Kim, D.Y.; Yang, W.; Song, C.; Baik, S.; Choi, I.Y.; Ki, S.K.; et al. Ceria-Zirconia Nanoparticles as an Enhanced Multi-Antioxidant for Sepsis Treatment. *Angew Chem. Int. Ed. Engl.* **2017**, *56*, 11399–11403. [CrossRef]

83. Yah, C.S.; Simate, G.S. Nanoparticles as potential new generation broad spectrum antimicrobial agents. *DARU J. Pharm. Sci.* **2015**, *23*, 43. [CrossRef]

84. Singh, R.; Nawale, L.; Arkile, M.; Wadhwani, S.; Shedbalkar, U.; Chopade, S.; Sarkar, D.; Chopade, B.A. Phytogenic silver, gold, and bimetallic nanoparticles as novel antitubercular agents. *Int. J. Nanomed.* **2016**, *11*, 1889–1897. [CrossRef]

85. Holy, J.; Perkins, E.; Yu, X. Adhesion, proliferation and differentiation of pluripotent stem cells on multi-walled carbon nanotubes. *IET Nanobiotechnol.* **2011**, *5*, 41–46. [CrossRef]

86. Ahmad, F.; Salem-Bekhit, M.M.; Khan, F.; Alshehri, S.; Khan, A.; Ghoneim, M.M.; Wu, H.-F.; Taha, E.I.; Elbagory, I. Unique Properties of Surface-Functionalized Nanoparticles for Bio-Application: Functionalization Mechanisms and Importance in Application. *Nanomaterials* **2022**, *12*, 1333. [CrossRef]

87. Wu, W.; Wu, Z.; Yu, T.; Jiang, C.; Kim, W.-S. Recent progress on magnetic iron oxide nanoparticles: Synthesis, surface functional strategies and biomedical applications. *Sci. Technol. Adv. Mater.* **2015**, *16*, 023501. [CrossRef] [PubMed]

88. Fu, C.; Zhou, H.; Wang, Y.; Liu, D.; Li, J.; Deng, H.; Qi, X.; Chen, T.; Zhang, L.-M.; Li, G. One-pot synthesis of dextran-coated iron oxide nanoclusters for real-time regional lymph node mapping. *Int. J. Nanomed.* **2017**, *12*, 3365. [CrossRef] [PubMed]

89. Qu, J.-B.; Shao, H.-H.; Jing, G.-L.; Huang, F. PEG-chitosan-coated iron oxide nanoparticles with high saturated magnetization as carriers of 10-hydroxycamptothecin: Preparation, characterization and cytotoxicity studies. *Colloids Surf. B Biointerfaces* **2013**, *102*, 37–44. [CrossRef] [PubMed]

90. Cheng, Y.; Meyers, J.D.; Broome, A.-M.; Kenney, M.E.; Basilion, J.P.; Burda, C. Deep penetration of a PDT drug into tumors by noncovalent drug-gold nanoparticle conjugates. *J. Am. Chem. Soc.* **2011**, *133*, 2583–2591. [CrossRef] [PubMed]

91. Nell, K.M.; Fontenot, S.A.; Carter, T.G.; Warner, M.G.; Warner, C.L.; Addleman, R.S.; Johnson, D.W. Non-covalent functionalization of high-surface area nanomaterials: A new class of sorbent materials. *Environ. Sci. Nano* **2016**, *3*, 138–145. [CrossRef]

92. Yue, L.; Sun, C.; Cheng, Q.; Ding, Y.; Wei, J.; Wang, R. Gold nanorods with a noncovalently tailorable surface for multi-modality image-guided chemo-photothermal cancer therapy. *Chem. Commun.* **2019**, *55*, 13506–13509. [CrossRef]

93. Nobs, L.; Buchegger, F.; Gurny, R.; Allémann, E. Current methods for attaching targeting ligands to liposomes and nanoparticles. *J. Pharm. Sci.* **2004**, *93*, 1980–1992. [CrossRef]

94. Lázaro, I.A.; Haddad, S.; Sacca, S.; Orellana-Tavra, C.; Fairen-Jimenez, D.; Forgan, R.S. Selective surface PEGylation of UiO-66 nanoparticles for enhanced stability, cell uptake, and pH-responsive drug delivery. *Chem* **2017**, *2*, 561–578. [CrossRef]

95. Oriana, S.; Fracassi, A.; Archer, C.; Yamakoshi, Y. Covalent surface modification of lipid nanoparticles by rapid potassium acyltrifluoroborate amide ligation. *Langmuir* **2018**, *34*, 13244–13251. [CrossRef]

96. Sakaguchi, M.; Makino, M.; Ohura, T.; Yamamoto, K.; Enomoto, Y.; Takase, H. Surface modification of Fe3O4 nanoparticles with dextran via a coupling reaction between naked Fe3O4 mechano-cation and naked dextran mechano-anion: A new mechanism of covalent bond formation. *Adv. Powder Technol.* **2019**, *30*, 795–806. [CrossRef]

97. Chen, H.; He, S. PLA–PEG coated multifunctional imaging probe for targeted drug delivery. *Mol. Pharm.* **2015**, *12*, 1885–1892. [CrossRef]

98. Luo, Y.; Cai, X.; Li, H.; Lin, Y.; Du, D. Hyaluronic acid-modified multifunctional Q-graphene for targeted killing of drug-resistant lung cancer cells. *ACS Appl. Mater. Interfaces* **2016**, *8*, 4048–4055. [CrossRef]

99. Slavin, Y.N.; Asnis, J.; Häfeli, U.O.; Bach, H. Metal nanoparticles: Understanding the mechanisms behind antibacterial activity. *J. Nanobiotechnol.* **2017**, *15*, 65. [CrossRef]

100. Galdiero, S.; Falanga, A.; Vitiello, M.; Cantisani, M.; Marra, V.; Galdiero, M. Silver nanoparticles as potential antiviral agents. *Molecules* **2011**, *16*, 8894–8918. [CrossRef]

101. Siddiqi, K.S.; Husen, A.; Rao, R.A. A review on biosynthesis of silver nanoparticles and their biocidal properties. *J. Nanobiotechnol.* **2018**, *16*, 14. [CrossRef]

102. Singh, S.; Park, I.; Shin, Y.; Lee, Y. Comparative study on antimicrobial efficiency of AgSiO2, ZnAg, and Ag-Zeolite for the application of fishery plastic container. *J. Mater. Sci. Eng.* **2015**, *4*, 2169-0022.

103. Rai, M.; Kon, K.; Ingle, A.; Duran, N.; Galdiero, S.; Galdiero, M. Broad-spectrum bioactivities of silver nanoparticles: The emerging trends and future prospects. *Appl. Microbiol. Biotechnol.* **2014**, *98*, 1951–1961. [CrossRef]

104. Korshed, P.; Li, L.; Liu, Z.; Wang, T. The molecular mechanisms of the antibacterial effect of picosecond laser generated silver nanoparticles and their toxicity to human cells. *PLoS ONE* **2016**, *11*, e0160078. [CrossRef]

105. Flores-López, L.Z.; Espinoza-Gómez, H.; Somanathan, R. Silver nanoparticles: Electron transfer, reactive oxygen species, oxidative stress, beneficial and toxicological effects. Mini review. *J. Appl. Toxicol.* **2019**, *39*, 16–26. [CrossRef]

106. Yin, I.X.; Zhang, J.; Zhao, I.S.; Mei, M.L.; Li, Q.; Chu, C.H. The antibacterial mechanism of silver nanoparticles and its application in dentistry. *Int. J. Nanomed.* **2020**, *15*, 2555. [CrossRef]

107. Raza, M.A.; Kanwal, Z.; Rauf, A.; Sabri, A.N.; Riaz, S.; Naseem, S. Size-and shape-dependent antibacterial studies of silver nanoparticles synthesized by wet chemical routes. *Nanomaterials* **2016**, *6*, 74. [CrossRef] [PubMed]

108. Kailasa, S.K.; Park, T.-J.; Rohit, J.; Koduru, J. *Nanoparticles in Pharmacotherapy*; Elsevier: Amsterdam, The Netherlands, 2019.

109. Gomaa, E.Z. Silver nanoparticles as an antimicrobial agent: A case study on Staphylococcus aureus and Escherichia coli as models for Gram-positive and Gram-negative bacteria. *J. Gen. Appl. Microbiol.* **2017**, *63*, 36–43. [CrossRef] [PubMed]

110. Quinteros, M.; Aristizábal, V.C.; Dalmasso, P.R.; Paraje, M.G.; Páez, P.L. Oxidative stress generation of silver nanoparticles in three bacterial genera and its relationship with the antimicrobial activity. *Toxicol. Vitr.* **2016**, *36*, 216–223. [CrossRef] [PubMed]

111. Tamayo, L.; Zapata, P.; Vejar, N.; Azócar, M.; Gulppi, M.; Zhou, X.; Thompson, G.; Rabagliati, F.; Páez, M. Release of silver and copper nanoparticles from polyethylene nanocomposites and their penetration into Listeria monocytogenes. *Mater. Sci. Eng. C* **2014**, *40*, 24–31. [CrossRef]

112. Rattanata, N.; Klaynongsruang, S.; Leelayuwat, C.; Limpaiboon, T.; Lulitanond, A.; Boonsiri, P.; Chio-Srichan, S.; Soontaranon, S.; Rugmai, S.; Daduang, J. Gallic acid conjugated with gold nanoparticles: Antibacterial activity and mechanism of action on foodborne pathogens. *Int. J. Nanomed.* **2016**, *11*, 3347.

113. Kundu, S. Gold nanoparticles: Their application as antimicrobial agents and vehicles of gene delivery. *Adv. Biotechnol. Microbiol.* **2017**, *4*, 555–658. [CrossRef]

114. Moghadam, B.Y.; Hou, W.-C.; Corredor, C.; Westerhoff, P.; Posner, J.D. Role of nanoparticle surface functionality in the disruption of model cell membranes. *Langmuir* **2012**, *28*, 16318–16326. [CrossRef]

115. Lee, H.; Lee, D.G. Gold nanoparticles induce a reactive oxygen species-independent apoptotic pathway in Escherichia coli. *Colloids Surf. B Biointerfaces* **2018**, *167*, 1–7. [CrossRef]

116. El-Borady, O.M.; Ayat, M.S.; Shabrawy, M.A.; Millet, P. Green synthesis of gold nanoparticles using Parsley leaves extract and their applications as an alternative catalytic, antioxidant, anticancer, and antibacterial agents. *Adv. Powder Technol.* **2020**, *31*, 4390–4400. [CrossRef]

117. Chmielewska, S.J.; Skłodowski, K.; Depciuch, J.; Deptuła, P.; Piktel, E.; Fiedoruk, K.; Kot, P.; Paprocka, P.; Fortunka, K.; Wollny, T.; et al. Bactericidal Properties of Rod-, Peanut-, and Star-Shaped Gold Nanoparticles Coated with Ceragenin CSA-131 against Multidrug-Resistant Bacterial Strains. *Pharmaceutics* **2021**, *13*, 425. [CrossRef]

118. Cui, Y.; Zhao, Y.; Tian, Y.; Zhang, W.; Lü, X.; Jiang, X. The molecular mechanism of action of bactericidal gold nanoparticles on Escherichia coli. *Biomaterials* **2012**, *33*, 2327–2333. [CrossRef]

119. Prasad, S.V.; Piktel, E.; Depciuch, J.; Maximenko, A.; Suprewicz, Ł.; Daniluk, T.; Spałek, J.; Wnorowska, U.; Zielinski, P.M.; Parlinska-Wojtan, M. Targeting bacteria causing otitis media using nanosystems containing nonspherical gold nanoparticles and ceragenins. *Nanomedicine* **2021**, *16*, 2657–2678. [CrossRef]

120. Piktel, E.; Suprewicz, Ł.; Depciuch, J.; Cieśluk, M.; Chmielewska, S.; Durnaś, B.; Król, G.; Wollny, T.; Deptuła, P.; Kochanowicz, J. Rod-shaped gold nanoparticles exert potent candidacidal activity and decrease the adhesion of fungal cells. *Nanomedicine* **2020**, *15*, 2733–2752. [CrossRef]

121. Piktel, E.; Wnorowska, U.; Depciuch, J.; Łysik, D.; Cieśluk, M.; Fiedoruk, K.; Mystkowska, J.; Parlińska-Wojtan, M.; Janmey, P.A.; Bucki, R. N-Acetyl-Cysteine Increases Activity of Peanut-Shaped Gold Nanoparticles Against Biofilms Formed by Clinical Strains of Pseudomonas aeruginosa Isolated from Sputum of Cystic Fibrosis Patients. *Infect. Drug Resist.* **2022**, *15*, 851. [CrossRef]

122. Majumdar, D.; Jung, K.-H.; Zhang, H.; Nannapaneni, S.; Wang, X.; Amin, A.R.; Chen, Z.; Chen, Z.; Shin, D.M. Luteolin nanoparticle in chemoprevention: In vitro and in vivo anticancer activity. *Cancer Prev. Res.* **2014**, *7*, 65–73. [CrossRef]

123. Korshed, P.; Li, L.; Liu, Z.; Mironov, A.; Wang, T. Size-dependent antibacterial activity for laser-generated silver nanoparticles. *J. Interdiscip. Nanomed.* **2019**, *4*, 24–33. [CrossRef]

124. Osonga, F.J.; Akgul, A.; Yazgan, I.; Akgul, A.; Eshun, G.B.; Sakhaee, L.; Sadik, O.A. Size and shape-dependent antimicrobial activities of silver and gold nanoparticles: A model study as potential fungicides. *Molecules* **2020**, *25*, 2682. [CrossRef]

125. Sohm, B.; Immel, F.; Bauda, P.; Pagnout, C. Insight into the primary mode of action of TiO2 nanoparticles on Escherichia coli in the dark. *Proteomics* **2015**, *15*, 98–113. [CrossRef]

126. Cheon, J.Y.; Kim, S.J.; Rhee, Y.H.; Kwon, O.H.; Park, W.H. Shape-dependent antimicrobial activities of silver nanoparticles. *Int. J. Nanomed.* **2019**, *14*, 2773–2780. [CrossRef]

127. El-Zahry, M.R.; Mahmoud, A.; Refaat, I.H.; Mohamed, H.A.; Bohlmann, H.; Lendl, B. Antibacterial effect of various shapes of silver nanoparticles monitored by SERS. *Talanta* **2015**, *138*, 183–189. [CrossRef]

128. Jung, W.K.; Koo, H.C.; Kim, K.W.; Shin, S.; Kim, S.H.; Park, Y.H. Antibacterial activity and mechanism of action of the silver ion in Staphylococcus aureus and Escherichia coli. *Appl. Environ. Microbiol.* **2008**, *74*, 2171–2178. [CrossRef] [PubMed]

129. Azam, A.; Ahmed, A.S.; Oves, M.; Khan, M.S.; Habib, S.S.; Memic, A. Antimicrobial activity of metal oxide nanoparticles against Gram-positive and Gram-negative bacteria: A comparative study. *Int. J. Nanomed.* **2012**, *7*, 6003. [CrossRef] [PubMed]

130. Rai, M.K.; Deshmukh, S.; Ingle, A.; Gade, A. Silver nanoparticles: The powerful nanoweapon against multidrug-resistant bacteria. *J. Appl. Microbiol.* **2012**, *112*, 841–852. [CrossRef] [PubMed]

131. Singh, I.R.; Chettri, U.; Maity, P.; Ghosh, A.K.; Joshi, S.; Mitra, S. Modulated Antimicrobial Activity and Drug-Protein Interaction Ability of Zinc Oxide and Cadmium Sulfide Nanoparticles: Effect of Doping with Few First-Row Transition Metals. *J. Clust. Sci.* **2022**, 1–13. [CrossRef]

132. Gayathri Manju, B.; Raji, P. Biological synthesis, characterization, and antibacterial activity of nickel-doped copper ferrite nanoparticles. *Appl. Phys. A* **2019**, *125*, 313. [CrossRef]

133. Sadaiyandi, K.; Kennedy, A.; Sagadevan, S.; Chowdhury, Z.Z.; Johan, M.; Bin, R.; Aziz, F.A.; Rafique, R.F.; Thamiz Selvi, R. Influence of Mg doping on ZnO nanoparticles for enhanced photocatalytic evaluation and antibacterial analysis. *Nanoscale Res. Lett.* **2018**, *13*, 229.

134. Niemirowicz, K.; Swiecicka, I.; Wilczewska, A.Z.; Misztalewska, I.; Kalska-Szostko, B.; Bienias, K.; Bucki, R.; Car, H. Gold-functionalized magnetic nanoparticles restrict growth of Pseudomonas aeruginosa. *Int. J. Nanomed.* **2014**, *9*, 2217.

135. Khan, M.; Khan, S.T.; Khan, M.; Adil, S.F.; Musarrat, J.; Al-Khedhairy, A.A.; Al-Warthan, A.; Siddiqui, M.R.H.; Alkhathlan, H.Z. Antibacterial properties of silver nanoparticles synthesized using Pulicaria glutinosa plant extract as a green bioreductant. *Int. J. Nanomed.* **2014**, *9*, 3551.

136. Ren, E.; Zhang, C.; Li, D.; Pang, X.; Liu, G. Leveraging metal oxide nanoparticles for bacteria tracing and eradicating. *View* **2020**, *1*, 20200052. [CrossRef]

137. Chauhan, S.; Upadhyay, L.S.B. Biosynthesis of iron oxide nanoparticles using plant derivatives of Lawsonia inermis (Henna) and its surface modification for biomedical application. *Nanotechnol. Environ. Eng.* **2019**, *4*, 8. [CrossRef]

138. Arakha, M.; Pal, S.; Samantarrai, D.; Panigrahi, T.K.; Mallick, B.C.; Pramanik, K.; Mallick, B.; Jha, S. Antimicrobial activity of iron oxide nanoparticle upon modulation of nanoparticle-bacteria interface. *Sci. Rep.* **2015**, *5*, 14813. [CrossRef]

139. Niyonshuti, I.I.; Krishnamurthi, V.R.; Okyere, D.; Song, L.; Benamara, M.; Tong, X.; Wang, Y.; Chen, J. Polydopamine surface coating synergizes the antimicrobial activity of silver nanoparticles. *ACS Appl. Mater. Interfaces* **2020**, *12*, 40067–40077. [CrossRef]

140. Lemire, J.A.; Kalan, L.; Bradu, A.; Turner, R.J. Silver oxynitrate, an unexplored silver compound with antimicrobial and antibiofilm activity. *Antimicrob. Agents Chemother.* **2015**, *59*, 4031–4039. [CrossRef]

141. Schweigert, N.; Zehnder, A.J.; Eggen, R.I. Chemical properties of catechols and their molecular modes of toxic action in cells, from microorganisms to mammals: Minireview. *Environ. Microbiol.* **2001**, *3*, 81–91. [CrossRef]

142. Skłodowski, K.; Chmielewska, S.J.; Depciuch, J.; Deptuła, P.; Piktel, E.; Daniluk, T.; Zakrzewska, M.; Czarnowski, M.; Cieśluk, M.; Durnaś, B. Ceragenin-Coated Non-Spherical Gold Nanoparticles as Novel Candidacidal Agents. *Pharmaceutics* **2021**, *13*, 1940. [CrossRef]

143. Bucki, R.; Niemirowicz-Laskowska, K.; Deptuła, P.; Wilczewska, A.Z.; Misiak, P.; Durnaś, B.; Fiedoruk, K.; Piktel, E.; Mystkowska, J.; Janmey, P.A. Susceptibility of microbial cells to the modified PIP 2-binding sequence of gelsolin anchored on the surface of magnetic nanoparticles. *J. Nanobiotechnol.* **2019**, *17*, 81. [CrossRef]

144. Niemirowicz-Laskowska, K.; Głuszek, K.; Piktel, E.; Pajuste, K.; Durnaś, B.; Król, G.; Wilczewska, A.Z.; Janmey, P.A.; Plotniece, A.; Bucki, R. Bactericidal and immunomodulatory properties of magnetic nanoparticles functionalized by 1, 4-dihydropyridines. *Int. J. Nanomed.* **2018**, *13*, 3411. [CrossRef]

145. Niemirowicz, K.; Surel, U.; Wilczewska, A.Z.; Mystkowska, J.; Piktel, E.; Gu, X.; Namiot, Z.; Kułakowska, A.; Savage, P.B.; Bucki, R. Bactericidal activity and biocompatibility of ceragenin-coated magnetic nanoparticles. *J. Nanobiotechnol.* **2015**, *13*, 32. [CrossRef]

146. Niemirowicz, K.; Durnaś, B.; Tokajuk, G.; Piktel, E.; Michalak, G.; Gu, X.; Kułakowska, A.; Savage, P.B.; Bucki, R. Formulation and candidacidal activity of magnetic nanoparticles coated with cathelicidin LL-37 and ceragenin CSA-13. *Sci. Rep.* **2017**, *7*, 4610. [CrossRef]

147. Tokajuk, G.; Niemirowicz, K.; Deptuła, P.; Piktel, E.; Cieśluk, M.; Wilczewska, A.Z.; Dąbrowski, J.R.; Bucki, R. Use of magnetic nanoparticles as a drug delivery system to improve chlorhexidine antimicrobial activity. *Int. J. Nanomed.* **2017**, *12*, 7833. [CrossRef]

148. Garibo, D.; Borbón-Nuñez, H.A.; de León, J.N.D.; García Mendoza, E.; Estrada, I.; Toledano-Magaña, Y.; Tiznado, H.; Ovalle-Marroquin, M.; Soto-Ramos, A.G.; Blanco, A. Green synthesis of silver nanoparticles using Lysiloma acapulcensis exhibit high-antimicrobial activity. *Sci. Rep.* **2020**, *10*, 12805. [CrossRef] [PubMed]

149. Ghetas, H.A.; Abdel-Razek, N.; Shakweer, M.S.; Abotaleb, M.M.; Paray, B.A.; Ali, S.; Eldessouki, E.A.; Dawood, M.A.; Khalil, R.H. Antimicrobial activity of chemically and biologically synthesized silver nanoparticles against some fish pathogens. *Saudi J. Biol. Sci.* **2022**, *29*, 1298–1305. [CrossRef] [PubMed]

150. Mousavi-Khattat, M.; Keyhanfar, M.; Razmjou, A. A comparative study of stability, antioxidant, DNA cleavage and antibacterial activities of green and chemically synthesized silver nanoparticles. *Artif. Cells Nanomed. Biotechnol.* **2018**, *46*, S1022–S1031. [CrossRef] [PubMed]

151. Swain, S.; Barik, S.; Behera, T.; Nayak, S.; Sahoo, S.; Mishra, S.; Swain, P. Green synthesis of gold nanoparticles using root and leaf extracts of Vetiveria zizanioides and Cannabis sativa and its antifungal activities. *BioNanoScience* **2016**, *6*, 205–213. [CrossRef]

152. Kumar, P.S.M.; Francis, A.P.; Devasena, T. Biosynthesized and chemically synthesized titania nanoparticles: Comparative analysis of antibacterial activity. *J. Environ. Nanotechnol.* **2014**, *3*, 73–81.

153. Qasim, S.; Zafar, A.; Saif, M.S.; Ali, Z.; Nazar, M.; Waqas, M.; Haq, A.U.; Tariq, T.; Hassan, S.G.; Iqbal, F. Green synthesis of iron oxide nanorods using Withania coagulans extract improved photocatalytic degradation and antimicrobial activity. *J. Photochem. Photobiol. B Biol.* **2020**, *204*, 111784. [CrossRef]

154. Menazea, A.; Ismail, A.; Samy, A. Novel green synthesis of zinc oxide nanoparticles using orange waste and its thermal and antibacterial activity. *J. Inorg. Organomet. Polym. Mater.* **2021**, *31*, 4250–4259. [CrossRef]

155. Attallah, N.G.; Elekhnawy, E.; Negm, W.A.; Hussein, I.A.; Mokhtar, F.A.; Al-Fakhrany, O.M. In vivo and in vitro antimicrobial activity of biogenic silver nanoparticles against Staphylococcus aureus clinical isolates. *Pharmaceuticals* **2022**, *15*, 194. [CrossRef]

156. Vanti, G.L.; Kurjogi, M.; Basavesha, K.; Teradal, N.L.; Masaphy, S.; Nargund, V.B. Synthesis and antibacterial activity of solanum torvum mediated silver nanoparticle against Xxanthomonas axonopodis pv. punicae and Ralstonia solanacearum. *J. Biotechnol.* **2020**, *309*, 20–28. [CrossRef]

157. Niemirowicz, K.; Swiecicka, I.; Wilczewska, A.Z.; Markiewicz, K.H.; Surel, U.; Kułakowska, A.; Namiot, Z.; Szynaka, B.; Bucki, R.; Car, H. Growth arrest and rapid capture of select pathogens following magnetic nanoparticle treatment. *Colloids Surf. B Biointerfaces* **2015**, *131*, 29–38. [CrossRef]

158. Mohana, S.; Sumathi, S. Multi-functional biological effects of palladium nanoparticles synthesized using Agaricus bisporus. *J. Clust. Sci.* **2020**, *31*, 391–400. [CrossRef]

159. Khashan, K.S.; Sulaiman, G.M.; Abdulameer, F.A.; Albukhaty, S.; Ibrahem, M.A.; Al-Muhimeed, T.; AlObaid, A.A. Antibacterial Activity of TiO2 Nanoparticles Prepared by One-Step Laser Ablation in Liquid. *Appl. Sci.* **2021**, *11*, 4623. [CrossRef]

160. Pachaiappan, R.; Rajendran, S.; Ramalingam, G.; Vo, D.-V.N.; Priya, P.M.; Soto-Moscoso, M. Green Synthesis of Zinc Oxide Nanoparticles by Justicia adhatoda Leaves and Their Antimicrobial Activity. *Chem. Eng. Technol.* **2021**, *44*, 551–558. [CrossRef]

161. Menon, S.; Agarwal, H.; Rajeshkumar, S.; Rosy, P.J.; Shanmugam, V.K. Investigating the antimicrobial activities of the biosynthesized selenium nanoparticles and its statistical analysis. *Bionanoscience* **2020**, *10*, 122–135. [CrossRef]

162. Cittrarasu, V.; Kaliannan, D.; Dharman, K.; Maluventhen, V.; Easwaran, M.; Liu, W.C.; Balasubramanian, B.; Arumugam, M. Green synthesis of selenium nanoparticles mediated from Ceropegia bulbosa Roxb extract and its cytotoxicity, antimicrobial, mosquitocidal and photocatalytic activities. *Sci. Rep.* **2021**, *11*, 1032. [CrossRef]

163. Baptista, P.V.; McCusker, M.P.; Carvalho, A.; Ferreira, D.A.; Mohan, N.M.; Martins, M.; Fernandes, A.R. Nano-strategies to fight multidrug resistant bacteria—"A Battle of the Titans". *Front. Microbiol.* **2018**, *9*, 1441. [CrossRef]

164. Madhi, M.; Hasani, A.; Mojarrad, J.S.; Rezaee, M.A.; Zarrini, G.; Davaran, S. Nano-strategies in pursuit of efflux pump activeness in Acinetobacter baumannii and Pseudomonas aeruginosa. *Gene Rep.* **2020**, *21*, 100915. [CrossRef]

165. Amaro, F.; Morón, Á.; Díaz, S.; Martín-González, A.; Gutiérrez, J.C. Metallic Nanoparticles—Friends or Foes in the Battle against Antibiotic-Resistant Bacteria? *Microorganisms* **2021**, *9*, 364. [CrossRef]

166. Ipe, D.S.; Kumar, P.; Love, R.M.; Hamlet, S.M. Silver nanoparticles at biocompatible dosage synergistically increases bacterial susceptibility to antibiotics. *Front. Microbiol.* **2020**, *11*, 1074. [CrossRef]

167. Salman, M.; Rizwana, R.; Khan, H.; Munir, I.; Hamayun, M.; Iqbal, A.; Rehman, A.; Amin, K.; Ahmed, G.; Khan, M. Synergistic effect of silver nanoparticles and polymyxin B against biofilm produced by Pseudomonas aeruginosa isolates of pus samples in vitro. *Artif. Cells Nanomed. Biotechnol.* **2019**, *47*, 2465–2472. [CrossRef]

168. Bankier, C.; Matharu, R.K.; Cheong, Y.K.; Ren, G.G.; Cloutman-Green, E.; Ciric, L. Synergistic Antibacterial Effects of Metallic Nanoparticle Combinations. *Sci. Rep.* **2019**, *9*, 16074. [CrossRef] [PubMed]

169. Agreles, M.A.A.; Cavalcanti, I.D.L.; Cavalcanti, I.M.F. Synergism between metallic nanoparticles and antibiotics. *Appl. Microbiol. Biotechnol.* **2022**, *106*, 3973–3984. [CrossRef] [PubMed]

170. Susanti, D.; Haris, M.S.; Taher, M.; Khotib, J. Natural Products-Based Metallic Nanoparticles as Antimicrobial Agents. *Front. Pharmacol.* **2022**, *13*, 1900. [CrossRef]

171. Heng, X.; Jiang, Y.; Chu, W. Influence of Fluconazole Administration on Gut Microbiome, Intestinal Barrier, and Immune Response in Mice. *Antimicrob. Agents Chemother.* **2021**, *65*, e02520–e02552. [CrossRef] [PubMed]

172. Patangia, D.V.; Anthony Ryan, C.; Dempsey, E.; Paul Ross, R.; Stanton, C. Impact of antibiotics on the human microbiome and consequences for host health. *MicrobiologyOpen* **2022**, *11*, e1260. [CrossRef]

173. Gupta, A.K.; Venkataraman, M.; Renaud, H.J.; Summerbell, R.; Shear, N.H.; Piguet, V. The increasing problem of treatment-resistant fungal infections: A call for antifungal stewardship programs. *Int. J. Dermatol.* **2021**, *60*, e474–e479. [CrossRef]

174. Yılmaz, Ç.; Özcengiz, G. Antibiotics: Pharmacokinetics, toxicity, resistance and multidrug efflux pumps. *Biochem. Pharmacol.* **2017**, *133*, 43–62. [CrossRef]

175. Blumenthal, K.G.; Peter, J.G.; Trubiano, J.A.; Phillips, E.J. Antibiotic allergy. *Lancet* **2019**, *393*, 183–198. [CrossRef]

176. Ranghar, S.; Sirohi, P.; Verma, P.; Agarwal, V. Nanoparticle-based drug delivery systems: Promising approaches against infections. *Braz. Arch. Biol. Technol.* **2014**, *57*, 209–222. [CrossRef]

177. WHO. *Global Tuberculosis Report 2020*; WHO: Geneva, Switzerland, 2020.

178. Khaled, J.M.; Alharbi, N.S.; Siddiqi, M.Z.; Alobaidi, A.S.; Nauman, K.; Alahmedi, S.; Almazyed, A.O.; Almosallam, M.A.; Al Jurayyan, A.N. A synergic action of colistin, imipenem, and silver nanoparticles against pandrug-resistant Acinetobacter baumannii isolated from patients. *J. Infect. Public Health* **2021**, *14*, 1679–1685. [CrossRef]

179. Niemirowicz, K.; Piktel, E.; Wilczewska, A.Z.; Markiewicz, K.H.; Durnaś, B.; Wątek, M.; Puszkarz, I.; Wróblewska, M.; Niklińska, W.; Savage, P.B.; et al. Core-shell magnetic nanoparticles display synergistic antibacterial effects against. *Int. J. Nanomed.* **2016**, *11*, 5443–5455. [CrossRef]

180. Nadhe, S.B.; Singh, R.; Wadhwani, S.A.; Chopade, B.A. Acinetobacter sp. mediated synthesis of AgNPs, its optimization, characterization and synergistic antifungal activity against C. albicans. *J. Appl. Microbiol.* **2019**, *127*, 445–458. [CrossRef]

181. Bayat, M.; Zargar, M.; Chudinova, E.; Astarkhanova, T.; Pakina, E. In vitro evaluation of antibacterial and antifungal activity of biogenic silver and copper nanoparticles: The first report of applying biogenic nanoparticles against Pilidium concavum and Pestalotia sp. fungi. *Molecules* **2021**, *26*, 5402. [CrossRef]

182. Al-Tawarah, N.M.; Qaralleh, H.; Khlaifat, A.M.; Nofal, M.N.; Alqaraleh, M.; Khleifat, K.M.; Al-limoun, M.O.; Al Shhab, M.A. Anticancer and Antibacterial Properties of Verthemia Iphionides Essential Oil/Silver Nanoparticles. *Biomed. Pharm. J.* **2020**, *13*, 1175–1185. [CrossRef]

183. Abdelsattar, A.S.; Nofal, R.; Makky, S.; Safwat, A.; Taha, A.; El-Shibiny, A. The Synergistic Effect of Biosynthesized Silver Nanoparticles and Phage ZCSE2 as a Novel Approach to Combat Multidrug-Resistant Salmonella enterica. *Antibiotics* **2021**, *10*, 678. [CrossRef]

184. Kapadia, C.; Alhazmi, A.; Patel, N.; Elesawy, B.H.; Sayyed, R.Z.; Lokhandwala, F.; Haque, S.; Datta, R. Nanoparticles combined with cefixime as an effective synergistic strategy against Salmonella enterica typhi. *Saudi J. Biol. Sci.* **2021**, *28*, 4164–4172. [CrossRef] [PubMed]

185. Mussin, J.E.; Roldán, M.V.; Rojas, F.; de los Ángeles Sosa, M.; Pellegri, N.; Giusiano, G. Antifungal activity of silver nanoparticles in combination with ketoconazole against Malassezia furfur. *AMB Express* **2019**, *9*, 131. [CrossRef]

186. Ahamad, I.; Aziz, N.; Zaki, A.; Fatma, T. Synthesis and characterization of silver nanoparticles using Anabaena variabilis as a potential antimicrobial agent. *J. Appl. Phycol.* **2021**, *33*, 829–841. [CrossRef]

187. Shaker Al-mawlawi, Z.; Obaid, H.H. Antibacterial activity of synergistic effect of colicin and gold nanoparticles against klebsiella pneumonia. *Indian J. Public Health* **2019**, *10*, 1041–1047. [CrossRef]

188. Alkawareek, M.Y.; Bahlool, A.; Abulateefeh, S.R.; Alkilany, A.M. Synergistic antibacterial activity of silver nanoparticles and hydrogen peroxide. *PLoS ONE* **2019**, *14*, e0220575. [CrossRef]

189. Chen, X.; Chen, H.; Zhang, H.; Peng, Y.; Deng, F.; Gao, J.; Chai, C.; Tang, S.; Zuo, X.; Lu, J.; et al. Characterization of synergistic antibacterial effect of silver nanoparticles and ebselen. *Artif. Cells Nanomed. Biotechnol.* **2019**, *47*, 3338–3349. [CrossRef] [PubMed]

190. Jyoti, A.; Agarwal, M.; Tomar, R.S. Synergistic effect of Zinc Oxide Nanoparticles and Guava Leaf extract for Enhanced antimicrobial activity against Enterotoxigenic Escherichia coli. *J. Biochem. Technol.* **2020**, *11*, 17–23.

191. Basavegowda, N.; Baek, K.-H. Multimetallic Nanoparticles as Alternative Antimicrobial Agents: Challenges and Perspectives. *Molecules* **2021**, *26*, 912. [CrossRef] [PubMed]

192. Buchwalter, P.; Rose, J.; Braunstein, P. Multimetallic catalysis based on heterometallic complexes and clusters. *Chem. Rev.* **2015**, *115*, 28–126. [CrossRef] [PubMed]

193. Zhang, J.; Ma, J.; Fan, X.; Peng, W.; Zhang, G.; Zhang, F.; Li, Y. Graphene supported Au-Pd-Fe3O4 alloy trimetallic nanoparticles with peroxidase-like activities as mimic enzyme. *Catal. Commun.* **2017**, *89*, 148–151. [CrossRef]

194. Prabhu, S.; Poulose, E.K. Silver nanoparticles: Mechanism of antimicrobial action, synthesis, medical applications, and toxicity effects. *Int. Nano Lett.* **2012**, *2*, 32. [CrossRef]

195. Al-Asfar, A.; Zaheer, Z.; Aazam, E.S. Eco-friendly green synthesis of Ag@ Fe bimetallic nanoparticles: Antioxidant, antimicrobial and photocatalytic degradation of bromothymol blue. *J. Photochem. Photobiol. B Biol.* **2018**, *185*, 143–152. [CrossRef]

196. Padilla-Cruz, A.L.; Garza-Cervantes, J.A.; Vasto-Anzaldo, X.G.; García-Rivas, G.; León-Buitimea, A.; Morones-Ramírez, J.R. Synthesis and design of Ag-Fe bimetallic nanoparticles as antimicrobial synergistic combination therapies against clinically relevant pathogens. *Sci. Rep.* **2021**, *11*, 5351. [CrossRef]

197. Zhao, X.; Jia, Y.; Dong, R.; Deng, J.; Tang, H.; Hu, F.; Liu, S.; Jiang, X. Bimetallic nanoparticles against multi-drug resistant bacteria. *Chem. Commun.* **2020**, *56*, 10918–10921. [CrossRef]

198. López Ruiz, A.; Bartomeu Garcia, C.; Navarro Gallón, S.; Webster, T.J. Novel Silver-Platinum Nanoparticles for Anticancer and Antimicrobial Applications. *Int. J. Nanomed.* **2020**, *15*, 169–179. [CrossRef]

199. Kamli, M.R.; Srivastava, V.; Hajrah, N.H.; Sabir, J.S.; Hakeem, K.R.; Ahmad, A.; Malik, M.A. Facile Bio-Fabrication of Ag-Cu-Co Trimetallic Nanoparticles and Its Fungicidal Activity against Candida auris. *J. Fungi* **2021**, *7*, 62. [CrossRef]

200. Mathur, P.; Jha, S.; Ramteke, S.; Jain, N. Pharmaceutical aspects of silver nanoparticles. *Artif. Cells Nanomed. Biotechnol.* **2018**, *46*, 115–126. [CrossRef]

201. Wang, Y.; Cao, A.; Jiang, Y.; Zhang, I.; Liu, J.; Liu, Y.; Wang, H. Superior antibacterial activity of zinc oxide/graphene oxide composites localized around bacteria. *ACS Appl. Mater. Interfaces* **2014**, *6*, 2791–2798. [CrossRef]

202. Ellis, T.; Chiappi, M.; García-Trenco, A.; Al-Ejji, M.; Sarkar, S.; Georgiou, T.K.; Shaffer, M.S.; Tetley, T.D.; Schwander, S.; Ryan, M.P. Multimetallic microparticles increase the potency of rifampicin against intracellular Mycobacterium tuberculosis. *ACS Nano* **2018**, *12*, 5228–5240. [CrossRef]

203. Mah, T.-F. Biofilm-specific antibiotic resistance. *Future Microbiol.* **2012**, *7*, 1061–1072. [CrossRef]

204. Ranpariya, B.; Salunke, G.; Karmakar, S.; Babiya, K.; Sutar, S.; Kadoo, N.; Kumbhakar, P.; Ghosh, S. Antimicrobial Synergy of Silver-Platinum Nanohybrids With Antibiotics. *Front. Microbiol.* **2020**, *11*, 610968. [CrossRef]

205. Fakhri, A.; Tahami, S.; Naji, M. Synthesis and characterization of core-shell bimetallic nanoparticles for synergistic antimicrobial effect studies in combination with doxycycline on burn specific pathogens. *J. Photochem. Photobiol. B* **2017**, *169*, 21–26. [CrossRef]

206. Tang, Z.; Yeo, B.C.; Han, S.S.; Lee, T.-J.; Bhang, S.H.; Kim, W.-S.; Yu, T. Facile aqueous-phase synthesis of Ag–Cu–Pt–Pd quadrometallic nanoparticles. *Nano Converg.* **2019**, *6*, 38. [CrossRef]

207. Sui, M.; Kunwar, S.; Pandey, P.; Pandit, S.; Lee, J. Improved localized surface plasmon resonance responses of multi-metallic Ag/Pt/Au/Pd nanostructures: Systematic study on the fabrication mechanism and localized surface plasmon resonance properties by solid-state dewetting. *New J. Phys.* **2019**, *21*, 113049. [CrossRef]

208. Formaggio, D.M.D.; de Oliveira Neto, X.A.; Rodrigues, L.D.A.; de Andrade, V.M.; Nunes, B.C.; Lopes-Ferreira, M.; Ferreira, F.G.; Wachesk, C.C.; Camargo, E.R.; Conceição, K. In vivo toxicity and antimicrobial activity of AuPt bimetallic nanoparticles. *J. Nanoparticle Res.* **2019**, *21*, 244. [CrossRef]

209. Diem, P.N.H.; Phuong, T.N.M.; Hien, N.Q.; Quang, D.T.; Hoa, T.T.; Cuong, N.D. Silver, gold, and silver-gold bimetallic nanoparticle-decorated dextran: Facile synthesis and versatile tunability on the antimicrobial activity. *J. Nanomater.* **2020**, *2020*, 7195048. [CrossRef]

210. Merugu, R.; Gothalwal, R.; Deshpande, P.K.; De Mandal, S.; Padala, G.; Chitturi, K.L. Synthesis of Ag/Cu and Cu/Zn bimetallic nanoparticles using toddy palm: Investigations of their antitumor, antioxidant and antibacterial activities. *Mater. Today Proc.* **2021**, *44*, 99–105. [CrossRef]

211. Dlugaszewska, J.; Dobrucka, R. Effectiveness of biosynthesized trimetallic Au/Pt/Ag nanoparticles on planktonic and biofilm Enterococcus faecalis and Enterococcus faecium forms. *J. Clust. Sci.* **2019**, *30*, 1091–1101. [CrossRef]

212. Ahmed, A.A.A.; Al-Mushki, A.A.; Al-Asbahi, B.A.; Abdulwahab, A.; Abduljalil, J.M.; Saad, F.A.; Qaid, S.M.; Ghaithan, H.M.; Farooq, W.; Omar, A.-E.H. Effect of ethylene glycol concentration on the structural and optical properties of multimetal oxide CdO–NiO–Fe2O3 nanocomposites for antibacterial activity. *J. Phys. Chem. Solids* **2021**, *155*, 110113. [CrossRef]

213. Paul, D.; Mangla, S.; Neogi, S. Antibacterial study of CuO-NiO-ZnO trimetallic oxide nanoparticle. *Mater. Lett.* **2020**, *271*, 127740. [CrossRef]

214. Gupta, A.; Khosla, N.; Govindasamy, V.; Saini, A.; Annapurna, K.; Dhakate, S.R. Trimetallic composite nanofibers for antibacterial and photocatalytic dye degradation of mixed dye water. *Appl. Nanosci.* **2020**, *10*, 4191–4205. [CrossRef]

215. Arsalan, A.; Younus, H. Enzymes and nanoparticles: Modulation of enzymatic activity via nanoparticles. *Int. J. Biol. Macromol.* **2018**, *118*, 1833–1847. [CrossRef]

216. Guliani, A.; Acharya, A. Nanomaterials as Protein, Peptide and Gene Delivery Agents. *Open Biotechnol. J.* **2018**, *12*, 154–165. [CrossRef]

217. McNamara, K.; Tofail, S.A. Nanoparticles in biomedical applications. *Adv. Phys. X* **2017**, *2*, 54–88. [CrossRef]

218. Shruthi, T.; Meghana, M.; Medha, M.; Sanjana, S.; Navya, P.; Daima, H.K. Streptomycin functionalization on silver nanoparticles for improved antibacterial activity. *Mater. Today Proc.* **2019**, *10*, 8–15. [CrossRef]

219. Shaikh, S.; Nazam, N.; Rizvi, S.M.D.; Ahmad, K.; Baig, M.H.; Lee, E.J.; Choi, I. Mechanistic Insights into the Antimicrobial Actions of Metallic Nanoparticles and Their Implications for Multidrug Resistance. *Int. J. Mol. Sci.* **2019**, *20*, 2468. [CrossRef]

220. Ramalingam, B.; Parandhaman, T.; Das, S.K. Antibacterial effects of biosynthesized silver nanoparticles on surface ultrastructure and nanomechanical properties of gram-negative bacteria viz. Escherichia coli and Pseudomonas aeruginosa. *ACS Appl. Mater. Interfaces* **2016**, *8*, 4963–4976. [CrossRef]

221. Rai, A.; Prabhune, A.; Perry, C.C. Antibiotic mediated synthesis of gold nanoparticles with potent antimicrobial activity and their application in antimicrobial coatings. *J. Mater. Chem.* **2010**, *20*, 6789–6798. [CrossRef]

222. Shaikh, S.; Rizvi, S.M.D.; Shakil, S.; Hussain, T.; Alshammari, T.M.; Ahmad, W.; Tabrez, S.; Al-Qahtani, M.H.; Abuzenadah, A.M. Synthesis and Characterization of Cefotaxime Conjugated Gold Nanoparticles and Their Use to Target Drug-Resistant CTX-M-Producing Bacterial Pathogens. *J. Cell. Biochem.* **2017**, *118*, 2802–2808. [CrossRef]

223. Sreedharan, S.M.; Singh, R. Ciprofloxacin Functionalized Biogenic Gold Nanoflowers as Nanoantibiotics Against Pathogenic Bacterial Strains. *Int. J. Nanomed.* **2019**, *14*, 9905–9916. [CrossRef]

224. Webber, M.; Piddock, L. The importance of efflux pumps in bacterial antibiotic resistance. *J. Antimicrob. Chemother.* **2003**, *51*, 9–11. [CrossRef]

225. Padwal, P.; Bandyopadhyaya, R.; Mehra, S. Biocompatible citric acid-coated iron oxide nanoparticles to enhance the activity of first-line anti-TB drugs in Mycobacterium smegmatis. *J. Chem. Technol. Biotechnol.* **2015**, *90*, 1773–1781. [CrossRef]

226. Brown, A.N.; Smith, K.; Samuels, T.A.; Lu, J.; Obare, S.O.; Scott, M.E. Nanoparticles functionalized with ampicillin destroy multiple-antibiotic-resistant isolates of Pseudomonas aeruginosa and Enterobacter aerogenes and methicillin-resistant Staphylococcus aureus. *Appl. Environ. Microbiol.* **2012**, *78*, 2768–2774. [CrossRef]

227. Bhattacharya, D.; Saha, B.; Mukherjee, A.; Santra, C.R.; Karmakar, P. Gold nanoparticles conjugated antibiotics: Stability and functional evaluation. *Nanosci. Nanotechnol.* **2012**, *2*, 14–21. [CrossRef]

228. Yeom, J.-H.; Lee, B.; Kim, D.; Lee, J.-k.; Kim, S.; Bae, J.; Park, Y.; Lee, K. Gold nanoparticle-DNA aptamer conjugate-assisted delivery of antimicrobial peptide effectively eliminates intracellular Salmonella enterica serovar Typhimurium. *Biomaterials* **2016**, *104*, 43–51. [CrossRef]

229. Kumar, C.G.; Poornachandra, Y. Biodirected synthesis of Miconazole-conjugated bacterial silver nanoparticles and their application as antifungal agents and drug delivery vehicles. *Colloids Surf. B Biointerfaces* **2015**, *125*, 110–119. [CrossRef] [PubMed]

230. Kumar, P.; Shivam, P.; Mandal, S.; Prasanna, P.; Kumar, S.; Prasad, S.R.; Kumar, A.; Das, P.; Ali, V.; Singh, S.K. Synthesis, characterization, and mechanistic studies of a gold nanoparticle–amphotericin B covalent conjugate with enhanced antileishmanial efficacy and reduced cytotoxicity. *Int. J. Nanomed.* **2019**, *14*, 6073. [CrossRef] [PubMed]

231. Ghosh, C.; Varela-Aramburu, S.; Eldesouky, H.E.; Salehi Hossainy, S.; Seleem, M.N.; Aebischer, T.; Seeberger, P.H. Non-Toxic Glycosylated Gold Nanoparticle-Amphotericin B Conjugates Reduce Biofilms and Intracellular Burden of Fungi and Parasites. *Adv. Ther.* **2021**, *4*, 2000293. [CrossRef]

232. Yeh, Y.-C.; Huang, T.-H.; Yang, S.-C.; Chen, C.-C.; Fang, J.-Y. Nano-based drug delivery or targeting to eradicate bacteria for infection mitigation: A review of recent advances. *Front. Chem.* **2020**, *8*, 286. [CrossRef] [PubMed]

233. Perni, S.; Prokopovich, P. Continuous release of gentamicin from gold nanocarriers. *RSC Adv.* **2014**, *4*, 51904–51910. [CrossRef]

234. Li, X.; Gui, R.; Li, J.; Huang, R.; Shang, Y.; Zhao, Q.; Liu, H.; Jiang, H.; Shang, X.; Wu, X. Novel Multifunctional Silver Nanocomposite Serves as a Resistance-Reversal Agent to Synergistically Combat Carbapenem-Resistant Acinetobacter baumannii. *ACS Appl. Mater. Interfaces* **2021**, *13*, 30434–30457. [CrossRef]

235. Zendegani, E.; Dolatabadi, S. The efficacy of imipenem conjugated with synthesized silver nanoparticles against Acinetobacter baumannii clinical isolates, Iran. *Biol. Trace Elem. Res.* **2020**, *197*, 330–340. [CrossRef]

236. Chavan, C.; Kamble, S.; Murthy, A.V.R.; Kale, S.N. Ampicillin-mediated functionalized gold nanoparticles against ampicillin-resistant bacteria: Strategy, preparation and interaction studies. *Nanotechnology* **2020**, *31*, 215604. [CrossRef]

237. Memarian, M.; Javadi, A.; Fateh, R. Antifungal effects of gold nanoparticles conjugated fluconazole against fluconazole resistant strains of candida albicans isolated from patients with chronic vulvovaginitis. *Qom Univ. Med. Sci. J.* **2016**, *10*, 10–19.

238. Nawaz, A.; Ali, S.M.; Rana, N.F.; Tanweer, T.; Batool, A.; Webster, T.J.; Menaa, F.; Riaz, S.; Rehman, Z.; Batool, F. Ciprofloxacin-Loaded Gold Nanoparticles against Antimicrobial Resistance: An In Vivo Assessment. *Nanomaterials* **2021**, *11*, 3152. [CrossRef]

239. Niemirowicz, K.; Durnaś, B.; Tokajuk, G.; Głuszek, K.; Wilczewska, A.Z.; Misztalewska, I.; Mystkowska, J.; Michalak, G.; Sodo, A.; Wątek, M. Magnetic nanoparticles as a drug delivery system that enhance fungicidal activity of polyene antibiotics. *Nanomed. Nanotechnol. Biol. Med.* **2016**, *12*, 2395–2404. [CrossRef]

240. Millenbaugh, N.J.; Baskin, J.B.; DeSilva, M.N.; Elliott, W.R.; Glickman, R.D. Photothermal killing of Staphylococcus aureus using antibody-targeted gold nanoparticles. *Int. J. Nanomed.* **2015**, *10*, 1953. [CrossRef]

241. Mocan, L.; Matea, C.; Tabaran, F.A.; Mosteanu, O.; Pop, T.; Puia, C.; Agoston-Coldea, L.; Gonciar, D.; Kalman, E.; Zaharie, G. Selective in vitro photothermal nano-therapy of MRSA infections mediated by IgG conjugated gold nanoparticles. *Sci. Rep.* **2016**, *6*, 39466. [CrossRef]

242. Al-Sharqi, A.; Apun, K.; Vincent, M.; Kanakaraju, D.; Bilung, L.M.; Sum, M.S.H. Investigation of the antibacterial activity of Ag-NPs conjugated with a specific antibody against Staphylococcus aureus after photoactivation. *J. Appl. Microbiol.* **2020**, *128*, 102–115. [CrossRef]

243. Shokri, R.; Salouti, M.; Zanjani, R.S. Anti protein A antibody-gold nanorods conjugate: A targeting agent for selective killing of methicillin resistant Staphylococcus aureus using photothermal therapy method. *J. Microbiol.* **2015**, *53*, 116–121. [CrossRef]

244. Di Pasqua, A.J.; Mishler II, R.E.; Ship, Y.-L.; Dabrowiak, J.C.; Asefa, T. Preparation of antibody-conjugated gold nanoparticles. *Mater. Lett.* **2009**, *63*, 1876–1879. [CrossRef]

245. Hashemi, H.; Varshosaz, J.; Fazeli, H.; Sharafi, S.M.; Mirhendi, H.; Chadeganipour, M.; Yousefi, H.; Manoochehri, K.; Chermahini, Z.A.; Jafarzadeh, L. Rapid differential diagnosis of vaginal infections using gold nanoparticles coated with specific antibodies. *Med. Microbiol. Immunol.* **2019**, *208*, 773–780. [CrossRef]

246. Shahbandeh, M.; Eghdami, A.; Moghaddam, M.M.; Nadoushan, M.J.; Salimi, A.; Fasihi-Ramandi, M.; Mohammadi, S.; Mirzaei, M.; Mirnejad, R. Conjugation of imipenem to silver nanoparticles for enhancement of its antibacterial activity against multidrug-resistant isolates of Pseudomonas aeruginosa. *J. Biosci.* **2021**, *46*, 26. [CrossRef]

247. Hamad, K.M.; Mahmoud, N.N.; Al-Dabash, S.; Al-Samad, L.A.; Abdallah, M.; Al-Bakri, A.G. Fluconazole conjugated-gold nanorods as an antifungal nanomedicine with low cytotoxicity against human dermal fibroblasts. *RSC Adv.* **2020**, *10*, 25889–25897. [CrossRef]

248. Salehi, Z.; Fattahi, A.; Lotfali, E.; Kazemi, A.; Shakeri-Zadeh, A.; Nasrollahi, S.A. Susceptibility Pattern of Caspofungin-Coated Gold Nanoparticles Against Clinically Important Candida Species. *Adv. Pharm. Bull.* **2020**, *11*, 693. [CrossRef]

249. Khan, M.; Shaik, M.R.; Khan, S.T.; Adil, S.F.; Kuniyil, M.; Al-Warthan, A.A.; Siddiqui, M.R.H.; Nawaz Tahir, M. Enhanced Antimicrobial Activity of Biofunctionalized Zirconia Nanoparticles. *ACS Omega* **2020**, *5*, 1987–1996. [CrossRef] [PubMed]

250. Halbus, A.F.; Horozov, T.S.; Paunov, V.N. Strongly enhanced antibacterial action of copper oxide nanoparticles with boronic acid surface functionality. *ACS Appl. Mater. Interfaces* **2019**, *11*, 12232–12243. [CrossRef] [PubMed]

251. Hussein, M.A.M.; Baños, F.G.D.; Grinholc, M.; Dena, A.S.A.; El-Sherbiny, I.M.; Megahed, M. Exploring the physicochemical and antimicrobial properties of gold-chitosan hybrid nanoparticles composed of varying chitosan amounts. *Int. J. Biol. Macromol.* **2020**, *162*, 1760–1769. [CrossRef] [PubMed]

252. Tiwari, V.; Tiwari, M.; Solanki, V. Polyvinylpyrrolidone-Capped Silver Nanoparticle Inhibits Infection of Carbapenem-Resistant Strain of. *Front. Immunol.* **2017**, *8*, 973. [CrossRef] [PubMed]

253. Bajaj, M.; Pandey, S.K.; Wangoo, N.; Sharma, R.K. Peptide functionalized metallic nanoconstructs: Synthesis, structural characterization, and antimicrobial evaluation. *ACS Biomater. Sci. Eng.* **2018**, *4*, 739–747. [CrossRef]

254. Algotiml, R.; Gab-Alla, A.; Seoudi, R.; Abulreesh, H.H.; El-Readi, M.Z.; Elbanna, K. Anticancer and antimicrobial activity of biosynthesized Red Sea marine algal silver nanoparticles. *Sci. Rep.* **2022**, *12*, 2421. [CrossRef]

255. Niemirowicz, K.; Prokop, I.; Wilczewska, A.Z.; Wnorowska, U.; Piktel, E.; Wątek, M.; Savage, P.B.; Bucki, R. Magnetic nanoparticles enhance the anticancer activity of cathelicidin LL-37 peptide against colon cancer cells. *Int. J. Nanomed.* **2015**, *10*, 3843. [CrossRef]

256. Sukhanova, A.; Bozrova, S.; Sokolov, P.; Berestovoy, M.; Karaulov, A.; Nabiev, I. Dependence of nanoparticle toxicity on their physical and chemical properties. *Nanoscale Res. Lett.* **2018**, *13*, 44. [CrossRef]

257. Mukhopadhyay, R.; Kazi, J.; Debnath, M.C. Synthesis and characterization of copper nanoparticles stabilized with Quisqualis indica extract: Evaluation of its cytotoxicity and apoptosis in B16F10 melanoma cells. *Biomed. Pharmacother.* **2018**, *97*, 1373–1385. [CrossRef]

258. Lokapur, V.; Jayakar, V.; Chalannavar, R.K.; Lasrado, L.; Shantaram, M. ZnO nanoparticles with spectroscopically controlled morphology, bioinspired from Holigarna grahamii (Wight) Kurz and delving its antioxidant and anticancer potential on A498 cell line. *Mater. Today Commun.* **2022**, *31*, 103338. [CrossRef]

259. Khan, S.A.; Shahid, S.; Hanif, S.; Almoallim, H.S.; Alharbi, S.A.; Sellami, H. Green synthesis of chromium oxide nanoparticles for antibacterial, antioxidant anticancer, and biocompatibility activities. *Int. J. Mol. Sci.* **2021**, *22*, 502. [CrossRef]

260. Pannerselvam, B.; Thiyagarajan, D.; Pazhani, A.; Thangavelu, K.P.; Kim, H.J.; Rangarajulu, S.K. Copperpod plant synthesized AgNPs enhance cytotoxic and apoptotic effect in cancer cell lines. *Processes* **2021**, *9*, 888. [CrossRef]

261. Piktel, E.; Markiewicz, K.H.; Wilczewska, A.Z.; Daniluk, T.; Chmielewska, S.; Niemirowicz-Laskowska, K.; Mystkowska, J.; Paprocka, P.; Savage, P.B.; Bucki, R. Quantification of Synergistic Effects of Ceragenin CSA-131 combined with iron oxide magnetic nanoparticles against cancer cells. *Int. J. Nanomed.* **2020**, *15*, 4573. [CrossRef]

262. Piktel, E.; Oscilowska, I.; Suprewicz, Ł.; Depciuch, J.; Marcińczyk, N.; Chabielska, E.; Wolak, P.; Głuszek, K.; Klimek, J.; Zieliński, P.M. Peanut-Shaped Gold Nanoparticles with Shells of Ceragenin CSA-131 Display the Ability to Inhibit Ovarian Cancer Growth In Vitro and in a Tumor Xenograft Model. *Cancers* **2021**, *13*, 5424. [CrossRef]

263. Magdolenova, Z.; Collins, A.; Kumar, A.; Dhawan, A.; Stone, V.; Dusinska, M. Mechanisms of genotoxicity. A review of in vitro and in vivo studies with engineered nanoparticles. *Nanotoxicology* **2014**, *8*, 233–278. [CrossRef]

264. Irrsack, E.; Schuller, J.; Petters, C.; Willmann, W.; Dringen, R.; Koch, M. Effects of Local Administration of Iron Oxide Nanoparticles in the Prefrontal Cortex, Striatum, and Hippocampus of Rats. *Neurotox. Res.* **2021**, *39*, 2056–2071. [CrossRef]

265. Lopez-Chaves, C.; Soto-Alvaredo, J.; Montes-Bayon, M.; Bettmer, J.; Llopis, J.; Sanchez-Gonzalez, C. Gold nanoparticles: Distribution, bioaccumulation and toxicity. In vitro and in vivo studies. *Nanomed. Nanotechnol. Biol. Med.* **2018**, *14*, 1–12. [CrossRef]

266. Xia, Q.; Huang, J.; Feng, Q.; Chen, X.; Liu, X.; Li, X.; Zhang, T.; Xiao, S.; Li, H.; Zhong, Z. Size-and cell type-dependent cellular uptake, cytotoxicity and in vivo distribution of gold nanoparticles. *Int. J. Nanomed.* **2019**, *14*, 6957. [CrossRef]

267. Woźniak, A.; Malankowska, A.; Nowaczyk, G.; Grześkowiak, B.F.; Tuśnio, K.; Słomski, R.; Zaleska-Medynska, A.; Jurga, S. Size and shape-dependent cytotoxicity profile of gold nanoparticles for biomedical applications. *J. Mater. Sci. Mater. Med.* **2017**, *28*, 92. [CrossRef]

268. Steckiewicz, K.P.; Barcinska, E.; Malankowska, A.; Zauszkiewicz–Pawlak, A.; Nowaczyk, G.; Zaleska-Medynska, A.; Inkielewicz-Stepniak, I. Impact of gold nanoparticles shape on their cytotoxicity against human osteoblast and osteosarcoma in in vitro model. Evaluation of the safety of use and anti-cancer potential. *J. Mater. Sci. Mater. Med.* **2019**, *30*, 22. [CrossRef]

269. Lee, Y.J.; Ahn, E.-Y.; Park, Y. Shape-dependent cytotoxicity and cellular uptake of gold nanoparticles synthesized using green tea extract. *Nanoscale Res. Lett.* **2019**, *14*, 129. [CrossRef] [PubMed]

270. Peng, C.; Shen, C.; Zheng, S.; Yang, W.; Hu, H.; Liu, J.; Shi, J. Transformation of CuO nanoparticles in the aquatic environment: Influence of pH, electrolytes and natural organic matter. *Nanomaterials* **2017**, *7*, 326. [CrossRef] [PubMed]

271. Hahn, A.; Fuhlrott, J.; Loos, A.; Barcikowski, S. Cytotoxicity and ion release of alloy nanoparticles. *J. Nanoparticle Res.* **2012**, *14*, 686. [CrossRef] [PubMed]

272. Sun, C.; Yin, N.; Wen, R.; Liu, W.; Jia, Y.; Hu, L.; Zhou, Q.; Jiang, G. Silver nanoparticles induced neurotoxicity through oxidative stress in rat cerebral astrocytes is distinct from the effects of silver ions. *Neurotoxicology* **2016**, *52*, 210–221. [CrossRef]

273. George, S.; Lin, S.; Ji, Z.; Thomas, C.R.; Li, L.; Mecklenburg, M.; Meng, H.; Wang, X.; Zhang, H.; Xia, T. Surface defects on plate-shaped silver nanoparticles contribute to its hazard potential in a fish gill cell line and zebrafish embryos. *ACS Nano* **2012**, *6*, 3745–3759. [CrossRef]

274. Soenen, S.J.; Parak, W.J.; Rejman, J.; Manshian, B. (Intra) cellular stability of inorganic nanoparticles: Effects on cytotoxicity, particle functionality, and biomedical applications. *Chem. Rev.* **2015**, *115*, 2109–2135. [CrossRef]

275. El Badawy, A.M.; Silva, R.G.; Morris, B.; Scheckel, K.G.; Suidan, M.T.; Tolaymat, T.M. Surface charge-dependent toxicity of silver nanoparticles. *Environ. Sci. Technol.* **2011**, *45*, 283–287. [CrossRef]

276. Rybak-Smith, M.J. Effect of surface modification on toxicity of nanoparticles. *Encycl. Nanotechnol.* **2012**, *2012*, 645–652.

277. Chen, N.-F.; Liao, Y.-H.; Lin, P.-Y.; Chen, W.-F.; Wen, Z.-H.; Hsieh, S. Investigation of the characteristics and antibacterial activity of polymer-modified copper oxide nanoparticles. *Int. J. Mol. Sci.* **2021**, *22*, 12913. [CrossRef]

278. Amooaghaie, R.; Saeri, M.R.; Azizi, M. Synthesis, characterization and biocompatibility of silver nanoparticles synthesized from Nigella sativa leaf extract in comparison with chemical silver nanoparticles. *Ecotoxicol. Environ. Saf.* **2015**, *120*, 400–408. [CrossRef]

279. Dowlath, M.J.H.; Musthafa, S.A.; Khalith, S.M.; Varjani, S.; Karuppannan, S.K.; Ramanujam, G.M.; Arunachalam, A.M.; Arunachalam, K.D.; Chandrasekaran, M.; Chang, S.W. Comparison of characteristics and biocompatibility of green synthesized iron oxide nanoparticles with chemical synthesized nanoparticles. *Environ. Res.* **2021**, *201*, 111585. [CrossRef]

280. Kummara, S.; Patil, M.B.; Uriah, T. Synthesis, characterization, biocompatible and anticancer activity of green and chemically synthesized silver nanoparticles–a comparative study. *Biomed. Pharmacother.* **2016**, *84*, 10–21. [CrossRef] [PubMed]

281. Hawkey, P.M.; Jones, A.M. The changing epidemiology of resistance. *J. Antimicrob. Chemother.* **2009**, *64*, i3–i10. [CrossRef] [PubMed]

282. Guo, J.; Gao, S.-H.; Lu, J.; Bond, P.L.; Verstraete, W.; Yuan, Z. Copper oxide nanoparticles induce lysogenic bacteriophage and metal-resistance genes in Pseudomonas aeruginosa PAO1. *ACS Appl. Mater. Interfaces* **2017**, *9*, 22298–22307. [CrossRef] [PubMed]

283. McQuillan, J.S.; Groenaga Infante, H.; Stokes, E.; Shaw, A.M. Silver nanoparticle enhanced silver ion stress response in Escherichia coli K12. *Nanotoxicology* **2012**, *6*, 857–866. [CrossRef]

284. Faghihzadeh, F.; Anaya, N.; Astudillo-Castro, C.; Oyanedel-Craver, V. Kinetic, metabolic and macromolecular response of bacteria to chronic nanoparticle exposure in continuous culture. *Environ. Sci. Nano* **2018**, *5*, 1386–1396. [CrossRef]

285. Mu, D.; Yu, X.; Xu, Z.; Du, Z.; Chen, G. Physiological and transcriptomic analyses reveal mechanistic insight into the adaption of marine Bacillus subtilis C01 to alumina nanoparticles. *Sci. Rep.* **2016**, *6*, 24474. [CrossRef]

286. Gou, N.; Onnis-Hayden, A.; Gu, A.Z. Mechanistic toxicity assessment of nanomaterials by whole-cell-array stress genes expression analysis. *Environ. Sci. Technol.* **2010**, *44*, 5964–5970. [CrossRef]

287. Wang, Q.; Kang, F.; Gao, Y.; Mao, X.; Hu, X. Sequestration of nanoparticles by an EPS matrix reduces the particle-specific bactericidal activity. *Sci. Rep.* **2016**, *6*, 21379. [CrossRef]

288. Ouyang, K.; Mortimer, M.; Holden, P.A.; Cai, P.; Wu, Y.; Gao, C.; Huang, Q. Towards a better understanding of Pseudomonas putida biofilm formation in the presence of ZnO nanoparticles (NPs): Role of NP concentration. *Environ. Int.* **2020**, *137*, 105485. [CrossRef]

289. Yang, Y.; Alvarez, P.J. Sublethal concentrations of silver nanoparticles stimulate biofilm development. *Environ. Sci. Technol. Lett.* **2015**, *2*, 221–226. [CrossRef]

290. Lamas, B.; Martins Breyner, N.; Houdeau, E. Impacts of foodborne inorganic nanoparticles on the gut microbiota-immune axis: Potential consequences for host health. *Part. Fibre Toxicol.* **2020**, *17*, 19. [CrossRef]

291. Ghebretatios, M.; Schaly, S.; Prakash, S. Nanoparticles in the food industry and their impact on human gut microbiome and diseases. *Int. J. Mol. Sci.* **2021**, *22*, 1942. [CrossRef]

292. Vitulo, M.; Gnodi, E.; Meneveri, R.; Barisani, D. Interactions between nanoparticles and intestine. *Int. J. Mol. Sci.* **2022**, *23*, 4339. [CrossRef]

293. Limage, R.; Tako, E.; Kolba, N.; Guo, Z.; García-Rodríguez, A.; Marques, C.N.; Mahler, G.J. TiO2 nanoparticles and commensal bacteria alter mucus layer thickness and composition in a gastrointestinal tract model. *Small* **2020**, *16*, 2000601. [CrossRef]

294. Williams, K.; Milner, J.; Boudreau, M.D.; Gokulan, K.; Cerniglia, C.E.; Khare, S. Effects of subchronic exposure of silver nanoparticles on intestinal microbiota and gut-associated immune responses in the ileum of Sprague-Dawley rats. *Nanotoxicology* **2015**, *9*, 279–289. [CrossRef]

295. Van Den Brûle, S.; Ambroise, J.; Lecloux, H.; Levard, C.; Soulas, R.; De Temmerman, P.-J.; Palmai-Pallag, M.; Marbaix, E.; Lison, D. Dietary silver nanoparticles can disturb the gut microbiota in mice. *Part. Fibre Toxicol.* **2015**, *13*, 38. [CrossRef]

296. Chen, H.; Zhao, R.; Wang, B.; Cai, C.; Zheng, L.; Wang, H.; Wang, M.; Ouyang, H.; Zhou, X.; Chai, Z. The effects of orally administered Ag, TiO2 and SiO2 nanoparticles on gut microbiota composition and colitis induction in mice. *NanoImpact* **2017**, *8*, 80–88. [CrossRef]

297. Das, P.; McDonald, J.A.; Petrof, E.O.; Allen-Vercoe, E.; Walker, V.K. Nanosilver-mediated change in human intestinal microbiota. *J. Nanomed. Nanotechnol.* **2014**, *5*, 1000235.

298. Dudefoi, W.; Moniz, K.; Allen-Vercoe, E.; Ropers, M.-H.; Walker, V.K. Impact of food grade and nano-TiO2 particles on a human intestinal community. *Food Chem. Toxicol.* **2017**, *106*, 242–249. [CrossRef]

299. Chen, Z.; Zhou, D.; Han, S.; Zhou, S.; Jia, G. Hepatotoxicity and the role of the gut-liver axis in rats after oral administration of titanium dioxide nanoparticles. *Part. Fibre Toxicol.* **2019**, *16*, 48. [CrossRef] [PubMed]

300. Xia, T.; Lai, W.; Han, M.; Han, M.; Ma, X.; Zhang, L. Dietary ZnO nanoparticles alters intestinal microbiota and inflammation response in weaned piglets. *Oncotarget* **2017**, *8*, 64878. [CrossRef] [PubMed]

301. Feng, Y.; Min, L.; Zhang, W.; Liu, J.; Hou, Z.; Chu, M.; Li, L.; Shen, W.; Zhao, Y.; Zhang, H. Zinc oxide nanoparticles influence microflora in ileal digesta and correlate well with blood metabolites. *Front. Microbiol.* **2017**, *8*, 992. [CrossRef] [PubMed]

10. Publikacja nr 2 (P.2)

Article

Ceragenin-Coated Non-Spherical Gold Nanoparticles as Novel Candidacidal Agents

Karol Skłodowski [1], Sylwia Joanna Chmielewska [1], Joanna Depciuch [2], Piotr Deptuła [1], Ewelina Piktel [1], Tamara Daniluk [1], Magdalena Zakrzewska [1], Michał Czarnowski [1], Mateusz Cieśluk [1], Bonita Durnaś [3], Magdalena Parlińska-Wojtan [2], Paul B. Savage [4] and Robert Bucki [1,*]

[1] Department of Medical Microbiology and Nanobiomedical Engineering, Medical University of Bialystok, 15-222 Bialystok, Poland; karol.sklodowsky@gmail.com (K.S.); sylwia.chmielewska@umb.edu.pl (S.J.C.); piotr.deptula@umb.edu.pl (P.D.); ewelina.piktel@wp.pl (E.P.); tamara.daniluk@umb.edu.pl (T.D.); magdalena.zakrzew@gmail.com (M.Z.); flaps.czarnowski@gmail.com (M.C.); mticv1@gmail.com (M.C.)
[2] Institute of Nuclear Physics, Polish Academy of Sciences, 31-342 Krakow, Poland; joanna.depciuch@ifj.edu.pl (J.D.); magdalena.parlinska@ifj.edu.pl (M.P.-W.)
[3] The Faculty of Medicine and Health Sciences, Collegium Modicum of the Jan Kochanowski University in Kielce, 25-734 Kielce, Poland; bonita.durnas@ujk.edu.pl
[4] Department of Chemistry and Biochemistry, Brigham Young University, Provo, UT 84602, USA; pbsavage@chem.byu.edu
* Correspondence: buckirobert@gmail.com; Tel.: +48-85-748-5493; Fax: +48-85-748-5416

Abstract: Background: Infections caused by *Candida* spp. have become one of the major causes of morbidity and mortality in immunocompromised patients. Therefore, new effective fungicides are urgently needed, especially due to an escalating resistance crisis. Methods: A set of nanosystems with rod- (AuR), peanut- (AuP), and star-shaped (AuS) metal cores were synthesized. These gold nanoparticles were conjugated with ceragenins CSA-13, CSA-44, and CSA-131, and their activity was evaluated against *Candida* strains ($n = 21$) through the assessment of MICs (minimum inhibitory concentrations)/MFCs (minimum fungicidal concentrations). Moreover, in order to determine the potential for resistance development, serial passages of *Candida* cells with tested nanosystems were performed. The principal mechanism of action of Au NPs was evaluated via ROS (reactive oxygen species) generation assessment, plasma membrane permeabilization, and release of the protein content. Finally, to evaluate the potential toxicity of Au NPs, the measurement of hemoglobin release from red blood cells (RBCs) was carried out. Results: All of the tested nanosystems exerted a potent candidacidal activity, regardless of the species or susceptibility to other antifungal agents. Significantly, no resistance development after 25 passages of *Candida* cells with AuR@CSA-13, AuR@CSA-44, and AuR@CSA-131 nanosystems was observed. Moreover, the fungicidal mechanism of action of the investigated nanosystems involved the generation of ROS, damage of the fungal cell membrane, and leakage of intracellular contents. Notably, no significant RBCs hemolysis at candidacidal doses of tested nanosystems was detected. Conclusions: The results provide rationale for the development of gold nanoparticles of rod-, peanut-, and star-shaped conjugated with CSA-13, CSA-44, and CSA-131 as effective candidacidal agents.

Keywords: *Candida* spp.; ceragenins; CSA-13; CSA-44; CSA-131; gold nanoparticles; nanosystems

1. Introduction

In recent years, the incidences of *Candida* fungal infections have substantially increased. According to various studies, the attributable mortality among all patients with candidaemia has been recorded to be between 10% and 47%; however, a more accurate estimate is approximately 10–20%, with the risk of death being strictly connected with the increasing age, the species of *Candida* strain causing the infection, the use of immunosuppressive agents, and the presence of the venous catheter, as well as pre-existing renal dysfunction and other comorbidities [1–5].

Systemic, potentially life-threatening infections are predominantly caused by *Candida* spp. It is worth emphasizing that nearly 10 million cases of mucosal candidiasis are reported globally and more than 150 million of people are affected by serious fungal diseases [6]. Moreover, *Candida* infections induce more than 3.6 million healthcare visits each year in the USA, resulting in $3 billion of direct medical costs [7].

It should be emphasized that *Candida albicans* is the most frequently identified species isolated in candidiasis-suffering patients. However, the role of other species such as *C. glabrata*, *C. tropicalis*, *C. parapsilosis*, and *C. krusei* have recently increased [8–11]. Most importantly, these species are more likely to be resistant to commonly used antifungal drugs and demonstrate the potential to lead to outbreaks [6]. All five of these species of *Candida* are isolated in more than 90% of invasive fungal infections [12,13]. The global burden of invasive candidiasis is approximately ~750,000 cases, and these infections cause high mortality rates, even in excess of 40% [6].

Despite the ongoing serious threat connected with candidiasis, the number of effective antimycotics available in therapy is still limited [14,15]. Additionally, growing resistance of fungi to available antimycotics poses a serious challenge to modern medicine. There is a growing number of drug-resistant fungi, including multi-drug resistant (MDR) strains on four continents, namely: Asia (Pakistan, India, and Japan), Africa (South Africa), South America (Venezuela) [16], and North America (USA/Canada) [17]. Furthermore, it is estimated that in 33,800 cases of hospitalized patients in the USA *Candida* drug-resistant species were isolated, which ultimately resulted in 1700 patient deaths in 2017. Crucially, the CDC in their last report warned against drug-resistant *Candida* and defined this pathogen as a serious threat that immediately necessitates new treatment options [7].

Antifungal drug resistance is a prominent aspect that negatively impacts the clinical outcome for patients with invasive candidiasis. It is worth noting that the most significance mechanisms of resistance to antifungal drugs involve (i) the reduction of drug intercellular accumulation through the activation of membrane-bound efflux pumps, (ii) the decrease in the affinity of agents to their targets (target mutation and target expression deregulation), and (iii) counteraction of the drug effect by metabolic modification triggered by, e.g., an echinocandins paradoxical effect or ergosterol biosynthesis pathway alteration [18–20].

Although advances in prophylaxis, diagnosis, and therapy have occurred, invasive *Candida* infections caused by resistant strains still contribute to significant mortality, particularly in immunocompromised patients, which underlines the urgent need to develop new antifungal drugs [6,21]. The search for newer antimycotics with improved pharmacokinetics and an enhanced ability to kill drug-resistant pathogens have led scientists to nanotechnology. It should be noted that the use of nanoparticles ameliorates the pharmacodynamic and pharmacokinetic parameters of the drug, including bioavailability, release time of the active substance, and prolongation of the pharmacological action [22–25].

Crucially, in the era of constantly increasing resistance to antibiotics and antimycotics, the use of nanomaterials is an innovative therapeutic approach to combat infections, notably those caused by resistant strains [26]. In this respect, several features of NPs make them an attractive alternative to traditional antibiotics and antimycotic agents [27]. First, a large surface area to volume ratio facilitates NP interactions with microbial membranes, exerting an antimicrobial activity even in low doses, as well as allowing for efficient surface functionalization, which optimizes the activity against preferred targets [28,29]. In addition, NPs possess the ability to penetrate microorganism cell membranes and cross barriers that are typically non-permeable for conventional agents [29,30]. The therapeutic potential of NPs is also highlighted by the improvement of pharmacokinetics of poorly water-soluble drugs and the prolongation of half-life or systemic circulation [22].

A vast range of NPs produced from diverse nanomaterials has been synthesized. However, gold nanoparticles (Au NPs) reflect an important role in nanotechnology, due to their advantageous properties including low toxicity, abilities to connect to various ligands, and antimicrobial activity against resistant strains [31,32]. Au NPs are widely proposed in the development of new therapeutic agents, with possible application in diagnostics,

cancer treatment, vaccines, or drug carriers [33]. It must be emphasized that many recent investigations show the antifungal activity of silver (Au) NPs against fungi. Results obtained by Paul et al. revealed that curcumin−silver nanoparticles (C–Ag–NPs) had a substantial activity against fluconazole-resistant *Candida* species isolated from patients with HIV [34]. Similar results were reported by Khatoon et al. and Edis et al., where a considerable reduction in the growth of *C. albicans, C. tropicalis* and *C. glabrata* by Au NPs was observed [35,36]. Nonetheless, the high toxicity of Au NPs significantly reduces their therapeutic applications [37]. This is why Au NPs that exhibit lower toxicity further highlight the valuable potential of use.

Although the antibacterial activities of Au NPs have been well reported, the impacts of Au NPs on fungi are not widely described in the literature. However, it is worth underlining that our previous studies proved the potent fungicidal activity of rod-shaped Au NPs against *Candida* strains and representatives of filamentous fungi from *Aspergillus, Cladosporium,* and *Fusarium* spp. at concentrations that are nontoxic to the host cells [38]. In line with this research direction, we decided to investigate whether Au NPs in three different shapes i.e., rods (AuR NPs), peanuts (AuP NPs), and stars (AuS NPs), can be successfully used as antifungal agents. The reason for choosing these shapes of nanoparticles was dictated by previous investigations. Piktel et al. demonstrated the paramount antimicrobial efficacy of rod-, peanut-, and star-shaped gold nanoparticles compared with spherical-shaped nanoparticles against representative isolates of *C. albicans* fungi, Gram-negative bacteria like *E. coli* and *P. aeruginosa* species, and Gram-positive strains involving *S. aureus* [39]. Moreover, the results presented by Penders et al. and Jebali et al. also confirmed that non-spherical gold nanoparticles (flowers, stars, and cubes) revealed a far superior activity than those in a spherical-shape [40,41]. The abovementioned observations therefore constitute a promising starting point for further investigations.

In recent times, more and more results have been reported indicating that the conjugation of Au NPs with other agents have shown a superior effect against microorganisms and may become a future alternative to conventional antibiotics and fungicides in the fight against MDR strains [27]. However, it has not been studied whether Au NPs coated with other agents like ceragenins are characterized by a pronounced antifungal potency. Hence, the primary goal of our investigation was to determine whether the functionalization of Au NPs with CSAs would make them prominent candidates to combat *Candida* strains. Ceragenins are synthetic compounds designed to mimic the structure and function of endogenous antimicrobial peptides (AMPs) [42]. The molecular structure of ceragenins is based on cholic acid, to which amino groups are attached to recreate the amphiphilic morphology of AMPs [43]. The chemical character between CSAs and AMP allows for the preservation of the broad-spectrum antimicrobial activity of AMPs [44]. However, ceragenins are not peptide-based; therefore, half-lives are not restricted by the action of proteases [45–47], and even long term storage in solutions does not affect the antimicrobial properties of ceragenins [48]. The leading mechanism of CSA action is determined by the same events as in antimicrobial peptides, which is a direct interaction with negatively charged fungal membrane components, resulting in changes in the membrane organization of phospholipids and sudden membrane disruption [49–52]. Moreover, other indirect of CSA-mediated mechanisms, such as increases in reactive oxygen species formation, have also be recognized [37,44,53]. Additionally, ceragenin functionalization on the surface of metallic nanoparticles provides the opportunity to achieve cumulative antimicrobial effects, including the ability to overwhelm some resistance mechanisms as well as obtain lower effective drug doses and a reduction of side effects of well-known antifungal agents.

To the best of our knowledge, this is the first report comparing the activities of rod-, peanut-, and star- shaped Au NPs functionalized by ceragenins involving CSA-13, CSA-44, and CSA-131 vs. ceragenins in a free form against *Candida* strains. It is noteworthy that one of the most crucial aspects of our studies was the assessment of whether fungi can develop resistance to AuR@CSA-13, AuR@CSA-44, and AuR@CSA-131 after 25 passages. Furthermore, in order to address the potential usefulness in the clinical use, the mechanisms

of action and biocompatibility of the Au NPs were evaluated. This study is a starting point for creating novel nanosystems with a potent antifungal activity and promising therapeutic properties [54].

2. Materials and Methods

2.1. Candida Strains, Media, and Growth Conditions

Two reference strains (*C. albicans* ATCC 26790 and *C. albicans* 1408) and 19 clinical isolates of fungi including, *C. albicans* ($n = 5$), *C. tropicalis* ($n = 5$), *C. krusei* ($n = 5$), and *C. glabrata* ($n = 4$), were used in our investigation. Clinical strains of *Candida* were collected from hematooncological patients of Holy Cross Cancer Center in Kielce (Kielce, Poland), and reference strains were purchased from the Polish Collection of Microorganisms, Polish Academy of Science (Wroclaw, Poland). The identification and antifungal sensitivity of *Candida* strains used in this study was determined using a VITEK® 2 (bioMérieux, Marcyl'Etoile, France) utilizing fungal cards YST and YS08. This system allows for an assessment of the antimycotic susceptibility of fungi to amphotericin B (AMB), caspofungin (CSF), fluconazole (FLU), flucytosine (FC), micafungin (MCF), and voriconazole (VOR). Fungal strains were cultured and maintained on Sabouraud Dextrose agar with chloramphenicol (Biomaxima, Lublin, Poland).

2.2. Antifungal Compounds

2.2.1. Ceragenins

Ceragenins: CSA-13, CSA-44, and CSA-131 were synthesized as described previously [55], and subsequently were dissolved in phosphate-buffered saline (PBS, Thermo Fisher Scientific, Saint Louis, MO, USA). Prepared solutions were stored in 4 °C. Tetrachloroaurate ($HAuCl_4$), sodium borohydride ($NaBH_4$), silver nitrate ($AgNO_3$), ascorbic acid ($C_6H_8O_6$), 16-mercaptohexadecanoic acid (MHDA), dimethylformamide (DMF), pentafluorophenyl (PFP), N,N-diisopropylethylamine (DIPEA), and N-cyclohexyl-N'-(2-morpholinoethyl) carbodiimide methyl-p-toluenesulfonate (CMC) were purchased from Merc (Darmstadt, Germany), while cetrimonium bromide (CTAB; $C_{19}H_{42}BrN$) was acquired from Carl Roth (Karlsruhe, Germany).

2.2.2. Gold Nanoparticles (Au NPs) Functionalized by CSA-13, CSA-44, and CSA-131

Star-, peanut-, and rod-shaped gold nanoparticles were synthesized using the seed-mediated method. In this method, two stages of synthesis were used. In first step, gold nanoseeds with a spherical shape were prepared. For this purpose, $C_{19}H_{42}BrN$ (5 mL; 5 μM), $HAuCl_4$ (5 mL of 0.5 mM), and $NaBH_4$ (0.6 mL; 0.1 M) were mixed with active stirring. The reaction was stopped when the solution turned red. In the second step, $C_{19}H_{42}BrN$ (5 mL; 5 μM), $AgNO_3$ (0.2 mL; 0.04 M), $HAuCl_4$ (5 mL; 1 mM), $C_6H_8O_6$ (70 μL; 78 mM), and 30 μL of Au nanoseeds were mixed under active stirring. For AuP NPs, the reaction was stopped after 3 h, while for AuR NPs and AuS NPs the reaction was stopped at 30 min. For AuS NPs, 210 μL of 78 mM $C_6H_8O_6$ was added. Nanoparticles were washed and functionalized by MHDA through overnight incubation at 4 °C. The functionalization process was verified using FT-Raman spectroscopy (Thermo Fisher Scientific, Saint Louis, MO, USA). In order to immobilize ceragenins with the Au NPs-MHDA complex, the solution consisting of PFP, DIPEA, and CMC was used to rinse Au NPs conjugated with MHDA for 30 min at 25 °C. In the next step, a solution of CSA-13, CSA-44, or CSA-131 was added to the resulting solution, which was washed with DMF and centrifuged. The incubation was continued for 30 min at 25 °C.

Finally, as a result of the synthesis, the nanosystems consisted of (i) ceragenin CSA-13, CSA-44 or CSA-131 (concentration: 2 mg/mL, which equals 0.002 M, i.e., 12.04×10^{20} molecules) and (ii) non-spherical nanoparticles (2.93 ng/mL, equivalent to 0.015×10^{-6} M, i.e., 9.03×10^{15} molecules). The consequence was that the ceragenin charge on the nanoparticle surface was 1.33×10^5 ceragenin molecules per nanoparticle. In preparing the nanosystems, we used MHDA in excess to ensure that all ceragenin molecules adhered to the

nanoparticle surface. Thus, the amount of ceragenin in the prepared nanosystem was not further calculated, and was determined by the amount of ceragenins that was used for the synthesis.

2.2.3. Physicochemical Properties of AuR NPs@CSA-13, AuP NPs@CSA-13, AuS NPs@CSA-13; AuR NPs@CSA-44, AuP NPs@CSA-44 and AuS NPs@CSA-44, and AuR NPs@CSA-131, AuP NPs@CSA-131, AuS NPs@CSA-131 Nanoparticles

Using scanning transmission electron microscopy (STEM, FEI, Hillsboro, OR, USA) with a high-angle annular dark field detector (HAADF) in conventional mode, the morphology and size of the obtained Au NPs were determined and performed in an aberration-corrected FEI Titan electron microscope operating at 300 kV, fitted with a FEG cathode (Field Emission Gun, FEI, Hillsboro, OR, USA). The measurements were carried out on an aberration-corrected FEI Titan electron microscope working at 300 kV equipped with a field emission gun (FEG) cathode (FEI, Hillsboro, OR, USA). The distribution of the particle size was obtained based on STEM images by counting the mean size from 100 nanoparticles placed in the different areas of the TEM grids using TIA Software version 4.0. The zeta potential distribution was determined by the microelectrophoretic method and Smoluchowski model. Each value was obtained as an average of three separate runs of the instrument with at least 20 measurements. All of the experiments were performed in water at 25 °C. Fourier transform Raman (FT-Raman, Thermo Fisher Scientific, Waltham, MA, USA) spectroscopy was used to define the efficiency of the nanoparticle functionalization and ceragenin immobilization. For this purpose, a Nicolet NXR 9650 FT-Raman spectrometer containing Nd:YAG laser (1064 nm, Thermo Fisher Scientific, Waltham, MA, USA) and a germanium detector was used (Thermo Fisher Scientific, Waltham, MA, USA). The measurements were carried out in the range of 150 to 3700 cm^{-1} with a spectral resolution of 8 cm^{-1}, 128 scans, and a 1W laser power. Raman spectra were developed using Omnic/Thermo Fisher Scientific software. However, baseline correction using rubber band methods and vector normalization were performed through OPUS software version 7.0. To obtain information about the zeta potential of the obtained nanoparticles, Zetasizer Nano Series (Malvern, Worcestershire, UK) was used.

2.3. Methods

2.3.1. MIC/MFC Measurements

The microdilution method described in the guidelines of the European Committee on Antimicrobial Susceptibility Testing (EUCAST), version 10.0-valid from 4 February 2020, was used to determine the minimum inhibitory concentrations (MICs) of the tested agents against fungal strains suspended at populations of 2×10^5 CFU (colony-forming units)/mL. The final concentrations of the tested compounds ranged from 0.1 to 51.2 µg/mL. MICs were determined visually and confirmed by spectrophotometer in an RPMI medium (Sigma-Aldrich, Saint Louis, MO, USA) supplemented with MOPS (Sigma-Aldrich, Saint Louis, MO, USA) and D-(+)-glucose (Sigma-Aldrich, Saint Louis, MO, USA) at the lowest concentration of tested agents that showed no visible microbial growth after 24 h. In turn, the minimum fungicidal concentration (MFC) was determined by plating each sample (10 µL) on Sabouraud Dextrose agar with the chloramphenicol (Biomaxima, Lublincity, Poland).

2.3.2. Induction of *C. albicans* ATCC 26790 and *C. krusei* 156 Resistance to AuR NPs@CSA-13, AuR NPs@CSA-44, and AuR NPs@CSA-131

MICs of AuR NPs@CSA-13, AuR NPs@CSA-44, and AuR NPs@CSA-131 against *C. albicans* ATCC 26790 and *C. krusei* 156 were determined visually and confirmed spectrophotometrically. After 24 h of incubation, the passaging was initiated by harvesting fungal cells growing at a concentration just below the MIC and inoculating into fresh RPMI medium.

Importantly, this inoculum was subjected to another MIC assay. After an 18–24 h incubation period, cells growing in the highest concentration of the antimicrobial from the

previous passage were once again harvested and assayed for the MIC. The process was repeated for 25 passages.

2.3.3. ROS Generation Assessment

The generation of ROS by *C. albicans* 1408 cells upon stimulation with ceragenin and Au NPs-conjugated with ceragenins was measured using 2′,7′-dichlorofluorescin diacetate (DFCH-DA, Sigma-Aldrich, Saint Louis, MO, USA) as a fluorescent probe. Fungal cells suspended in PBS (OD_{600} = 0.5) were placed in 96-well black plates and then antifungal agents were added to each well at concentrations ranging from 1 to 10 µg/mL. DFCH-DA at 20 µM was supplied and mixed. After 1 h of incubation, the relative fluorescent signals were measured at excitation/emission = 485/530 nm using a microplate reader—Labsystem Varioscan Lux (Thermo Fisher Scientific, Waltham, MA, USA). The results obtained were compared to the 5 mM concentration of the hydrogen peroxide (Sigma Aldrich, Saint Louis, MO, USA). The fungal cell visualization was achieved by DCFH-DA staining and was performed using a fluorescence microscope (Zeiss AxioObserver.A1 Fluorescence Version Inverted Optical Microscope, JPK Instruments, Berlin, Germany).

2.3.4. Membrane Permeabilization Assay

Measurement of the capacity of ceragenins and ceragenins attached to the surface of gold nanoparticles to disrupt the plasma membrane of *C. albicans* 1408 cells was performed using N-phenyl-1-napthylamine (NPN; Sigma Aldrich, Saint Louis, MO, USA) as a fluorescent probe. Fungal cells suspended in PBS (OD_{600} = 0.5) were subjected to incubation with the tested agents at concentrations ranging from 1 to 10 µg/mL. Next, NPN was added to a final concentration of 0.5 mM, and the mixture was incubated for 5 min. Increases in fluorescence intensity at 348/408 nm (excitation/emission) were measured using Labsystem Varioscan Lux (Thermo Fisher Scientific, Waltham, MA, USA). Finally, the comparison of the results with the 1 µg/mL concentration of the amphotericin B (Chemat, Los Angeles, CA, USA) was prepared.

2.3.5. diSC$_{(3)}$ Assay

The ability of the studied ceragenins and ceragenin-coated nanosystems to depolarize the fungal cell membrane was investigated using a 3,3′-dipropylthiadicarbocyanine iodide (diSC$_{(3)}$) assay. Briefly, a *C. albicans* 1408 suspension was adjusted to OD_{600} ~ 0.5. In the next step, diSC$_{(3)}$ (Sigma Aldrich, Saint Louis, MO, USA) was added to give a final concentration of 0.4 µM, and it was incubated for 60 min at room temperature and protected from the light until a stable fluorescence signal was obtained. Thereafter, a solution of KCl (Chempur, Piekary Śląskie, Poland) (100 mM) in PBS was added to align the intra- and extra-cellular potassium concentrations, followed by 5 min of incubation. Finally, the fungal cells in suspension were incubated with studied nanosystems at concentrations of 1–10 µg/mL for 1 h. The final fluorescence value was recorded after incubation lasting 1 h using a microplate reader at 622/670 nm (excitation/emission)—Varioskan Lux (Thermo Fisher Scientific, Waltham, MA, USA). In the last step, the obtained results were compared to a 1 µg/mL concentration of the amphotericin B (Chemat, Los Angeles, CA, USA).

2.3.6. Assessment of Protein Leakage

Protein leakage analysis was performed using the Bradford assay. *C. albicans* 1408 cells were resuspended in PBS with adjustment to OD_{600} ~ 0.5 prior to exposure to nanoparticles at concentrations of 1, 2, 5, and 10 µg/mL for 1 h. At the end of incubation, samples were centrifuged (5000 rpm) for 10 min. Supernatant was mixed with the Bradford reagent, i.e., Coomassie Brilliant Blue G-250 (Sigma-Aldrich, Saint Louis, MO, USA) in a 1:1 ratio. Mixtures were incubated in the dark for 10 min. The absorbance of the samples was measured at 595 nm using Labsystem Varioscan Lux (Thermo Fisher Scientific, Waltham, MA, USA). Finally, a comparison of the results with the 1 µg/mL concentration of the amphotericin B (Chemat, Los Angeles, CA, USA) was prepared.

2.3.7. Haemolytic Activity Assessment

The haemolytic activity of both free and ceragenins attached to the surface of gold nanoparticles was determined with a suspension of human RBC (red blood cells) in PBS (hematocrit ~ 5%) collected from the healthy volunteers. Compounds in a concentration range of 1–50 µg/mL were incubated with RBCs for 1, 6, and 12 h at 37 °C. Upon incubation, plates were centrifuged (2500 rpm, 10 min) and the optical density of the sample was measured at 595 nm using Labsystem Varioscan Lux (Thermo Fisher Scientific, Waltham, MA, USA). A supernatant from the samples treated with 1% Triton X-100 (Sigma-Aldrich, Saint Louis, MO, USA) was used as a positive control (100% hemolysis), whereas RBCs in PBS were used as a negative control (0% hemolysis). The relative absorbance compared with that treated with 1% Triton X-100 was defined as the percentage of haemolysis.

2.3.8. Statistical Analysis

All of the statistical analyses were performed sing Graph Pad Prism, version 8 (San Diego, CA, USA). The results were presented as mean $\pm$ standard deviation (SD) consisting of three to six replicate experiments. The two-tailed Student's test was used to determine the significance of differences. A p-value < 0.05 was considered statistically significant.

3. Results

3.1. Physicochemical Nature of Rod-, Peanut-, and Star-Shaped Au NPs

Au NPs with different shapes and sizes of the Au NPs, depending on the synthetic methods used, were prepared. Nanoparticles with rod-like (Figure 1(A1,A2)), peanut-like (Figure 1(B1,B2)), and star-like (Figure 1(C1,C2)) shapes were obtained. However, 20% of non-rod-shaped nanoparticles and 40% of non-peanut-shaped nanoparticles were recognized. Additionally, among the rod-shape AuR NPs, rounded ends were observed along with spherical Au NPs. Sizes, measured on the longitudinal and transverse axes in AuP NPs and AuR NPs, were used to compare NPs. In the case of AuR NPs, the sizes of the axes were 45 ± 8 nm and 10 ± 3, respectively, while, in the case of the AuP NPs, the sizes were 55–65 nm and 24–34 nm, respectively. The size of AuS NPs was 243 nm. Zeta potential plots of AuR NPs, AuP NPs, and AuS NPs (Figure 1D) showed that all of the gold nanoparticles were positively charged in the entire range of pH. For AuR NPs, the zeta potential values were 49 mV for pH 3.5 to 18 mV for pH 12.5, while for AuP NPs, these values were between 42 mV and 19 mV, and for AuS NPs, the zeta potentials were from 33 mV to 16 mV. For all of these nanoparticles, the potential value decreased as the pH value increased.

Successful functionalization and immobilization of ceragenins on NPs was verified using FT Raman spectroscopy. In Figure 1E, which is a representative spectrum, the corresponding Au-S stretching vibration peaks are observed at 278 cm^{-1}, which are the bonds in charge of forming the bond between the gold nanoparticles and the sulfur surface with MHDA [56]. Furthermore, successful ceragenins immobilization in the surface of the AuR NPs, AuP NPs, and AuS NPs was confirmed by the presence of peaks at 1680 cm^{-1}, corresponding to the N-H vibrations created between COOH groups from MHDA and NH$_2$ groups from CSA-13, CSA-44, and CSA-131, respectively [57].
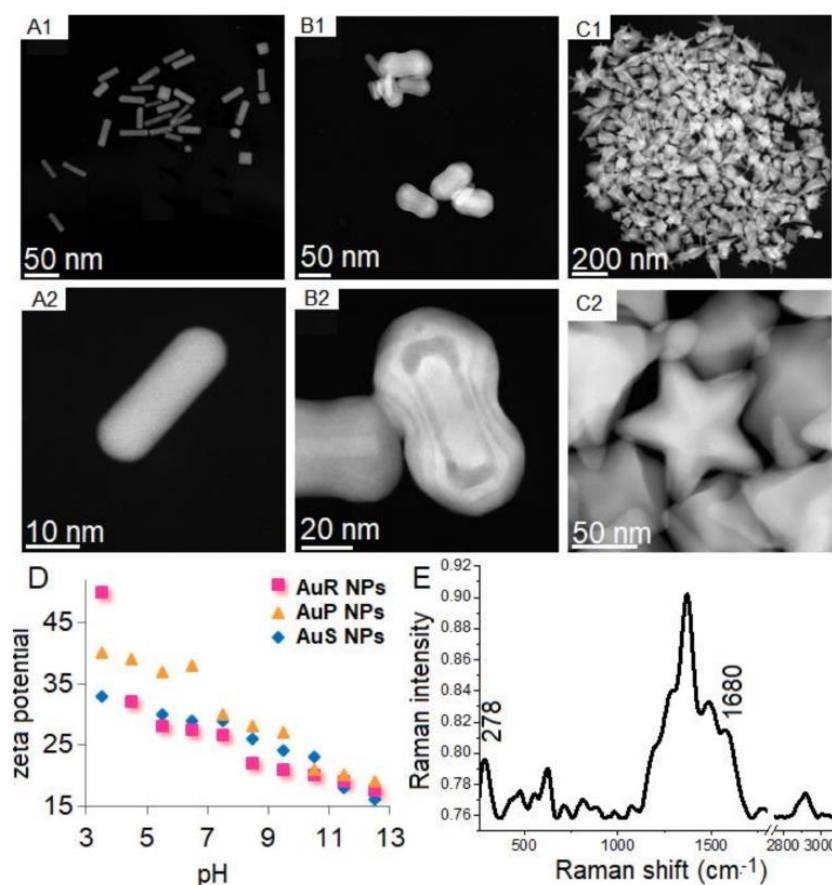
Figure 1. HAADF-STEM over view (1) and magnified (2) images of AuR (**A**), AuP (**B**), and AuS (**C**). Zeta potential values of synthesized AuR, AuP, and AuS (**D**). Representative FT-Raman spectrum showing the chemical mechanism of ceragenins CSA-13 immobilized on the AuP NPs surface (**E**).

3.2. Susceptibility of Tested Candida Strains to Antimycotics and Developed Nanoparticles

MICs and MFCs are used to determine the therapeutic potential of the antimicrobial agents. In this study, almost half of the *Candida* isolates were resistant to fluconazole. In addition, multiple strains showed intermediate resistance to caspofungin ($n = 8$) and voriconazole ($n = 2$) (according to EUCAST interpretation; Table 1). MICs and MFCs of ceragenin-appended NPs are presented in Figure 2A–C. Activities of ceragenin-based nanosystems (AuR NPs@CSA-13, AuR NPs@CSA-44, and AuR NPs@CSA-131; AuP NPs@CSA-13, AuP NPs@CSA-44, and AuP NPs@CSA-131; and AuS NPs@CSA-13, AuS NPs@CSA-44, and AuS NPs@CSA-131) in the majority of cases were higher (MIC values ranging from 0.4 to 3.2 μg/mL) compared with those determined for ceragenins alone (i.e., CSA-13, CSA-44, and CSA-131, MICs ranging from 0.8 to 6.4 μg/mL). Moreover, ceragenin-based nanosystems with CSA-13 and CSA-131 were more effective than those with CSA-44 (Figure 2B).

Table 1. Susceptibility of tested *Candida* isolates to conventional antimitotic agents. S—susceptible; R—resistance; I—intermediate; AMB—Amphotericin B; FLU—Fluconazole; VOR—Voriconazole; CSF–Caspofungin; MCF–Micafungin; FC–Flucytosine; "-"—no breakpoints.

Fungal Strain	Antimycotic Susceptibility ([μg/mL]/Interpretation)					
	AMB	FLU	VOR	CSF	MCF	FC
C. albicans 138	0.25/S	0.5/S	0.12/S	0.12/S	0.06/S	1/S
C. albicans 166	0.5/S	0.5/S	0.12/S	0.12/S	0.06/S	1/S
C. albicans 177	1/S	0.5/S	0.12/S	0.12/S	0.06/S	1/S
C. albicans 185	0.25/S	0.5/S	0.12/S	0.12/S	0.06/S	1/S
C. albicans 197	0.5/S	0.5/S	0.12/S	0.12/S	0.06/S	1/S
C. albicans 1408	1/S	1/S	0.12/S	0.12/S	0.06/S	1/S
C. albicans ATCC 26790	1/S	0.5/S	0.12/S	0.12/S	0.06/S	1/S
C. glabrata 132	1/S	-/R	0.25/I	0.25/I	0.06/S	1/S
C. glabrata 145	1/S	-/R	0.25/I	0.25/I	0.06/S	1/S
C. glabrata 154	0.5/S	-/R	0.12/S	0.25/I	0.06/S	1/S
C. krusei 137	0.5/S	-/R	0.12/S	0.5/I	0.12/S	16/I
C. krusei 148	0.5/S	-/R	0.12/S	0.5/S	0.12/S	16/I
C. krusei 156	0.5/S	-R	0.12/S	0.5/I	0.12/S	16/I
C. krusei 163	0.5/S	-/R	0.12/S	0.5/I	0.12/S	16/I
C. krusei 176	0.5/S	-/R	0.12/S	0.5/I	0.12/S	16/I
C. krusei 184	0.5/S	-/R	0.12/S	0.5/I	0.12/S	16/I
C. tropicalis 133	0.25/S	0.5/S	0.12/S	0.12/S	0.06/S	1/S
C. tropicalis 157	0.5/S	1/S	0.12/S	0.12/S	0.06/S	1/S
C. tropicalis 165	0.25/S	1/S	0.12/S	0.12/S	0.06/S	1/S
C. tropicalis 178	0.5/S	0.5/S	0.12/S	0.12/S	0.06/S	1/S
C. tropicalis 191	0.25/S	0.5/S	0.12/S	0.12/S	0.06/S	1/S

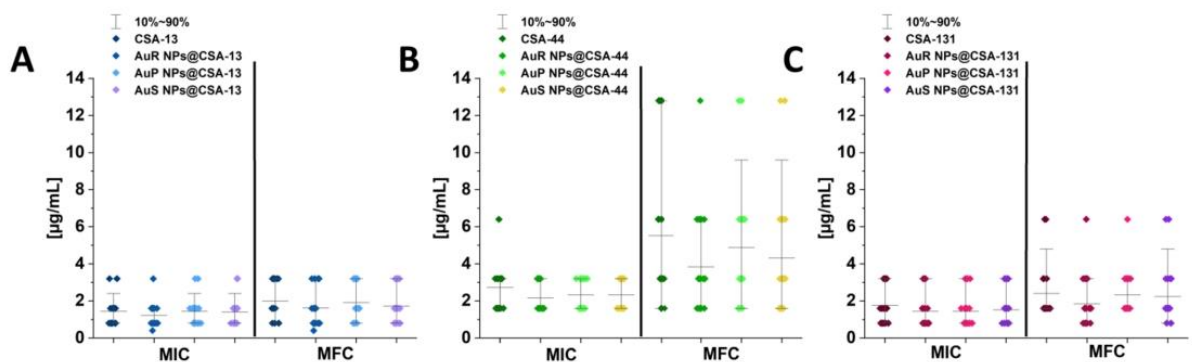**Figure 2.** MIC (minimal inhibitory concentration; μg/mL) and MFC (minimal fungicidal concentration; μg/mL) values of CSA-13, AuR NPs@CSA-13, AuP NPs@CSA-13, AuS NPs@CSA-13 (**A**); CSA-44, AuR NPs@CSA-44, AuP NPs@CSA-44, AuS NPs@CSA-44 (**B**); and CSA-131, AuR NPs@CSA-131, AuP NPs@CSA-131, AuS NPs@CSA-131 (**C**) against 19 fungal clinical strains and 2 reference fungal strains.

3.3. Serial Passaging Experiment to Induce Development of Resistance towards AuR NPs@CSA-13, AuR NPs@CSA-44, and AuR NPs@CSA-131 by Candida Cells

The initial MICs of AuR NPs@CSA-13, AuR NPs@CSA-44, and AuR NPs@CSA-131 for *C. albicans* ATCC 26790 were 1.6 µg/mL, 3.2 µg/mL, and 1.6 µg/mL, respectively. After two serial passages, the MIC of AuR NPs@CSA-13 increased two-fold, and after 13 serial passages it was enhanced four-fold. It is noteworthy that this value remained to the end of the experiment (Figure 3A). In turn, in relation to AuR NPs@CSA-44 after four serial passages, the MIC of increased two-fold, and no further changes were observed through the rest of the experiment (Figure 3C). On the other hand, the MIC of AuR NPs@CSA-131 was unchanged through 23 passages, and after this passage, the MIC grew two-fold through the end of the investigation (Figure 3E).
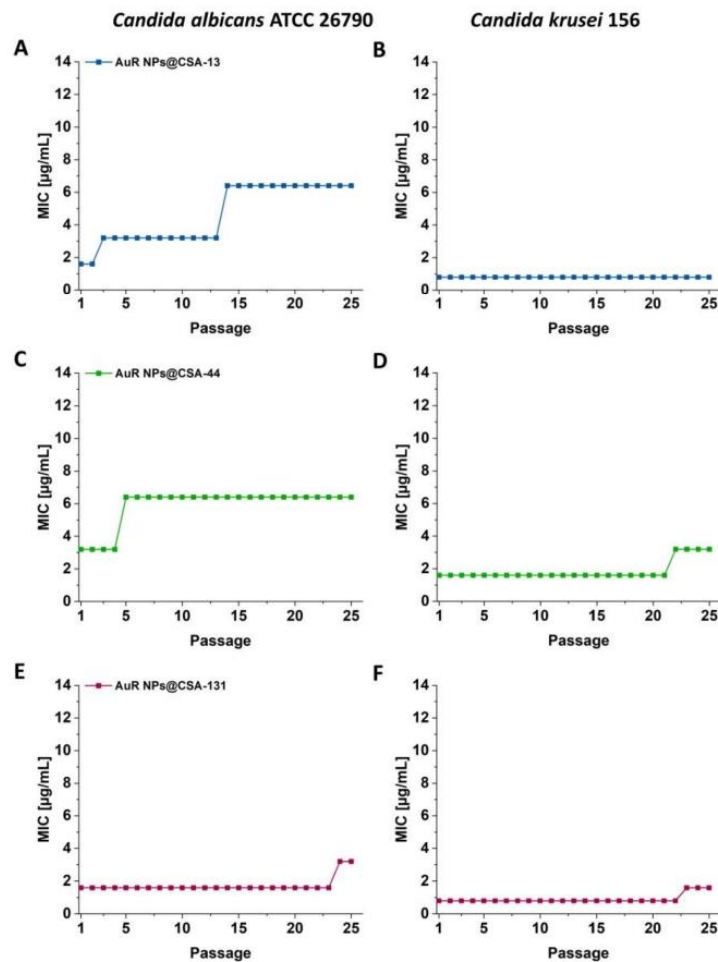

Figure 3. MIC/MFC values for *C. albicans* 26790 (**A**,**C**,**E**) and for *C. krusei* 156 (**B**,**D**,**F**) of the AuR NPs@CSA-13, AuR NPs@CSA-44, and AuR NPs@CSA-131 after 25 serial passages indicated.

With regard to *C. krusei* 156, the initial MICs of AuR NPs@CSA-13, AuR NPs@CSA-44, and AuR NPs@CSA-131 were 0.8 µg/mL, 1.6 µg/mL, and 0.8 µg/mL, respectively. Notably, no change of MIC of AuR NPs@CSA-13 was observed until the end of the experiment (Figure 3B). In the case of AuR NPs@CSA-44 and AuR NPs@CSA-131, the MIC increased

two-fold after 21 or 22 passages, respectively (Figure 3D,F). Moreover, no substantial changes through the rest of the experiment were observed.

3.4. Antifungal Activity of Nanosystems Involves Generation of Reactive Oxygen Species, Depolarization, and Disruption of the Cell Membrane as Well as Protein Leakage

Reactive oxygen species (ROS) are synthesized in various metabolic pathways during the reduction and oxidation, and constitute a mechanism of action of some antifungal agents [58]. For the assessment of the generation of the ROS by *C. albicans* 1408 cells in response to ceragenins and ceragenins conjugated with NPs, the DCFH-DA assay was performed (Figure 4A–C). The application of a 10 μg/mL concentration of the antifungal agents resulted in a 1.31 to 2.52-fold increase of ROS generation in comparison with the 5 mM hydrogen peroxide. Significantly, this effect was observed for all of the developed nanosystems. On the other hand, free ceragenins, i.e., CSA-13, CSA-44, and CSA-131, enhanced ROS generation from 1.22 to 1.7-fold in relation to the 5 mM hydrogen peroxide.
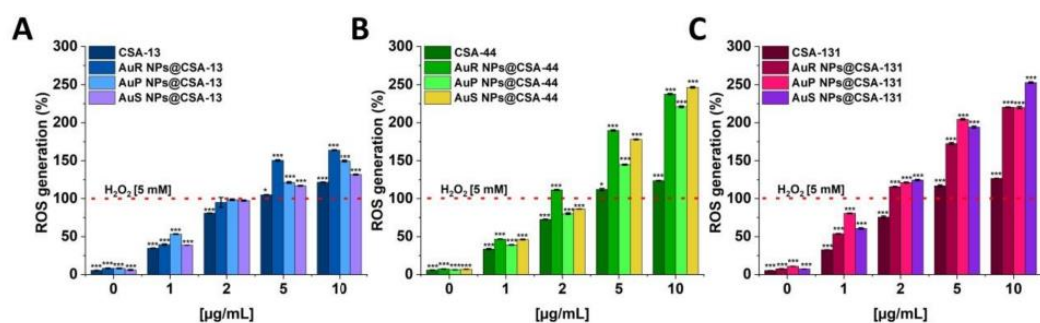

Figure 4. Induction of reactive oxygen species (ROS) generation in *C. albicans* 1408 was evaluated by the DFCH-DA fluorimetric assay. Formation of ROS in cells subjected to CSA-13, AuR NPs@CSA-13, AuP NPs@CSA-13, AuS NPs@CSA-13 (**A**); CSA-44, AuR NPs@CSA-44, AuP NPs@CSA-44, AuS NPs@CSA-44 (**B**); and CSA-131, AuR NPs@CSA-131, AuP NPs@CSA-131, AuS NPs@CSA-131 (**C**) ranging from 1 to 10 μg/mL was presented. The dashed line corresponds to the effect obtained with the 5 mM hydrogen peroxide. The results show the mean ± SD, $n = 3$; * indicates statistical significance at $\leq$0.05 and *** $\leq$0.001.

As shown in Figure 5, no fluorescent signal was detected after the incubation of *C. albicans* 1408 without the test agents, whereas a strong signal from the DFCH-DA fluorescent probe was observed under the treatment with increasing concentrations of nanoparticles.

Activities of the ceragenins and gold nanosystems with ceragenins to cytoplasmic membrane depolarization were determined using the membrane potential-sensitive dye, i.e., diSC$_{(3)}$. The highest increase of fluorescence signals was detected for peanut-shaped Au NPs functionalized with CSA-13, and CSA-131. It should be highlighted that treatment with nanosystems at a concentration of 10 μg/mL resulted in an approximately 1.27 to 2.30-fold increase of the fluorescence intensity compared with a 1 μg/mL concentration of the amphotericin B (Figure 6A–C). In contrast, the same dose of CSA-13, CSA-44, and CSA-131, caused only 1.22 to 1.41-fold increases of fluorescence as compared to 1 μg/mL concentration of the amphotericin B.
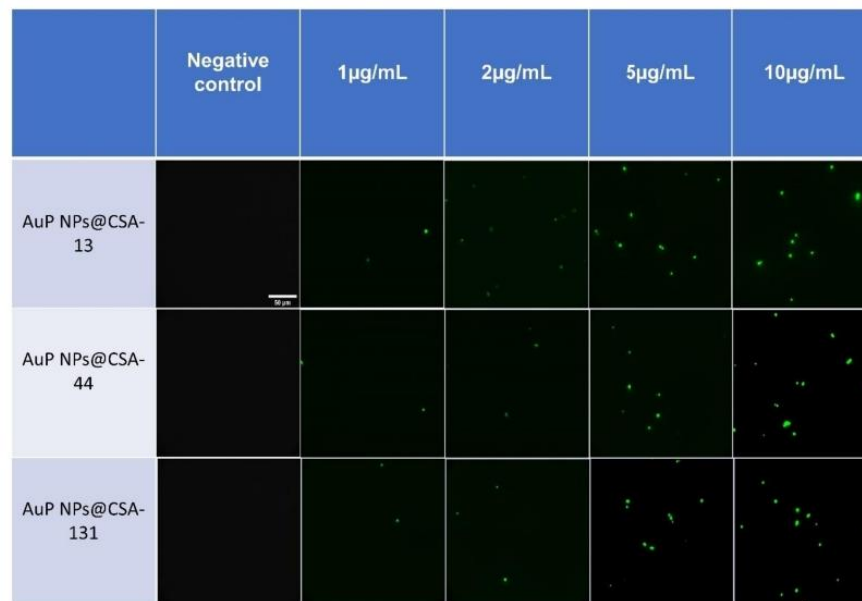
Figure 5. Generation of reactive oxygen species in AuP NPs@CSA-13, AuP NPs@CSA-44, and AuP NPs@CSA-131 -treated *Candida* cells. Increase in dichlorofluorescin diacetate–derived fluorescence signal after 1 h of treatment of *C. albicans* 1408 isolate with tested compounds in concentrations ranging from 1 to 10 µg/mL.
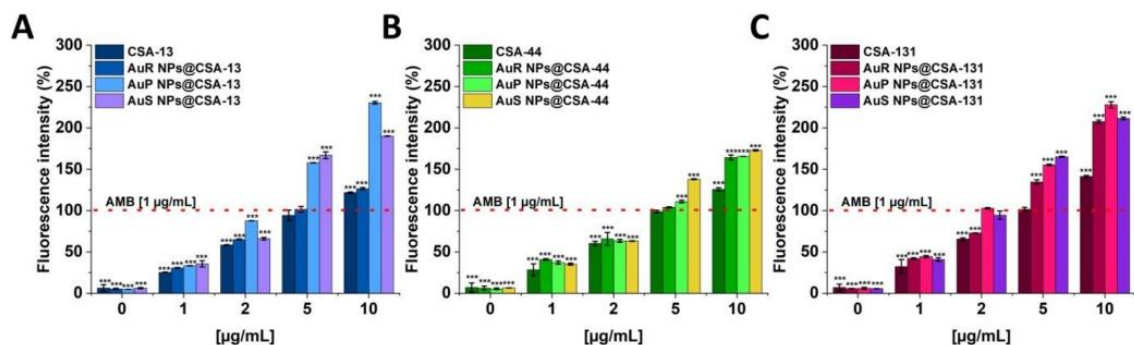

Figure 6. Depolarization of the fungal membrane of *C. albicans* 1408 cell fungal membrane was assessed using diSC$_{(3)}$ assay. The evaluation of the degree of cell membrane depolarization in the presence of CSA-13, AuR NPs@CSA-13, AuP NPs@CSA-13, AuS NPs@CSA-13 (**A**); CSA-44, AuR NPs@CSA-44, AuP NPs@CSA-44, AuS NPs@CSA-44 (**B**); and CSA-131, AuR NPs@CSA-131, AuP NPs@CSA-131, AuS NPs@CSA-131 (**C**) ranging from 1 to 10 µg/mL was evaluated by monitoring the enhancement of intensity of the fluorescence. The dashed line represents the effect obtained with the amphotericin B at a concentration of 1 µg/mL. Results show the mean ± SD, $n = 3$; *** indicates statistical significance at ≤0.001.

The ability of ceragenin-based nanosystems and ceragenins to disrupt the outer layer of *C. albicans* 1408 was determined using the NPN uptake assay (Figure 7A–C). The highest level of membrane permeabilization was observed for rod-shaped Au NPs. In general, the antifungal activities of nanosystems were higher than those observed for CSA-13, CSA-44, and CSA-131 in a free form. For instance, under treatment with AuR NPs@CSA-44 at a concentration of 10 µg/mL, an approximately 2.18-fold (Figure 7B) increase of intensity of the fluorescence signal was recorded compared to 1 µg/mL concentration of the amphotericin B.
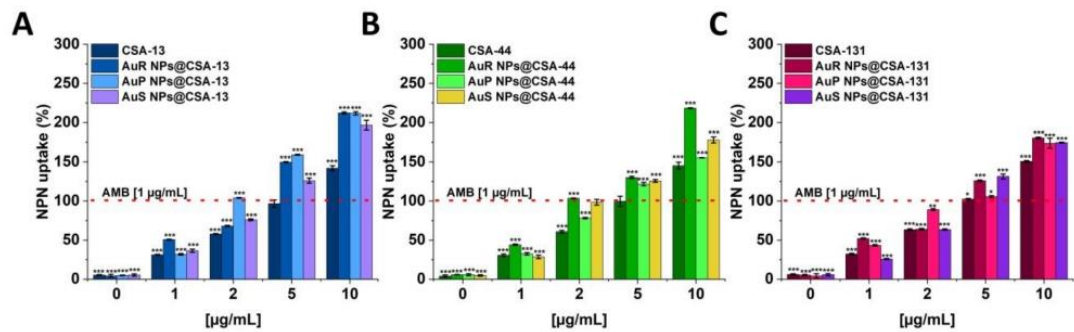
Figure 7. The increase of the membrane permeability of *C. albicans* 1408 subjected to CSA-13, AuR NPs@CSA-13, AuP NPs@CSA-13, AuS NPs@CSA-13 (**A**); CSA-44, AuR NPs@CSA-44, AuP NPs@CSA-44, AuS NPs@CSA-44 (**B**); and CSA-131, AuR NPs@CSA-131, AuP NPs@CSA-131, AuS NPs@CSA-131 (**C**) at doses of 1–10 μg/mL was investigated using the fluorimetric method. The dashed line corresponds to the effect obtained with amphotericin B at a concentration of 1 μg/mL. The results show the mean ± SD, *n* = 3; * indicates statistical significance at ≤0.05, ** ≤0.01, and *** ≤0.001.

To verify whether the treatment of *C. albicans* with ceragenins and ceragenins attachment to Au NPs leads to the release of the protein content, a protein leakage assay was performed. The results shown in Figure 8 (panels A–C) indicate a significant release of cytoplasmic proteins as a consequence of the damage to the fungal membrane. The results obtained were reported for all of the synthesized nanosystems in a dose-dependent manner. It is worth noting that in case of AuP NPs@CSA-131 the greatest leakage of intracellular content was detected with 2.51-fold increase in comparison to the 1 μg/mL concentration of the amphotericin B. With ceragenins, substantially lower absorbance values were determined in relation to the nanosystems.
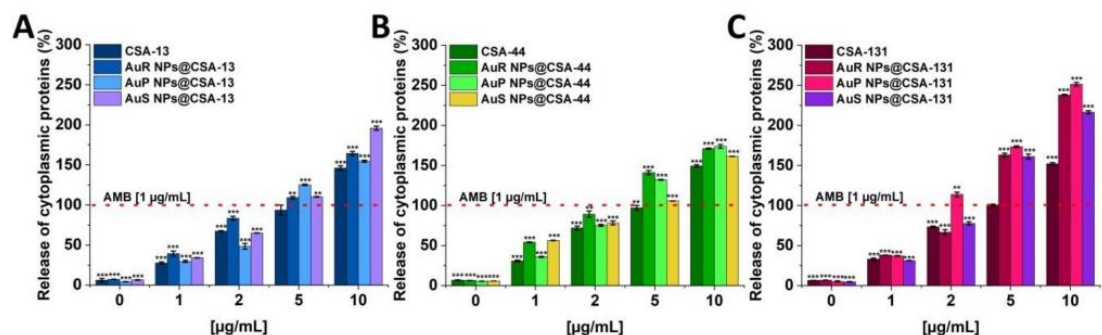

Figure 8. The release of cytoplasmic proteins from *C. albicans* 1408 after treatment with CSA-13, AuR NPs@CSA-13, AuP NPs@CSA-13, AuS NPs@CSA-13 (**A**); CSA-44, AuR NPs@CSA-44, AuP NPs@CSA-44, AuS NPs@CSA-44 (**B**); and CSA-131, AuR NPs@CSA-131, AuP NPs@CSA-131, AuS NPs@CSA-131 (**C**) at concentrations of 1–10 μg/mL was evaluated by the Bradford protein assay. The dashed line represents the effect obtained with the amphotericin B at a concentration of 1 μg/mL. The results show the mean ± SD, *n* = 3; ** indicates statistical significance at ≤0.01, and *** ≤0.001.

3.5. Ceragenin-Based Nanosystems Exhibit Biocompatibility at Fungicidal Doses

To assess the potential toxicity of the tested nanosystems, a haemolysis assay was performed at concentrations corresponding to their range of candidacidal activity. As demonstrated in Figure 9 (panels A–I), the nanosystems did not induce significant haemolysis at doses from 1 to 10 μg/mL, even if the incubation was extended until 12 h. After 1 h of incubation at concentrations ranging from 1 to 10 μg/mL, haemolysis was not higher than 3.5%. Moreover, only 1.68–9.60% of erythrocytes were injured after 6 h of exposure to the nanosystems, and merely 2.23–9.78% after incubation for 12 h.
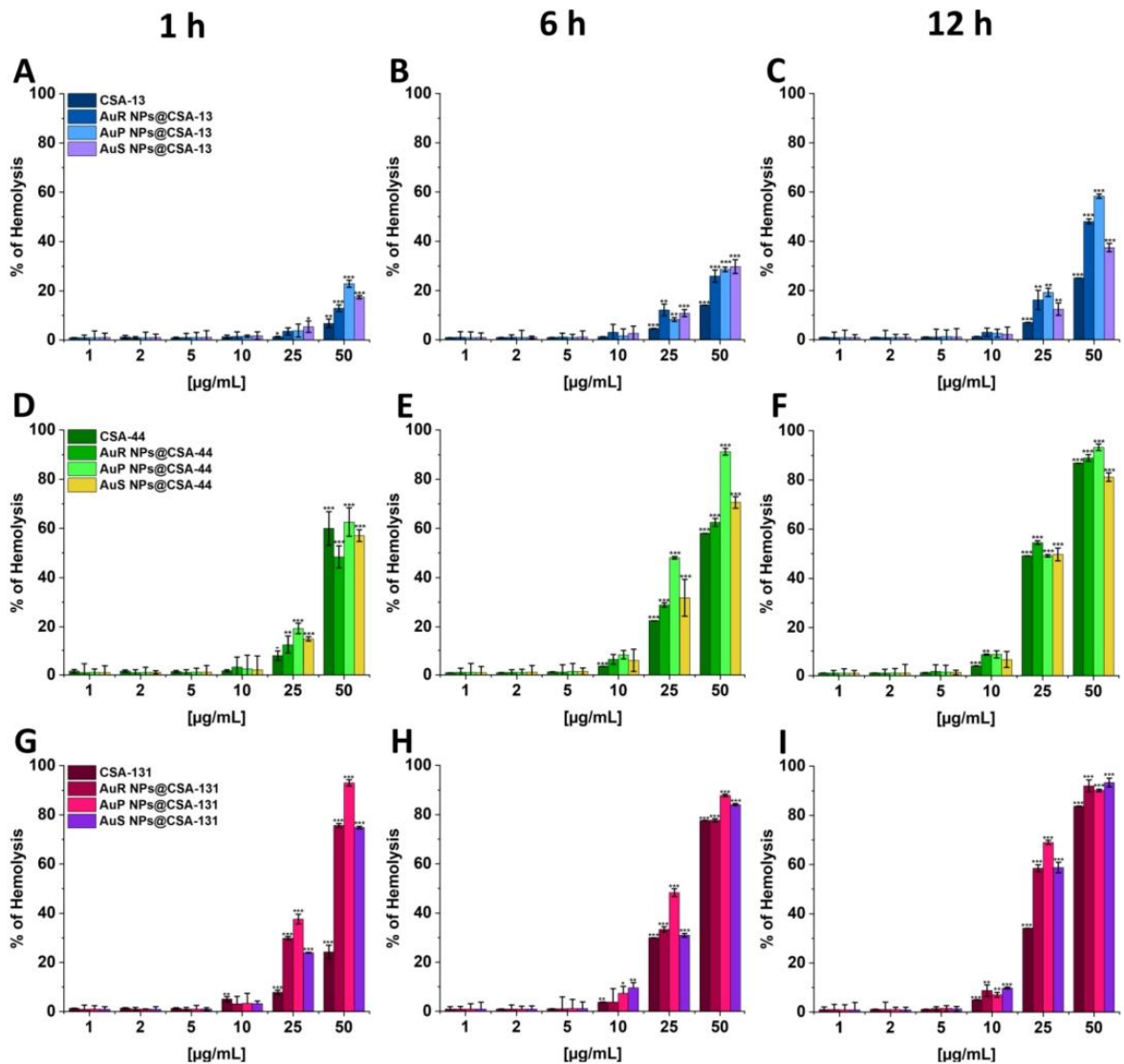
100

Figure 9. Hemoglobin release from human red blood cells (RBCs) incubated in the presence of CSA-13; AuR-NPs, AuP-NPs, and AuS-NPs containing CSA-13 (**A–C**); CSA-44; AuR-NPs, AuP-NPs, and AuS-NPs containing CSA-44 (**D–F**); and CSA-131; AuR-NPs, AuP-NPs, and AuS-NPs containing CSA-131 (**G–I**) at doses of 1–50 μg/mL after 1 h (**A,D,G**), 6 h (**B,E,H**), and 12 h (**C,F,I**) of incubation. Results show the mean ± SD, *n* = 3; * indicates statistical significance at ≤ 0.05, ** ≤ 0.01, and *** ≤ 0.001.

4. Discussion

Despite significant efforts to develop new antimicrobial agents, escalating resistance is still a global public health concern [59,60]. It is noteworthy that *Candida* spp. are the most common opportunistic fungal pathogens [61,62]. Currently, it is assumed that *Candida* spp. colonize the mucosal surfaces in approximately 50–70% of healthy humans. However, it should be underlined that if breaches in the gastrointestinal and cutaneous barriers appear, for example, after gastrointestinal surgery or venous catheters, the commensal fungi can translocate and invade the bloodstream causing candidaemia [5]. It is important to note that fungi interact with the host's immune system and then exit the intravascular spaces to invade deep tissues of target organs such as the liver, spleen, kidneys, heart, and brain [63].

101

The characteristics of the fungi involved in this pathogenicity include the adhesion of tissues, the ability to exhibit yeast−hyphal dimorphism, the hydrophobicity of the cell surface, and finally secretion of proteinases and phenotypic switching [14,64,65].

The studies presented herein demonstrate the potent antifungal activity of rod-, peanut-, and star-shaped Au NPs functionalized by CSA-13, CSA-44, and CSA-131 at low concentrations. Importantly, MICs did not exceed 3.2 µg/mL for both referential and clinical strains, which points out the considerable fungicidal activity of ceragenin-based nanosystems (Figure 2). The lowest MIC values were observed for Au NPs functionalized by CSA-13, where in more than half of the cases this value was 0.8 µg/mL (Figure 2).

It is assumed that electrostatic interactions between positively charged gold nanoparticles and the negative charges on the surface of the fungus play an important role [66]. The positive charge of nanosystems results from the (i) method of synthesis, which involves the use of CTAB, and (ii) the positive charge of ceragenins [42]. On the other hand, the chemical groups responsible for the negative charge on the fungal surface most likely contain acidic amino acids and charged polysaccharides as, perhaps, mannoproteins [67], where the phosphomannosylation has an essential role. Phosphomannosylation is a modification of cell wall proteins and thus modified mannans provide a negative charge to the fungus wall [68].

Gold nanoparticles have been proposed in the development of new fungicidal agents. The high activity of indolicidin-gold NP conjugates against fluconazole-resistant *Candida* strains was observed (four-fold decrease in MIC value compared with free indolicidin) [69, 70]. Khan et al. also demonstrated that Au NPs are able to increase the activity of methylene blue in combination with nanosystems against *C. albicans* [71]. Likewise, another study showed that free triangular gold nanoparticles and all conjugated triangular gold nanoparticles demonstrate a significant antifungal activity against clinical *C. albicans* strains in contrast to free peptide ligands [72]. According to above mentioned information, Au NPs seems to be a very good carrier for antimicrobial agents like ceragenins used in this study.

The size and shape of metallic nanoparticles have an influence on their chemical, optical, and thermal properties [73]. Wani et al. proved that smaller sized gold nanodiscs have superior fungicidal effects than larger sized gold polyhedral nanocrystals against *C. albicans* [74]. On the other hand, Jebali et al. confirmed that the antifungal properties of silver and gold nanocubes against *Candida* isolates were greater than gold and silver nanospheres and wires [41]. The above assumption was further supported by other results where a potent bactericidal activity of non-spherical nanosystems in comparison to spherical-nanoparticles was observed [39].

Growing resistance to antimicrobials constitute one of the principal public health problems in the 21st century [75]. Therefore, gold nanoparticles appear to be good candidates for the development of new candidacidal agents, not only due to their intrinsic activity, but also in the view of the infrequent development of resistance in pathogens, including fungi [76]. It should be highlighted that the results obtained in this study induced no emergence of significant resistance in relation to fungi against gold nanoparticles. The motivation for selecting rod-shaped nanoparticles to the induction of the development of resistance of *Candida* strains was dictated by the previous research. The results obtained by Piktel et al. showed no substantial differences between rod-, peanut-, and star-shaped gold nanoparticles [39]. Comparable conclusions were also drawn in our other research, where the negligible distinction on viability of *Staphylococcus aureus* Xen30, *S. epidermidis* 175, *Klebsiella pneumoniae* 700603, *K. oxytoca* 329, *Pseudomonas aeruginosa* LESB58, and *P. aeruginosa* 510 among rod-, peanut-, and star-shaped gold nanosystems was observed. It should be emphasized that all of the mentioned nanoparticles were characterized by similar bactericidal effectiveness [37]. In view of the above, we decided to examine only one type of shape. We considered that the outcomes obtained for the rod-shape will be analogue and comparable to star- and peanut-shaped nanosystems.

Importantly, our series of experiments demonstrate no increase or only a two-fold raise in the MICs of nanosystems with *C. krusei* 156 and only two- or four- fold increases with *C. albicans* 26790 after 25 passages (Figure 3A–F). Similarly, Xie et al. [77] and Zheng et al. [78] obtained no resistance development of gold nanoparticles against *S. aureus*. However, Elbehiry et al. [79] showed resistance to the 10-nm Ag NPs ($n = 4$) and to 20-mm Ag NPs ($n = 10$) after 10 passages utilizing 10-nm and 20-nm silver and gold nanoparticles. In contrast, only two strains developed resistance to the 10-nm Au NPs, and three strains to the 20-nm Au NPs.

The wide range of biomedical applications of gold nanosystems prompted the determination of the mechanism of action. Nanoparticles enter *Candida* cells, and release metal ions from their surface, which inhibit the activity or cause the cell damage and finally lead to the cell death [80]. An important role in the mechanism of the fungicidal action of gold nanoparticles is played by ROS. It is estimated that due to Au NP membrane incorporation and penetration ability, interaction with fungal mitochondria leads to membrane disruption, which interferes with the reduction of molecular oxygen during ATP synthesis. Some amount of oxygen is not reduced causing the formation of superoxide anion and other ROS. This results in a chain reaction involving protein oxidation and oxidation of fatty acid double bonds in the cell membrane, which drastically reduces the fungal membrane integrity. Additionally, ROS are involved in DNA-strand breaks resulting in the loss of cell metabolic function [81–85]. To assess the mechanism of action of ceragenin nanosystems, examination of the ROS generation (Figure 4A–C and Figure 5), diSC$_{(3)}$ assay (Figure 6A–C), NPN assay (Figure 7A–C), and the protein leakage assay (Figure 8A–C) were performed. The results obtained suggest that the principal mechanism of fungicidal action of ceragenin-based nanosystems involves the production of ROS, causing destruction of the fungal membrane and leading to the leakage of intracellular constituents, which ultimately may affect the fungal death. The numbers of reports related to the generation of ROS by Au NPs against fungal strains are still limited, although there is compelling evidence indicating the crucial role of the ROS generation by gold nanoparticles in the antibacterial activity. Mohamed et al. described the antimicrobial effects of Au NPs against *Corynebacterium pseudotuberculosis* via the ROS generation [86]. Furthermore, the ROS-dependent mechanism that ultimately leads to the eradication of pathogens like MDR *E. coli* and methicillin-resistant *S. aureus* was observed by Xie et al. [77] or in the case of ESKAPE strains (*Enterococcus faecium*, *S. aureus*, *K. pneumoniae*, *Acinetobacter baumannii*, *P. aeruginosa*, and *Enterobacter* spp.) by Zheng et al. [78]. According to the protein leakage, Piktel et al. investigated that the cell death upon AuR NP treatment resulted from the loss of membrane integrity, the destabilization, and finally the release of intracellular content from the fungus cells [38].

Knowledge about the potential toxicity and health impact of gold nanoparticles is essential before nanomaterials can be used in clinical settings [87]. In our investigation, an assessment of the haemolytic activity of Au NPs at doses corresponding to MICs and to the fungicidal range was performed (Figure 9A–I). It should be highlighted that no significant differences between the haemolytic activity and the shape of the gold core of nanosystems were observed. Moreover, "candidacidal doses" of Au NPs did not cause significant damage of human RBCs (Figure 9A–I). The results obtained by Rahimi et al. are compatible with the outcomes presented in this research [69]; that is, the hemolytic activity of gold nanoparticles at fungicidal doses is not significant. It is worth noting that the results from the cytotoxic evaluation performed by Raja et al. [88] indicate much higher haemolytic activity of silver nanoparticles (Ag NPs) after 12 h of incubation; haemolysis under treatment with Ag NPs at concentrations of 5 µg/mL, 10 µg/mL, and 25 µg/mL reached 6%, 12.5%, and 85%, respectively. However, in comparison to our investigation, only 1.76%, 9.78%, and 68.99% of the erythrocytes were damaged upon exposure to the same doses of Au NPs, which clearly underlines a greater potential for the use of gold nanomaterials considering their low toxicity.

Collectively, our results suggest that ceragenin nanosystems can be potentially used as a novel and an effective antifungals or drug-delivery carriers to enhance the therapy

induced by *Candida*-strains. Nevertheless, further studies are required to determine pharmacodynamic and pharmacokinetic characteristics.

5. Conclusions

Functionalization of rod-, peanut-, and star- gold-shaped nanoparticles with CSA-13, CSA-44, and CSA-131 increased fungicidal activity in comparison to the free molecules of ceragenins. Moreover, an important finding of this study is the lack of resistance development to these nanosystems by strains of *Candida*. The fungicidal activity of the developed nanosystems is mediated by the generation of ROS that leads to membrane-permeabilization and release of intracellular content. Additionally, the low hemolytic activity of tested nanosystems at fungicidal doses further underline their high potential in development of new methods to combat infections caused by various *Candida*-strains.

Author Contributions: Conceptualization, K.S., S.J.C. and R.B.; methodology, S.J.C., K.S., P.D., M.C. (Mateusz Cieśluk), M.C. (Michał Czarnowski) and T.D.; software, K.S., P.D., M.C. (Mateusz Cieśluk), B.D., T.D. and M.Z.; validation, J.D., E.P., P.B.S. and R.B.; formal analysis, S.J.C., K.S., T.D., E.P., M.C. (Mateusz Cieśluk), P.B.S. and R.B.; investigation, S.J.C., J.D., K.S. and M.C. (Michał Czarnowski); resources, J.D., E.P., B.D., M.C. (Michał Czarnowski) and R.B.; data curation, K.S. and S.J.C.; writing—original draft preparation, S.J.C., K.S., P.D., J.D., B.D., M.Z. and T.D.; writing—review and editing, K.S., S.J.C., B.D., P.D., J.D., E.P., T.D., M.P.-W., P.B.S. and R.B.; visualization, K.S., M.C. (Mateusz Cieśluk) and P.D.; supervision, M.P.-W., P.B.S. and R.B.; project administration, S.J.C., K.S. and E.P.; funding acquisition, R.B. and K.S. All authors have read and agreed to the published version of the manuscript.

Institutional Review Board Statement: Hemolytic activity of tested agents was evaluated in blood samples from adult healthy volunteers under IRB approval: R-I-002/231/2019 from 28 March 2019. This study was ap-proved by the institutional review board (IRB) of The Medical University of Bialystok. The study was in accordance with the Declaration of Helsinki and written informed consent was provided by the blood donors.

Informed Consent Statement: Informed consent was obtained from all subjects involved in the study.

Data Availability Statement: The data that support the findings of this study are available from the corresponding author upon reasonable request.

Conflicts of Interest: The authors declare no conflict of interest.

References

1. Schwab, F.; Geffers, C.; Behnke, M.; Gastmeier, P. ICU mortality following ICU-acquired primary bloodstream infections according to the type of pathogen: A prospective cohort study in 937 Germany ICUs (2006–2015). *PLoS ONE* **2018**, *13*, e0194210. [CrossRef] [PubMed]
2. Ghanem-Zoubi, N.; Zorbavel, D.; Khoury, J.; Geffen, Y.; Qasum, M.; Predescu, S.; Paul, M. The association between treatment appropriateness according to EUCAST and CLSI breakpoints and mortality among patients with candidemia: A retrospective observational study. *Eur. J. Clin. Microbiol. Infect. Dis.* **2018**, *37*, 2397–2404. [CrossRef] [PubMed]
3. Bassetti, M.; Giacobbe, D.R.; Vena, A.; Trucchi, C.; Ansaldi, F.; Antonelli, M.; Adamkova, V.; Alicino, C.; Almyroudi, M.P.; Atchade, E.; et al. Incidence and outcome of invasive candidiasis in intensive care units (ICUs) in Europe: Results of the EUCANDICU project. *Crit. Care* **2019**, *23*, 219. [CrossRef] [PubMed]
4. Luzzati, R.; Merelli, M.; Ansaldi, F.; Rosin, C.; Azzini, A.; Cavinato, S.; Brugnaro, P.; Vedovelli, C.; Cattelan, A.; Marina, B.; et al. Nosocomial candidemia in patients admitted to medicine wards compared to other wards: A multicentre study. *Infection* **2016**, *44*, 747–755. [CrossRef]
5. Pappas, P.G.; Lionakis, M.S.; Arendrup, M.C.; Ostrosky-Zeichner, L.; Kullberg, B.J. Invasive candidiasis. *Nat. Rev. Dis. Primers* **2018**, *4*, 18026. [CrossRef]
6. Bongomin, F.; Gago, S.; Oladele, R.O.; Denning, D.W. Global and Multi-National Prevalence of Fungal Diseases-Estimate Precision. *J. Fungi* **2017**, *3*, 57. [CrossRef]

7. CDC Antibiotic Resistance Threats in the United States. 2019. Available online: https://www.cdc.gov/drugresistance/biggest-threats.html (accessed on 15 November 2021).
8. Mayer, F.L.; Wilson, D.; Hube, B. *Candida albicans* pathogenicity mechanisms. *Virulence* **2013**, *4*, 119–128. [CrossRef]
9. Ferreira, A.V.; Prado, C.G.; Carvalho, R.R.; Dias, K.S.; Dias, A.L. *Candida albicans* and non-*C. albicans Candida* species: Comparison of biofilm production and metabolic activity in biofilms, and putative virulence properties of isolates from hospital environments and infections. *Mycopathologia* **2013**, *175*, 265–272. [CrossRef]
10. Brunke, S.; Hube, B. Two unlike cousins: *Candida albicans* and *C. glabrata* infection strategies. *Cell Microbiol.* **2013**, *15*, 701–708. [CrossRef]
11. Patil, S.; Rao, R.S.; Majumdar, B.; Anil, S. Clinical Appearance of Oral *Candida* Infection and Therapeutic Strategies. *Front. Microbiol.* **2015**, *6*, 1391. [CrossRef]
12. Maccallum, D.M. Hosting infection: Experimental models to assay *Candida* virulence. *Int. J. Microbiol.* **2012**, *2012*, 363764. [CrossRef]
13. Pfaller, M.A.; Diekema, D.J. Epidemiology of invasive candidiasis: A persistent public health problem. *Clin. Microbiol. Rev.* **2007**, *20*, 133–163. [CrossRef]
14. Naglik, J.R.; Challacombe, S.J.; Hube, B. *Candida albicans* secreted aspartyl proteinases in virulence and pathogenesis. *Microbiol. Mol. Biol. Rev.* **2003**, *67*, 400–428. [CrossRef]
15. Cannon, R.D.; Lamping, E.; Holmes, A.R.; Niimi, K.; Baret, P.V.; Keniya, M.V.; Tanabe, K.; Niimi, M.; Goffeau, A.; Monk, B.C. Efflux-mediated antifungal drug resistance. *Clin. Microbiol. Rev.* **2009**, *22*, 291–321. [CrossRef]
16. Lockhart, S.R.; Etienne, K.A.; Vallabhaneni, S.; Farooqi, J.; Chowdhary, A.; Govender, N.P.; Colombo, A.L.; Calvo, B.; Cuomo, C.A.; Desjardins, C.A.; et al. Simultaneous Emergence of Multidrug-Resistant *Candida auris* on 3 Continents Confirmed by Whole-Genome Sequencing and Epidemiological Analyses. *Clin. Infect. Dis.* **2017**, *64*, 134–140. [CrossRef]
17. Pfaller, M.A.; Andes, D.R.; Diekema, D.J.; Horn, D.L.; Reboli, A.C.; Rotstein, C.; Franks, B.; Azie, N.E. Epidemiology and outcomes of invasive candidiasis due to non-albicans species of *Candida* in 2,496 patients: Data from the Prospective Antifungal Therapy (PATH) registry 2004-2008. *PLoS ONE* **2014**, *9*, e101510. [CrossRef]
18. Kanafani, Z.A.; Perfect, J.R. Antimicrobial resistance: Resistance to antifungal agents: Mechanisms and clinical impact. *Clin. Infect. Dis.* **2008**, *46*, 120–128. [CrossRef]
19. Vandeputte, P.; Ferrari, S.; Coste, A.T. Antifungal resistance and new strategies to control fungal infections. *Int. J. Microbiol.* **2012**, *2012*, 713687. [CrossRef]
20. Perlin, D.S. Antifungal drug resistance: Do molecular methods provide a way forward? *Curr. Opin. Infect. Dis.* **2009**, *22*, 568–573. [CrossRef]
21. Pagano, L.; Mayor, S. Invasive fungal infections in high-risk patients: Report from TIMM-8 2017. *Future Sci. OA* **2018**, *4*, FSO307. [CrossRef]
22. Huh, A.J.; Kwon, Y.J. "Nanoantibiotics": A new paradigm for treating infectious diseases using nanomaterials in the antibiotics resistant era. *J. Control. Release* **2011**, *156*, 128–145. [CrossRef] [PubMed]
23. Sousa, F.; Ferreira, D.; Reis, S.; Costa, P. Current Insights on Antifungal Therapy: Novel Nanotechnology Approaches for Drug Delivery Systems and New Drugs from Natural Sources. *Pharmaceuticals* **2020**, *13*, 248. [CrossRef] [PubMed]
24. Kischkel, B.; Rossi, S.A.; Santos, S.R.; Nosanchuk, J.D.; Travassos, L.R.; Taborda, C.P. Therapies and Vaccines Based on Nanoparticles for the Treatment of Systemic Fungal Infections. *Front. Cell. Infect. Microbiol.* **2020**, *10*, 463. [CrossRef] [PubMed]
25. Souza, A.C.; Amaral, A.C. Antifungal Therapy for Systemic Mycosis and the Nanobiotechnology Era: Improving Efficacy, Biodistribution and Toxicity. *Front. Microbiol.* **2017**, *8*, 336. [CrossRef]
26. Lima, R.; Del Fiol, F.S.; Balcão, V.M. Prospects for the Use of New Technologies to Combat Multidrug-Resistant Bacteria. *Front. Pharmacol.* **2019**, *10*, 692. [CrossRef]
27. Lee, N.Y.; Ko, W.C.; Hsueh, P.R. Nanoparticles in the Treatment of Infections Caused by Multidrug-Resistant Organisms. *Front. Pharmacol.* **2019**, *10*, 1153. [CrossRef]
28. Gatoo, M.A.; Naseem, S.; Arfat, M.Y.; Dar, A.M.; Qasim, K.; Zubair, S. Physicochemical properties of nanomaterials: Implication in associated toxic manifestations. *Biomed. Res. Int.* **2014**, *2014*, 498420. [CrossRef]
29. Patra, J.K.; Das, G.; Fraceto, L.F.; Campos, E.V.R.; Rodriguez-Torres, M.D.P.; Acosta-Torres, L.S.; Diaz-Torres, L.A.; Grillo, R.; Swamy, M.K.; Sharma, S.; et al. Nano based drug delivery systems: Recent developments and future prospects. *J. Nanobiotechnology* **2018**, *16*, 71. [CrossRef]
30. Durnas, B.; Piktel, E.; Watek, M.; Wollny, T.; Gozdz, S.; Smok-Kalwat, J.; Niemirowicz, K.; Savage, P.B.; Bucki, R. Anaerobic bacteria growth in the presence of cathelicidin LL-37 and selected ceragenins delivered as magnetic nanoparticles cargo. *BMC Microbiol.* **2017**, *17*, 167. [CrossRef]
31. Okkeh, M.; Bloise, N.; Restivo, E.; De Vita, L.; Pallavicini, P.; Visai, L. Gold Nanoparticles: Can They Be the Next Magic Bullet for Multidrug-Resistant Bacteria? *Nanomaterials* **2021**, *11*, 312. [CrossRef]
32. Shaikh, S.; Nazam, N.; Rizvi, S.M.D.; Ahmad, K.; Baig, M.H.; Lee, E.J.; Choi, I. Mechanistic Insights into the Antimicrobial Actions of Metallic Nanoparticles and Their Implications for Multidrug Resistance. *Int. J. Mol. Sci.* **2019**, *20*, 468. [CrossRef]
33. Kong, F.Y.; Zhang, J.W.; Li, R.F.; Wang, Z.X.; Wang, W.J.; Wang, W. Unique Roles of Gold Nanoparticles in Drug Delivery, Targeting and Imaging Applications. *Molecules* **2017**, *22*, 1445. [CrossRef]

34. Paul, S.; Mohanram, K.; Kannan, I. Antifungal activity of curcumin-silver nanoparticles against fluconazole-resistant clinical isolates of *Candida* species. *Ayu* **2018**, *39*, 182–186. [CrossRef]
35. Khatoon, N.; Sharma, Y.; Sardar, M.; Manzoor, N. Mode of action and anti-*Candida* activity of Artemisia annua mediated-synthesized silver nanoparticles. *J. Mycol. Med.* **2019**, *29*, 201–209. [CrossRef]
36. Edis, Z.; Haj Bloukh, S.; Ibrahim, M.R.; Abu Sara, H. "Smart" Antimicrobial Nanocomplexes with Potential to Decrease Surgical Site Infections (SSI). *Pharmaceutics* **2020**, *12*, 361. [CrossRef]
37. Chmielewska, S.J.; Skłodowski, K.; Depciuch, J.; Deptuła, P.; Piktel, E.; Fiedoruk, K.; Kot, P.; Paprocka, P.; Fortunka, K.; Wollny, T.; et al. Bactericidal Properties of Rod-, Peanut-, and Star-Shaped Gold Nanoparticles Coated with Ceragenin CSA-131 against Multidrug-Resistant Bacterial Strains. *Pharmaceutics* **2021**, *13*, 425. [CrossRef]
38. Piktel, E.; Suprewicz, Ł.; Depciuch, J.; Cieśluk, M.; Chmielewska, S.; Durnaś, B.; Król, G.; Wollny, T.; Deptuła, P.; Kochanowicz, J. Rod-shaped gold nanoparticles exert potent candidacidal activity and decrease the adhesion of fungal cells. *Nanomedicine* **2020**, *15*, 2733–2752. [CrossRef]
39. Piktel, E.; Suprewicz, Ł.; Depciuch, J.; Chmielewska, S.; Skłodowski, K.; Daniluk, T.; Król, G.; Kołat-Brodecka, P.; Bijak, P.; Pajor-Świerzy, A.; et al. Varied-shaped gold nanoparticles with nanogram killing efficiency as potential antimicrobial surface coatings for the medical devices. *Sci. Rep.* **2021**, *11*, 12546. [CrossRef]
40. Penders, J.; Stolzoff, M.; Hickey, D.J.; Andersson, M.; Webster, T.J. Shape-dependent antibacterial effects of non-cytotoxic gold nanoparticles. *Int. J. Nanomed.* **2017**, *12*, 2457–2468. [CrossRef]
41. Jebali, A.; Hajjar, F.H.; Pourdanesh, F.; Hekmatimoghaddam, S.; Kazemi, B.; Masoudi, A.; Daliri, K.; Sedighi, N. Silver and gold nanostructures: Antifungal property of different shapes of these nanostructures on *Candida* species. *Med. Mycol.* **2014**, *52*, 65–72. [CrossRef]
42. Ding, B.; Taotofa, U.; Orsak, T.; Chadwell, M.; Savage, P.B. Synthesis and characterization of peptide-cationic steroid antibiotic conjugates. *Org. Lett.* **2004**, *6*, 3433–3436. [CrossRef]
43. Lai, X.Z.; Feng, Y.; Pollard, J.; Chin, J.N.; Rybak, M.J.; Bucki, R.; Epand, R.F.; Epand, R.M.; Savage, P.B. Ceragenins: Cholic acid-based mimics of antimicrobial peptides. *Acc. Chem. Res.* **2008**, *41*, 1233–1240. [CrossRef]
44. Chmielewska, S.J.; Skłodowski, K.; Piktel, E.; Suprewicz, Ł.; Fiedoruk, K.; Daniluk, T.; Wolak, P.; Savage, P.B.; Bucki, R. NDM-1 Carbapenemase-Producing Enterobacteriaceae are Highly Susceptible to Ceragenins CSA-13, CSA-44, and CSA-131. *Infect. Drug Resist.* **2020**, *13*, 3277–3294. [CrossRef]
45. Savage, P.B.; Li, C.; Taotafa, U.; Ding, B.; Guan, Q. Antibacterial properties of cationic steroid antibiotics. *FEMS Microbiol. Lett.* **2002**, *217*, 1–7. [CrossRef]
46. Wnorowska, U.; Niemirowicz, K.; Myint, M.; Diamond, S.L.; Wróblewska, M.; Savage, P.B.; Janmey, P.A.; Bucki, R. Bactericidal activity of cathelicidin LL-37 and select cationic lipids against the hypervirulent *P. aeruginosa* strain LESB58. *Antimicrob. Agents Chemother.* **2015**, *59*, 3808–3815. [CrossRef]
47. Bucki, R.; Niemirowicz, K.; Wnorowska, U.; Byfield, F.J.; Piktel, E.; Wątek, M.; Janmey, P.A.; Savage, P.B. Bactericidal activity of ceragenin CSA-13 in cell culture and an animal model of peritoneal infection. *Antimicrob. Agents Chemother.* **2015**, *59*, 6274–6282. [CrossRef]
48. Wnorowska, U.; Fiedoruk, K.; Piktel, E.; Prasad, S.V.; Sulik, M.; Janion, M.; Daniluk, T.; Savage, P.B.; Bucki, R. Nanoantibiotics containing membrane-active human cathelicidin LL-37 or synthetic ceragenins attached to the surface of magnetic nanoparticles as novel and innovative therapeutic tools: Current status and potential future applications. *J. Nanobiotechnol.* **2020**, *18*, 3. [CrossRef]
49. Mangoni, M.L.; Luca, V.; McDermott, A.M. Fighting microbial infections: A lesson from amphibian skin-derived esculentin-1 peptides. *Peptides* **2015**, *71*, 286–295. [CrossRef]
50. Kodedová, M.; Sychrová, H. Synthetic antimicrobial peptides of the halictines family disturb the membrane integrity of *Candida* cells. *Biochim. Biophys. Acta Biomembr.* **2017**, *1859*, 1851–1858. [CrossRef] [PubMed]
51. Durnaś, B.; Wnorowska, U.; Pogoda, K.; Deptuła, P.; Wątek, M.; Piktel, E.; Głuszek, S.; Gu, X.; Savage, P.B.; Niemirowicz, K.; et al. Candidacidal Activity of Selected Ceragenins and Human Cathelicidin LL-37 in Experimental Settings Mimicking Infection Sites. *PLoS ONE* **2016**, *11*, e0157242. [CrossRef] [PubMed]
52. Wnorowska, U.; Piktel, E.; Durnaś, B.; Fiedoruk, K.; Savage, P.B.; Bucki, R. Use of ceragenins as a potential treatment for urinary tract infections. *BMC Infect. Dis.* **2019**, *19*, 369. [CrossRef] [PubMed]
53. Niemirowicz, K.; Durnaś, B.; Tokajuk, G.; Piktel, E.; Michalak, G.; Gu, X.; Kułakowska, A.; Savage, P.B.; Bucki, R. Formulation and candidacidal activity of magnetic nanoparticles coated with cathelicidin LL-37 and ceragenin CSA-13. *Sci. Rep.* **2017**, *7*, 4610. [CrossRef] [PubMed]
54. Pelgrift, R.Y.; Friedman, A.J. Nanotechnology as a therapeutic tool to combat microbial resistance. *Adv. Drug Deliv. Rev.* **2013**, *65*, 1803–1815. [CrossRef] [PubMed]
55. Ding, B.; Guan, Q.; Walsh, J.P.; Boswell, J.S.; Winter, T.W.; Winter, E.S.; Boyd, S.S.; Li, C.; Savage, P.B. Correlation of the antibacterial activities of cationic peptide antibiotics and cationic steroid antibiotics. *J. Med. Chem.* **2002**, *45*, 663–669. [CrossRef]
56. Levin, C.S.; Janesko, B.G.; Bardhan, R.; Scuseria, G.E.; Hartgerink, J.D.; Halas, N.J. Chain-length-dependent vibrational resonances in alkanethiol self-assembled monolayers observed on plasmonic nanoparticle substrates. *Nano Lett.* **2006**, *6*, 2617–2621. [CrossRef]
57. Bazylewski, P.; Divigalpitiya, R.; Fanchini, G. In situ Raman spectroscopy distinguishes between reversible and irreversible thiol modifications in L-cysteine. *RSC Adv.* **2017**, *7*, 2964–2970. [CrossRef]

58. Abdal Dayem, A.; Hossain, M.K.; Lee, S.B.; Kim, K.; Saha, S.K.; Yang, G.M.; Choi, H.Y.; Cho, S.G. The Role of Reactive Oxygen Species (ROS) in the Biological Activities of Metallic Nanoparticles. *Int. J. Mol. Sci.* **2017**, *18*, 120. [CrossRef]
59. Prasad, R.; Kapoor, K. Multidrug resistance in yeast *Candida*. *Int. Rev. Cytol.* **2005**, *242*, 215–248. [CrossRef]
60. Spampinato, C.; Leonardi, D. *Candida* infections, causes, targets, and resistance mechanisms: Traditional and alternative antifungal agents. *Biomed. Res. Int.* **2013**, *2013*, 204237. [CrossRef]
61. Badiee, P.; Hashemizadeh, Z. Opportunistic invasive fungal infections: Diagnosis & clinical management. *Indian J. Med. Res.* **2014**, *139*, 195–204.
62. Canela, H.M.S.; Cardoso, B.; Vitali, L.H.; Coelho, H.C.; Martinez, R.; Ferreira, M.E.D.S. Prevalence, virulence factors and antifungal susceptibility of *Candida* spp. isolated from bloodstream infections in a tertiary care hospital in Brazil. *Mycoses* **2018**, *61*, 11–21. [CrossRef]
63. McCarty, T.P.; Pappas, P.G. Invasive Candidiasis. *Infect. Dis. Clin. N. Am.* **2016**, *30*, 103–124. [CrossRef]
64. Gauthier, G.M. Fungal Dimorphism and Virulence: Molecular Mechanisms for Temperature Adaptation, Immune Evasion, and In Vivo Survival. *Mediat. Inflamm.* **2017**, *2017*, 8491383. [CrossRef]
65. Modrzewska, B.; Kurnatowski, P. Adherence of *Candida* sp. to host tissues and cells as one of its pathogenicity features. *Ann. Parasitol.* **2015**, *61*, 3–9.
66. Pal, I.; Brahmkhatri, V.P.; Bera, S.; Bhattacharyya, D.; Quirishi, Y.; Bhunia, A.; Atreya, H.S. Enhanced stability and activity of an antimicrobial peptide in conjugation with silver nanoparticle. *J. Colloid Interface Sci.* **2016**, *483*, 385–393. [CrossRef]
67. Jones, L.; Hobden, C.; Oshea, P. Use of a Real-Time Fluorescent-Probe to Study the Electrostatic Properties of the Cell-Surface of *Candida albicans*. *Mycol. Res.* **1995**, *99*, 969–976. [CrossRef]
68. Gonzalez-Hernandez, R.J.; Jin, K.; Hernandez-Chavez, M.J.; Diaz-Jimenez, D.F.; Trujillo-Esquivel, E.; Clavijo-Giraldo, D.M.; Tamez-Castrellon, A.K.; Franco, B.; Gow, N.A.R.; Mora-Montes, H.M. Phosphomannosylation and the Functional Analysis of the Extended *Candida albicans* MNN4-Like Gene Family. *Front. Microbiol.* **2017**, *8*, 2156. [CrossRef]
69. Rahimi, H.; Roudbarmohammadi, S.; Delavari, H.H.; Roudbary, M. Antifungal effects of indolicidin-conjugated gold nanoparticles against fluconazole-resistant strains of. *Int. J. Nanomed.* **2019**, *14*, 5323–5338. [CrossRef]
70. de Alteriis, E.; Maselli, V.; Falanga, A.; Galdiero, S.; Di Lella, F.M.; Gesuele, R.; Guida, M.; Galdiero, E. Efficiency of gold nanoparticles coated with the antimicrobial peptide indolicidin against biofilm formation and development of. *Infect. Drug Resist.* **2018**, *11*, 915–925. [CrossRef]
71. Khan, S.; Alam, F.; Azam, A.; Khan, A.U. Gold nanoparticles enhance methylene blue-induced photodynamic therapy: A novel therapeutic approach to inhibit *Candida albicans* biofilm. *Int. J. Nanomed.* **2012**, *7*, 3245–3257. [CrossRef]
72. Jebali, A.; Hajjar, F.H.; Hekmatimoghaddam, S.; Kazemi, B.; De La Fuente, J.M.; Rashidi, M. Triangular gold nanoparticles conjugated with peptide ligands: A new class of inhibitor for *Candida albicans* secreted aspartyl proteinase. *Biochem. Pharmacol.* **2014**, *90*, 349–355. [CrossRef]
73. El-Sayed, M.A. Some interesting properties of metals confined in time and nanometer space of different shapes. *Acc. Chem. Res.* **2001**, *34*, 257–264. [CrossRef]
74. Wani, I.A.; Ahmad, T.; Manzoor, N. Size and shape dependant antifungal activity of gold nanoparticles: A case study of *Candida*. *Colloids Surf. B Biointerfaces* **2013**, *101*, 162–170. [CrossRef]
75. Prestinaci, F.; Pezzotti, P.; Pantosti, A. Antimicrobial resistance: A global multifaceted phenomenon. *Pathog. Glob. Health* **2015**, *109*, 309–318. [CrossRef] [PubMed]
76. Baptista, P.V.; McCusker, M.P.; Carvalho, A.; Ferreira, D.A.; Mohan, N.M.; Martins, M.; Fernandes, A.R. Nano-Strategies to Fight Multidrug Resistant Bacteria—"A Battle of the Titans". *Front. Microbiol.* **2018**, *9*, 1441. [CrossRef] [PubMed]
77. Xie, Y.; Liu, Y.; Yang, J.; Liu, Y.; Hu, F.; Zhu, K.; Jiang, X. Gold Nanoclusters for Targeting Methicillin-Resistant *Staphylococcus aureus* In Vivo. *Angew Chem. Int. Ed. Engl.* **2018**, *57*, 3958–3962. [CrossRef] [PubMed]
78. Zheng, Y.K.; Liu, W.W.; Qin, Z.J.; Chen, Y.; Jiang, H.; Wang, X.M. Mercaptopyrimidine-Conjugated Gold Nanoclusters as Nanoantibiotics for Combating Multidrug-Resistant Superbugs. *Bioconjugate Chem.* **2018**, *29*, 3094–3103. [CrossRef] [PubMed]
79. Elbehiry, A.; Al-Dubaib, M.; Marzouk, E.; Moussa, I. Antibacterial effects and resistance induction of silver and gold nanoparticles against *Staphylococcus aureus*-induced mastitis and the potential toxicity in rats. *Microbiologyopen* **2019**, *8*, e00698. [CrossRef]
80. Slavin, Y.N.; Asnis, J.; Häfeli, U.O.; Bach, H. Metal nanoparticles: Understanding the mechanisms behind antibacterial activity. *J. Nanobiotechnol.* **2017**, *15*, 65. [CrossRef]
81. Stadtman, E.R.; Berlett, B.S. Reactive oxygen-mediated protein oxidation in aging and disease. *Drug Metab. Rev.* **1998**, *30*, 225–243. [CrossRef]
82. Poli, G.; Leonarduzzi, G.; Biasi, F.; Chiarpotto, E. Oxidative stress and cell signalling. *Curr. Med. Chem.* **2004**, *11*, 1163–1182. [CrossRef]
83. Shi, H.; Hudson, L.G.; Liu, K.J. Oxidative stress and apoptosis in metal ion-induced carcinogenesis. *Free Radic. Biol. Med.* **2004**, *37*, 582–593. [CrossRef]
84. Qiu, Y.; Liu, Y.; Wang, L.; Xu, L.; Bai, R.; Ji, Y.; Wu, X.; Zhao, Y.; Li, Y.; Chen, C. Surface chemistry and aspect ratio mediated cellular uptake of Au nanorods. *Biomaterials* **2010**, *31*, 7606–7619. [CrossRef]
85. Sun, N.; Parrish, R.S.; Calderone, R.A.; Fonzi, W.A. Unique, Diverged, and Conserved Mitochondrial Functions Influencing *Candida albicans* Respiration. *mBio* **2019**, *10*, e00300-19. [CrossRef]

86. Mohamed, M.M.; Fouad, S.A.; Elshoky, H.A.; Mohammed, G.M.; Salaheldin, T.A. Antibacterial effect of gold nanoparticles against. *Int. J. Vet. Sci. Med.* **2017**, *5*, 23–29. [CrossRef]

87. Khan, M.S.; Vishakante, G.D.; Siddaramaiah, H. Gold nanoparticles: A paradigm shift in biomedical applications. *Adv. Colloid Interface Sci.* **2013**, *199*, 44–58. [CrossRef]

88. Raja, A.; Salique, S.M.; Gajalakshmi, P.; James, A. Antibacterial and Hemolytic Activity of Green Silver Nanoparticles from Catharanthus roseus. *Int. J. Pharm. Sci. Nanotechnol.* **1970**, *9*, 3112–3117. [CrossRef]

11. Streszczenie w języku polskim

Narastająca lekooporność drobnoustrojów jest jednym z najważniejszych wyzwań współczesnej medycyny. W związku z tym, konieczne jest poszukiwane nowych metod terapeutycznych, które skutecznie zwalczą drobnoustroje lekooporne, jednocześnie minimalizując ryzyko rozwoju oporności. Jednym z obszarów, który przyciąga szczególną uwagę, jest nanotechnologia, a w szczególności wykorzystanie nanocząstek jako alternatywy w leczeniu zakażeń. Nanocząstki metaliczne oferują unikalne właściwości, które sprawiają, że są obiecującym narzędziem w walce z infekcjami. Ich rozmiar pozwala na ukierunkowane dostarczanie leków do miejsc zakażenia, co zwiększa skuteczność terapii. Dodatkowo, nanocząstki jako nośniki leków wykazują zdolność do pokonywania barier biologicznych, takich jak błony komórkowe czy złożone struktury biofilmu drobnoustrojów.

Celem badań była ocena aktywności przeciwbakteryjnej oraz przeciwgrzybiczej nanocząstek złota w kształcie patyczków, fistaszków i gwiazdek, których powierzchnia została sfunkcjonalizowana cerageninami: CSA-13, CSA-44 oraz CSA-131. Aktywność przeciwdrobnoustrojową wobec bakterii z grupy ESKAPE oraz szczepów *Candida* określono wykorzystując ocenę MIC/MBC/MFC. Przeprowadzono także test zliczania kolonii (killing assay) oraz zapis kinetyki wzrostu bakterii z użyciem resazuryny. Oceniono również aktywność przeciwbakteryjną badanych nanosystemów w stosunku do bakterii zewnątrzkomórkowych za pomocą testu adhezji oraz wewnątrzkomórkowych, za pomocą testu internalizacji z wykorzystaniem komórek A549. Ponadto w celu określenia potencjału rozwoju oporności przeprowadzono seryjne pasażowanie komórek *Candida* z testowanymi nanosystemami. Główny mechanizm działania nanocząstek złota określono badając wytwarzanie ROS, przepuszczalność błony komórkowej i uwalnianie zawartego białka. Aby ocenić potencjalną toksyczność nanocząsteczek złota, przeprowadzono test MTT wobec A549 oraz pomiar uwalniania hemoglobiny z krwinek czerwonych.

W wyniku funkcjonalizacji powierzchni nanocząstek złota oraz modyfikacji ich kształtu oraz wielkości zaobserwowano wzrost aktywności przeciwbakteryjnej oraz przeciwgrzybiczej, zarówno w stosunku do patogenów zewnątrzkomórkowych, jak i wewnątrzkomórkowych w porównaniu do ceragenin w postaci wolnej oraz antybiotyków. Wykazano, iż mechanizmy przeciwdrobnoustrojowego działania badanych nanocząstek obejmują wytwarzanie reaktywnych form tlenu, co wiąże się ze zmianą struktury błon i wypływem zawartości wewnątrzkomórkowej. Uzyskane wyniki potwierdzają niskie ryzyko indukcji oporności wśród badanych patogenów przy zachowaniu silnej aktywności przeciwdrobnoustrojowej również

w stosunku do wielolekoopornych drobnoustrojów. Dodatkowo, badane nanosystemy w dawkach bakterio- oraz grzybobójczych wykazują niską toksyczność wobec ludzkich krwinek czerwonych oraz komórek A549, co podkreśla ich istotny potencjał w opracowywaniu innowacyjnych metod zwalczania infekcji.

12. Streszczenie w języku angielskim

The increasing drug resistance of microorganisms is becoming one of the most significant challenges for modern medicine. Consequently, new therapeutic approaches are being sought to effectively combat drug-resistant microorganisms while minimizing the risk of resistance development. One area that is attracting particular attention is nanotechnology, particularly the use of nanoparticles as an alternative for treating infections. Metallic nanoparticles offer unique properties that make them a promising tool in the fight against infections. Their size at the nanometer scale allows for targeted delivery of drugs to sites of infection, increasing the effectiveness of therapy. In addition, nanoparticles as drug carriers show the ability to overcome biological barriers such as cell membranes and complex biofilm structures, making them potentially effective against resistant strains of microorganisms.

This study aimed to evaluate the antimicrobial and antifungal activity of rod-, peanut-, and star-shaped gold nanoparticles whose surface was functionalized with ceragenins CSA-13, CSA-44, and CSA-131. Antimicrobial activity against ESKAPE bacteria and *Candida* strains was determined by evaluating MIC/MBC/MFC, and a colony counting assay (killing assay) and growth kinetics evaluation with resazurin was performed against bacterial strains. The antimicrobial activity of the tested nanosystems was also evaluated against extracellular bacteria using an adhesion assay and intracellular bacteria using an internalization assay with A549 cells. In addition, serial passaging of *Candida* cells with the tested nanosystems was carried out to determine the potential for resistance development. The primary mechanism of action of the gold nanoparticles was determined by evaluating the production of ROS, cell membrane permeability, and release of the intracellular protein. To assess the potential toxicity of the gold nanoparticles, an MTT assay was performed against A549, and the release of hemoglobin from red blood cells was measured.

As a result of the functionalization of the surface of the gold nanoparticles and modification of their shape and size, an increase in antimicrobial and antifungal activity was observed against both extracellular and intracellular pathogens compared to ceragenins in free form and antibiotics. It was shown that the mechanisms of antimicrobial action of the studied nanoparticles include the production of reactive oxygen species, which is associated with changes in membrane structure and leakage of intracellular contents. The results confirm the low risk of resistance induction among the tested pathogens while maintaining strong antimicrobial activity against multidrug-resistant microorganisms. In addition, the tested nanosystems at bactericidal and fungicidal doses show low toxicity against human red blood

cells and A549 cells, highlighting their significant potential in developing innovative methods for fighting infections.

13. Piśmiennictwo

1. Prestinaci F, Pezzotti P, Pantosti A. Antimicrobial resistance: a global multifaceted phenomenon. Pathog Glob Health. 2015;109(7):309-18.

2. Kainz K, Bauer MA, Madeo F, Carmona-Gutierrez D. Fungal infections in humans: the silent crisis. Microbial Cell. 2020;7(6):143.

3. Ikuta KS, Swetschinski LR, Aguilar GR, Sharara F, Mestrovic T, Gray AP, et al. Global mortality associated with 33 bacterial pathogens in 2019: a systematic analysis for the Global Burden of Disease Study 2019. The Lancet. 2022;400(10369):2221-48.

4. Murray CJ, Ikuta KS, Sharara F, Swetschinski L, Aguilar GR, Gray A, et al. Global burden of bacterial antimicrobial resistance in 2019: a systematic analysis. The Lancet. 2022;399(10325):629-55.

5. Available from: https://www.who.int/news/item/29-04-2019-new-report-calls-for-urgent-action-to-avert-antimicrobial-resistance-crisis.

6. Munir MU, Ahmed A, Usman M, Salman S. Recent Advances in Nanotechnology-Aided Materials in Combating Microbial Resistance and Functioning as Antibiotics Substitutes. Int J Nanomedicine. 2020;15:7329-58.

7. Aslam B, Wang W, Arshad MI, Khurshid M, Muzammil S, Rasool MH, et al. Antibiotic resistance: a rundown of a global crisis. Infect Drug Resist. 2018;11:1645-58.

8. Van Boeckel TP, Brower C, Gilbert M, Grenfell BT, Levin SA, Robinson TP, et al. Global trends in antimicrobial use in food animals. Proceedings of the National Academy of Sciences. 2015;112(18):5649-54.

9. Singh S, Singh SK, Chowdhury I, Singh R. Understanding the Mechanism of Bacterial Biofilms Resistance to Antimicrobial Agents. Open Microbiol J. 2017;11:53-62.

10. Manyi-Loh C, Mamphweli S, Meyer E, Okoh A. Antibiotic use in agriculture and its consequential resistance in environmental sources: potential public health implications. Molecules. 2018;23(4):795.

11. Sachdev C, Anjankar A, Agrawal J. Self-medication with antibiotics: an element increasing resistance. Cureus. 2022;14(10).

12. Mah TF, O'Toole GA. Mechanisms of biofilm resistance to antimicrobial agents. Trends Microbiol. 2001;9(1):34-9.

13. Roy R, Tiwari M, Donelli G, Tiwari V. Strategies for combating bacterial biofilms: A focus on anti-biofilm agents and their mechanisms of action. Virulence. 2018;9(1):522-54.

14. Rice LB. Federal funding for the study of antimicrobial resistance in nosocomial pathogens: no ESKAPE. The University of Chicago Press; 2008. p. 1079-81.

15. Santajit S, Indrawattana N. Mechanisms of antimicrobial resistance in ESKAPE pathogens. BioMed research international. 2016;2016.

16. Tacconelli E, Carrara E, Savoldi A, Harbarth S, Mendelson M, Monnet DL, et al. Discovery, research, and development of new antibiotics: the WHO priority list of antibiotic-resistant bacteria and tuberculosis. The Lancet infectious diseases. 2018;18(3):318-27.

17. Fiore E, Van Tyne D, Gilmore MS. Pathogenicity of enterococci. Microbiology spectrum. 2019;7(4):7.4. 9.

18. Pendleton JN, Gorman SP, Gilmore BF. Clinical relevance of the ESKAPE pathogens. Expert review of anti-infective therapy. 2013;11(3):297-308.

19. Lindsay JA, Ruzin A, Ross HF, Kurepina N, Novick RP. The gene for toxic shock toxin is carried by a family of mobile pathogenicity islands in Staphylococcus aureus. Molecular microbiology. 1998;29(2):527-43.

20. Navon-Venezia S, Kondratyeva K, Carattoli A. Klebsiella pneumoniae: a major worldwide source and shuttle for antibiotic resistance. FEMS microbiology reviews. 2017;41(3):252-75.

21. Effah CY, Sun T, Liu S, Wu Y. Klebsiella pneumoniae: an increasing threat to public health. Annals of clinical microbiology and antimicrobials. 2020;19(1):1-9.

22. Ophir T, Gutnick DL. A role for exopolysaccharides in the protection of microorganisms from desiccation. Applied and environmental microbiology. 1994;60(2):740-5.

23. Potts M. Desiccation tolerance of prokaryotes. Microbiological reviews. 1994;58(4):755-805.

24. Aranda J, Bardina C, Beceiro A, Rumbo S, Cabral MP, Barbé J, et al. Acinetobacter baumannii RecA protein in repair of DNA damage, antimicrobial resistance, general stress response, and virulence. Journal of bacteriology. 2011;193(15):3740-7.

25. Wright MS, Mountain S, Beeri K, Adams MD. Assessment of insertion sequence mobilization as an adaptive response to oxidative stress in Acinetobacter baumannii using IS-seq. Journal of Bacteriology. 2017;199(9):10.1128/jb. 00833-16.

26. Hu Y, Zhang X, Deng S, Yue C, Jia X, Lyu Y. Non-antibiotic prevention and treatment against Acinetobacter baumannii infection: Are vaccines and adjuvants effective strategies? Frontiers in Microbiology. 2023;14:1049917.

27. Kalpana S, Lin W-Y, Wang Y-C, Fu Y, Lakshmi A, Wang H-Y. Antibiotic Resistance Diagnosis in ESKAPE Pathogens—A Review on Proteomic Perspective. Diagnostics. 2023;13(6):1014.

28. Mancuso G, Midiri A, Gerace E, Biondo C. Bacterial antibiotic resistance: The most critical pathogens. Pathogens. 2021;10(10):1310.

29. Hancock RE. The bacterial outer membrane as a drug barrier. Trends in microbiology. 1997;5(1):37-42.

30. Tümmler B. Emerging therapies against infections with Pseudomonas aeruginosa. F1000Research. 2019;8.

31. Terzi HA, Kulah C, Atasoy AR, Ciftci IH. Investigation of OprD porin protein levels in carbapenem-resistant Pseudomonas aeruginosa isolates. Jundishapur journal of microbiology. 2015;8(12).

32. Glen KA, Lamont IL. β-lactam resistance in Pseudomonas aeruginosa: Current status, future prospects. Pathogens. 2021;10(12):1638.

33. Fukuoka T, Ohya S, Narita T, Katsuta M, Iijima M, Masuda N, et al. Activity of the carbapenem panipenem and role of the OprD (D2) protein in its diffusion through the Pseudomonas aeruginosa outer membrane. Antimicrobial agents and chemotherapy. 1993;37(2):322-7.

34. Elsner H-A, Sobottka I, Mack D, Laufs R, Claussen M, Wirth R. Virulence factors of Enterococcus faecalis and Enterococcus faecium blood culture isolates. European Journal of Clinical Microbiology and Infectious Diseases. 2000;19:39-42.

35. Teng J, Imani S, Zhou A, Zhao Y, Du L, Deng S, et al. Combatting resistance: Understanding multi-drug resistant pathogens in intensive care units. Biomedicine & Pharmacotherapy. 2023;167:115564.

36. Davin-Regli A, Lavigne J-P, Pagès J-M. Enterobacter spp.: update on taxonomy, clinical aspects, and emerging antimicrobial resistance. Clinical microbiology reviews. 2019;32(4):10.1128/cmr. 00002-19.

37. Seeberg AH, Tolxdorff-Neutzling R, Wiedemann B. Chromosomal beta-lactamases of Enterobacter cloacae are responsible for resistance to third-generation cephalosporins. Antimicrobial Agents and Chemotherapy. 1983;23(6):918-25.

38. Flury BB, Ellington MJ, Hopkins KL, Turton JF, Doumith M, Woodford N. The differential importance of mutations within AmpD in cephalosporin resistance of Enterobacter aerogenes and Enterobacter cloacae. International journal of antimicrobial agents. 2016;48(5):555-8.

39. Kang KN, Klein DR, Kazi MI, Guerin F, Cattoir V, Brodbelt JS, et al. Colistin heteroresistance in Enterobacter cloacae is regulated by PhoPQ-dependent 4-amino-4-deoxy-l-arabinose addition to lipid A. Molecular microbiology. 2019;111(6):1604-16.

40. Huang L, Feng Y, Zong Z. Heterogeneous resistance to colistin in Enterobacter cloacae complex due to a new small transmembrane protein. Journal of Antimicrobial Chemotherapy. 2019;74(9):2551-8.

41. Control CfD, Prevention. Increasing threat of spread of antimicrobial-resistant fungus in health care facilities. Ultimo accesso. 2023;3.

42. Schwab F, Geffers C, Behnke M, Gastmeier P. ICU mortality following ICU-acquired primary bloodstream infections according to the type of pathogen: A prospective cohort study in 937 Germany ICUs (2006-2015). PLoS One. 2018;13(3):e0194210.

43. Ghanem-Zoubi N, Zorbavel D, Khoury J, Geffen Y, Qasum M, Predescu S, et al. The association between treatment appropriateness according to EUCAST and CLSI breakpoints and mortality among patients with candidemia: a retrospective observational study. Eur J Clin Microbiol Infect Dis. 2018;37(12):2397-404.

44. Pappas PG, Lionakis MS, Arendrup MC, Ostrosky-Zeichner L, Kullberg BJ. Invasive candidiasis. Nat Rev Dis Primers. 2018;4:18026.

45. Bassetti M, Giacobbe DR, Vena A, Trucchi C, Ansaldi F, Antonelli M, et al. Incidence and outcome of invasive candidiasis in intensive care units (ICUs) in Europe: results of the EUCANDICU project. Crit Care. 2019;23(1):219.

46. Luzzati R, Merelli M, Ansaldi F, Rosin C, Azzini A, Cavinato S, et al. Nosocomial candidemia in patients admitted to medicine wards compared to other wards: a multicentre study. Infection. 2016;44(6):747-55.

47. Matthaiou DK, Christodoulopoulou T, Dimopoulos G. How to treat fungal infections in ICU patients. BMC infectious diseases. 2015;15(1):1-8.

48. Mayer FL, Wilson D, Hube B. Candida albicans pathogenicity mechanisms. Virulence. 2013;4(2):119-28.

49. Ferreira AV, Prado CG, Carvalho RR, Dias KS, Dias AL. Candida albicans and non-C. albicans Candida species: comparison of biofilm production and metabolic activity in biofilms, and putative virulence properties of isolates from hospital environments and infections. Mycopathologia. 2013;175(3-4):265-72.

50. Brunke S, Hube B. Two unlike cousins: Candida albicans and C. glabrata infection strategies. Cell Microbiol. 2013;15(5):701-8.

51. Patil S, Rao RS, Majumdar B, Anil S. Clinical Appearance of Oral Candida Infection and Therapeutic Strategies. Front Microbiol. 2015;6:1391.

52. Maccallum DM. Hosting infection: experimental models to assay Candida virulence. Int J Microbiol. 2012;2012:363764.

53. Pfaller MA, Diekema DJ. Epidemiology of invasive candidiasis: a persistent public health problem. Clin Microbiol Rev. 2007;20(1):133-63.

54. Bongomin F, Gago S, Oladele RO, Denning DW. Global and Multi-National Prevalence of Fungal Diseases-Estimate Precision. J Fungi (Basel). 2017;3(4):57.

55. Naglik JR, Challacombe SJ, Hube B. Candida albicans secreted aspartyl proteinases in virulence and pathogenesis. Microbiol Mol Biol Rev. 2003;67(3):400-28, table of contents.

56. Cannon RD, Lamping E, Holmes AR, Niimi K, Baret PV, Keniya MV, et al. Efflux-mediated antifungal drug resistance. Clin Microbiol Rev. 2009;22(2):291-321, Table of Contents.

57. Lockhart SR, Etienne KA, Vallabhaneni S, Farooqi J, Chowdhary A, Govender NP, et al. Simultaneous Emergence of Multidrug-Resistant Candida auris on 3 Continents Confirmed by Whole-Genome Sequencing and Epidemiological Analyses. Clin Infect Dis. 2017;64(2):134-40.

58. Pfaller MA, Andes DR, Diekema DJ, Horn DL, Reboli AC, Rotstein C, et al. Epidemiology and outcomes of invasive candidiasis due to non-albicans species of Candida in 2,496 patients: data from the Prospective Antifungal Therapy (PATH) registry 2004-2008. PLoS One. 2014;9(7):e101510.

59. Control CfD, Prevention. CDC antibiotic resistance threats in the United States, 2019. Web citation: https://www.cdc.gov/drugresistance/biggest-threats html Accessed. 2021;20.

60. Vandeputte P, Ferrari S, Coste AT. Antifungal resistance and new strategies to control fungal infections. Int J Microbiol. 2012;2012:713687.

61. Perlin DS. Antifungal drug resistance: do molecular methods provide a way forward? Curr Opin Infect Dis. 2009;22(6):568-73.

62. Kanafani ZA, Perfect JR. Antimicrobial resistance: resistance to antifungal agents: mechanisms and clinical impact. Clin Infect Dis. 2008;46(1):120-8.

63. Ghannoum MA, Rice LB. Antifungal agents: mode of action, mechanisms of resistance, and correlation of these mechanisms with bacterial resistance. Clinical microbiology reviews. 1999;12(4):501-17.

64. Pagano L, Mayor S. Invasive fungal infections in high-risk patients: report from TIMM-8 2017. Future Sci OA. 2018;4(6):FSO307.

65. Durand GA, Raoult D, Dubourg G. Antibiotic discovery: history, methods and perspectives. International journal of antimicrobial agents. 2019;53(4):371-82.

66. Vanreppelen G, Wuyts J, Van Dijck P, Vandecruys P. Sources of antifungal drugs. Journal of Fungi. 2023;9(2):171.

67. Bush K, Bradford PA. Interplay between β-lactamases and new β-lactamase inhibitors. Nature Reviews Microbiology. 2019;17(5):295-306.

68. Naas T, Oueslati S, Bonnin RA, Dabos ML, Zavala A, Dortet L, et al. Beta-lactamase database (BLDB)–structure and function. Journal of enzyme inhibition and medicinal chemistry. 2017;32(1):917-9.

69. De Pascale G, Wright GD. Antibiotic resistance by enzyme inactivation: from mechanisms to solutions. ChemBioChem. 2010;11(10):1325-34.

70. Uddin TM, Chakraborty AJ, Khusro A, Zidan BRM, Mitra S, Emran TB, et al. Antibiotic resistance in microbes: History, mechanisms, therapeutic strategies and future prospects. Journal of infection and public health. 2021;14(12):1750-66.

71. Munita JM, Arias CA. Mechanisms of antibiotic resistance. Virulence mechanisms of bacterial pathogens. 2016:481-511.

72. Capek A, Simek A. Antimicrobial agente XII. Relationships between biochemical resistance and microbial degradation, of antimycotics. Folia Microbiologica, Praha. 1971;16(6):472-5.

73. Piddock LJ. Clinically relevant chromosomally encoded multidrug resistance efflux pumps in bacteria. Clinical microbiology reviews. 2006;19(2):382-402.

74. Du D, Wang-Kan X, Neuberger A, Van Veen HW, Pos KM, Piddock LJ, et al. Multidrug efflux pumps: structure, function and regulation. Nature Reviews Microbiology. 2018;16(9):523-39.

75. Jenkinson HF. Ins and outs of antimicrobial resistance: era of the drug pumps. Journal of dental research. 1996;75(2):736-42.

76. Egorov A, Ulyashova M, Rubtsova MY. Bacterial enzymes and antibiotic resistance. Acta Naturae (англоязычная версия). 2018;10(4 (39)):33-48.

77. Fyfe C, Grossman TH, Kerstein K, Sutcliffe J. Resistance to macrolide antibiotics in public health pathogens. Cold Spring Harbor Perspectives in Medicine. 2016;6(10).

78. Nabili M, Gohar AA, Badali H, Mohammadi R, Moazeni M. Amino acid substitutions in Erg11p of azole-resistant Candida glabrata: possible effective substitutions and homology modelling. Journal of Global Antimicrobial Resistance. 2016;5:42-6.

79. Limansky AS, Mussi MA, Viale AM. Loss of a 29-kilodalton outer membrane protein in Acinetobacter baumannii is associated with imipenem resistance. Journal of clinical microbiology. 2002;40(12):4776-8.

80. Mago N, Khuller G. Influence of lipid composition on the sensitivity of Candida albicans to antifungal agents. Indian journal of biochemistry & biophysics. 1989;26(1):30-3.

81. Hitchcock C, Barrett-Bee K, Russell N. The lipid composition and permeability to azole of an azole-and polyene-resistant mutant of Candida albicans. Journal of medical and veterinary mycology. 1987;25(1):29-37.

82. Karygianni L, Ren Z, Koo H, Thurnheer T. Biofilm matrixome: extracellular components in structured microbial communities. Trends in microbiology. 2020;28(8):668-81.

83. Vestby LK, Grønseth T, Simm R, Nesse LL. Bacterial biofilm and its role in the pathogenesis of disease. Antibiotics. 2020;9(2):59.

84. Mendhe S, Badge A, Ugemuge S, Chandi D. Impact of Biofilms on Chronic Infections and Medical Challenges. Cureus. 2023;15(11).

85. Karygianni L, Ruf S, Follo M, Hellwig E, Bucher M, Anderson A, et al. Novel broad-spectrum antimicrobial photoinactivation of in situ oral biofilms by visible light plus water-filtered infrared A. Applied and environmental microbiology. 2014;80(23):7324-36.

86. Koo H, Allan RN, Howlin RP, Stoodley P, Hall-Stoodley L. Targeting microbial biofilms: current and prospective therapeutic strategies. Nature Reviews Microbiology. 2017;15(12):740-55.

87. Hall CW, Mah T-F. Molecular mechanisms of biofilm-based antibiotic resistance and tolerance in pathogenic bacteria. FEMS microbiology reviews. 2017;41(3):276-301.

88. Tuon FF, Suss PH, Telles JP, Dantas LR, Borges NH, Ribeiro VST. Antimicrobial treatment of Staphylococcus aureus biofilms. Antibiotics. 2023;12(1):87.

89. Raheem N, Straus SK. Mechanisms of action for antimicrobial peptides with antibacterial and antibiofilm functions. Frontiers in microbiology. 2019;10:2866.

90. Wnorowska U, Fiedoruk K, Piktel E, Prasad SV, Sulik M, Janion M, et al. Nanoantibiotics containing membrane-active human cathelicidin LL-37 or synthetic ceragenins attached to the surface of magnetic nanoparticles as novel and innovative therapeutic tools: current status and potential future applications. J Nanobiotechnology. 2020;18(1):3.

91. Ding B, Taotofa U, Orsak T, Chadwell M, Savage PB. Synthesis and characterization of peptide− cationic steroid antibiotic conjugates. Organic letters. 2004;6(20):3433-6.

92. Chmielewska SJ, Skłodowski K, Piktel E, Suprewicz Ł, Fiedoruk K, Daniluk T, et al. NDM-1 Carbapenemase-Producing Enterobacteriaceae are Highly Susceptible to Ceragenins CSA-13, CSA-44, and CSA-131. Infect Drug Resist. 2020;13:3277-94.

93. Suprewicz Ł, Szczepański A, Lenart M, Piktel E, Fiedoruk K, Barreto-Duran E, et al. Ceragenins exhibit antiviral activity against SARS-CoV-2 by increasing the expression and release of type I interferons upon activation of the host's immune response. Antiviral Research. 2023;217:105676.

94. Durnaś B, Wnorowska U, Pogoda K, Deptuła P, Wątek M, Piktel E, et al. Candidacidal activity of selected ceragenins and human cathelicidin LL-37 in experimental settings mimicking infection sites. PloS one. 2016;11(6):e0157242.

95. Bozkurt-Guzel C, Hacioglu M, Savage PB. Investigation of the in vitro antifungal and antibiofilm activities of ceragenins CSA-8, CSA-13, CSA-44, CSA-131, and CSA-138 against Candida species. Diagnostic Microbiology and Infectious Disease. 2018;91(4):324-30.

96. Piktel E, Prokop I, Wnorowska U, Król G, Cieśluk M, Niemirowicz K, et al. Ceragenin CSA-13 as free molecules and attached to magnetic nanoparticle surfaces induce caspase-dependent apoptosis in human breast cancer cells via disruption of cell oxidative balance. Oncotarget. 2018;9(31):21904-20.

97. Durnaś B, Piktel E, Wątek M, Wollny T, Góźdź S, Smok-Kalwat J, et al. Anaerobic bacteria growth in the presence of cathelicidin LL-37 and selected ceragenins delivered as magnetic nanoparticles cargo. BMC Microbiol. 2017;17(1):167.

98. Piktel E, Pogoda K, Roman M, Niemirowicz K, Tokajuk G, Wróblewska M, et al. Sporicidal activity of ceragenin CSA-13 against Bacillus subtilis. Scientific reports. 2017;7(1):44452.

99. Hashemi MM, Mmuoegbulam AO, Holden BS, Coburn J, Wilson J, Taylor MF, et al. Susceptibility of multidrug-resistant bacteria, isolated from water and plants in Nigeria, to Ceragenins. International Journal of Environmental Research and Public Health. 2018;15(12):2758.

100. Spałek J, Daniluk T, Godlewski A, Deptuła P, Wnorowska U, Ziembicka D, et al. Assessment of Ceragenins in prevention of damage to voice prostheses caused by Candida biofilm formation. Pathogens. 2021;10(11):1371.

101. Epand RF, Pollard JE, Wright JO, Savage PB, Epand RM. Depolarization, bacterial membrane composition, and the antimicrobial action of ceragenins. Antimicrobial agents and chemotherapy. 2010;54(9):3708-13.

102. Bucki R, Sostarecz AG, Byfield FJ, Savage PB, Janmey PA. Resistance of the antibacterial agent ceragenin CSA-13 to inactivation by DNA or F-actin and its activity in cystic fibrosis sputum. Journal of antimicrobial chemotherapy. 2007;60(3):535-45.

103. Ding B, Guan Q, Walsh JP, Boswell JS, Winter TW, Winter ES, et al. Correlation of the antibacterial activities of cationic peptide antibiotics and cationic steroid antibiotics. J Med Chem. 2002;45(3):663-9.

104. Lai XZ, Feng Y, Pollard J, Chin JN, Rybak MJ, Bucki R, et al. Ceragenins: cholic acid-based mimics of antimicrobial peptides. Acc Chem Res. 2008;41(10):1233-40.

105. Lima R, Del Fiol FS, Balcão VM. Prospects for the Use of New Technologies to Combat Multidrug-Resistant Bacteria. Front Pharmacol. 2019;10:692.

106. Gatoo MA, Naseem S, Arfat MY, Dar AM, Qasim K, Zubair S. Physicochemical properties of nanomaterials: implication in associated toxic manifestations. Biomed Res Int. 2014;2014:498420.

107. Huh AJ, Kwon YJ. "Nanoantibiotics": a new paradigm for treating infectious diseases using nanomaterials in the antibiotics resistant era. Journal of controlled release. 2011;156(2):128-45.

108. Niemirowicz-Laskowska K, Głuszek K, Piktel E, Pajuste K, Durnaś B, Król G, et al. Bactericidal and immunomodulatory properties of magnetic nanoparticles functionalized by 1, 4-dihydropyridines. International journal of nanomedicine. 2018;13:3411.

109. Shruthi T, Meghana M, Medha M, Sanjana S, Navya P, Daima HK. Streptomycin functionalization on silver nanoparticles for improved antibacterial activity. Materials Today: Proceedings. 2019;10:8-15.

110. Gupta A, Mumtaz S, Li C-H, Hussain I, Rotello VM. Combatting antibiotic-resistant bacteria using nanomaterials. Chemical Society Reviews. 2019;48(2):415-27.

111. Shaikh S, Nazam N, Rizvi SMD, Ahmad K, Baig MH, Lee EJ, et al. Mechanistic Insights into the Antimicrobial Actions of Metallic Nanoparticles and Their Implications for Multidrug Resistance. Int J Mol Sci. 2019;20(10).

112. Ramalingam B, Parandhaman T, Das SK. Antibacterial effects of biosynthesized silver nanoparticles on surface ultrastructure and nanomechanical properties of gram-negative bacteria viz. Escherichia coli and Pseudomonas aeruginosa. ACS applied materials & interfaces. 2016;8(7):4963-76.

113. Rai A, Prabhune A, Perry CC. Antibiotic mediated synthesis of gold nanoparticles with potent antimicrobial activity and their application in antimicrobial coatings. Journal of Materials Chemistry. 2010;20(32):6789-98.

114. Shaikh S, Rizvi SMD, Shakil S, Hussain T, Alshammari TM, Ahmad W, et al. Synthesis and Characterization of Cefotaxime Conjugated Gold Nanoparticles and Their Use to Target Drug-Resistant CTX-M-Producing Bacterial Pathogens. Journal of Cellular Biochemistry. 2017;118(9):2802-8.

115. Yeh Y-C, Huang T-H, Yang S-C, Chen C-C, Fang J-Y. Nano-based drug delivery or targeting to eradicate bacteria for infection mitigation: a review of recent advances. Frontiers in chemistry. 2020;8:286.

116. Zendegani E, Dolatabadi S. The efficacy of imipenem conjugated with synthesized silver nanoparticles against Acinetobacter baumannii clinical isolates, Iran. Biological trace element research. 2020;197(1):330-40.

117. Memarian M, Javadi A, Fateh R. Antifungal effects of gold nanoparticles conjugated fluconazole against fluconazole resistant strains of Candida albicans isolated from patients with chronic vulvovaginitis. 2016.

118. Habibullah G, Viktorova J, Ruml T. C urrent strategies for noble metal nanoparticle synthesis. Nanoscale Research Letters. 2021;16:1-12.

119. Xiao T, Huang J, Wang D, Meng T, Yang X. Au and Au-Based nanomaterials: Synthesis and recent progress in electrochemical sensor applications. Talanta. 2020;206:120210.

120. Li S, Zhang L, Wang T, Li L, Wang C, Su Z. The facile synthesis of hollow Au nanoflowers for synergistic chemo-photothermal cancer therapy. Chemical Communications. 2015;51(76):14338-41.

121. Folorunso A, Akintelu S, Oyebamiji AK, Ajayi S, Abiola B, Abdusalam I, et al. Biosynthesis, characterization and antimicrobial activity of gold nanoparticles from leaf extracts of Annona muricata. Journal of Nanostructure in Chemistry. 2019;9:111-7.

122. Daniel M-C, Astruc D. Gold nanoparticles: assembly, supramolecular chemistry, quantum-size-related properties, and applications toward biology, catalysis, and nanotechnology. Chemical reviews. 2004;104(1):293-346.

123. Pissuwan D, Gazzana C, Mongkolsuk S, Cortie MB. Single and multiple detections of foodborne pathogens by gold nanoparticle assays. Wiley Interdisciplinary Reviews: Nanomedicine and Nanobiotechnology. 2020;12(1):e1584.

124. Ramalingam V. Multifunctionality of gold nanoparticles: Plausible and convincing properties. Advances in colloid and interface science. 2019;271:101989.

125. Thakor A, Jokerst J, Zavaleta C, Massoud T, Gambhir S. Gold nanoparticles: a revival in precious metal administration to patients. Nano letters. 2011;11(10):4029-36.

126. Slavin YN, Asnis J, Häfeli UO, Bach H. Metal nanoparticles: understanding the mechanisms behind antibacterial activity. J Nanobiotechnology. 2017;15(1):65.

127. Cheon JY, Kim SJ, Rhee YH, Kwon OH, Park WH. Shape-dependent antimicrobial activities of silver nanoparticles. Int J Nanomedicine. 2019;14:2773-80.

128. Padmavathy N, Vijayaraghavan R. Enhanced bioactivity of ZnO nanoparticles—an antimicrobial study. Science and technology of advanced materials. 2008.

129. Yates PD, Franks GV, Biggs S, Jameson GJ. Heteroaggregation with nanoparticles: effect of particle size ratio on optimum particle dose. Colloids and Surfaces A: Physicochemical and Engineering Aspects. 2005;255(1-3):85-90.

130. Sharifi S, Behzadi S, Laurent S, Forrest ML, Stroeve P, Mahmoudi M. Toxicity of nanomaterials. Chem Soc Rev. 2012;41(6):2323-43.

131. Stensberg MC, Wei Q, McLamore ES, Porterfield DM, Wei A, Sepúlveda MS. Toxicological studies on silver nanoparticles: challenges and opportunities in assessment, monitoring and imaging. Nanomedicine (Lond). 2011;6(5):879-98.

132. Joshi AS, Singh P, Mijakovic I. Interactions of gold and silver nanoparticles with bacterial biofilms: Molecular interactions behind inhibition and resistance. International Journal of Molecular Sciences. 2020;21(20):7658.

133. Warren EA, Payne CK. Cellular binding of nanoparticles disrupts the membrane potential. RSC Adv. 2015;5(18):13660-6.

134. Dwivedi S, Wahab R, Khan F, Mishra YK, Musarrat J, Al-Khedhairy AA. Reactive oxygen species mediated bacterial biofilm inhibition via zinc oxide nanoparticles and their statistical determination. PloS one. 2014;9(11):e111289.

135. Makabenta JMV, Nabawy A, Li C-H, Schmidt-Malan S, Patel R, Rotello VM. Nanomaterial-based therapeutics for antibiotic-resistant bacterial infections. Nature Reviews Microbiology. 2021;19(1):23-36.

136. Hsueh Y-H, Lin K-S, Ke W-J, Hsieh C-T, Chiang C-L, Tzou D-Y, et al. The antimicrobial properties of silver nanoparticles in Bacillus subtilis are mediated by released Ag+ ions. PloS one. 2015;10(12):e0144306.

137. Kumar N, Das S, Jyoti A, Kaushik S. Synergistic effect of silver nanoparticles with doxycycline against Klebsiella pneumoniae. Int J Pharm Pharm Sci. 2016;8(7):183-6.

138. Durán N, Nakazato G, Seabra AB. Antimicrobial activity of biogenic silver nanoparticles, and silver chloride nanoparticles: an overview and comments. Appl Microbiol Biotechnol. 2016;100(15):6555-70.

139. Dakal TC, Kumar A, Majumdar RS, Yadav V. Mechanistic basis of antimicrobial actions of silver nanoparticles. Frontiers in microbiology. 2016:1831.

14. Wykaz tabel i rycin

15. Dorobek naukowy

15.1 Wykaz publikacji stanowiących rozprawę doktorską

Publikacja nr 1

Karol Skłodowski, Sylwia Joanna Chmielewska-Deptuła, Ewelina Piktel, Przemysław Wolak, Tomasz Wollny, Robert Bucki. Metallic Nanosystems in the Development of Antimicrobial *Strategies with High Antimicrobial Activity and High Biocompatibility*. International Journal of Molecular Sciences, 2023, 24(3), 2104. DOI: 10.3390/ijms24032104.
IF:5,6; MEiN: 140.

Publikacja nr 2

Karol Skłodowski, Sylwia Joanna Chmielewska, Joanna Depciuch, Piotr Deptuła, Ewelina Piktel, Tamara Daniluk, Magdalena Zakrzewska, Michał Czarnowski, Mateusz Cieśluk, Bonita Durnaś, Magdalena Parlińska-Wojtan, Paul B. Savage, Robert Bucki. *Ceragenin-Coated Non-Spherical Gold Nanoparticles as Novel Candidacidal Agents*. Pharmaceutics, 2021, 13, 1940. DOI: 10.3390/pharmaceutics13111940.
IF: 6,525; MEiN: 100.

15.2 Wykaz innych publikacji naukowych

Karol Skłodowski, Łukasz Suprewicz, Sylwia Joanna Chmielewska-Deptuła, Szczepan Kaliniak, Sławomir Okła, Magdalena Zakrzewska, Łukasz Minarowski, Robert Mróz, Tamara Daniluk, Paul B. Savage, Krzysztof Fiedoruk, Robert Bucki. *Ceragenins exhibit bactericidal properties that are independent of the ionic strength in the environment mimicking cystic fibrosis sputum*. Frontiers in Microbiology. 2023;14. DOI: 10.3389/fmicb.2023.1290952.
IF: 5,2; MEiN: 140.

Maciej Karasiński, Urszula Wnorowska, Bonita Durnaś, Grzegorz Król, Tamara Daniluk, **Karol Skłodowski**, Katarzyna Głuszek, Ewelina Piktel, Sławomir Okła, Robert Bucki. *Ceragenins and Ceragenin-Based Core-Shell Nanosystems as New Antibacterial Agents against Gram-Negative Rods Causing Nosocomial Infections*. Pathogens. 2023;12(11):1346. DOI: 10.3390/pathogens12111346.
IF: 3,7; MEiN: 100.

Robert Bucki, Daniel V Iwamoto, Xuechen Shi, Katherine E Kerr, Fitzroy J Byfield, Łukasz Suprewicz, **Karol Skłodowski**, Julian Sutaria, Paweł Misiak, Agnieszka Z Wilczewska, Sekar Ramachandran, Aaron Wolfe, Minh-Tri Ho Thanh, Eli Whalen, Alison E. Patteson, Paul A. Janmey. *Extracellular vimentin is sufficient to promote cell attachment, spreading, and motility by a mechanism involving N-acetyl glucosamine-containing structures*. Journal of Biological Chemistry. 2023;299(8). DOI: 10.1016/j.jbc.2023.104963.
IF: 4,8; MEiN: 140.

Łukasz Suprewicz, **Karol Skłodowski**, Alicja Walewska, Piotr Deptuła, Alicja Sadzyńska, Andrzej Eljaszewicz, Marcin Moniuszko, Paul A. Janmey, Robert Bucki. *Plasma Gelsolin Enhances Phagocytosis of Candida auris by Human Neutrophils through Scavenger Receptor Class B*. Microbiology Spectrum. 2023;11(2):e04082-22. DOI: 10.1128/spectrum.04082-22.
IF: 3,7; MEiN: 100.

Mateusz Cieśluk, Ewelina Piktel, Urszula Wnorowska, **Karol Skłodowski**, Jan Kochanowicz, Alina Kułakowska, Robert Bucki, Katarzyna Pogoda. *Substrate viscosity impairs temozolomide-mediated inhibition of glioblastoma cells' growth*. Biochimica et Biophysica Acta (BBA)-Molecular Basis of Disease. 2022;1868(11):166513. DOI: 10.1016/j.bbadis.2022.166513
IF: 6,2; MEiN: 140.

Dawid Łysik, Piotr Deptuła, Sylwia Chmielewska, **Karol Skłodowski**, Katarzyna Pogoda, LiKang Chin, Dawei Song, Joanna Mystkowska, Paul A Janmey, Robert Bucki. *Modulation of Biofilm Mechanics by DNA Structure and Cell Type*. ACS Biomaterials Science & Engineering. 2022;8(11):4921-9. DOI: 10.1021/acsbiomaterials.2c00777.
IF: 5,7; MEiN: 140.

Katarzyna Pogoda, Fitzroy Byfield, Piotr Deptuła, Mateusz Cieśluk, Łukasz Suprewicz, **Karol Skłodowski**, Jordan L Shivers, Anne Van Oosten, Katrina Cruz, Ekaterina Tarasovetc, Ekaterina L. Grishchuk, Fred C Mackintosh, Robert Bucki, Alison E. Patteson, Paul A. Janmey. *Unique Role of Vimentin Networks in Compression Stiffening of Cells and Protection of Nuclei from Compressive Stress*. Nano Letters. 2022. DOI: 10.1021/acs.nanolett.2c00736.
IF: 10,8; MEiN: 200.

Paulina Paprocka, Angelika Mańkowska, **Karol Skłodowski**, Grzegorz Król, Tomasz Wollny, Agata Lesiak, Katarzyna Głuszek, Paul B Savage, Bonita Durnaś, Robert Bucki. *Bactericidal Activity of Ceragenin in Combination with Ceftazidime, Levofloxacin, Co-Trimoxazole, and Colistin against the Opportunistic Pathogen Stenotrophomonas maltophilia*. Pathogens. 2022;11(6):621. DOI: 10.3390/pathogens11060621.
IF: 3,7; MEiN: 100.

Joanna Tokajuk, Piotr Deptuła, Sylwia Joanna Chmielewska, **Karol Skłodowski**, Żaneta Anna Mierzejewska, Małgorzata Grądzka-Dahlke, Adam Tołstoj, Tamara Daniluk, Paulina Paprocka, Paul B. Savage, Robert Bucki. *Ceragenin CSA-44 as a Means to Control the Formation of the Biofilm on the Surface of Tooth and Composite Fillings*. Pathogens. 2022;11(5):491. DOI: 10.3390/pathogens11050491.
IF: 3,7; MEiN: 100.

Paulina Paprocka, Bonita Durnaś, Angelika Mańkowska, **Karol Skłodowski**, Grzegorz Król, Magdalena Zakrzewska, Michał Czarnowski, Patrycja Kot, Kamila Fortunka, Stanisław Góźdź, Paul B. Savage, Robert Bucki. *New β-lactam antibiotics and ceragenins–a study to assess their potential in treatment of infections caused by multidrug-resistant strains of Pseudomonas aeruginosa*. Infection and Drug Resistance. 2021:5681-98. DOI: 10.2147/IDR.S338827.
IF: 4,177; MEiN: 100.

Ewelina Piktel, Łukasz Suprewicz, Joanna Depciuch, Sylwia Chmielewska, **Karol Skłodowski**, Tamara Daniluk, Grzegorz Król, Paulina Kołat-Brodecka, Piotr Bijak, Anna Pajor-Świerzy, Krzysztof Fiedoruk, Magdalena Parlinska-Wojtan, Robert Bucki. *Varied-shaped gold nanoparticles with nanogram killing efficiency as potential antimicrobial surface coatings for the medical devices*. Scientific Reports. 2021;11(1):12546. DOI: 10.1038/s41598-021-91847-3.
IF: 4,997; MEiN: 140.

Sylwia Joanna Chmielewska, **Karol Skłodowski**, Joanna Depciuch, Piotr Deptuła, Ewelina Piktel, Krzysztof Fiedoruk, Patrycja Kot, Paulina Paprocka, Kamila Fortunka, Tomasz Wollny, Przemysław Wolak, Magdalena Parlinska-Wojtan, Paul B. Savage, Robert Bucki. *Bactericidal Properties of Rod-, Peanut-, and Star-Shaped Gold Nanoparticles Coated with Ceragenin CSA-131 against Multidrug-Resistant Bacterial Strains*. Pharmaceutics. 2021;13(3). DOI: 10.3390/pharmaceutics13030425.
IF: 6,525; MEiN: 100.

Sylwia Joanna Chmielewska, **Karol Skłodowski**, Ewelina Piktel, Łukasz Suprewicz, Krzysztof Fiedoruk, Tamara Daniluk, Przemysław Wolak, Paul B. Savage, Robert Bucki. *NDM-1 Carbapenemase-Producing Enterobacteriaceae are Highly Susceptible to Ceragenins CSA-13, CSA-44, and CSA-131*. Infect Drug Resist. 2020;13:3277-94. DOI: 10.2147/IDR.S261579.
IF: 4,003; MEiN: 100.

15.3 Wykaz doniesień zjazdowych

Karol Skłodowski, Sylwia Joanna Chmielewska-Deptuła, Łukasz Suprewicz, Joanna Depciuch, Magdalena Parlińska-Wojtan, Paul B. Savage, Bucki Robert. *Core-shell gold nanoparticles functionalized with ceragenin CSA-13 display strong antibacterial activity against of multidrug-resistant Klebsiella pneumoniae.* 10th Congress of European Microbiologists, Hamburg, Niemcy, 9-13 lipiec 2023.

Łukasz Suprewicz, **Karol Skłodowski**, Magdalena Zakrzewska, Krzysztof Fiedoruk, Robert Bucki. *Extracellular vimentin enhances phagocytosis of Escherichia coli and Candida albicans by human neutrophils*. 10th Congress of European Microbiologists, Hamburg, Niemcy, 9-13 lipiec 2023.

Karol Skłodowski, Sylwia Chmielewska, Łukasz Suprewicz, Tomasz Wollny, Grzegorz Król, Joanna Depciuch, Magdalena Parlińska-Wojtan, Paul Savage, Robert Bucki. *Antimicrobial activity of gold nanoparticles coated with ceragenin CSA-13 against highly-virulent and antibiotic-resistant Acinetobacter baumannii*. 40TH Annual Meeting of the European Society for Paediatric Infectious Diseases. Ateny, 9-13 maj 2022.

Łukasz Suprewicz, Ewelina Piktel, Piotr Deptuła, Sylwia Chmielewska, **Karol Skłodowski**, Alicja Walewska, Sylwia Księżak, Tomasz Wollny, Grzegorz Król, Robert Bucki. *Recombinant human plasma gelsolin significantly increases phagocytosis of Candida auris cells by human neutrophils*. 40TH Annual Meeting of the European Society for Paediatric Infectious Diseases. Ateny, 9-13 maj 2022.

Łukasz Suprewicz, Alicja Walewska, **Karol Skłodowski**, Anna Gutowska. *Antibiotic resistance patterns and the prevalence of macrolide-lincosamide-streptogramin B (MLS_B) resistance in Streptoccocus agalactiae clinical isolates*. 14TH Bialystok International Medical Congress for Young Scientists. Białystok, 17-18 maj 2019.

16. Informacje o charakterze udziału współautorów w publikacjach

Informacja o charakterze udziału współautorów w publikacjach wraz z szacunkowym określeniem procentowego wkładu

Karol Skłodowski, Sylwia Joanna Chmielewska-Deptuła, Ewelina Piktel, Przemysław Wolak, Tomasz Wollny, Robert Bucki: *Metallic nanosystems in the development of antimicrobial strategies with high antimicrobial activity and high biocompatibility*. International Journal of Molecular Sciences, 2023, 24(3), 2104. DOI: 10.3390/ijms24032104.

Imię i nazwisko współautora	Charakter udziału	Procentowy wkład
doktorant – mgr Karol Skłodowski	wiodący udział w opracowaniu koncepcji pracy, opracowaniu manuskryptu, akceptacja roboczej i końcowej wersji manuskryptu, przygotowanie figur, pozyskanie środków finansowych	60%
dr n. med. Sylwia Joanna Chmielewska-Deptuła	udział w opracowaniu koncepcji pracy, pozyskaniu środków finansowych, opracowaniu manuskryptu, akceptacji roboczej i końcowej wersji manuskryptu oraz nadzorze merytorycznym	12%
dr hab. n. med. Ewelina Piktel	udział w opracowaniu koncepcji pracy, opracowaniu manuskryptu, akceptacji roboczej i końcowej wersji manuskryptu oraz nadzorze merytorycznym	10%
dr n. med. Przemysław Wolak	udział w przygotowaniu figur oraz opracowaniu manuskryptu	3%
dr n. med. Tomasz Wollny	udział w przygotowaniu figur oraz opracowaniu manuskryptu	3%
prof. dr. hab. n. med. Robert Bucki	udział w opracowaniu koncepcji pracy, pozyskaniu środków finansowych, opracowaniu manuskryptu, akceptacji roboczej i końcowej wersji manuskryptu oraz nadzorze merytorycznym	12%

Oświadczam, że wszyscy współautorzy wyrazili zgodę na wykorzystanie powyższej publikacji w pracy doktorskiej mgr Karola Skłodowskiego.

Karol Skłodowski

Potwierdzam opisany powyżej merytoryczny wkład kandydata w powstanie publikacji wchodzącej w skład rozprawy doktorskiej.

Signed by / Podpisano przez:
Robert Antoni Bucki
Date / Data: 2024-04-03 10:56

Informacja o charakterze udziału współautorów w publikacjach wraz z szacunkowym określeniem procentowego wkładu

Karol Skłodowski, Sylwia Joanna Chmielewska, Joanna Depciuch, Piotr Deptuła, Ewelina Piktel, Tamara Daniluk, Magdalena Zakrzewska, Michał Czarnowski, Mateusz Cieśluk, Bonita Durnaś, Magdalena Parlińska-Wojtan, Paul B. Savage, Robert Bucki: *Ceragenin-Coated Non-Spherical Gold Nanoparticles as Novel Candidacidal Agents*. Pharmaceutics, 2021, 13, 1940. DOI: 10.3390/pharmaceutics13111940.

Imię i nazwisko współautora	Charakter udziału	Procentowy wkład
doktorant – mgr Karol Skłodowski	wiodący udział w opracowaniu koncepcji pracy i metodologii, opracowaniu manuskryptu, przeprowadzeniu badań, weryfikacji wyników, przygotowaniu figur, pozyskaniu środków finansowych na badania, akceptacji roboczej i końcowej wersji manuskryptu	60%
dr n. med. Sylwia Joanna Chmielewska	udział w opracowaniu koncepcji pracy, przeprowadzeniu badań, weryfikacji wyników, analizie formalnej, opracowaniu manuskryptu oraz akceptacji roboczej i końcowej wersji manuskryptu	5%
dr inż. Joanna Depciuch	synteza nanocząstek złota funkcjonalizowanych ceragenimami, ocena właściwości fizykochemicznych, przedstawienie graficzne uzyskanych wyników oraz zredagowanie części manuskryptu dotyczącej syntezy nanosystemów złota	3%
dr inż. Piotr Deptuła	udział w przeprowadzeniu badań, weryfikacji wyników, przygotowaniu figur oraz opracowaniu manuskryptu	3%
Dr hab. n. med. Ewelina Piktel	udział w analizie formalnej, weryfikacji wyników, opracowaniu manuskryptu oraz akceptacji roboczej i końcowej wersji manuskryptu	3%
dr n. med. Tamara Daniluk	udział w przeprowadzeniu badań oraz weryfikacji wyników	3%
mgr Magdalena Zakrzewska	udział w opracowaniu manuskryptu oraz weryfikacji wyników	3%
lek. – dent. Michał Czarnowski	udział w przeprowadzeniu badań oraz weryfikacji wyników	3%
dr n. med. Mateusz Cieśluk	udział w analizie formalnej, przygotowaniu figur, przeprowadzeniu badań oraz weryfikacji wyników	3%

dr. hab. N. med., prof. UJK Bonita Durnaś	udział w opracowaniu manuskryptu oraz weryfikacji wyników	3%
prof. dr hab. inż. Magdalena Parlińska-Wojtan	synteza nanocząstek złota funkcjonalizowanych cerageninami, ocena właściwości fizykochemicznych, przedstawienie graficzne uzyskanych wyników oraz zredagowanie części manuskryptu dotyczącej syntezy nanosystemów złota	3%
Dr Paul B. Savage	synteza ceragenin, udział w analizie formalna, przygotowanie manuskryptu oraz nadzorze merytorycznym	3%
prof. dr. hab. n. med. Robert Bucki	udział w opracowaniu koncepcji badania i metodologii, zapewnieniu materiałów badawczych, opracowaniu manuskryptu, weryfikacji wyników, pozyskaniu środków finansowych na badania, akceptacji roboczej i końcowej wersji manuskryptu oraz nadzorze merytorycznym	5%

Oświadczam, że wszyscy współautorzy wyrazili zgodę na wykorzystanie powyższej publikacji w pracy doktorskiej mgr Karola Skłodowskiego.

Karol Skłodowski

Potwierdzam opisany powyżej merytoryczny wkład kandydata w powstanie publikacji wchodzącej w skład rozprawy doktorskiej.

Signed by / Podpisano przez:

Robert Antoni Bucki

Date / Data: 2024-04-03 10:57

17. Oświadczenia współautorów

Białystok, 20.02.2023

Dr n. med. Sylwia Joanna Chmielewska
Zakład Mikrobiologii Lekarskiej i Inżynierii
Nanobiomedycznej
Uniwersytet Medyczny w Białymstoku
ul. Mickiewicza 2C
15-222 Białystok

OŚWIADCZENIE

Oświadczam, iż mój udział w przygotowaniu publikacji:

„*Ceragenin-Coated Non-Spherical Gold Nanoparticles as Novel Candidacidal Agents*"
autorstwa: Karol Skłodowski, Sylwia Joanna Chmielewska, Joanna Depciuch, Piotr Deptuła,
Ewelina Piktel, Tamara Daniluk, Magdalena Zakrzewska, Michał Czarnowski, Mateusz
Cieśluk, Bonita Durnaś, Magdalena Parlińska-Wojtan, Paul B. Savage, Robert Bucki
opublikowanej w czasopiśmie *Pharmaceutics*, 2021, 13, 1940. DOI:
10.3390/pharmaceutics13111940

wchodzącej w skład rozprawy doktorskiej „*Wpływ kształtu i rozmiaru nanocząstek złota na
efekt przeciwbakteryjny i przeciwgrzybiczy ceragenin związanych z ich powierzchnią – badania
in vitro*", wynoszący 5%, polegał na udziale w opracowaniu koncepcji pracy, przeprowadzeniu
badań, weryfikacji wyników, analizie formalnej, opracowaniu manuskryptu oraz akceptacji
roboczej i końcowej wersji manuskryptu.

Jednocześnie wyrażam zgodę na wykorzystanie przez mgr Karola Skłodowskiego
powyższej publikacji w postępowaniu o nadanie stopnia doktora w dziedzinie nauk
medycznych i nauk o zdrowiu w dyscyplinie nauki medyczne.

ADIUNKT
Zakład Mikrobiologii Lekarskiej
I Inżynierii Nanobiomedycznej
S. Chmielewska-Deptuła
dr n. med. Sylwia Chmielewska-Deptuła

Dr inż. Joanna Depciuch
Zakład Nanomateriałów Funkcjonalnych
Instytut Fizyki Jądrowej
im. Henryka Niewodniczańskiego
Polskiej Akademii Nauk
ul. Radzikowskiego 152
31-342 Kraków

OŚWIADCZENIE

Oświadczam, iż mój udział w przygotowaniu publikacji:

„*Ceragenin-Coated Non-Spherical Gold Nanoparticles as Novel Candidacidal Agents*"
autorstwa: Karol Skłodowski, Sylwia Joanna Chmielewska, Joanna Depciuch, Piotr Deptuła,
Ewelina Piktel, Tamara Daniluk, Magdalena Zakrzewska, Michał Czarnowski, Mateusz
Cieśluk, Bonita Durnaś, Magdalena Parlińska-Wojtan, Paul B. Savage, Robert Bucki
opublikowanej w czasopiśmie *Pharmaceutics*, 2021, 13, 1940. DOI:
10.3390/pharmaceutics13111940

wchodzącej w skład rozprawy doktorskiej „*Wpływ kształtu i rozmiaru nanocząstek złota na
efekt przeciwbakteryjny i przeciwgrzybiczy ceragenin związanych z ich powierzchnią – badania
in vitro*", wynoszący 3%, polegał na syntezie nanocząstek złota funkcjonalizowanych
ceргeninami, ocenie właściwości fizykochemicznych, przedstawieniu graficznym uzyskanych
wyników oraz zredagowaniu części manuskryptu dotyczącej syntezy nanosystemów złota.

Jednocześnie wyrażam zgodę na wykorzystanie przez mgr Karola Skłodowskiego
powyższej publikacji w postępowaniu o nadanie stopnia doktora w dziedzinie nauk
medycznych i nauk o zdrowiu w dyscyplinie nauki medyczne.

Białystok, 20.02.2023

Dr inż. Piotr Deptuła
Samodzielna Pracowania Nanomedycyny
Uniwersytet Medyczny w Białymstoku
ul. Mickiewicza 2B
15-222 Białystok

OŚWIADCZENIE

Oświadczam, iż mój udział w przygotowaniu publikacji:

„*Ceragenin-Coated Non-Spherical Gold Nanoparticles as Novel Candidacidal Agents*" autorstwa: Karol Skłodowski, Sylwia Joanna Chmielewska, Joanna Depciuch, Piotr Deptuła, Ewelina Piktel, Tamara Daniluk, Magdalena Zakrzewska, Michał Czarnowski, Mateusz Cieśluk, Bonita Durnaś, Magdalena Parlińska-Wojtan, Paul B. Savage, Robert Bucki opublikowanej w czasopiśmie *Pharmaceutics*, 2021, 13, 1940. DOI: 10.3390/pharmaceutics13111940

wchodzącej w skład rozprawy doktorskiej „*Wpływ kształtu i rozmiaru nanocząstek złota na efekt przeciwbakteryjny i przeciwgrzybiczy ceragenin związanych z ich powierzchnią – badania in vitro*", wynoszący 3%, polegał na udziale w przeprowadzeniu badań, weryfikacji wyników, przygotowaniu figur oraz opracowaniu manuskryptu.

Jednocześnie wyrażam zgodę na wykorzystanie przez mgr Karola Skłodowskiego powyższej publikacji w postępowaniu o nadanie stopnia doktora w dziedzinie nauk medycznych i nauk o zdrowiu w dyscyplinie nauki medyczne.

ADIUNKT
Samodzielna Pracownia Nanomedycyny

dr inż. Piotr Deptuła

133

Dr hab. n. med. Ewelina Piktel
Samodzielna Pracowania Nanomedycyny
Uniwersytet Medyczny w Białymstoku
ul. Mickiewicza 2B
15-222 Białystok

OŚWIADCZENIE

Oświadczam, iż mój udział w przygotowaniu publikacji:

„*Ceragenin-Coated Non-Spherical Gold Nanoparticles as Novel Candidacidal Agents*"
autorstwa: Karol Skłodowski, Sylwia Joanna Chmielewska, Joanna Depciuch, Piotr Deptuła,
Ewelina Piktel, Tamara Daniluk, Magdalena Zakrzewska, Michał Czarnowski, Mateusz
Cieśluk, Bonita Durnaś, Magdalena Parlińska-Wojtan, Paul B. Savage, Robert Bucki
opublikowanej w czasopiśmie *Pharmaceutics*, 2021, 13, 1940. DOI:
10.3390/pharmaceutics13111940

wchodzącej w skład rozprawy doktorskiej „*Wpływ kształtu i rozmiaru nanocząstek złota na
efekt przeciwbakteryjny i przeciwgrzybiczy ceragenin związanych z ich powierzchnią – badania
in vitro*", wynoszący 3%, polegał na udziale w analizie formalnej, weryfikacji wyników,
opracowaniu manuskryptu oraz akceptacji roboczej i końcowej wersji manuskryptu.

Jednocześnie wyrażam zgodę na wykorzystanie przez mgr Karola Skłodowskiego
powyższej publikacji w postępowaniu o nadanie stopnia doktora w dziedzinie nauk
medycznych i nauk o zdrowiu w dyscyplinie nauki medyczne.

ADIUNKT
Samodzielnej Pracowni Nanomedycyny
dr hab. n. med. Ewelina Piktel

Dr n. med. Tamara Daniluk
Zakład Mikrobiologii Lekarskiej i Inżynierii
Nanobiomedycznej
Uniwersytet Medyczny w Białymstoku
ul. Mickiewicza 2C
15-222 Białystok

OŚWIADCZENIE

Oświadczam, iż mój udział w przygotowaniu publikacji:

„Ceragenin-Coated Non-Spherical Gold Nanoparticles as Novel Candidacidal Agents" autorstwa: Karol Skłodowski, Sylwia Joanna Chmielewska, Joanna Depciuch, Piotr Deptuła, Ewelina Piktel, Tamara Daniluk, Magdalena Zakrzewska, Michał Czarnowski, Mateusz Cieśluk, Bonita Durnaś, Magdalena Parlińska-Wojtan, Paul B. Savage, Robert Bucki opublikowanej w czasopiśmie Pharmaceutics, 2021, 13, 1940. DOI: 10.3390/pharmaceutics13111940

wchodzącej w skład rozprawy doktorskiej „Wpływ kształtu i rozmiaru nanocząstek złota na efekt przeciwbakteryjny i przeciwgrzybiczy ceragenin związanych z ich powierzchnią – badania in vitro", wynoszący 3%, polegał na udziale w przeprowadzeniu badań oraz weryfikacji wyników.

Jednocześnie wyrażam zgodę na wykorzystanie przez mgr Karola Skłodowskiego powyższej publikacji w postępowaniu o nadanie stopnia doktora w dziedzinie nauk medycznych i nauk o zdrowiu w dyscyplinie nauki medyczne.

Mgr Magdalena Zakrzewska
Zakład Mikrobiologii Lekarskiej i Inżynierii
Nanobiomedycznej
Uniwersytet Medyczny w Białymstoku
ul. Mickiewicza 2C
15-222 Białystok

Białystok, 20.02.2023

OŚWIADCZENIE

Oświadczam, iż mój udział w przygotowaniu publikacji:

„*Ceragenin-Coated Non-Spherical Gold Nanoparticles as Novel Candidacidal Agents*" autorstwa: Karol Skłodowski, Sylwia Joanna Chmielewska, Joanna Depciuch, Piotr Deptuła, Ewelina Piktel, Tamara Daniluk, Magdalena Zakrzewska, Michał Czarnowski, Mateusz Cieśluk, Bonita Durnaś, Magdalena Parlińska-Wojtan, Paul B. Savage, Robert Bucki opublikowanej w czasopiśmie *Pharmaceutics*, 2021, 13, 1940. DOI: 10.3390/pharmaceutics13111940

wchodzącej w skład rozprawy doktorskiej „*Wpływ kształtu i rozmiaru nanocząstek złota na efekt przeciwbakteryjny i przeciwgrzybiczy ceragenin związanych z ich powierzchnią – badania in vitro*", wynoszący 3%, polegał na udziale w opracowaniu manuskryptu oraz weryfikacji wyników.

Jednocześnie wyrażam zgodę na wykorzystanie przez mgr Karola Skłodowskiego powyższej publikacji w postępowaniu o nadanie stopnia doktora w dziedzinie nauk medycznych i nauk o zdrowiu w dyscyplinie nauki medyczne.

Zakrzewska Magdalene

136

Białystok, 20.02.2023

Lek. – dent. Michał Czarnowski
Zakład Mikrobiologii Lekarskiej i Inżynierii
Nanobiomedycznej
Uniwersytet Medyczny w Białymstoku
ul. Mickiewicza 2C
15-222 Białystok

OŚWIADCZENIE

Oświadczam, iż mój udział w przygotowaniu publikacji:

„*Ceragenin-Coated Non-Spherical Gold Nanoparticles as Novel Candidacidal Agents*"
autorstwa: Karol Skłodowski, Sylwia Joanna Chmielewska, Joanna Depciuch, Piotr Deptuła,
Ewelina Piktel, Tamara Daniluk, Magdalena Zakrzewska, Michał Czarnowski, Mateusz
Cieśluk, Bonita Durnaś, Magdalena Parlińska-Wojtan, Paul B. Savage, Robert Bucki
opublikowanej w czasopiśmie *Pharmaceutics*, 2021, 13, 1940. DOI:
10.3390/pharmaceutics13111940

wchodzącej w skład rozprawy doktorskiej „*Wpływ kształtu i rozmiaru nanocząstek złota na
efekt przeciwbakteryjny i przeciwgrzybiczy ceragenin związanych z ich powierzchnią – badania
in vitro*", wynoszący 3%, polegał na udziale w przeprowadzeniu badań oraz weryfikacji
wyników.

Jednocześnie wyrażam zgodę na wykorzystanie przez mgr Karola Skłodowskiego
powyższej publikacji w postępowaniu o nadanie stopnia doktora w dziedzinie nauk
medycznych i nauk o zdrowiu w dyscyplinie nauki medyczne.

Michał Czarnowski

Białystok, 20.02.2023

Dr n. med. Mateusz Cieśluk
Zakład Mikrobiologii Lekarskiej i Inżynierii
Nanobiomedycznej
Uniwersytet Medyczny w Białymstoku
ul. Mickiewicza 2C
15-222 Białystok

OŚWIADCZENIE

Oświadczam, iż mój udział w przygotowaniu publikacji:

„*Ceragenin-Coated Non-Spherical Gold Nanoparticles as Novel Candidacidal Agents*"
autorstwa: Karol Skłodowski, Sylwia Joanna Chmielewska, Joanna Depciuch, Piotr Deptuła,
Ewelina Piktel, Tamara Daniluk, Magdalena Zakrzewska, Michał Czarnowski, Mateusz
Cieśluk, Bonita Durnaś, Magdalena Parlińska-Wojtan, Paul B. Savage, Robert Bucki
opublikowanej w czasopiśmie *Pharmaceutics*, 2021, 13, 1940. DOI:
10.3390/pharmaceutics13111940

wchodzącej w skład rozprawy doktorskiej „*Wpływ kształtu i rozmiaru nanocząstek złota na
efekt przeciwbakteryjny i przeciwgrzybiczy ceragenin związanych z ich powierzchnią – badania
in vitro*", wynoszący 3%, polegał na udziale w analizie formalnej, przygotowaniu figur,
przeprowadzeniu badań oraz weryfikacji wyników.

Jednocześnie wyrażam zgodę na wykorzystanie przez mgr Karola Skłodowskiego
powyższej publikacji w postępowaniu o nadanie stopnia doktora w dziedzinie nauk
medycznych i nauk o zdrowiu w dyscyplinie nauki medyczne.

Dr hab. n. med., prof. UJK Bonita Durnaś
Collegium Medicum
Uniwersytet Jana Kochanowskiego w Kielcach
ul. IX Wieków Kielc 19A
25-516 Kielce

OŚWIADCZENIE

Oświadczam, iż mój udział w przygotowaniu publikacji:

„*Ceragenin-Coated Non-Spherical Gold Nanoparticles as Novel Candidacidal Agents*" autorstwa: Karol Skłodowski, Sylwia Joanna Chmielewska, Joanna Depciuch, Piotr Deptuła, Ewelina Piktel, Tamara Daniluk, Magdalena Zakrzewska, Michał Czarnowski, Mateusz Cieśluk, Bonita Durnaś, Magdalena Parlińska-Wojtan, Paul B. Savage, Robert Bucki opublikowanej w czasopiśmie *Pharmaceutics*, 2021, 13, 1940. DOI: 10.3390/pharmaceutics13111940

wchodzącej w skład rozprawy doktorskiej „*Wpływ kształtu i rozmiaru nanocząstek złota na efekt przeciwbakteryjny i przeciwgrzybiczy ceragenin związanych z ich powierzchnią – badania in vitro*", wynoszący 3%, polegał na udziale w opracowaniu manuskryptu oraz weryfikacji wyników.

Jednocześnie wyrażam zgodę na wykorzystanie przez mgr Karola Skłodowskiego powyższej publikacji w postępowaniu o nadanie stopnia doktora w dziedzinie nauk medycznych i nauk o zdrowiu w dyscyplinie nauki medyczne.

Prof. dr hab. inż. Magdalena Parlińska-Wojtan
Zakład Nanomateriałów Funkcjonalnych
Instytut Fizyki Jądrowej
im. Henryka Niewodniczańskiego
Polskiej Akademii Nauk
ul. Radzikowskiego 152
31-342 Kraków

OŚWIADCZENIE

Oświadczam, iż mój udział w przygotowaniu publikacji:

„*Ceragenin-Coated Non-Spherical Gold Nanoparticles as Novel Candidacidal Agents*"
autorstwa: Karol Skłodowski, Sylwia Joanna Chmielewska, Joanna Depciuch, Piotr Deptuła,
Ewelina Piktel, Tamara Daniluk, Magdalena Zakrzewska, Michał Czarnowski, Mateusz
Cieśluk, Bonita Durnaś, Magdalena Parlińska-Wojtan, Paul B. Savage, Robert Bucki
opublikowanej w czasopiśmie *Pharmaceutics*, 2021, 13, 1940. DOI:
10.3390/pharmaceutics13111940

wchodzącej w skład rozprawy doktorskiej „*Wpływ kształtu i rozmiaru nanocząstek złota na
efekt przeciwbakteryjny i przeciwgrzybiczy ceragenin związanych z ich powierzchnią – badania
in vitro*", wynoszący 3%, polegał na wykonaniu oraz zanalizowaniu zdjęć TEM nanocząstek
złota.

Jednocześnie wyrażam zgodę na wykorzystanie przez mgr Karola Skłodowskiego
powyższej publikacji w postępowaniu o nadanie stopnia doktora w dziedzinie nauk
medycznych i nauk o zdrowiu w dyscyplinie nauki medyczne.

DEPARTMENT OF CHEMISTRY
AND BIOCHEMISTRY
BRIGHAM YOUNG UNIVERSITY
C-100 BNSN
PROVO, UT 84602
(801) 422-3667 / FAX: (801) 422-0153

12-20-2023

Dr Paul B. Savage
Department of Chemistry and Biochemistry
Brigham Young University
C100 Benson Building
Provo, UT 84602, United States

STATEMENT

I declare that my participation in the preparation of the publication:
"*Ceragenin-Coated Non-Spherical Gold Nanoparticles as Novel Candidacidal Agents*" by: Karol Skłodowski, Sylwia Joanna Chmielewska, Joanna Depciuch, Piotr Deptuła, Ewelina Piktel, Tamara Daniluk, Magdalena Zakrzewska, Michał Czarnowski, Mateusz Cieśluk, Bonita Durnaś, Magdalena Parlińska-Wojtan, Paul B. Savage, Robert Bucki published in the journal *Pharmaceutics*, 2021, 13, 1940. DOI: 10.3390/pharmaceutics13111940 included in the doctoral dissertation "*Effect of the shape and size of gold nanoparticles on the antimicrobial and antifungal effects of ceragenins bound to their surface - in vitro studies*," amounting to 3% of the total effort and consisted of the synthesis of ceragenins, formal analysis, preparation of the manuscript and supervision.

I approve for Karol Sklodowski, M.D., to use the above publication in the proceedings for the conferral of the doctoral degree in medical and health sciences in the discipline of medical sciences.

Sincerely,

Paul B. Savage
Reed M. Izatt Professor of Chemistry
Karl G. Maeser Distinguished University Professor

Białystok, 20.02.2023

Prof. dr hab. Robert Bucki
Zakład Mikrobiologii Lekarskiej i Inżynierii
Nanobiomedycznej
Uniwersytet Medyczny w Białymstoku
ul. Mickiewicza 2C
15-222 Białystok

OŚWIADCZENIE

Oświadczam, iż mój udział w przygotowaniu publikacji:

„*Ceragenin-Coated Non-Spherical Gold Nanoparticles as Novel Candidacidal Agents*"
autorstwa: Karol Skłodowski, Sylwia Joanna Chmielewska, Joanna Depciuch, Piotr Deptuła,
Ewelina Piktel, Tamara Daniluk, Magdalena Zakrzewska, Michał Czarnowski, Mateusz
Cieśluk, Bonita Durnaś, Magdalena Parlińska-Wojtan, Paul B. Savage, Robert Bucki
opublikowanej w czasopiśmie *Pharmaceutics*, 2021, 13, 1940. DOI:
10.3390/pharmaceutics13111940

wchodzącej w skład rozprawy doktorskiej „*Wpływ kształtu i rozmiaru nanocząstek złota na
efekt przeciwbakteryjny i przeciwgrzybiczy ceragenin związanych z ich powierzchnią – badania
in vitro*", wynoszący 5%, polegał na udziale w opracowaniu koncepcji badania i metodologii,
zapewnieniu materiałów badawczych, opracowaniu manuskryptu, weryfikacji wyników,
pozyskaniu środków finansowych na badania, akceptacji roboczej i końcowej wersji
manuskryptu oraz nadzorze merytorycznym.

Jednocześnie wyrażam zgodę na wykorzystanie przez mgr Karola Skłodowskiego
powyższej publikacji w postępowaniu o nadanie stopnia doktora w dziedzinie nauk
medycznych i nauk o zdrowiu w dyscyplinie nauki medyczne.

Dr n. med. Sylwia Joanna Chmielewska-Deptuła
Zakład Mikrobiologii Lekarskiej i Inżynierii
Nanobiomedycznej
Uniwersytet Medyczny w Białymstoku
ul. Mickiewicza 2C
15-222 Białystok

OŚWIADCZENIE

Oświadczam, iż mój udział w przygotowaniu publikacji:

„*Metallic Nanosystems in the Development of Antimicrobial Strategies with High Antimicrobial Activity and High Biocompatibility*" autorstwa: Karol Skłodowski, Sylwia Joanna Chmielewska-Deptuła, Ewelina Piktel, Przemysław Wolak, Tomasz Wollny, Robert Bucki opublikowanej w czasopiśmie *International Journal of Molecular Sciences*, 2023, 24(3), 2104. DOI: 10.3390/ijms24032104

wchodzącej w skład rozprawy doktorskiej „*Wpływ kształtu i rozmiaru nanocząstek złota na efekt przeciwbakteryjny i przeciwgrzybiczy ceragenin związanych z ich powierzchnią – badania in vitro*", wynoszący 12%, polegał na udziale w opracowaniu koncepcji pracy, pozyskaniu środków finansowych, opracowaniu manuskryptu, akceptacji roboczej i końcowej wersji manuskryptu oraz nadzorze merytorycznym.

Jednocześnie wyrażam zgodę na wykorzystanie przez mgr Karola Skłodowskiego powyższej publikacji w postępowaniu o nadanie stopnia doktora w dziedzinie nauk medycznych i nauk o zdrowiu w dyscyplinie nauki medyczne.

ADIUNKT
Zakład Mikrobiologii Lekarskiej
i Inżynierii Nanobiomedycznej
S. Chmielewska-Deptuła

Białystok, 30.03.2023

Dr hab. n. med. Ewelina Piktel
Samodzielna Pracowania Nanomedycyny
Uniwersytet Medyczny w Białymstoku
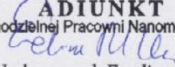ul. Mickiewicza 2B
15-222 Białystok

OŚWIADCZENIE

Oświadczam, iż mój udział w przygotowaniu publikacji:

„*Metallic Nanosystems in the Development of Antimicrobial Strategies with High Antimicrobial Activity and High Biocompatibility*" autorstwa: Karol Skłodowski, Sylwia Joanna Chmielewska-Deptuła, Ewelina Piktel, Przemysław Wolak, Tomasz Wollny, Robert Bucki opublikowanej w czasopiśmie *International Journal of Molecular Sciences*, 2023, 24(3), 2104. DOI: 10.3390/ijms24032104

wchodzącej w skład rozprawy doktorskiej „*Wpływ kształtu i rozmiaru nanocząstek złota na efekt przeciwbakteryjny i przeciwgrzybiczy ceragenin związanych z ich powierzchnią – badania in vitro*", wynoszący 10%, polegał na udziale w opracowaniu koncepcji pracy, opracowaniu manuskryptu, akceptacji roboczej i końcowej wersji manuskryptu oraz nadzorze merytorycznym.

Jednocześnie wyrażam zgodę na wykorzystanie przez mgr Karola Skłodowskiego powyższej publikacji w postępowaniu o nadanie stopnia doktora w dziedzinie nauk medycznych i nauk o zdrowiu w dyscyplinie nauki medyczne.

ADIUNKT
Samodzielnej Pracowni Nanomedycyny
dr hab. n. med. Ewelina Piktel

Dr n. med. Przemysław Wolak
Instytut Nauk Medycznych,
Uniwersytet Jana Kochanowskiego
Aleja IX Wieków Kielc 19A
25-317 Kielce

Białystok, 30.03.2023

OŚWIADCZENIE

Oświadczam, iż mój udział w przygotowaniu publikacji:

„*Metallic Nanosystems in the Development of Antimicrobial Strategies with High Antimicrobial Activity and High Biocompatibility*" autorstwa: Karol Skłodowski, Sylwia Joanna Chmielewska-Deptuła, Ewelina Piktel, Przemysław Wolak, Tomasz Wollny, Robert Bucki opublikowanej w czasopiśmie *International Journal of Molecular Sciences*, 2023, 24(3), 2104. DOI: 10.3390/ijms24032104

wchodzącej w skład rozprawy doktorskiej „*Wpływ kształtu i rozmiaru nanocząstek złota na efekt przeciwbakteryjny i przeciwgrzybiczy ceragenin związanych z ich powierzchnią – badania in vitro*", wynoszący 3%, polegał na udziale w przygotowaniu figur oraz opracowaniu manuskryptu.

Jednocześnie wyrażam zgodę na wykorzystanie przez mgr Karola Skłodowskiego powyższej publikacji w postępowaniu o nadanie stopnia doktora w dziedzinie nauk medycznych i nauk o zdrowiu w dyscyplinie nauki medyczne.

145

Dr n. med. Tomasz Wollny
Świętokrzyskie Centrum Onkologii
ul. Artwińskiego 3,
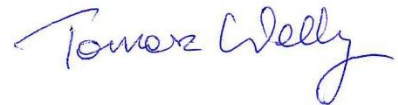25-734 Kielce, Poland

Białystok, 30.03.2023

OŚWIADCZENIE

Oświadczam, iż mój udział w przygotowaniu publikacji:

„*Metallic Nanosystems in the Development of Antimicrobial Strategies with High Antimicrobial Activity and High Biocompatibility*" autorstwa: Karol Skłodowski, Sylwia Joanna Chmielewska-Deptuła, Ewelina Piktel, Przemysław Wolak, Tomasz Wollny, Robert Bucki opublikowanej w czasopiśmie *International Journal of Molecular Sciences*, 2023, 24(3), 2104. DOI: 10.3390/ijms24032104

wchodzącej w skład rozprawy doktorskiej „*Wpływ kształtu i rozmiaru nanocząstek złota na efekt przeciwbakteryjny i przeciwgrzybiczy ceragenin związanych z ich powierzchnią – badania in vitro*", wynoszący 3%, polegał na udziale w przygotowaniu figur oraz opracowaniu manuskryptu.

Jednocześnie wyrażam zgodę na wykorzystanie przez mgr Karola Skłodowskiego powyższej publikacji w postępowaniu o nadanie stopnia doktora w dziedzinie nauk medycznych i nauk o zdrowiu w dyscyplinie nauki medyczne.

146

Białystok, 30.03.2023

Prof. dr hab. Robert Bucki
Zakład Mikrobiologii Lekarskiej i Inżynierii
Nanobiomedycznej
Uniwersytet Medyczny w Białymstoku
ul. Mickiewicza 2C
15-222 Białystok

OŚWIADCZENIE

Oświadczam, iż mój udział w przygotowaniu publikacji:

„*Metallic Nanosystems in the Development of Antimicrobial Strategies with High Antimicrobial Activity and High Biocompatibility*" autorstwa: Karol Skłodowski, Sylwia Joanna Chmielewska-Deptuła, Ewelina Piktel, Przemysław Wolak, Tomasz Wollny, Robert Bucki opublikowanej w czasopiśmie *International Journal of Molecular Sciences*, 2023, 24(3), 2104. DOI: 10.3390/ijms24032104

wchodzącej w skład rozprawy doktorskiej „*Wpływ kształtu i rozmiaru nanocząstek złota na efekt przeciwbakteryjny i przeciwgrzybiczy ceragenin związanych z ich powierzchnią – badania in vitro*", wynoszący 12%, polegał na udziale w opracowaniu koncepcji pracy, pozyskaniu środków finansowych, opracowaniu manuskryptu, akceptacji roboczej i końcowej wersji manuskryptu oraz nadzorze merytorycznym.

Jednocześnie wyrażam zgodę na wykorzystanie przez mgr Karola Skłodowskiego powyższej publikacji w postępowaniu o nadanie stopnia doktora w dziedzinie nauk medycznych i nauk o zdrowiu w dyscyplinie nauki medyczne.

18. Zgoda komisji bioetycznej

KOMISJA BIOETYCZNA
UNIWERSYTETU MEDYCZNEGO w BIAŁYMSTOKU
ul. Jana Kilińskiego 1
15-089 Białystok
tel. (085) 748 54 07, (085) 686 52 20, fax. (085) 748 55 08
prorektorkl@umb.edu.pl

Białystok, 28-03-2019

Uchwała nr: R-I-002/231/2019

Komisja Bioetyczna Uniwersytetu Medycznego w Białymstoku, po zapoznaniu się z projektem badania zgodnie z zasadami GCP/ Guidelines for Good Clinical Practice /- **w y r a ż a z g o d ę** na prowadzenie tematu badawczego: „Ocena wpływu bakteriofagów typu Pf1 produkowanych przez szczepy *Pseudomonas aeruginosa* na odpowiedź zapalną organizmu" przez prof. dr hab. Roberta Buckiego wraz z zespołem badawczym z UMB.

Przewodnicząca Komisji Bioetycznej UMB

prof. dr hab. Otylia Kowal-Bielecka